DOCTORAL THESES IN FOOD SCIENCES AT THE UNIVERSITY OF TURKU

# Molecular Insights to Gut–Brain Communication: Metabolomics Approach on Lifestyle Influences

**HANY AHMED**

**Food Sciences**
**Department of Life Technologies**

DOCTORAL THESES IN FOOD SCIENCES AT THE UNIVERSITY OF TURKU
Food Chemistry

# Molecular Insights to Gut–Brain Communication: Metabolomics Approach on Lifestyle Influences

HANY AHMED

**Food Sciences**
**Department of Life Technologies**

**TURKU, FINLAND – 2025**

University of Turku
Department of Life Technologies, Faculty of Technology
Food Sciences
Doctoral Programme in Technology

Supervised by
Professor Kati Hanhineva, Ph.D.
Department of Life Technologies
University of Turku
Turku, Finland

Docent Ville Koistinen, Ph.D.
Department of Life Technologies
University of Turku
Turku, Finland

Senior Researcher Olli Kärkkäinen, Ph.D.
School of Pharmacy
University of Eastern Finland
Kuopio, Finland

Reviewed by
Associate Professor Nicholas Rattray, Ph.D.
Strathclyde Institute of Pharmacy and Biomedical Sciences
University of Strathclyde
Glasgow, Scotland

Associate Professor Tiina Sikanen, Ph.D.
Faculty of Pharmacy
University of Helsinki
Helsinki, Finland

Opponent
Professor Jonathan Swann, Ph.D.
Faculty of Medicine
University of Southampton
Southampton, UK

Research director
Professor Baoru Yang, Ph.D.
Department of Life Technologies
University of Turku
Turku, Finland

The originality of this dissertation has been checked in accordance with the University of Turku quality assurance system using the Turnitin OriginalityCheck service

ISBN 978-952-02-0317-7 (print)
ISBN 978-952-02-0318-4 (pdf)
ISSN 2323-9395 (print)
ISSN 2323-9409 (pdf)
Painosalama – Turku, Finland 2025

*To Remi, for being there late into the night during the final stretch*

# TABLE OF CONTENTS

# ABSTRACT

Alterations in the gut microbiota composition and function have been implicated in various human diseases. Gut–brain axis, a bidirectional communication network involving the neural, immune, and endocrine systems, facilitates the crosstalk between the gut microbiota and the central nervous system (CNS). Small molecules produced through host and microbial metabolism, known as metabolites, play a focal role in this signaling. Metabolomics, the comprehensive profiling of metabolites in biological samples, has been instrumental in identifying these active compounds. Applied to fecal and blood samples, metabolomics has revealed the significant influence of lifestyle factors, such as nutrition or substance use, on human metabolome. However, the connections between lifestyle factors and neuroactive metabolites remain poorly understood.

This doctoral thesis aimed to discover metabolites with neuroactive potential and provide insights on how lifestyle factors may influence them. The primary methodology across the included studies was nontargeted metabolic profiling using liquid chromatography–high-resolution mass spectrometry (LC-HRMS), enabling broad detection of chemically diverse metabolites in human clinical samples. These samples were collected from clinical interventions examining the effects of alcohol use and withdrawal in individuals with alcohol use disorder (AUD), inulin supplementation in individuals with AUD or obesity, and high-intensity interval training in individuals with metabolic-dysfunction associated steatotic liver disease (MASLD).

The findings show that AUD has a profound effect on plasma metabolome, particularly affecting lipid intermediates, bile acids, steroids, and diet- and microbiota-derived metabolites. Notably, many of these changes showed reversible trends following a three-week withdrawal period, underscoring the independent impact of AUD. Several diet- and microbiota-derived metabolites were inversely associated with psychological symptoms and were also detected in the brains of deceased individuals with a history of heavy alcohol use. Inulin supplementation during withdrawal had modest effects on fecal and plasma metabolites, with minor reductions in fecal secondary bile acids and amines and increases in plasma lipid species. These changes showed moderate correlations with gut microbiota composition. Overall, alcohol use, inulin supplementation and exercise each produced distinct effects on fecal and plasma metabolomes. The relationships between fecal and plasma metabolites were treatment- and time-specific, and not consistent across interventions.

This doctoral thesis uncovered several plasma metabolites with neuroactive potential and emphasized the role of diet and microbiota in shaping their abundance. It also demonstrated that microbiota-targeted interventions do not necessarily induce broad metabolic changes, as evidenced by the specific

outcomes of inulin supplementation. Furthermore, the distinct metabolic effects of different lifestyle interventions, influenced by environmental and individual factors, may explain the inconsistent associations between fecal and plasma metabolomes. The findings highlight the importance of assessing and considering the individual variability in microbiota composition, diet, lifestyle, and health when investigating pivotal metabolites involved in the gut–brain axis communication

.

# SUOMENKIELINEN ABSTRAKTI

Suolistomikrobiston koostumuksen ja toiminnan muutokset on yhdistetty lukuisiin sairauksiin. Suoli–aivo-akseli on kaksisuuntainen kokonaisuus, jossa hermosto, immuunijärjestelmä ja enteroendokriininen järjestelmä mahdollistavat viestinnän suolistomikrobiston ja keskushermoston välillä. Sekä oman aineenvaihduntamme että mikrobien aineenvaihdunnan tuottamat pienet molekyylit ovat keskeisiä toimijoita tässä viestintäverkostossa. Metabolomiikka, eli biologisissa näytteissä olevien aineenvaihduntatuotteiden kattava profilointi, on keskeinen tieteenala näiden aineenvaihduntatuotteiden määrittämisessä ja tunnistamisessa. Uloste- ja verinäytteiden tutkiminen metabolomiikan keinoin on paljastanut, kuinka merkittävästi elämäntapatekijät, kuten ravitsemus tai päihteiden käyttö, vaikuttavat ihmisen metaboliittiprofiiliin. Toistaiseksi on kuitenkin epäselvää, millainen vaikutus elämäntapatekijöillä on aineenvaihduntatuotteisiimme, joilla on hermostoon toimintaa muuttavia ominaisuuksia.

Tämän väitöskirjan tavoitteena oli tunnistaa hermostoon vaikuttavia aineenvaihduntatuotteita ja selvittää, miten elämäntapatekijät voivat vaikuttaa niiden määriin kehossa. Tutkimuksissa käytettiin tutkimusmetodina kohdentamatonta metaboliittiprofilointia perustuen nestekromatografiaan ja korkean resoluution massaspektrometrilaitteisiin, mikä mahdollisti kemiallisesti monimuotoisten ja matalan pitoisuuden aineenvaihduntatuotteiden määrittämisen veri- ja ulostenäytteistä. Näytteet olivat peräisin interventiotutkimuksista, joihin oli sisällytetty potilasryhmiä, joilla oli diagnosoitu alkoholiriippuvuussairaus, lihavuussairaus tai ei-alkoholiperäinen rasvamaksa. Interventioiden aikana alkoholiriippuvaiset potilaat osallistuivat alkoholivieroitukseen tai saivat vierotuksen aikana inuliinikuitulisää. Kolmannessa interventiotutkimuksessa inuliinikuitulisää ja ravitsemusohjausta annettiin lihavuussairaille potilaille. Neljännessä interventiotutkimuksessa ei-alkoholiperäistä rasvamaksaa sairastavat potilaat osallistuivat korkean intensiteetin intervalliharjoitteluun.

Tulokset osoittivat, että alkoholiriippuvuus vaikuttaa voimakkaasti veren metaboliittiprofiiliin, erityisesti sappihappojen, steroidien, rasvahappoja sisältävien sekä ravintoon ja mikrobeihin liittyvien aineenvaihduntatuotteiden osalta. Huomionarvoista on, että useat alkoholisairaudessa muuttuneista aineenvaihduntatuotteista osoittivat päinvastaisia muutoksia vieroitusjakson jälkeen korostaen alkoholin vaikutusta aineenvaihduntaan. Useat ravinto- ja mikrobiperäiset aineenvaihduntatuotteet olivat käänteisesti yhteydessä psykologisiin oireisiin ja niitä havaittiin runsaasti alkoholia käyttäneiden henkilöiden aivoista. Alkoholivieroituksen aikana annostellulla inuliinilisällä oli hyvin vähäinen vaikutus ulosteen ja veren metaboliittiprofiiliin, sillä muutoksia havaittiin lähinnä ulosteen sekundaarisissa sappihapoissa ja amiineissa, jotka laskivat sekä veren rasvahappoja sisältävissä aineenvaihduntatuotteissa, jotka nousivat. Nämä

muutokset olivat kohtalaisesti yhteydessä suolistomikrobiston koostumukseen. Tulosten mukaan alkoholin käyttö, inuliinilisä ja liikuntaharjoittelu aiheuttivat kukin erilaisia vaikutuksia ulosteen ja veren metaboliittiprofiiliin. Havaitut yhteydet ulosteen ja veren aineenvaihduntatuotteiden olivat ryhmästä ja ajasta riippuvaisia, eikä samoja yhteyksiä havaittu johdonmukaisesti eri interventiotutkimusten välillä.

Tässä väitöskirjassa tunnistettiin useita veren aineenvaihduntatuotteita, joilla saattaa olla hermostoon vaikuttavia ominaisuuksia. Tulokset osoittavat ravitsemuksen ja suolistomikrobiston olevan keskeisiä tekijöitä niiden määrän säätelyssä. On kuitenkin huomioitava, että suolistomikrobistoon kohdistuvat interventiotutkimukset eivät välttämättä muuta aineenvaihduntatuotteiden määriä selkeästi, kuten inuliinilisän maltilliset vaikutukset osoittivat. Eri elämäntapatekijöiden aineenvaihdunnalliset vaikutukset olivat selvästi toisistaan poikkeavia, mitä selittävät ympäristö sekä yksilölliset tekijät. Tulokset korostavat yksilöllisten erojen, kuten mikrobiston koostumuksen, ruokavalion, elämäntapojen ja terveydentilan huomioimisen tärkeyttä suoli–aivo-akselin toimintaan keskeisesti osallistuvien aineenvaihduntatuotteiden tutkimuksessa.

# LIST OF ABBREVIATIONS

| | |
|---|---|
| 5-AVAB | 5-aminovaleric acid betaine |
| ASD | Autism spectrum disorder |
| AUD | Alcohol use disorder |
| BBB | Blood–brain barrier |
| CMPF | 3-carboxy-4-methyl-5-propyl-2-furanpropionic acid |
| CNS | Central nervous system |
| CSF | Cerebrospinal fluid |
| ENS | Enteric nervous system |
| ESI | Electrospray ionization |
| FMT | Fecal microbiota transplantation |
| GABA | Gamma-aminobutyric acid |
| GC | Gas chromatography |
| GF | Germ-free |
| GLP-1 | Glucagon-like peptide 1 |
| HILIC | Hydrophilic interaction chromatography |
| IPA | 3-indolepropionic acid |
| (UHP)LC | (Ultra-high performance) liquid chromatography |
| LPC | Lysophosphatidylcholine |
| LPE | Lysophosphatidylethanolamine |
| MASLD | Metabolic dysfunction-associated steatotic liver disease |
| (HR)MS | (High-resolution) mass spectrometry |
| M/Z | Mass-to-charge ratio |
| NMR | Nuclear magnetic resonance |
| PC | Phosphatidylcholine |
| PE | Phosphatidylethanolamine |
| PYY | Peptide YY |
| QC | Quality control |
| QTOF | Quadrupole time-of-flight |
| RP | Reversed-phase |
| SCFA | Short-chain fatty acid |
| sPLS-DA | Sparse Partial Least-Squares Discriminant Analysis |
| TLR | Toll-like receptor |
| TMAO | Trimethylamine-*N*-oxide |
| VIP | Variable Importance in Projection |
| ZO | Zonula occludens |

# LIST OF ORIGINAL PUBLICATIONS

I. Leclercq, S.*; Ahmed, H.*; Amadieu, C.; Petit, G.; Koistinen, V.; Leyrolle, Q.; Poncin, M.; Stärkel, P.; Kok, E.; Karhunen, P.; De Timary, P.; Laye, S.; Neyrinck, A.; Kärkkäinen, O.; Hanhineva, K.[#]; Delzenne, N[#]. Blood metabolomic profiling reveals new targets in the management of psychological symptoms associated with severe alcohol use disorder. *eLife*. **2024**, 13, RP96937.

II. Amadieu, C.*; Ahmed, H*.; Leclercq, S.*; Koistinen, V.; Leyrolle, Q.; Stärkel, P.; Bindels, L.; Laye, S.; Neyrinck, A.; Kärkkäinen, O.; De Timary, P.; Hanhineva, K.[#]; Delzenne, N[#]. Effect of inulin supplementation on fecal and blood metabolome in alcohol use disorder patients: A randomised, controlled dietary intervention. *Clin. Nutr. ESPEN.* **2025**. S2405-4577(25)00047-6.

III. Ahmed, H.; Kärkkäinen, O.; Babu, A.F.; Meuronen, T.; Koistinen, V.; Leclercq, S.; Amadieu, C.; Leyrolle, Q.; Neyrinck, A.; Rodriguez, J.; Csader, S.; Schwab, U.; Thissen, J-P.; Starkel, P.; De Timary, P.; Layé, S.; Delzenne, N.; Hanhineva, K. Assessment of common fecal and plasma metabolic crosstalk during nutritional or exercise interventions. *Submitted*

*,[#] Equal contribution

# 1 INTRODUCTION

Metabolomics is the scientific field dedicated to the comprehensive analysis of small molecules, metabolites, within biological systems[1]. It emerged in the late 20th century as an extension of other omics fields, such as genomics, transcriptomics, and proteomics, driven by advances in analytical technologies. Techniques like mass spectrometry (MS) and nuclear magnetic resonance (NMR) spectroscopy enable the simultaneous measurement of chemically broad range of metabolites in complex biological samples. As end products of cellular processes, metabolites reflect the functional state of a biological system. Quantitative profiling of metabolites offers insight into metabolic processes, physiological conditions, and cellular interactions influenced by both intrinsic and environmental factors[2]. When integrated with other omics approaches, an area known as multiomics, metabolomics helps elucidate the complex interplay between genotype and phenotype and their roles in health and disease.

Blood and feces are two commonly analyzed biological samples that capture host and gut microbiota metabolism, as well as lifestyle factors like diet, drug use, and environmental exposures[3-7]. Blood metabolite profiles provide a systemic perspective into the metabolic status, where altered levels may serve as biomarkers of conditions such as metabolic syndrome or cognitive and mood disorders[8-13]. These changes can also generate novel hypotheses about disease origins. In contrast, fecal metabolite profile primarily reflects gut microbiota metabolism with smaller contributions from dietary- and host-derived compounds[14]. These profiles offer a window into the local gut environment and may hold biomarker potential for gastrointestinal disorders[10, 15]. Importantly, integrating blood and fecal metabolic profiles enables the study of dynamic host–microbiota interactions, a rapidly growing area of research in the 21st century.

Neurological and mental disorders are often accompanied by gastrointestinal symptoms and altered gut microbiota composition, sparking interest in the gut–brain axis and its health implications[16]. This axis comprises bidirectional communication pathways between the gut and the brain. While the brain influences gastrointestinal function, signals originating from the gut can also affect brain activity. Numerous preclinical studies have demonstrated causal links between gut microbiota or their metabolites and neurodevelopmental disorders or behavior[17-21]. Microbial metabolites can act as neurotransmitters, modulate immune responses, and influence inflammation, all of which are relevant to brain function[22-26]. These findings have opened promising avenues for lifestyle-based interventions, as factors like diet, exercise or substance use shape the microbiota. Proof-of-concept studies using probiotics or nutritional strategies have shown potential in targeting mood and behavioral symptoms by modifying gut microbiota composition or function[27-30]. However, research in this

area is still in its early stages, and the current evidence is insufficient to draw definitive conclusions.

This thesis investigates the metabolic effects of alcohol consumption, fiber supplementation and high-intensity interval training, three lifestyle factors potentially relevant to the gut–brain axis. The core methodology is nontargeted metabolite profiling of both plasma and fecal samples to explore the role and systemic relevance of microbial metabolites. First, the alcohol-related metabolome was characterized to identify circulating metabolites with neuroactive potential. Next, the metabolic impact of inulin fiber supplementation, which targets gut microbiota, during alcohol withdrawal was assessed. Finally, the shared effects of the mentioned lifestyle factors were examined by comparing associations between fecal and plasma metabolomes across studies involving patients with alcohol use disorder (AUD), obesity or metabolic-dysfunction associated steatotic liver disease (MASLD). The findings offer insights into how lifestyle factors distinctly influence systemic and gut-localized metabolic profiles, contributing to our understanding of the gut–brain interactions. To contextualize these results, the literature review covers the principles of gut–brain axis, the application of metabolomics in its study, neuroactive metabolites associated with gut microbiota, and the role of lifestyle factors, with a focus on alcohol and inulin fiber.

# 2 REVIEW OF THE LITERATURE

## 2.1 Gut–brain axis

### 2.1.1 Definition and implications of the gut–brain axis in human health

The human gastrointestinal tract hosts a diverse microbial community including bacteria, archea, viruses and fungi[31]. While present in the small intestine, this community is mainly concentrated in the large intestine and dominated by obligately anaerobic bacteria collectively known as gut microbiota. The relationship between the host and the microbiota can be described as mutualistic and beneficial to both parties. Maintaining healthy gut microbiota is essential for the host as it supports local and systemic immune development, pathogen protection, metabolism of indigestible dietary fibers and production of essential vitamins[32, 33]. The metabolic capacity of the microbiota complements host's biochemistry as the number of bacterial cells and their genetic potential both outnumber the host's counterparts by 10–100 times. Products of microbial metabolism, microbial metabolites, are not only unique to microorganisms as they include molecules such as neurotransmitters[24, 34] or uremic toxins[35, 36] that are also produced by the host. Moreover, metabolizing dietary components yields metabolites with anti-inflammatory[37, 38] or energetic[39] properties. Together, these metabolites act as neuromodulators, signaling molecules, or energy sources for host cells.

The central nervous system (CNS), comprising the brain and spinal cord, regulates physiological processes and cognitive functions. Bidirectional communication between peripheral organs, the nervous system and the immune system is essential for homeostasis. CNS, along with the peripheral nervous system, forms crosstalk networks with organs like the liver, pancreas and gastrointestinal tract. In the latter, the intricate communication network between the gut and the brain is referred to as the gut–brain axis[40]. Within the gut–brain axis, the gut microbiota interacts with the local nervous, endocrine and immune systems that convey signals to the brain. While the full extent of microbial signaling pathways is yet to be elucidated, microbial metabolites are considered key players in both local and systemic activation. Currently established mechanisms include education of immune systems[41], activation of sympathetic[42] and parasympathetic[43] neurons, production of neurotransmitters[23, 44] and gut hormone secretion[45, 46].

Current knowledge does not support the existence of fetal microbiota[47]. Seeding of the gut microbiota is initiated during birth and the composition of the gut microbiota changes during maturation and aging[33]. However, the maternal

microbiota has been shown to have an impact on fetal development in preclinical models[48]. Further, preclinical reports also suggests that the presence of gut microbiota is essential for normal brain and immune development and growth as evidenced in germ-free (GF) animals, animals born and developing without gastrointestinal flora, exhibiting altered brain development, behavioral abnormalities and immune dysfunction[49, 50]. Bacterial molecules, such as antigens and metabolites derived from the maternal microbiota can enter the maternal circulation and reach the fetal environment, thereby influencing prenatal development[51]. Hence, albeit coming from experimental models, these findings underline the critical roles prenatal exposure to microbiota and associated molecules possess in shaping host's early-life development.

Early-life gut microbiota composition is determined by factors such as delivery mode, genetics, environment and diet[52]. Nevertheless, a newborn's microbiota closely resembles maternal microbiota during the first postpartum months. The first 3–6 months post-birth are considered as the window of opportunity where beneficial, or detrimental, microorganism–host interactions are established. Perturbations during this period, due to factors such as antibiotic treatment, may lead to cognitive and behavioral alterations later in life[53]. Without significant stressors, such as severe inflammations or malnourishment, the introduction of solid foods initiates gut microbiota maturation. By the age of 2 years, the compositional and functional diversity of the microbiota reaches an adult-like state intertwined with host metabolism, gastrointestinal well-being and immune homeostasis. With ageing, the microbiota composition changes as the gut flora of the elderly are characterized by a decrease in previously dominant bacteria replaced by other bacteria groups and pathobionts[54].

Interest in the gut–brain axis has been fueled by accumulating evidence of altered gut microbial composition in neurological disorders[55]. Moreover, findings go beyond observational as preclinical models have demonstrated that selected neurological symptoms can be recapitulated by transferring the disease-associated gut microbiota from humans to GF mice[56]. While it is too early to establish robust causal link between gut microbiota and neurodevelopmental or behavioral disorders in humans, the potential of gut microbiota as a health modulator is widely recognized. Hence, characterizing pathways of action and mapping candidate biomarkers or metabolites implicated within the gut–brain axis is essential for unraveling the nature of microbiota–host crosstalk in the context of brain function. Documented pathways of communication within the gut–brain axis involve components of enteric nervous system and the immune system which are discussed in more detail in the following chapters and illustrated in **Figure 1**.

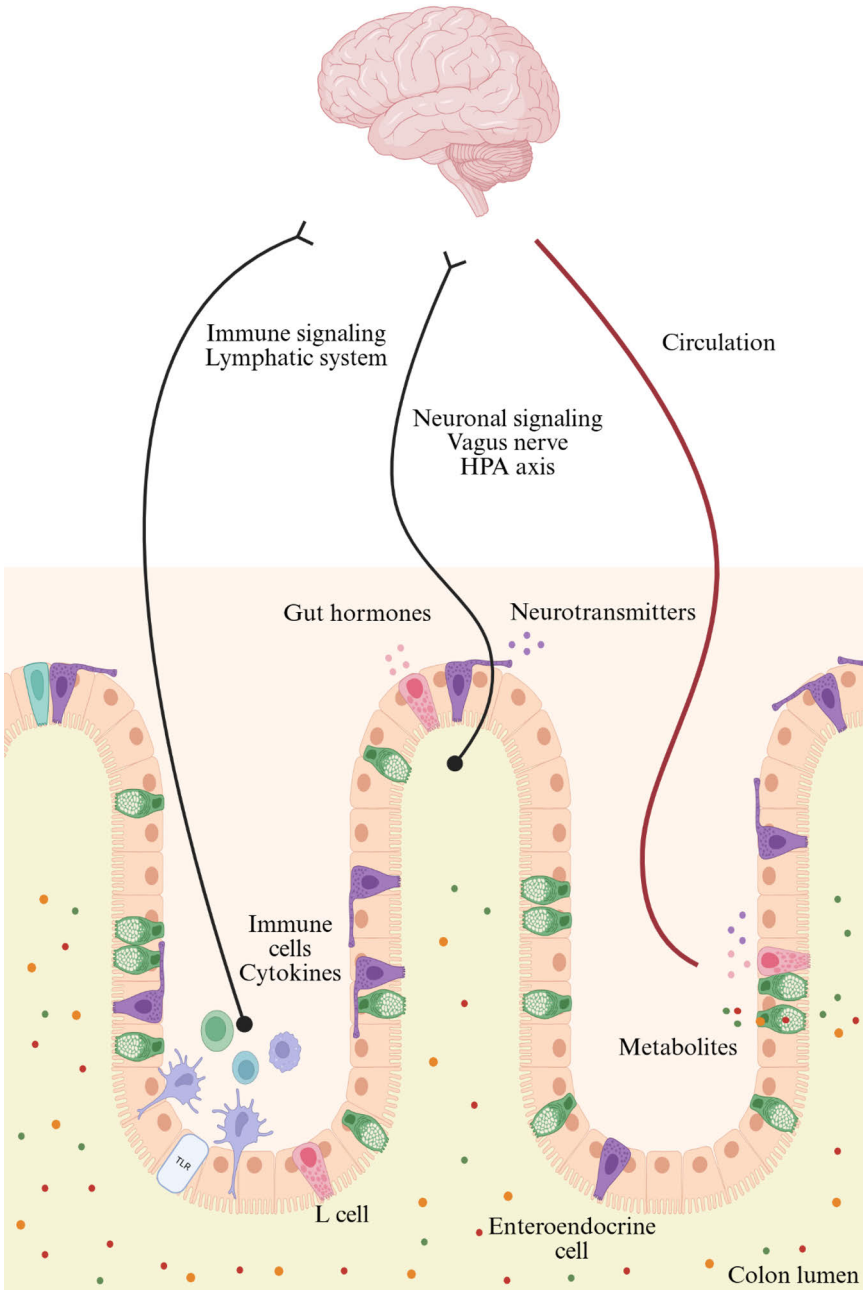


Figure 1. Key communication pathways within the gut–brain axis. Gut-derived molecules or immune cells can translocate from the gut to the brain via circulation or lymphatic system. Microbial metabolites, neurotransmitters and gut hormones can activate neurons of enteric nervous system carrying signals through vagal or spinal branches to the central nervous system. Additionally, cells of both adaptive and innate immune systems are widely present in the gut and interact with the compartments of systemic immunity. HPA, hypothalamic-pituitary-adrenal axis. Figure created in Biorender.com.

### 2.1.2 Enteric nervous system as a communication pathway

The enteric nervous system (ENS) is a crucial component of the autonomic nervous system spread throughout the gastrointestinal tract[57]. The ENS forms a complex network of sensory, motor, and interneurons, along with supporting glial cells innervated within the intestinal wall. As a part of the autonomic nervous system, the ENS is capable of operating local motility, secretion and blood flow autonomously emphasizing its role as a frontline sensory network. However, ENS is also connected to the CNS through sympathetic and parasympatethic routes forming a bidirectional gut–brain crosstalk loop. The first neuronal interface, endings of the intrinsic primary afferent neurons, that can be directly or indirectly activated by intestinal content is in the submucosal plexus. These afferent neurons are extensions of the vagal and spinal branches thus offering a direct neuronal pathway from mucosal lining to the CNS.

Vagus nerve has been highlighted as the most direct route of signaling between the gut and brain[16]. 80 % of vagal neuronal fibers are afferent and transmit signals from the intestinal muscle and mucosal layers towards the CNS while remaining efferent fibers carry signals from the CNS to the periphery. Depending on the location and type of the vagal afferents in the gastrointestinal tract, the excitatory signaling can be triggered directly via motion, stretch or molecules such as neurotransmitters. Moreover, microbiota or its metabolites can mediate the excitation of vagal sensory neurons through binding to G-protein-coupled receptors resulting in activation of selected brainstem areas[34, 42]. Microbial metabolites can also induce neurotransmitter production in enteral cells and consequently via enteroendocrine function trigger activation of the vagal afferents[58]. Enteroendocrine cells have also been shown to form physical connections with vagal afferents and this neuroepithelial circuit, referred to as neuropods, carry signals from the intestinal lumen to brainstem within milliseconds[59]. Furthermore, vagal stimulation has been shown to modulate mood[16] and severing the vagus nerve to modify behavior and brain function[43, 60]. Vagus nerve stimulation has also been linked to the hypothalamic-pituitary-adrenal axis which is a major neuroendocrine system modulating stress responses[61]. Vagus stimulation resulted in the activation of hypothalamic stress pathways and increase in the plasma stress hormones corticosterone and cortisol-release stimulating adrenocorticotropic hormone.

In addition to vagal stimulation, enteroendocrine signaling is in the nexus of relaying microbial cues into nerve activating signaling[16, 44]. Majority of the circulating serotonin is produced by colonic enterochromaffin cells, and the rate of synthesis is influenced by microbial metabolites[44, 62]. Besides activating enteric neurons, serotonin has been shown to play a role in the development and function of the ENS[63]. Colonic L cells are another type of enteroendocrine cells

that synthesize glucagon-like peptide 1 (GLP-1) and peptide YY (PYY), both of which participate locally in gut motility and modulate food intake and eating behaviour via CNS[64-66]. Moreover, the ENS expresses several receptors binding hormones released by the L cells[67]. Similar to enterochromaffin cells, microbial metabolites can also regulate the enteroendocrine function of colonic L cells[16]. While selected species of the gut microbiota are indeed adept to synthesize neurotransmitters such as serotonin or histamine and thus directly activate the ENS, it is debatable whether their synthesis can reach physiologically relevant quantities[67]. However, the ENS also expresses receptors towards other microbial molecules. The most notorious example of such pattern recognition receptors are the Toll-like receptors (TLR). TLRs are vital for physiologically sound gut function and development as their knock-out produces neuronal defects and reduces intestinal motility reverted by TLR agonism[68]. Hence, molecular cues from the gut microbiota are essential for the development and maintenance of a functional ENS and thus gastrointestinal physiology[69].

### 2.1.3 Immune system as a communication pathway

The gastrointestinal tract hosts a diverse array of innate and adaptive immune system cells that are the frontline responders to immune challenges generated by the gut microbiota[32]. It has been established that gut microbiota is in the apex of normal immune development and that microbiota–host immune crosstalk is established early in life[52]. Evidence shows that the offspring's immunity is shaped by the maternal microbiota and that the microbial molecules and metabolites are the key transmitters[48]. After birth, the wealth of microbial molecules that challenge the developing immune system mediate the immune imprinting that is severely dysfunctional in GF mice[70]. Pattern-recognizing receptors, such as the mentioned TLRs, are the central receptors for detecting microbiota-associated molecules like lipopeptides and -polysaccharides and further training the immune system[41, 71]. Recognition of microbiota-associated molecular patterns will trigger innate immunity response resulting in a cascade of signals that eventually drive the production of cytokines and chemokines and infiltration of macrophages and dendritic cells in the site of inflammation. In infants the immaturity of the immune system protects the infant from excessive inflammatory responses towards microbial clues[52].

The signaling cascade initiated by the innate immunity is also required for the response of adaptive immunity cells, mainly circulating T- and B lymphocytes[52]. By its name, the adaptive immune system adapts to challenges through regulation, specification and tolerance facilitated by the memory T and B cells. Thus, exposure to microbes and their metabolites is reflected on immunoregulation of the adaptive immune system[16]. Recently, a link between this immune system and

the gut–brain axis was demonstrated by antidepressant-like behavioral changes induced by transferring lymphocytes from stressed mice to their immune-deficient counterparts[72]. Short-chain fatty acids (SCFA) produced by the gut microbiota can also modulate the homeostasis of intestinal T cells through maturation of regulatory T cells[22, 73].

During the inflammatory response, immune cells produce pro- and anti-inflammatory cytokines that are signaling proteins interacting with other cells and membranes. Pro-inflammatory cytokines have the potential to induce depressive-like behavior and reduce appetite which are characteristic to sickness behavior[74]. This implies that cytokines signal the brain via peripheral routes, or they can be transported to the CNS. Unlike immune cells or most microbiota-derived metabolites, cytokines can cross the blood–brain barrier (BBB) and increase its permeability. Alternatively, the lymphatic system can also pertain passage of cytokines, immune cells and even microbial components to the CNS[75]. As a part of the lymphatic system, the meningeal lymphatic vessels are responsible for the exchange and draining of the cerebrospinal and interstitial fluid from the CNS providing a potential opening for translocation of peripheral cells and molecules. Induction of immune reaction in the CNS, neuroinflammation, also activates microglia and astrocytes both of which are presumed targets of microbiota-derived metabolites[76]. While the repertoire of mechanisms by which microbiota signals the brain remains undisclosed, the findings of microbial modulation on the CNS immunity emphasizes the significance of gut–brain axis on brain homeostasis[77]. With the communication pathways described, the following chapter will cover currently established microbial-derived metabolites and their properties in the context of gut–brain axis.

## 2.2 Metabolomics in the study of the gut–brain axis

### 2.2.1 Metabolomics approaches

Progress in high-throughput technologies has revolutionized scientific research[78]. Large-scale assessment of biological molecules in a short period of time is characteristic to the scientific field called omics. Different omics applications focus on specific molecules like DNA (genomics), RNA (transcriptomics, proteins (proteomics) or metabolites (metabolomics). Metabolomics studies the small molecules (<1500 Da) derived from cellular metabolism, reflecting the functional output of other omics levels at the time of sample collection. Existing sub-fields within metabolomics can focus on specific metabolite classes such as lipids (lipidomics) or volatiles (volatilomics), or particular areas of science such foodomics. Metabolic profiling, the comprehensive assessment of metabolites in a sample, is for mapping dietary or disease biomarkers and characterizing

cellular metabolism (**Figure 2**)[1]. Integrating multiple layers of omics data in multi-omics studies provides a holistic view of the intrinsic factors driving disease risks. In the context of gut–brain axis, integrating metagenomics data from gut microbiota with host metabolomes offers insights into microbial influence on host metabolic profiles associations with emotional or cognitive functions[79]. In the following paragraphs, the main methodologies and general aspects of sample treatment are discussed.

A targeted, quantitative metabolomics approach studies specific metabolites of interest, usually a few tens, though newer methods can quantify even hundreds accurately[80]. Targeted metabolomics, or rather targeted metabolite analysis as metabolomics is by definition nontargeterd, is hypothesis-driven, selecting metabolites based on common pathways, chemical class or other relevant physicochemical for the hypothesis. Strengths include specificity, accuracy and possibility to quantify absolute concentrations. Although developing validated targeted metabolomics method is laborious and may require additional sample concentration steps for the low-abundant metabolites, downstream data processing is more straightforward than in nontargeted methods. Moreover, targeted approaches can achieve higher analytical sensitivity than nontargeted approaches by focusing on selected precursor ions, mass-to-charge ratios (*m/z*) or retention time ranges. Since microbial metabolites belonging to classes of bile or amino acids are relevant for the gut–brain axis signaling, several studies have implemented targeted assays focusing on them[81-83].

Contrary to targeted approaches, nontargeted metabolomics (also known as metabolic profiling, nontargeted or global metabolomics) aims to cover the full range of metabolites in a sample detectable by the chosen analytical technique[84]. These studies are hypothesis-generating, typically focusing on differentiating metabolites between case and control groups, measured by their relative abundances. Consequently, this approach enables the detection of known, suspected and unknown metabolites, expanding the pool of potentially interesting metabolites to thousands. Since the aim is to cover a broad range of analytes, sample treatment procedures are usually straightforward, enabling high-throughput and sensitive analysis. However, the richness of the data requires several downstream processing steps to align and normalize data, reduce background noise and account for missing data. Confirming compound identities requires analysis of analytical standards to match the molecular features, limiting identification to established compounds. To address some of the limitations, semi-targeted approaches combine standards with nontargeted methods to determine absolute concentrations of selected metabolites complementing metabolic profiling[79]. Nevertheless, metabolic profiling is widely utilized to probe how neurological disorders alter metabolism or how microbiota presence or absence affects the host[85-87].

Regardless of the metabolomics approach, metabolites need to be extracted from biological matrixes[84]. First, snap-freezing or embedding is used at collection to stop metabolic reactions. Metabolite extraction is facilitated by extraction solvent which also acts as a dilutant, quenches the metabolism and precipitates proteins. The choice of extraction solvent is crucial for metabolite coverage with methanol or acetonitrile mixed with water being common choices[79]. Combining different organic solvents like methyl tert-butyl ether or dichloromethane improves extraction coverage. Liquid samples such as plasma or urine can use simple and rapid liquid-liquid extraction. Solid samples like tissues or fecal material may require mechanical homogenization to break down the matrix and release metabolites. Extraction may include additional steps like derivatization or concentration by evaporation but generally ends with centrifugation and filtration to remove extra material from the sample. Together, combining different extraction methods and biological matrices provides comprehensive insight into an organism's metabolic landscape.

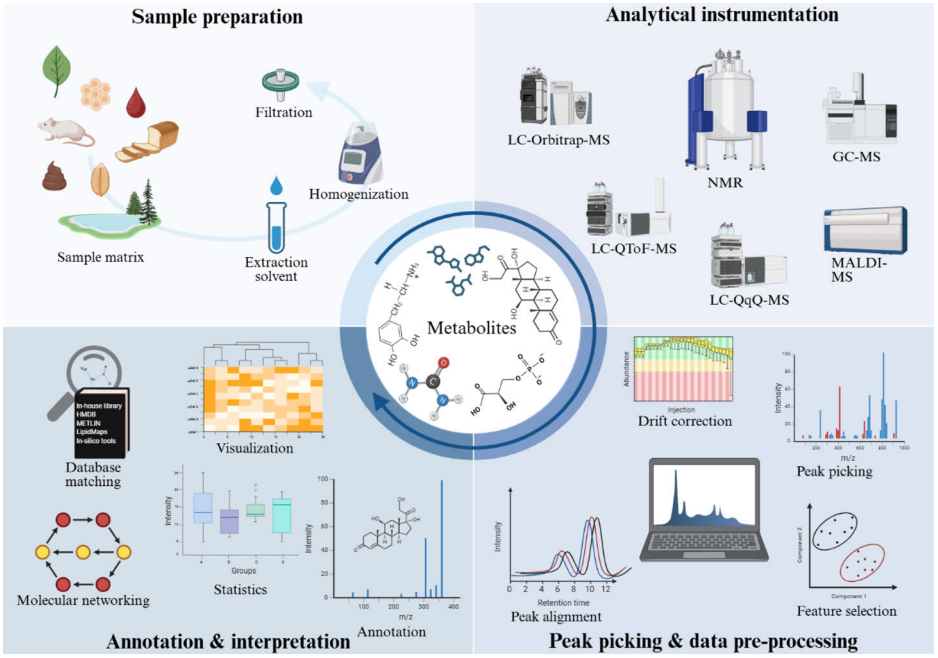


Figure 2. Metabolomics workflow from sample treatment to metabolite identification. Metabolites can be extracted from virtually any type of biological samples. Choice of the analytical instrument, or their combinations, depend on the approach or target metabolites. Data handling requires bioinformatics tools and several preprocessing steps. Annotation is facilitated by chemical standards, spectral databases and in silico tools. GC, gas chromatography; LC, liquid chromatography; MALDI, matrix-assisted laser desorption ionization; MS, mass spectrometry; NMR, nuclear magnetic resonance spectroscopy; QToF, quadrupole-time-of-flight; QqQ, triple-quadrupole. Figure created in Biorender.com.

### 2.2.2 Analytical instrumentation

Similar to the extraction method, no single analytical platform can comprehensively cover the entire metabolome[84]. Combining different platforms enables capturing most metabolites regardless of their chemical properties and concentrations ranging from picomolar to millimolar. Common platforms in metabolomics include NMR spectroscopy and MS. Both have their advantages and limitations, which are discussed in detail later, but they can be used in parallel to provide complementary information on the metabolome. Within MS techniques, the mass analyzer is chosen based on the study aim and resources. For example, triple quadrupoles are commonly used in targeted approaches, while quadrupole time-of-flights (QToF) or Orbitraps in nontargeted approaches. The latter two HRMS instruments provide information on analytes' accurate masses and isotopic patterns. MS is rarely used alone; coupling it with a chromatographic separation method, such as ultra-high performance liquid chromatography (UHPLC) or gas chromatography (GC), permits efficient analysis of chemically rich samples and supports metabolite identification. Additionally, mass spectrometry imaging is increasingly used to determine the spatial distribution of metabolites within tissue. The following paragraphs briefly review the advantages and disadvantages of NMR, GC-MS and LC-MS platforms.

NMR spectroscopy offers robustness, reproducibility, structural elucidation, non-destructive and high-throughput capabilities[84]. It is the only metabolomics platform capable of determining the chemical structure of unknown compounds, making it ideal for novel metabolite identification when a high-concentration sample of the unknown compound is available. For instance, while MS suggested the presence of a known microbiota-derived metabolite in mice brain, NMR revealed their identity as two novel isomers of carnitine derivatives[88]. NMR samples do not require pretreatment, analysis is quantitative, can be completed in minutes, and the resulting spectra are robust and reproducible, enabling the reliance on spectral databases[2]. Moreover, samples can be used for other analysis after measurement. However, NMR has limited sensitivity (around few micromoles) and requires high liquid sample volumes (few hundred microliters). The widely used $^{1}$H NMR requires protonated molecules, and with limited sensitivity, the NMR spectrum from a biological sample can contain signals from around 100 metabolites[89]. Despite these limitations, NMR spectroscopy is broadly applied in metabolomics due to its robustness, quantitative nature, and wide range of organic metabolite coverage.

GC-MS is ideal for analyzing thermally stable and volatile organic compounds or non-polar metabolites such as SCFAs, alcohols and ketones[84]. The range of detectable metabolites can be increased to (semi)polar metabolites like amino acids and amines by including a derivatization or other chemical

modification step in sample treatment. In GC-MS, volatiles vaporized at high temperature, are moved by inert carrier gas through a column where they interact with the column material based on their chemical characteristics. Volatiles spend varying time in the column before reaching the MS side. Commonly, volatiles are ionized by electron impact, producing reproducible fragmentation spectra, enabling the use of spectral libraries. In terms of sensitivity, GC-MS outperforms NMR reaching sub-millimolar concentrations. However, electron impact is a hard ionization technique not suitable for all metabolites, and GC gradients usually extend analysis time to tens of minutes. GC-MS has been extensively applied to measure microbial metabolites, like SCFAs, from fecal and blood samples in both targeted and nontargeted manner[79, 90].

UHPLC-MS offers the widest coverage of non-volatile analytes, tailored by extraction and MS techniques according to the research question[80]. In chromatographic separation, analytes are carried by liquid phase through a column covered in material with affinity towards, for example polar or nonpolar analytes. Targeted approaches can apply a single LC method for optimal separation of selected analytes, while nontargeted approaches can combine methods, like reversed-phase (RP) and hydrophilic interaction (HILIC) chromatography to separate both hydrophobic and hydrophilic analytes. Electrospray ionization (ESI) is the most used ionization technique in metabolomics, creating fewer fragments and preserving analytes compared to electron impact ionization. ESI allows ionization of a wide range of co-eluting compounds in a single assay, and together with LC separation, outperforms most metabolic profiling techniques. Ion-mobility spectrometry, useful for stereoisomer separation post-ionization, separates ions in gas-phase based on their structural features. LC-MS does not require extensive sample treatment, and analysis time can be limited to around ten minutes per sample, producing data on potentially thousands of metabolites. However, the resulting data in nontargeted approaches requires extensive data processing[84]. The next topic covers the steps in nontargeted LC-MS metabolomics data processing and how such data has been utilized to understand the molecular landscape within the gut–brain axis.

### 2.2.3 Utilization of nontargeted metabolomics data

The acquired spectral data from nontargeted liquid chromatography–high-resolution mass spectrometry (LC-HRMS) metabolomics analysis is complex and redundant, containing information from the sample, pre-treatment materials, eluents, instrument noise, and in-source adducts and fragments[91]. Analyzing a single sample can produce thousands of molecular features, with the number of detected features increasing with each sample. Signal abundances are relative to

the ionization efficiency and analyte concentration, further complicated by individual differences in metabolomes. To translate this high-dimensional data into identifiable metabolic signatures and meaningful biological information, peak-picking, alignment, data correction, quality control and reduction are essential procedures to ascertain data validity.

Data processing begins with peak picking and alignment where spectral peaks are detected based on pre-set parameters defining peak height, mass accuracy, scan and retention time, and aligned across all samples[1]. Instrumental drift causes systematic distortion in the abundances of molecular features, which must be corrected before further processing. Drift correction is done by algorithms that correct feature abundances against those from regularly analyzed pooled quality control (QC) samples, representing a 'mean' sample[92]. After correction, quality metrics can be calculated for the molecular features' abundances based on their coefficient of variation and residual standard deviation, followed by the removal of low-quality features originating from random variation or artefacts. Metabolomics data can contain missing values due to various reasons and data imputation methods such as Random Forest, K-Nearest Neighbors or minimum value can be used to address missing data[93]. Before proceeding to annotation and identification, the number of interesting features can be narrowed by applying filters such as sample-to-blank or signal-to-noise ratios, and multivariate or univariate analysis or machine-learning tools to reveal molecular features that are most discriminating or significantly different between sample groups. Several online platforms offer the entire pipeline from peak picking to statistical analysis, as well as vendor-specific and freeware community-maintained applications and programming tools that can be used in parallel to facilitate data processing and analysis[1].

Despite methodological approaches, metabolite identification remains the major bottleneck in nontargeted metabolomics[91]. Measurement of accurate mass and calculation of probable molecular formula can still result in tens of matching metabolites, and while chromatographic separation adds another data dimension, retention times are method and lab specific. Inspection of MS/MS fragmentation spectra significantly improves annotation rates, as MS/MS spectrum are metabolite-specific, although not enough to distinguish stereoisomers. Moreover, characteristic fragments are relatively reproducible between different MS instruments when the same fragmentation energy is applied, allowing querying of spectral libraries for possible candidates. Nevertheless, confident identification requires matching the accurate mass, retention time and MS/MS fragments against data from analytical standard analyzed with the same instrument and conditions. With over 100,000 known human metabolites[94], creating and maintaining such internal libraries is impossible for a single research group or facility. Hence, annotation is assisted by public spectral

libraries, *in silico* tools predicting fragmentation patterns, and machine-learning approaches utilizing large databases for spectral matching and similarity scoring. Since chemically similar metabolites share some common fragments, molecular networking approaches are increasingly used to provide insight into chemically connected metabolites, bridging the gap between knowns and unknowns.

In the context of gut–brain axis, a seminal 2009 study using nontargeted UHPLC-QToF-MS approach showed that over 200 unique mice blood molecular features were microbiota-associated, with particular enrichment in amino acid derivatives and sulfated metabolites[95]. Since then, metabolic profiling studies have verified the broad influence of gut microbiota on our metabolome, with one study suggesting that almost 50 % of variation in circulating metabolites is explained by the microbiota[6]. Metabolic profiling of circulating metabolites can also unravel metabolic signatures or altered metabolic pathways in neurological and mental disorders[96, 97]. Profiling of the fecal metabolome has been used as a proxy for microbial functionality and can reveal metabolic dysregulation linked to neurodevelopmental disorders where gastrointestinal symptoms are common[14, 98]. Constantly accumulating metabolomics data has been translated into interactive platforms where users can inspect the metabolic signatures and their associations with background variables[6, 11]. With the establishment of community-sourced repositories, researchers can now mine millions of microbiota-associated MS/MS spectra and link them to specific microbial species or genera[99]. Mining public repositories has been used to identify novel microbiota-modified bile acid signatures in humans[100]. In an approach called reverse metabolomics, specific MS/MS patterns of novel metabolites are mined from public repositories to explore their biological significance in existing data[101].

## 2.3 Neuroactive properties of microbial metabolites

### 2.3.1 Neurodevelopment

Neurodevelopmental processes begin in the prenatal phase and continue throughout life, involving the generation, organization and reshaping of the nervous system. Recent studies indicate that microbial metabolites, such as butyrate, amino, and bile acid derivatives, modulate the formation of intestinal structures through cell proliferation[102, 103]. A seminal study in a mouse model of autism spectrum disorder (ASD) showed that maternal microbiota can drastically affect brain development in descendants[17]. ASD-related behavior abnormalities and defects in intestinal integrity and microbial composition in descendants are induced by immune activation in pregnant dams. Descendants exhibit increased intestinal permeability due to alterations in serum metabolite profiles,

particularly a 46-fold increase in 4-ethylphenylsulfate, a tyrosine derivative and uremic toxin. Microbiota-dependency was demonstrated by normalization of ASD-related behavior and metabolic abnormalities after administering *Bacteroides fragilis*, a human commensal. Underlining the significance of the 4-ethylphenylsulfate, treating naïve wild-type mice induced anxiety-like behavior. A follow-up study linked the detrimental effects of 4-ethylphenylsulfate to interference in brain myelination, oligodendrocyte maturation and activity patterns in the limbic system[19].

4-ethylphenylsulfate has also been detected in the plasma of children with ASD, aligning with preclinical findings[86]. Another molecule, 4-methylphenylsulfate also called *p*-cresol sulfate, differing from 4-ethylphenylsulfate by methyl instead of ethyl substitution in the phenyl ring, impairs social behavior in mice, and this behavior was transferred by fecal microbiota transplantation (FMT)[35]. High circulating levels of *p*-cresol sulfate were measured in recipient, along with decreased myelination in the medial prefrontal cortex. In humans, urinary and fecal levels of *p*-cresol sulfate have been shown to be elevated in children with ASD compared to children without ASD[104, 105].

Conversely, some microbial metabolites have protective effects in humanized mouse model of ASD-like behavior. When GF mice received an FMT from ASD donors, circulating levels of 5-aminovaleric acid and taurine were significantly lower compared to control mice[106]. Taurine, a non-proteinogenic amino sulfonic acid, and 5-aminovaleric acid, a lysine degradation product, ameliorated ASD-like features when administered to pregnant dams or offspring before reaching four weeks of age. Cognitive and social defects in offspring were ameliorated when acetic and propionic acids, two prominent SCFAs, were administered post-weaning[107]. These beneficial effects were accompanied by improvements in hippocampal synaptic ultrastructure and microglial maturation. Microbial metabolism has also been associated with fear extinction learning, where appropriate response to environmental stimuli develops[108]. Neuronal plasticity necessary for learning processes was diminished in GF or antibiotic-treated mice but not in gnotobiotic mice, and this was associated with four phenolic metabolites and sulfates: 3-(3-sulfooxyphenyl)propanoic acid, phenyl, pyrocatechol and indoxyl sulfates.

Continuing the notion that microbial metabolites affect behavior through neurodevelopment modulation, a study implicated maternal microbiota products in fetal thalamocortical axonogenesis[18]. This process involves axonal branching connecting the thalamus to cortical brain areas, and absence of maternal microbiota interfered with the process, causing neurobehavioral defects in offspring. Restoration of axonogenesis was achieved even in the absence of gut microbiota by selected microbial metabolites: 5-aminovaleric acid, its betainized

form 5-aminovaleric acid betaine (5-AVAB), trimethylamine-*N*-oxide (TMAO), hippuric acid and imidazolepropionic acid. The microbiota-dependency of these metabolites and their translocation to the fetal brain have been previously reported, but their neurogenic properties were a novel finding[85, 95, 109]. Neurogenic metabolites have also been detected in adult mice, where tryptophan metabolites promote neurogenesis in the hippocampus or axonal regeneration after sciatic nerve injury[110, 111]. In the former, indole stimulation through the aryl hydrocarbon receptor was necessary to induce neurogenesis, while in the latter, regeneration was stimulated by 3-indolepropionic acid (IPA) mediated inhibition of neutrophil chemotaxis. Beyond neurodevelopment, gut microbiota-associated metabolites may also influence neurological functions such as neurotransmission, modulation of BBB integrity, neuroinflammation, neuronal energy metabolism, and neuroprotection, as illustrated in **Figure 3**.

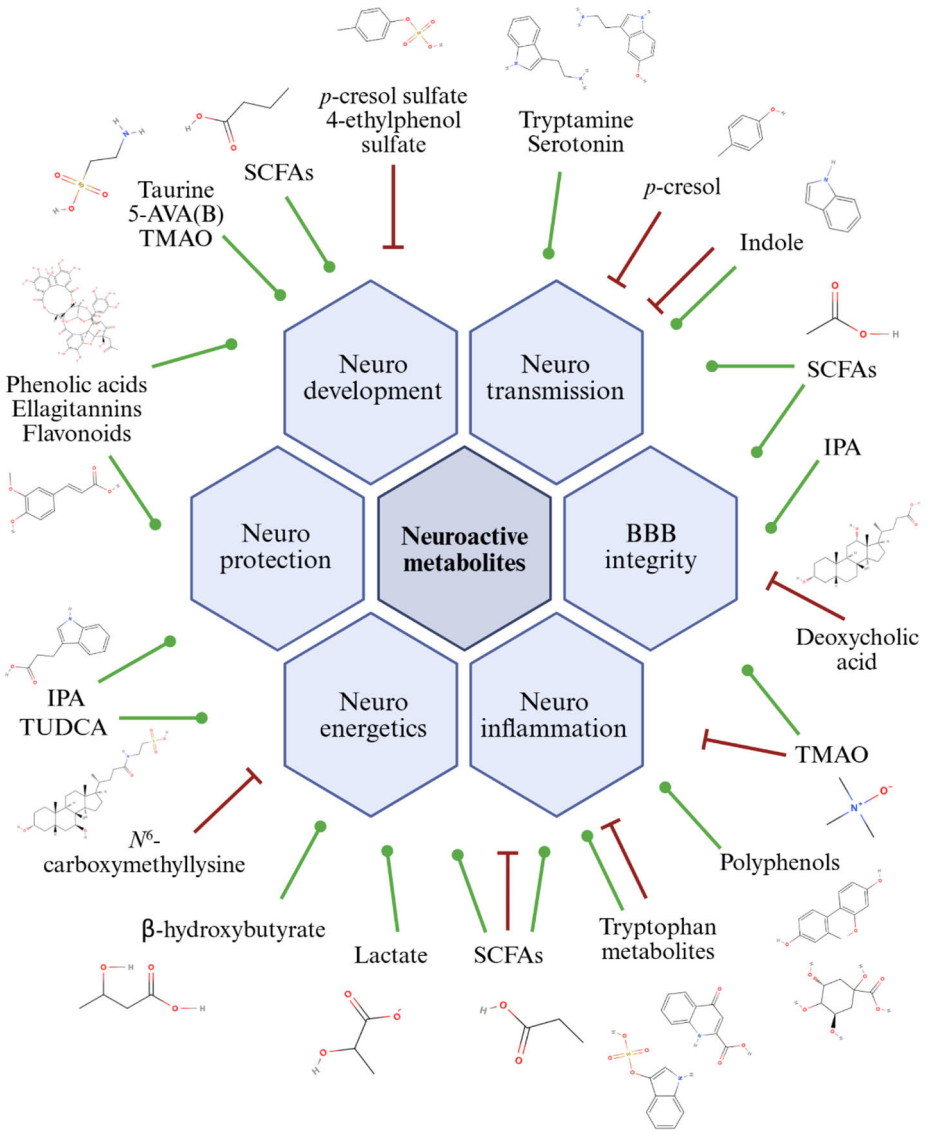


Figure 3. Overarching neuronal functions of microbiota-associated neuroactive metabolites. Red arrows illustrate detrimental effects such as induction of neuroinflammation, disruption of blood–brain barrier, altered neurodevelopment, interference with neuronal signaling and mitochondrial function. Green arrows illustrate beneficial effect such as support of blood–brain barrier integrity or mitochondrial function, alleviation of neuroinflammation and rescue of neurodevelopmental processes or neuronal signaling. 5-AVA(B), 5-aminovaleric acid (betaine); BBB, blood–brain barrier; IPA, 3-indolepropionic acid; SCFA, short-chain fatty acid; TMAO, trimethylamine-N-oxide; TUDCA, tauroursodeoxycholic acid. Figure created in Biorender.com.

### 2.3.2 Neurotransmission

The gut microbiota, through its enzymatic activities, significantly modulates the host's production of various neurotransmitters[95] within the gut lumen and can synthesize neurotransmitters *de novo*[112]. Prominent examples of bacteria-derived neurotransmitters include dopamine, norepinephrine, pipecolic acid and gamma-aminobutyric acid (GABA)[24, 112]. Additionally, bacterial β-glucuronidase cleaves the glucuronide-conjugate from host-derived dopamine and norepinephrine, transforming inactive conjugated catecholamines into biologically active forms within the gut lumen[23]. Some microbial-species in the normal gut flora produce tryptophan-derived serotonin, a neurotransmitter associated with depression and substance-use disorders, though the impact of this serotonin supply on host physiology remains unclear[113, 114]. Microbial products may also act as neurotransmitter receptor agonists, binding to receptors and initiate signaling. For example, phenylethylamine, produced by microbial fermentation, can pass the BBB and act as a dopamine receptor agonist[34]. The previously mentioned 5-aminovaleric acid and taurine are weak $GABA_A$ receptor agonists[106], while tryptamine, a tryptophan derivative, can bind to serotonin receptor 5-$HT_4$, increasing colonic secretion and gut transit time[115].

Despite of microbial potential for *de novo* serotonin synthesis, over 90% of the host's serotonin is produced by the enterochromaffin cells in the gut, with gut microbiota playing a crucial regulatory role[44, 116]. Microbial metabolites can stimulate enterochromaffin cells to synthesize and release serotonin to the lamina propria. Tyrosine-derivative tyramine, a secondary bile acid deoxycholic acid, and 4-aminobenzoic acid have been shown to stimulate serotonin synthesis[44]. The ENS has nerve fibers expressing serotonin receptors, and inducing serotonin release increases enteric and vagal neuronal signaling towards the CNS. Serotonin-releasing properties have been observed with several microbiota-associated metabolites, including tryptophan derivatives indole and indole-3-aldehyde, norepinephrine and SCFAs like butyric, isobutyric and isovaleric acids[58, 117]. Recently, the small intestine and cecal SCFAs (acetic, butyric and propionic acids), secondary bile acids and indoxyl sulfate, were shown to promote vagal nerve activity by receptor-mediated activation of the enteroendocrine cells[26]. Indole and SCFAs also promote the release of gut hormones that modulate motility, secretion and satiety. Indole can transiently promote the release of GLP-1 from colonic L cells[118], while SCFAs induce enteroendocrine cells to secrete PYY and GLP-1 and release leptin from adipocytes, collectively regulating food intake and satiety[45, 46, 119, 120]. However, indole overproduction can stimulate vagal afferents in the intestine and induce anxiety-like behavior in mice but only under chronic stress[121]. Conversely, tryptophan-derived indoles have been associated with reduced anxiety-like

behavior in humanized mice receiving FMT from patients with irritable bowel syndrome and subsequent probiotic supplementation[122]. A recent study observed overexcitability of principal neurons in the basolateral amygdala, a key brain structure in anxiety-related behavior, in GF mice[123]. Indole supplementation in the absence of gut microbiota reverted amygdala neuronal overactivity and ameliorated anxiety-like behavior, suggesting a mechanism for indole's anxiety-relieving effects. Although not reported, the anxiety-ameliorating effect may be related to shifts in plasma serotonin or norepinephrine levels[124] or SCFA production, as butyric and propionic acid have stress-relieving properties via downregulation of genes involved in hypothalamic stress signaling[125].

The variety of luminal microbiota-associated neurotransmitters is considerable, but their impact on CNS signaling and levels is not straightforward. In conventionalized mice, the substantially higher peripheral and colon GABA levels were not reflected in brain levels compared to GF mice[109]. Instead, GF mice had higher levels of both dopamine and GABA[109, 126]. However, indirect modulation of CNS neurotransmitters and subsequent signaling by microbiota-associated metabolites has been recorded. Glutamate, a neurotransmitter and precursor of GABA, participates in hippocampal glutamatergic signaling[127]. Tryptophan-derived kynurenic acid can modulate extracellular glutamate levels, and limiting kynurenic acid supply has been shown to increase hippocampal glutamate levels, enhancing memory and cognitive performance *in vivo*[127-129]. Following an FMT from schizophrenic patients, recipient mice showed decreased hippocampal glutamate and increased GABA without notable effects on circulating GABA[130]. Treatment with probiotic *Lactobacillus rhamnosus* increased brain levels of glutamate, GABA and *N*-acetyl aspartate, with levels returning to baseline after treatment cessation[121]. Previously, *L. rhamnosus* treatment modulated regional brain GABA receptor expression and reduce anxiety- and depression-like behavior in mice[43].

Other examples of GABA-linked microbiota-associated metabolites are lysine-derived pipecolic acid and lactate. Pipecolic acid has been detected in the brain and is involved in GABAergic signaling or GABA release within the CNS[131, 132]. Lactate has been linked with hippocampal and frontal cortex GABA expression and has been shown to improve memory and learning through neuroplasticity in mice[133, 134]. In addition to GABA-related signaling, lactate induced the expression of hippocampal brain-derived neurotrophic factor, a neuronal growth factor involved in learning and memory functions[135]. SCFAs like butyric acid may also regulate the production of neurotrophic factors, such as brain-derived neurotrophic factor, in the CNS[39]. However, negative neuromodulatory effects are also possible as demonstrated with *p*-cresol administration, which induced negative traits in anxiety-like and social behavior through alterations in dopamine turnover and receptor activity and signaling in

oxytocinergic and opioidergic systems[136-138]. Recently, significant elevations of prefrontal cortex *p*-cresol were linked with altered dopaminergic signaling in the prefrontal cortex and increased abundance of protein-fermenting gut bacteria families in a preclinical model of post-traumatic stress disorder[139].

While preclinical studies have provided preliminary mechanisms and pathways in which the neuromodulatory potential of microbial metabolites manifests as behavioral symptoms or altered cognitive performance, similar observations in humans are scarce. Decreased serotonin levels have been suggested as indicators of depression, or alcohol use disorder, or even causal factors for neurological and cognitive symptoms associated with COVID-19[140-142]. However, serotonin homeostasis is complex with considerable external modulators such as diet[143] influencing circulating levels independently from strictly regulated cerebral levels[140, 141]. Tryptophan metabolism and its relationship with mental health have been studied in different populations, with meta-analysis supporting a decreasing trend in tryptophan and related metabolites in patients with major depressive disorder[144]. Tryptophan catabolism through the kynurenine pathway has been linked to depression[145] and cognitive functions in obese individuals[146] and females with medically diagnosed depression[83]. Alternatively, the microbiota-orchestrated indole pathway, specifically end-product urinary indoxyl sulfate, has been associated with recurrent depressive symptoms, and circulating indoxyl sulfate with anxiety[147, 148]. There are also indications that psychobiotics, probiotics conferring mental health benefits, modulate tryptophan metabolism by favoring serotonin pathway[27] instead of kynurenine pathway[149]. Beyond serotonin, a dopamine-related microbial pathway synthetizing 3,4-dihydroxyphenylacetic acid has been associated with mental quality of life score[114] but also suggested as a biomarker of Alzheimer's disease[150]. Understanding these interactions opens new avenues for exploring therapeutic strategies targeting the microbiota-neurotransmitter relationship.

### 2.3.3 Blood–brain barrier integrity

The BBB is a selective barrier separating circulating blood from the brain, except for the circumventricular organs[151]. The BBB has a significant neuroprotective role, preventing the translocation of toxins, pathogens, cells and large molecules from circulation, thus preserving brain homeostasis and functions. Consequently, the BBB also limits the passage of most gut-derived metabolites or neurotransmitters. It is formed by endothelial cells connected by tight junctions composed of transmembrane proteins like claudins and occludins, connected to cytoskeleton actin filaments via zonula occludens 1 and 2 proteins, along with adherent junctions sealing the vascular wall. However, supporting cells such as

astrocytes, pericytes and microglia also contribute to barrier maintenance and connect the BBB to surrounding neurons and vasculature. Semipermeability is enabled through selective transport mechanisms, including diffusion of small hydrophilic molecules such as ethanol, ion transporters, carrier-mediated transporters, and receptor-mediated or adsorptive transcytosis. Findings of altered barrier function and increased permeability in pathological conditions have highlighted the effect of gut microbiota and its metabolites on BBB function[152].

Although the BBB prevents translocation of most molecules, studies in GF mice have indicated that some microbial metabolites can pass the barrier, likely via transporters mentioned previously[18, 85]. Metabolite translocation is not limited to preclinical models as analysis of postmortem human brain samples has shown detectable levels of microbial products like TMAO, hippuric acid and 5-AVAB[153]. Secondary bile acids, such as taurolithocholic, ursodeoxycholic, and 3-dehydrochenodeoxycholic acids, have been measured in the brains of Alzheimer's disease patients in significantly higher proportions than in control samples[154]. However, it is unclear whether altered barrier integrity results from metabolites or the pathological condition. Nevertheless, serum levels of deoxycholic acid and its taurine or glycine conjugated forms are associated with cognitive impairment in Alzheimer's disease patients[81], and gradual increases in lithocholic acid over disease progression have been recorded[155]. Moreover, a distinct group of bacterial species drives the metabolism of these bile acids, but their significance in disease progression is yet to be established[156].

GF mice display signs of disrupted BBB compared to specific pathogen-free mice highlighting microbial interplay developing a functional BBB[157]. Dysfunction was evident in the embryonic state, emphasizing the significance of the prenatal environment and maternal microbiota. However, administration of butyrate or monocolonization with butyrate-producing bacterial species restored tight junction protein levels and barrier integrity to control levels. Increased expression of tight junction protein also partly restored BBB integrity after a single intraperitoneal injection of sodium butyrate in a mouse model of traumatic brain injury[158]. Propionic acid alone has been shown to improve BBB integrity by mitigating oxidative and pro-inflammatory pathways *in vitro*[159]. The beneficial effects of SCFAs reach the blood–cerebrospinal fluid barrier, as microbial colonization or administration improved barrier integrity in a mouse model of Alzheimer's disease[160]. In the same study, the beneficial effect was likely exerted by direct interaction between the barrier and butyrate/propionate, as vagotomy did not diminish the improvement, nor were the SCFAs detectable in the cerebrospinal fluid. Endothelial cells in the barrier express monocarboxylate transporters and free fatty acid receptors, which could be responsible for the observed effects without substantial translocation to the brain,

although similar receptors are expressed in neurons and astrocytes[39]. Within the brain, SCFAs may promote histone acetylation and participate in gene regulation. However, contrary to the preclinical *in vivo* and *in vitro* models, the uptake of SCFAs to the human brain is nominal.

Apart from SCFAs, other microbial metabolites are associated with BBB integrity. Secondary bile acids have varying effects on BBB permeability. Injection of deoxycholic acid in rats increased barrier permeability by disrupting the tight junction protein zonula occludens 1 and 2 and occludin[161]. In contrast, in an *in vitro* model of severe hyperbilirubinemia, ursodeoxycholic acid partially restored barrier integrity by protecting endothelial cells from apoptosis[162]. Trimethylamine (TMA) and its oxidized form, TMAO, have opposing effects on BBB integrity[163]. TMA impairs barrier integrity *in vitro* by degrading the actin cytoskeleton and inducing metabolic stress. Conversely, physiological levels of TMAO enhance BBB integrity both *in vitro* and *in vivo* by promoting anti-inflammatory pathways and protecting from lipopolysaccharide-induced stress. Another metabolite protecting BBB from lipopolysaccharide-induced damage is the host–gut co-metabolite *p*-cresol glucuronide[164]. Interestingly, the protective mechanism depends on the presence of lipopolysaccharide, as the *p*-cresol glucuronide acts as BBB TLR4 antagonist, inhibiting endotoxin binding and subsequent BBB degradation. IPA was recently shown to rescue the degradation of tight junction proteins and downregulate disruptive signaling pathways in an *in vitro* model of ischemic brain injury[165] Finally, indoxyl sulfate was shown to induce BBB disruption and cognitive impairment in a rat model of renal dysfunction, with barrier disruption mediated through aryl hydrocarbon receptor activation[166]. Together, these data indicate that microbial metabolites modulate BBB integrity through various mechanisms, but the evidence is still preliminary and largely from preclinical models.

### 2.3.4 Neuroinflammation

The pivotal role gut microbiota plays modulating the host's immune system, influencing both local and systemic immune responses, was demonstrated in GF mice[71, 77, 167, 168]. Bacteria and microbiota-associated molecular patterns educate the host’s immune system to maintain immune homeostasis, discriminating pathogenic bacteria from symbiotic bacteria. Microbial metabolites can also have pro- or anti-inflammatory effects that reach the CNS[168]. Within the CNS, the inflammatory responses initiate the production of reactive oxygen species, pro-inflammatory cytokines, and chemokines by the resident brain cells or migrating immune cells, leading to neurofinlammation[169, 170]. Neuroinflammatory cascades can be triggered by central infection or trauma, but systemic conditions such as metabolic disease or aging also induce neuroinflammation. Depending on the

magnitude and duration of neuroinflammation and the counteracting measures by microglia and macrophages, the outcome may support brain homeostasis or sustain neuropathological processes[171].

The dualistic properties of microbial metabolites on neuroinflammation are robustly portrayed by the SCFAs and tryptophan derivatives. From the perspective of immune homeostasis, SCFAs have fundamental properties, as SCFA administration can reinstate T cell maturation and balance and increase microglial function in the CNS, even in the absence of the microbiota[77, 172]. In a mouse model of cerebral hypoperfusion, SCFA administration or colonization with SCFA-producing bacterial species mitigated neuronal apoptosis and hippocampal neuroinflammation[25]. Conversely, propionic acid has been associated with detrimental effects on CNS neuroinflammation and behavioral abnormalities in ASD rat models[173-176]. Acetate alone promoted microglial maturation and mitochondrial function but limited phagocytic capacity, resulting in a net-negative effect on amyloid beta protein deposition, the assumed driver of Alzheimer's disease progression[177]. SCFAs increased both alpha-synuclein deposition in an *in vivo* model of Parkinson's disease and amyloid beta protein deposition in an *in vivo* model of Alzheimer's disease but these effects were not repeated *in vitro*[25, 56]. Additionally, the limited number of clinical trials with SCFA supplementation have not resolved the inconclusive preclinical results[178, 179].

Tryptophan-derived metabolites, especially products of the kynurenine pathway have both pro- and anti-inflammatory properties through the agonism of the aryl hydrocarbon receptor pathway[180, 181]. Indoxyl sulfate promoted neuroinflammation and cell death *in vitro* in astrocytes and glial cells and induced histological brain alterations *in vivo*[36]. In a rat model of chronic kidney disease, indoxyl sulfate supplementation impaired behavior and spatial memory performance[182]. However, indoxyl sulfate, along with indolepropionic acid and indole-3-aldehyde, also alleviated CNS inflammation *in vitro* and *in vivo* in a mouse model of multiple sclerosis[183, 184]. Suppression of proinflammatory gene expression was observed in human astrocytes after indoxyl sulfate treatment, along with reduced aryl hydrocarbon receptor-dependent activation[184]. Parkinson's disease patients display increased cerebrospinal fluid levels of indoxyl sulfate compared to controls, even in the absence of renal dysfunction[185]. Activation of aryl hydrocarbon receptor also drove the beneficial effects of urolithin A supplementation, a polyphenol metabolite, inhibiting neuroinflammatory processes and microglia activation in mouse models of multiple sclerosis and stroke[186-188]. Another polyphenol, quinic acid, alleviated neuroinflammation and amyloid beta protein deposition likely by increasing indole-3-acetic and kynurenic acids and inhibiting the nuclear factor-kappa B signaling pathway[189]. Anti-inflammatory effects of polyphenols may also be

mediated by the suppression of cytokine secretion, as dihydrocaffeic acid, a derivative of caffeic acid, decreased circulating interleukin-6 levels in a mouse model of stress-induced depression[190].

As demonstrated by SCFAs and tryptophan metabolites, the overall influence on neuroinflammation can differ depending on the disease state. Age can also play a role, as ingestion of the advanced glycation end product $N^6$-carboxymethyllysine induced microglial dysfunction only in aged mice, but not in young mice[191]. The effect was dependent on age-related microbiota composition, jeopardizing gut barrier integrity and increasing translocation of the metabolite to circulation and the brain. In the same study, TMAO was among the upregulated metabolites in aged mice's brain and circulation. Elsewhere, TMAO has been shown to aggravate post-operative cognitive dysfunction in aged rodents and promote hippocampal cytokine release in a Parkinson's disease model through neuroinflammatory mechanisms[192-195]. Both $N^6$-carboxymethyllysine and TMAO have been detected in the CNS of Alzheimer's or Parkinson's disease patients[185, 196, 197]. In elderly humans, an inverse correlation has been recorded between cognitive performance and TMAO[192] while $N^6$-carboxymethyllysine has been associated with oxidative stress[198]. Hence, the physiological state is an important mediator of the overall relationship between microbial metabolites and neuroinflammation.

### 2.3.5 Neuronal energy metabolism

Despite accounting for roughly 2 % of the total body mass, the brain consumes around 20 % of our resting energy expenditure[199]. Cognitive functions are energetically costly, primarily driven by neurons, the principal component of nervous tissue. To maintain synaptic excitability, glucose is primarily used as fuel, but lactate and ketone bodies can be utilized if glucose supply falls short. The properties of lactate and ketone bodies extend beyond maintaining energy balance. Astrocytes produce lactate through glycolysis, which is subsequently used by neurons. This astrocyte-neuron lactate shuttle is central to long-term memory formation and synaptic plasticity[200]. Lactate supply from astrocytes is also linked with the neural glutamine-glutamate cycle, affecting downstream glutamate and GABA, both associated with learning and memory[201, 202]. Lactate receptors are widely expressed throughout the cerebral neocortex, hippocampus and BBB, promoting neural activity independently, emphasizing its role beyond being mere energy source.

Ketogenic diet rich in fat and low in carbohydrates, has gained attention for symptom improvement in treatment-resistant epilepsy patients and protective effects in preclinical models of neurodegenerative disorders[203]. Administration of ketogenic meals or the ketone body β-hydroxybutyrate has been found to

promote cognitive performance and memory function in elderly individuals or patients with type 2 diabetes[204, 205]. Similar to lactate, β-hydroxybutyrate is involved in the glutamate and GABA pathways, as GABAergic neurons can use β-hydroxybutyrate as a substrate in neurotransmitter synthesis[206]. Moreover, alterations in GABA and β-hydroxybutyrate have also been recorded in subjects with heavy alcohol use. A gut microbiota-dependent depletion of β-hydroxybutyrate was observed in individuals with alcohol use disorder (AUD) along with changes in social and depressive behavior[207]. In line with the depletion of circulating β-hydroxybutyrate, GABA levels were reduced in the brains of deceased subjects with a history of chronic alcohol use[153].

Fasting increases the production of ketone bodies and could theoretically alter cognitive function. In diabetic mice, intermittent fasting enhanced cognitive function and improved mitochondrial gene expression in the hippocampus[208]. While depletion of microbiota abolished the observed effect of fasting, administration of IPA, tauroursodeoxycholic acid or SCFAs recapitulated the effect of fasting on hippocampal energy metabolism and cognition. IPA has been previously linked with improved mitochondrial respiratory rates and function in neuroblastoma cells or mice brain cell cultures[209, 210]. Although mitochondrial defects have been associated with ASD[211], the butyric acid-induced improvement in mitochondrial function *in vitro*[212] was not observed in an *in vivo* model of ASD where both butyric and propionic acid treatment interfered with brain mitochondrial fatty acid metabolism[213]. In contrast, in an *in vivo* model of aged mice, neither sodium acetate nor propionate halted microglial mitochondrial function, but $N^6$-carboxymethyllysine damaged mitochondrial structures, inducing microglial metabolic dysfunction[191]. Alterations in mitochondrial fatty acid oxidation rate are not unique to SCFAs, as other microbial-derived metabolites have similar properties. Carnitine mediates fatty acid oxidation, and carnitine analogues 3-methyl-4-(trimethylammonio)butanoate and 4-(trimethylammonio)pentanoate colocalize with carnitine in brain white matter, interfering with mitochondrial function[88]. An isomer of these compounds, 5-AVAB, also limited fatty acid oxidation by altering carnitine transportation into cells in mouse cardiomyocytes[214]. Together, findings of altered mitochondrial function in neurological or neurodegenerative disorders and the variety of metabolites with potential to regulate neuronal bioenergetics warrant continued research in brain energy metabolism and gut–brain axis.

### 2.3.6 Neuroprotection

Neuroprotective actions or measures preserve, recover or protect neuronal structures or homeostasis. Many compounds described in the previous chapters possess neuroprotective qualities, such as mitigating inflammation or oxidative

stress and promoting neuronal regeneration. Mapping neuroprotective compounds is crucial due to the wide variety of conditions characterized by neuronal damage, including aging, neurodegenerative disorders, and traumatic brain injuries all. In addition to previously mentioned metabolites, a significant group of neuroprotective compounds is phytochemicals[215]. Present in plant-based products and released from the plant matrix by digestion or activated by gut microbiota metabolism, many phytochemical metabolites have shown promise in preclinical models of neurodevelopmental disorders.

Phytochemical metabolites, including ellagitannins, isoflavones, flavonoids, and phenolic acids, have preliminary evidence of neuroprotective features. However, due to the chemical complexity of phytochemicals that are further amplified by microbial metabolism, neuroprotective potential is rather compound specific as exampled by BBB perfusion capability[216]. Examples of microbiota-produced phytochemical derivatives, 3-hydroxybenzoic acid and 3-(3′-hydroxyphenyl)propionic acid, were found to accumulate in mice brains after administration of grape seed extract or red wine and decrease amyloid β protein build-up *in vitro*[217]. Ergothioneine, a histidine-derivative, was able to cross the BBB and protected against amyloid β protein-induced cellular damage both *in vitro* and *in vivo*[218, 219]. Ferulic acid, a phenolic compound in plant fiber matrix, reduced pathological brain changes and improved memory in a model of cerebral amyloidosis[220]. Preliminary evidence also links other gut microbiota-related phytochemical metabolites like hesperitin, sulforaphane, and s-equol to neuroprotective benefits against neurodegenerative diseases[221].

Some previously mentioned metabolites, like tauroursodeoxycholic acid, IPA, and urolithin A, also have specific neuroprotective characteristics observed in *in vitro* and *in vivo* models of amyloid beta protein-associated illnesses. For instance, IPA alleviated cell apoptosis and oxidative stress in neuroblastoma cultures treated with amyloid β protein[222]. Tauroursodeoxycholic acid mitigated neuronal apoptosis and interfered with amyloid β protein build-up in preclinical models of Alzheimer's and Parkinson's disease[223, 224]. In a mouse model of cerebral ischemia, ferulic acid limited neuronal cell death and improved memory performance post-ischemia[37]. A downstream microbial product of ferulic acid showed antioxidative properties in an *in vitro* model of human neuroblastoma cells[38]. Besides its neuroprotective qualities against amyloid β deposits, ferulic acid has potential in mitigating depression and neuronal damage post-ischemia. In a mouse model of corticosterone-induced depression, ferulic acid alleviated depressive behavior and oxidative stress in the brain[225]. Urolithin A protected mice from aging-related cognitive decline and pathological changes in brain neuronal structure, likely mediated through nerve factor kappa B and mTOR signaling[226].

Despite the accumulating evidence of phytochemicals' neuroprotective characteristics, current research remains speculative. A healthy dietary regimen is associated with brain-related benefits, but such studies do not provide molecular-level resolution to isolate molecules driving the effects. However, administrating plant or fruit extracts typically yields cognitive improvements or mood benefits, but extracts are mixtures of different molecules rather than pure isolates227. Identifying potential compounds and revealing the microbiota-assisted molecular pathways behind the compounds' health-promoting effects is crucial to unfold the diet-microbiota-health crosstalk.

## 2.4 Lifestyle factors and the gut–brain axis

### 2.4.1 Lifestyle factors influencing the gut–brain axis

The preceding chapters detailed the complex communication network within the gut–brain axis and the role of microbiota-related metabolites. While genetics and both pre- and postnatal periods influence the establishment and development of the gut–brain axis, lifestyle factors are crucial for maintaining gut function and brain health later in life (**Figure 4**). Approaches to promote overall health through optimal lifestyle choices may rely on gut–brain axis-dependent signaling[33]. A balanced diet rich in fiber and fermented products promotes a diverse gut microbiota in terms of composition and function[228]. Conversely, an unhealthy diet promotes dysbiosis, increased gut barrier permeability, and systemic low-grade inflammation. Harmful factors such as smoking, substance use, or alcohol use induce inflammatory and neuronal damage[229]. Exercise, recognized for its metabolic benefits, also regulates mood and cognitive function and is advocated as a tool for stress management[230]. Thus, the net influence of lifestyle factors on the gut–brain axis and health should not be overlooked. The following paragraphs discuss the role of selected lifestyle factors in the context of gut–brain axis, with an emphasis on alcohol intake and inulin fiber.

Obesity is associated with systemic low-grade inflammation, characterized by chronically elevated levels of circulating pro-inflammatory cytokines[231]. This pro-inflammatory setting drives β-cell exhaustion and interferes with tissue insulin signaling, contributing to the development of type 2 diabetes and further accelerating inflammation. The main drivers of this low-grade inflammation are the number and function of adipose tissue macrophages in obesity. As adipose tissue expands, the number of macrophages in the adipose tissue increases, and their polarization shifts towards a pro-inflammatory state, increasing the production of TNF-α, IL-6 and IL-1β among other cytokines or chemokines. Similar macrophage accumulation and differentiation occur in the liver, promoting steatosis and steatohepatitis. Hypoxia, or insufficient oxygen supply,

triggers adipose tissue inflammation when vasculature formation does not keep up with the oxygen needs of expanding tissue. Obesity also alters gut microbiota composition and increases gut and brain barrier permeability, subjecting the intestinal and cerebral immune systems to increased influx of microbial metabolites and inflammatory molecules[232]. Reports of transferring depressive-like behavior and neuroinflammatory signatures through FMT to recipient mice in the absence of obesity suggests a major role of microbiota composition and function in developing obesity-associated neuroinflammation[233, 234]. These mechanisms may explain neuroinflammatory responses associated with obesity in preclinical models. Moreover, obesity-associated neuroinflammation has been linked to poorer performance cognitive test[235, 236]. While obesity predisposes to neuroinflammation, dietary factors contributing to obesity and inflammation should not be overlooked.

Several dietary patterns have been studied in the context of brain health and cognitive function[237]. Despite differences, whether it's the Mediterranean diet, the Dietary Approach to Stop Hypertension, the Mediterranean–DASH diet intervention for neurodegenerative delay, or the Inflammatory diet, these patterns share common core features. They emphasize consuming vegetables, fruits, whole grains, oils rich in unsaturated fatty acids, fish, lean meat, and low-fat dairy products while discouraging the use of red and processed meat, convenience foods, and foods high in saturated fat or cholesterol. Apart from the Mediterranean diet, which has shown significant effects on cognitive outcomes in clinical trials, evidence of positive effects between dietary patterns and cognitive outcomes primarily comes from observational studies. Rather than pinpointing a single biological pathway behind the neuroprotective effects, it is likely that neurological health benefits are conferred synergistically, including slowing neurodegenerative or neuroinflammatory processes, improving cerebral vascular or bioenergetic states, and modifying epigenetics or host–microbiota interactions.

As diet strongly modulates gut microbiota composition, and plant-rich diet provides ample feed for microbial metabolism, the gut–brain axis is acknowledged as a core regulator in observed diet-related benefits[238]. For example, microbial products of carbohydrate fermentation or bile acid metabolism, SCFAs and secondary bile acids, interact with local immune and nervous networks, inducing signaling cascades that regulate satiety and immunomodulatory responses. Polyunsaturated fatty acids have also been scrutinized for their ability to modulate microbiota composition, interlink with microbial metabolism, and influence cognitive function. Thus, targeting microbiota through selected dietary components is an intriguing option for adjunctive therapies in brain-related disorders.

Prebiotics or probiotics are increasingly used to improve mood or cognitive functions by targeting the gut microbiota. Prebiotics contain substrates selectively used by gut microorganisms, while probiotics contain live microorganisms, both conferring health benefits on the host[239]. Synbiotics combine prebiotics and probiotics synergistically, while postbiotics consist of non-living microorganisms or their components. Prebiotics or probiotics can be acquired from natural sources like fermented foods or vegetables, but dietary supplements containing isolates of single or a mixed prebiotic or probiotic components are usually used in studies. Species from the *Lactobacillus* and *Bifidobacterium* genera are most used in probiotics, and prebiotics stimulate the proliferation of these species due to their SCFA production capability[229]. Some evidence suggests that psychobiotics, like L. *plantarum* species, may confer benefits for the gut–brain axis, resulting in antidepressant and anxiolytic effects or improvements in cognitive and memory functions[29, 240]. Mechanisms hypothesized to mediate probiotics' brain health benefits include amelioration of local and systemic inflammation, neuroinflammation and immune modulation[229, 240].

Regarding prebiotics, the most studied fermentable carbohydrates with prebiotic effects are fructooligosaccharides, galactooligosaccharides and inulin-type fructans[241]. The properties of inulin, a widely used long-chain cross-linked fructooligosaccharide, will be discussed more in depth in a separate chapter. Compared to probiotics, the evidence for prebiotics is thinner as meta-analysis showed no support for antidepressant or anxiolytic effect[29]. In terms of cognitive function, results have been controversial, with some benefits observed in acute supplementation studies but not on a similar scale in studies continuing supplementation for several weeks[242]. Aging may also be a factor, as positive results on cognition have been recorded among elderly subjects[242, 243]. Nevertheless, with prebiotics' established effects on SCFA-producing species and indicative evidence on cognitive performance, prebiotics are a factor to consider when targeting the gut–brain axis.

The beneficial effects of exercise on overall health are well documented, and maintaining regular physical activity is recommended regardless of age or health status. Different types of exercise are important for preventing and treating neurodegenerative diseases or mental disorders[229, 244]. While different exercise modes, regimens, and intensities may have unique benefits, this discussion focuses on the overall influence of physical exercise. Findings on exercise's influence on gut microbiota composition have accelerated the discussion on whether microbiota and the gut–brain axis mediate some positive effects associated with exercise. Generally, the documented effects of exercise are driven by immunological, neuronal, epigenetic and metabolic mechanisms that extend from peripheral tissues to the brain. Physical activity is particularly

favorable for the aging brain, as demonstrated by the induction of neurotrophic regulation and improvement in cognitive function and brain volume selected areas in elderly subjects[230]. Clinical studies have also established microbial signatures concomitant with physical activity that promote functional alterations. Interestingly, the genera responding to exercise include species recognized for SCFA production, and the metabolic adaptation enriches the pathways associated with amino acids and carbohydrates metabolism. Hence, exercise can alter the gut microenvironment to support the proliferation of selected bacterial genera producing metabolites relevant for gut physiology and gut–brain communication. Moreover, the gut microenvironment is altered by reduced transit time, favoring symbiotic bacteria that protect against opportunistic pathogens. It is worth mentioning that some local effects of exercise can be unfavorable, but their long-term impacts are unknow. For instance, strenuous and prolonged exercise decreases the blood flow to the intestine, induces metabolic stress and increases gut permeability, predisposing to temporary gastrointestinal distress[244]. Nevertheless, clinical studies exploring the interplay between exercise and gut–brain axis remain scarce, but further mechanistic hypotheses based on preclinical models suggest roles for the local immune system, alteration of neurotransmission, and gut hormones in mediating the crosstalk.

Substance use disorders are among the most prominent mental health disorders, inflicting substantial mental and physiological disease burdens along with socioeconomic issues[245]. Widespread misuse of substances such as alcohol, stimulants, opioids, and cannabis is reflected in the constant increase in addiction problems, where current treatment options are characterized by a high risk of relapses. The neurobiological basis for addiction lies in the interplay of neurotransmitters and the brain's reward system as substances induce short-term dopamine release, resulting in feelings of pleasure and reward. However, long-term substance use poses serious risk of dysregulated neuronal circuits, influencing cognitive and emotional well-being or lethal overdosing[246]. Mounting preclinical evidence suggests that substance use is also associated with deteriorating intestinal permeability, proinflammatory responses, altered gut microbiota and behavioral abnormalities[245]. Considering that gut microbiota is involved in many of the same processes affected by substance use, harnessing the gut–brain axis in substance use disorder treatment is an appealing approach. Much of the research has focused on AUD, which will be discussed in more detail in the following chapter. However, stimulants and opioids also interact with the gut microbiota. For instance, cocaine increased intestinal norepinephrine levels, promoting colonization of ɣ-Proteobacteria, which enhanced addiction-like behavior through alterations in brain glutamatergic signaling[247]. Moreover, microbiota depletion by antibiotic treatment may increase drug-seeking behavior and sensitivity to cocaine reward sensation, likely linked to the reduced

availability of SCFAs[248, 249]. Similar effects have been demonstrated with opioid administration to mice[250]. Furthermore, FMT of methamphetamine-associated microbiota promotes anxiety- and depressive-like behavior in recipient mice, suggesting microbiota-dependent psychiatric symptomology[251].

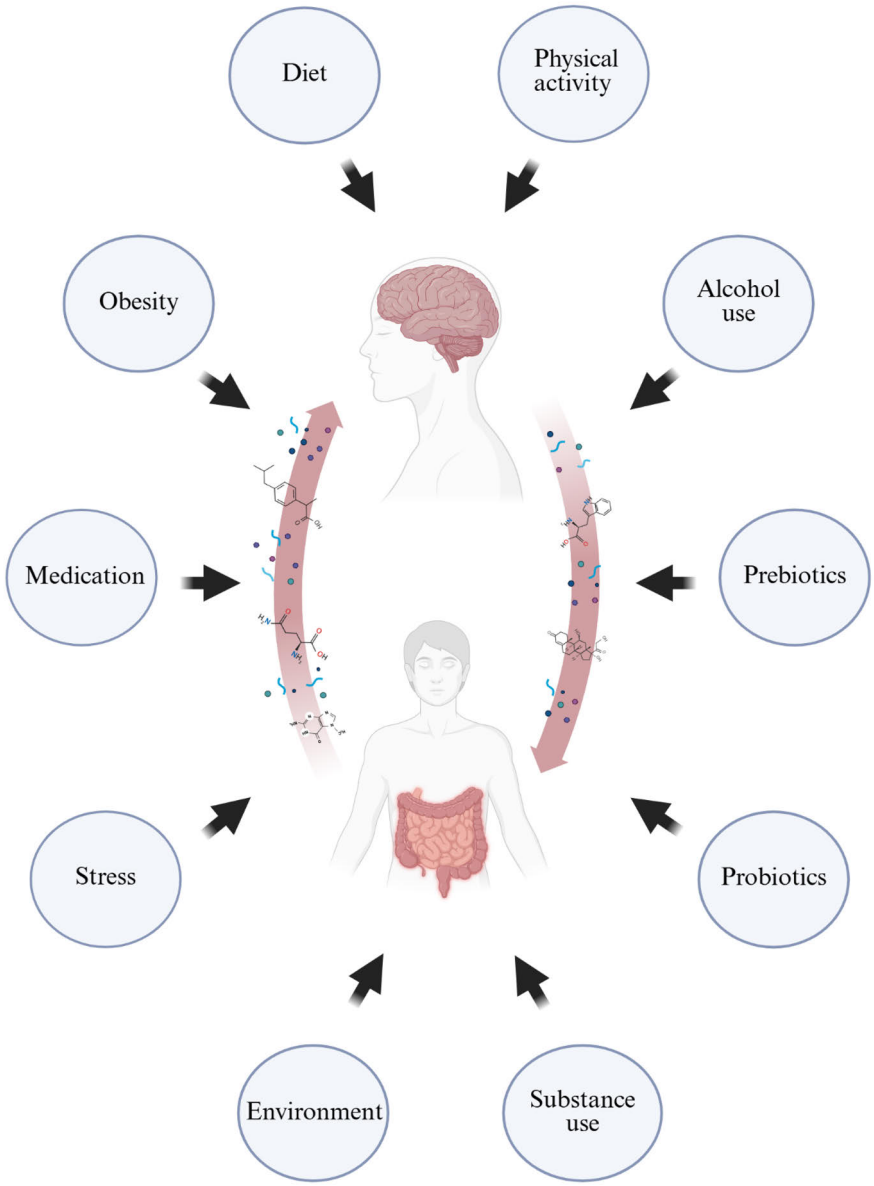


Figure 4. Lifestyle factors influencing the gut–brain axis. Wide range of factors can alter the homeostasis present in the gut–brain axis communication. While many induce changes in the gut microbiota that are reflected in the gut–brain communication, lifestyle factors can also alter physiological or psychological compartments predisposing to brain-related diseases. Figure created in Biorender.com.

### 2.4.2 Special focus on the effect of excessive alcohol use in the context of gut–brain axis

Alcoholic beverages have been an integral part of human dietary, social and economic landscapes for thousands of years. However, with the growing understanding of alcohol-related physiological, psychiatric and societal issues, health guidelines advocate to limit alcohol intake below 1–2 "drinks" per day, as there is no safe amount of alcohol consumption for health[252]. Generally, 1–2 "drinks" refers to ethanol amount of 16–28 grams per day, considered light to moderate alcohol intake[253]. Anything above this is considered as excessive alcohol use, where binge drinking (several drinks and intoxication at a single occasion) or AUD (drinking with one or more signs of addiction) stand out as major health risks. AUD can be assessed for its severity – mild, moderate or severe – depending on the number of criteria the individual's symptoms meet in an assessment by a medical professional. AUD is characterized by both physiological and psychological symptoms which, is why effective treatment tends to combine nutritional, medicinal and behavioral approaches in a personalized manner.

Upon ingestion, ethanol is rapidly distributed throughout the body as it passes freely through most biological membranes[254]. The liver is the primary site of ethanol metabolism due to its size, exposure to intestinal uptake through the portal vein, and high content of alcohol dehydrogenase, the primary enzyme for alcohol oxidation. Alcohol dehydrogenase produces toxic acetaldehyde, which is rapidly oxidized into acetate. Acetate becomes the primary energy source, limiting the use of long-chain fatty acids, amino acids and glucose in peripheral tissues. Ethanol oxidation occurs at a constant rate and can cover over 50 % of sedentary energy consumption if blood ethanol levels (i.e. alcohol intake) are kept constant. Hence, long-term excessive alcohol intake is usually accompanied by nutritional deficiencies. Consistent with these, alcohol use is reflected in alterations of systemic levels of amino acids, lipids, dietary- and microbiota-derived metabolites[255]. For instance, increases in lysophosphatidylcholines (LPC), phosphatidylcholine (PC) diacyls, long-chain fatty acids, steroids, lactate and alanine while decreases in levels of sphingomyelins, PC acyl-alkyls, citrate and glutamine are associated with alcohol use. Due to the robust shift in metabolism induced by excessive, long-term alcohol use, endogenous metabolites like phosphatidylethanolamines (PE) and fatty acid derivatives have been suggested as potential biomarkers for excessive alcohol use[253]. Sustained alcohol consumption and metabolism exhibit harmful effects, especially in the liver and the brain[254]. In the liver, inhibition of fatty acid oxidation and parallel activation of fatty acid synthesis causes steatosis, metabolic dysfunction, and stress reflected in the liver's detoxification rate. In the brain, alcohol

consumption impairs neuronal function through altered dopaminergic and glutamatergic signaling, mediating the neurobiology of addictive behavior and withdrawal symptoms, and leading to long-term neuronal injury.

Although dysbiosis is not uniformly associated with alcohol use, it is a potent modulator of gut microbiota composition and function, decreasing beneficial bacteria like *Lactobacillus* and increasing pro-inflammatory bacteria like *Proteobacteria*[256, 257]. Dysbiosis has also been associated with AUD symptoms like alcohol craving and anxiety, especially bacteria from the family *Ruminococcaceae*, suggesting a microbial modulator of individual susceptibility to excessive alcohol consumption or AUD. Moreover, alcohol-induced changes in microbiota composition can persist even after longer periods of abstinence. Ethanol is also a microbial metabolite, and recent reports have demonstrated that ethanol production by selected symbiotic bacteria can reach amounts sufficient to induce liver diseases or, in rare cases, intoxification[258]. Alongside dysbiosis, increased intestinal permeability has been suggested as a key characteristic of alcohol's detrimental effects mediated by the gut–brain axis. Binge drinking deteriorates barrier function, resulting in increased circulating levels of bacterial endotoxins and metabolites[257]. Higher intestinal permeability in persons with AUD was reversed following a three-week withdrawal period, indicating the acute harmful effect of alcohol but also the possibility to overturn some pathological changes with relatively short-term alcohol cessation[259]. In the same study, AUD symptomology correlated strongly with increased permeability and dysbiosis. As alcohol intake is promptly followed by a peripheral immune reaction resulting in the production of pro-inflammatory signaling molecules, and their continuous production in chronic alcohol use, altered intestinal permeability potentiates the passage of inflammatory mediators from the intestine to the systemic circulation[256]. Coupling these findings with preclinical evidence of transfer of AUD-related symptomology via FMT and amelioration of symptoms via probiotic supplementation further underlines the role of gut–brain axis in the development of alcohol use-related pathology.

### 2.4.3 Inulin metabolism – the host–microbiota crosstalk

Dietary fibers present in plant products are nutrients indigestible by the human gastrointestinal tract but fermentable by gut microbiota[241]. Due to their physicochemical and prebiotic properties, dietary fibers are acknowledged for their benefits against non-communicable diseases and are indispensable in healthy dietary patterns. Dietary fiber can be roughly divided into non-starch polysaccharides, resistant starches or resistant oligosaccharides, with the molecular compositions varying within these categories. Inulin is a fructan comprised of fructose monomers linked by glycosidic linkages, and the number

of monomeric units in the polymer affects its solubility and fermentability[260]. Inulin is a common storage carbohydrate in plants, with rich natural sources including Jerusalem artichoke, chicory, grains and onions. Besides natural sources, inulin is widely applied in food processing due to its safety and technological characteristics like gelation, foaming and thickening. As with other dietary fibers, the health benefits of inulin are linked to improvements in lipid metabolism, blood glucose levels, weight maintenance, gastrointestinal homeostasis, and modulation of gut microbiota composition and function[241].

Despite inulin's prebiotic qualities, clinical interventions have not demonstrated a significant effect on microbiota diversity or relative abundances following inulin supplementation[261]. However, like other accepted prebiotics, inulin stimulates the proliferation of several members of the genus *Bifidobacterium* and *Lactobacillus*. These genera include species known for their SCFA and lactic acid production, molecules that can modulate the intestinal environment and promote the growth of bacteria utilizing them as substrates. Hence, the lack of effect on microbiota diversity may result from the selective blooming of certain species at the expense of others. Significant increases in fecal butyrate have been observed after inulin supplementation but not in acetate or propionate[261]. Apart from butyrate, the effect of inulin on other metabolites has been limited or understudied. Preclinical models have demonstrated increases in fecal bile acids, dicarboxylic acids and indoles along with circulating indoles and phosphocholines[262, 263]. However, clinical trials lasting 4 to 6 weeks did not show inulin-dependent effects on fecal volatiles in healthy adults or circulating metabolites in adults with overweight[264, 265]. Extending supplementation to 12 weeks induced subtle alterations in fecal fatty acid metabolites but not in systemic or urinary metabolites[266, 267]. These findings suggest that if inulin metabolism alters metabolite levels and host metabolism, intestinal metabolism and gut-derived signaling are likely key mediators driving the benefits of inulin.

The metabolic benefits of inulin have been associated with maintaining normoglycemia, reducing body weight, and lowering blood cholesterol levels in individuals with obesity or related metabolic diseases[241]. However, the mechanisms behind such effects are not fully understood, but several plausible pathways intersect with the gut–brain axis, including production of anti-inflammatory mediators by the intestinal immune system, SCFA-mediated influence on satiety, vagal stimulation, energy metabolism or production of gut hormones, and improvement of gut barrier integrity. There are indications supporting these theories and promising results in the context of brain and behavior. In a preclinical model of chronic mild stress, inulin administration decreased anxiety and depressive behavior, along with a decrease in neuroinflammatory markers and increase in hippocampal markers of

neurogenesis[268]. Neurogenic properties of inulin have also been recorded in a mouse model of traumatic brain injury, along with increased cecal and serum levels of SCFAs[269]. Preliminary clinical evidence has also been presented. For instance, a 12-week intervention with snack bars containing inulin-type fructans significantly decreased desire to eat, increased satiety, and improved composite mental score in subjects with overweight or obesity[270]. Consistently, females with overweight showed decreased neural activation towards high-caloric food stimuli after 2 weeks of inulin supplementation[271]. Elsewhere, combined inulin and resistant maltodextrin supplementation during a weight loss diet increased the activity of gut microbial genes involved in the synthesis of neurotransmitter precursors and GABA and decreased levels of secondary bile acids in participants with overweight[272]. Additionally, in elderly twins, 12-week inulin+branched chain amino acid supplementation combined with resistance training improved cognition and memory test scores when compared to controls receiving only branched chain amino acid supplementation with resistance training[243]. Although the findings are preliminary and study populations small, the effects of inulin on the gut–brain axis warrants for further and larger-scale investigations.

# 3 AIMS OF THE STUDY

The primary aim of this study was to identify circulating microbiota-derived metabolites with neuroactive potential using a nontargeted LC-HRMS-based metabolomics approach on human biospecimens collected from five independent clinical trials. The research is structured into three studies, each with specific objectives:

**I.** Characterize the impact of severe AUD and a three-week alcohol withdrawal period on plasma metabolome, and identify circulating metabolites associated with alcohol craving, anxiety and depression scores in individuals with AUD.

**II.** Investigate the modulatory effect of inulin fiber supplementation during a three-week alcohol withdrawal on both plasma and fecal metabolomes and explore their associations with gut microbiota and clinical markers related to inflammation, liver function, sociability and neuroplasticity.

**III.** Examine the common associations between fecal and plasma metabolites across three different lifestyle interventions: (1) individuals with AUD undergoing inulin supplementation during a three-week alcohol withdrawal, (2) individuals with obesity receiving inulin supplementation for three months and (3) individuals with MASLD participating in a three-month high-intensity interval training program.

# 4 MATERIALS AND METHODS

## 4.1 Clinical samples

The studies utilized clinical samples of plasma, feces, frontal cortex and cerebrospinal fluid (CSF) obtained from participants in pre-existing trials as shown in **Figure 5**. Study **I** used samples from three distinct cohorts. Two cohorts (*AlcoholBis* and *Gut2Brain*) were clinical trials involving individuals with AUD in the area of Brussels, Belgium. The third cohort (*Tampere Sudden Death Series*) comprised of deceased individuals with a history of heavy alcohol use, with samples collected during forensic autopsies in the area of Pirkanmaa, Finland. Study **II** included samples from the *Gut2Brain* study comprising of individuals with AUD in the area of Brussels. Study **III** combined samples from three intervention trials involving patients with either AUD (*Gut2Brain*) or obesity (*Food4Gut*) in Brussels, and patients with MASLD (*BestTreat*) in the area of Kuopio, Finland. Details on the cohorts and sample sizes are provided in the following sections.

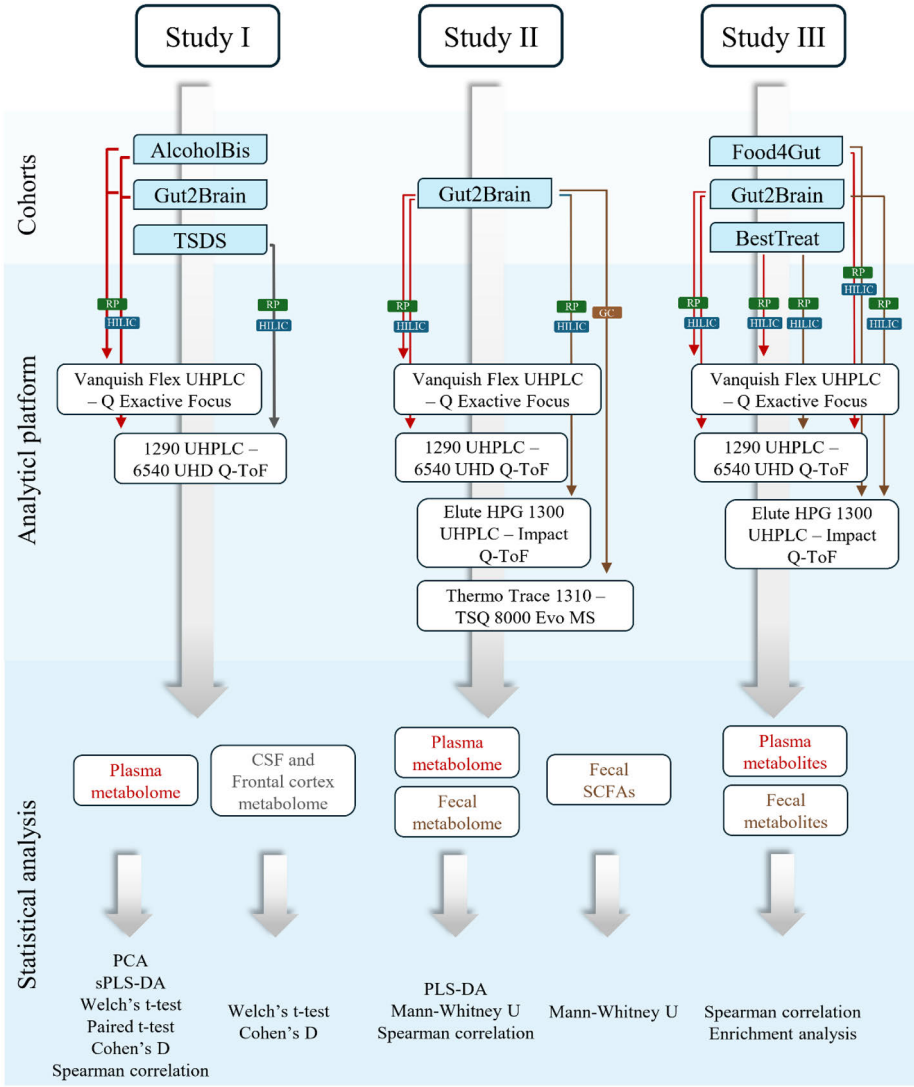


Figure 5. Flowchart of cohorts, analytical platforms, acquired datasets and applied statistical analysis in the studies included in this thesis. CSF, cerebrospinal fluid; MS, mass spectrometer; PCA, prinicpal component analysis; Q-ToF; quadrupole time-of-flight; SCFA, short-chain fatty acids; sPLS-DA, sparse partial least-squares discriminant analysis; UHPLC, ultra-high performance liquid chromatography.

### 4.1.1 Study I

In the study **I**, male and female patients with AUD were drawn from two different cohorts: *Alcoholbis*[273], with participants recruited in 2015 and 2019, and *Gut2Brain*[274], with recruitment in 2018–2019. Population characteristics are detailed in the original publications[273, 274]. In both cohorts, patients underwent a 3-week detoxification program at the alcohol withdrawal unit of Cliniques

Universitaires Saint-Luc, Brussels, Belgium. Together, the cohorts included 48 actively drinking patients. AUD severity was confirmed by a psychiatrist using the diagnostic criteria of the Diagnostic and Statistical Manual of Mental Disorders. *AlcoholBis* utilized the fourth version of the manual to diagnose 'alcohol dependence,' while *Gut2Brain* utilized the fifth version to diagnose 'severe AUD'. For consistency, the term 'AUD' is used throughout to refer to both diagnoses.

Exclusion criteria included chronic inflammatory disease, liver disease, cancer, metabolic disorder, diabetes or severe cognitive impairment or bariatric surgery. Participants were also excluded if they had used probiotics, prebiotics or antibiotics in the previous two months, or non-steroidal anti-inflammatory drugs or glucocorticoids in the past month. Blood samples and psychological data were collected on the day after admission (T1) and at end of the alcohol withdrawal (T2). Blood samples were stored at -80°C until analysis. However, since the *Gut2Brain* cohort included a placebo-controlled prebiotic fiber intervention, only T1 data from this cohort were used in the study. This resulted in group sizes of $n = 96$ for T1 and $n = 48$ for T2. Both cohorts also included age-, biological sex- and BMI-matched healthy controls without AUD, recruited from the same region, with a pooled total $n = 32$. The study was approved by the local ethics committee, registered at ClinicalTrial.gov (NCT03803709), and conducted in accordance with the Declaration of Helsinki.

To investigate whether circulating metabolites were also present in the CNS, Study **I** incorporated metabolomics data from the *Tampere Sudden Death Series* cohort conducted in the area of Pirkanmaa Hospital District, Finland[153]. Frontal cortex and CSF samples were collected during forensic autopsies from 700 deceased individuals and stored in -80°C until analysis. Autopsy reports and medical records were reviewed to identify individuals with a history of heavy alcohol use, alcohol-related disease, or elevated clinical markers of alcohol consumption. The alcohol group included of $n = 97$ individuals, while the control group comprised $n = 100$ individuals without signs of excessive alcohol use, whose primary cause of death was cardiovascular disease. Population characteristics for these groups have been published previously[153].

### 4.1.2 Study II

Study **II** was based on a randomized, double-blind, placebo-controlled trial investigating the effects of inulin supplementation during a 3-week alcohol withdrawal program in patients with AUD[274]. Participants were males and females aged 18–65, actively drinking, and diagnosed with AUD by a psychiatrist at Cliniques Universitaires Saint-Luc, Brussels, Belgium. Exclusion criteria included the presence of any addiction other than tobacco, chronic

inflammatory disease, liver disease, cancer, metabolic disease, bariatric surgery or severe cognitive impairment. Patients who had used probiotics, prebiotics or antibiotics in the previous two months, or non-steroidal anti-inflammatory drugs or glucocorticoids in the past month were also excluded. The *Gut2Brain* trial was registered at ClinicalTrials.gov (NCT03803709), approved by the local ethics committee and conducted in accordance with the declaration of Helsinki.

Study protocol consisted of two inpatients weeks (weeks 1 and 3) at the withdrawal clinic, separated by one outpatient week (week 2). Eligible participants were randomized in 1:1 ratio to receive either inulin or maltodextrin (placebo). A total of 50 patients were enrolled, with 21 in the placebo and 22 in the inulin group completing the study. Inulin and maltodextrin were provided in identical sachets in powder form. The dosage was gradually increased: 4 g (days 3–4), 8 g (days 5–14), and 16 g (days 15–19), which was the target dose. Fasting blood and fecal samples, along with psychological symptom data, were collected the day after admission (T1) and at the end of the intervention (T2). All samples were stored at -80°C until analysis.

### 4.1.3 Study III

Study **III** compared plasma and fecal metabolomics data from three separate clinical intervention trials. The first intervention was the *Gut2Brain* trial (see section 4.1.2). A subset of participants with complete nontargeted plasma and fecal metabolomics data at both T1 and T2 was included, resulting in $n = 19$ for the placebo and $n = 17$ for the inulin group. The second intervention, *Food4Gut*, was a multicenter, single-blind, placebo-controlled trial conducted in the area of Brussels, Belgium, between 2016 and 2018[275]. The trial was registered at ClinicalTrials.gov (NCT03852069) and approved by the local ethics committee. Eligible participants were obese Caucasian adults (18–65 years) with at least one obesity-related metabolic condition (e.g. dyslipidemia or (pre)diabetes). Exclusion criteria included restricted diet, use of probiotics, prebiotics or antibiotics (within 6 weeks), psychiatric issues, or alcohol consumption exceeding three portions per day.

Participants were randomized 1:1 to receive either inulin or maltodextrin (placebo) and their baseline characteristics have been previously published[275]. The intervention lasted three months, with inulin dosage increasing from 8 g/day (after the first week) to 16 g/day. The placebo group received an identical dose of maltodextrin. Additionally, the inulin group was advised to consume at least one meal per day containing fructan-rich vegetables, while the placebo group was advised to consume fructan-poor vegetables. Fasting blood and fecal samples were collected at the baseline (T1) and at the end of the trial (T2) and stored in -80°C. A subset of participants with complete nontargeted fecal and

plasma metabolomics data at both timepoints was included in study **III**: $n = 14$ for the placebo group and $n = 12$ for the inulin group.

The third intervention named *BestTreat*, was a 3-month randomized controlled exercise trial conducted in Kuopio, Finland between 2019 and 2020[276]. The trial was approved by the local ethics committee, registered at ClinicalTrials.gov (NCT03995056), and conducted in accordance with the declaration of Helsinki and. Eligible participants had imaging-confirmed MASLD, a BMI under 35 kg/m$^2$, and were aged 18–70. Exclusion criteria included inflammatory or infectious diseases, diabetes, conditions posing a risk during exercise, recent participation in diet or exercise programs (within 3 months), smoking, excessive alcohol use, or psychological illness. Participants were randomized and matched by BMI, age and biological sex into either exercise or control group. The exercise group underwent supervised high-intensity interval training on a cycle ergometer twice weekly, with intensity tailored to baseline ergospirometry results. They were also instructed to follow a home-based aerobic exercise program. The control group was asked to maintain their usual physical activity. A total of 43 participants completed trial ($n = 21$ in the exercise group, $n = 22$ in the control group) with all characteristics available in the original publication[276]. Fasting blood and fecal samples were collected at baseline (T1) and at week 12 (T2). Study **III** included a subset of participants with complete nontargeted fecal and plasma metabolomics at both timepoints: $n = 20$ in both the exercise and control groups.

## 4.2 Nontargeted metabolomics analysis

### 4.2.1 Plasma and CSF metabolite extraction

All plasma and CSF samples were prepared following the general guidelines with minor study-specific deviations, based on a previously published protocol[277]. Typically, randomized samples were kept on wet ice, and metabolite extraction was performed by adding 400 µL of cold acetonitrile to 100 µL of plasma or CSF. Mixing was done either by pipetting[273, 276] or vortexing[278]. For the *Food4Gut* plasma samples, an additional 5-minute sonication was included, which was not applied in the other studies[278]. Centrifugation and filtration were carried out using one of the two approaches: when using 96-well plates topped with 0.2 µm filter plates (Captiva ND, Agilent Technologies), centrifugation was performed at 700*g* for 5 minutes at 4 °C[273, 276] or when using sample tubes, centrifugation was done at 16,200*g* for 5 minutes at 4°C, followed by filtration of the supernatant through 0.45 µm PTFE syringe filters (Acrodisc, Pall Life Science) into HPLC vials using plastic syringes[153, 278]. Study-specific pooled quality control (QC) samples were created by combining aliquots from each

extract to form a representative sample. Extraction blanks, containing only acetonitrile, were processed identically to experimental samples. Solvent blanks, consisting solely of acetonitrile, were not subjected to any treatment.

### 4.2.2 Fecal and frontal cortex metabolite extraction

Fecal and frontal cortex metabolite extraction followed a previously published tissue metabolite extraction workflow, with minor deviations in the homogenization steps between studies[277]. In general, samples were weighed prior to treatment, and extraction was performed using ice-cold $H_2O$:MeOH solvent mixture. For the frontal cortex samples, 80 % MeOH was added at a ratio of 1,000 µL solvent per 100 mg of tissue. For fecal samples, the solvent ratio ranged from 500 to 900 µL per 100 mg of sample. In study **I**, frontal cortex tissue was homogenized using a Teflon-coated plastic stick, followed by 10 minutes of water sonication. Samples were then centrifuged at 16,200*g* for 5 minutes at 4°C and filtered through 0.45 µm PTFE syringe filters into HPLC vials[153]. In Studies **II** and **III**, *Gut2Brain* fecal samples were first diluted in 3:1 ratio (v/w) with ultra-pure $H_2O$ to create a fecal-water slurry. MeOH was then added in 3:1 (v/v) ratio to $H_2O$, followed by vortexing, centrifugation at 17,000*g* for 20 min at 4 °C, and filtration through 0.2 µm PTFE filter membranes into HPLC vials using plastic syringes[279]. In study **III**, *BestTreat* fecal samples were extracted using 500 µL of 80 % MeOH. Homogenization was performed with Bead Ruptor 24 Elite homogenizer at 6 m/s for 30 s at 0 °C. Samples were then centrifuged and filtrated at 700*g* for 5 minutes at 4 °C using 96-well plates topped with 0.2 µm filter plates (Captiva ND, Agilent Technologies)[276]. *Food4Gut* fecal samples were extracted with 500 µL of 80 % MeOH, vortexed for 5 minutes, centrifuged at 17,000*g* for 20 minutes at 4 °C, and filtered through 0.2 µm PTFE filter membrane into HPLC vials using plastic syringes[279].

### 4.2.3 LC-MS data acquisition

All nontargeted metabolomics data presented in this thesis were generated using an LC-HRMS platform comprising Q-TOFs (Agilent Technologies and Bruker Daltonik) or a Q Exactive Focus Orbitrap (Thermo Fischer Scientific). Key instrument specifications are summarized in **Table 1**, and the corresponding datasets are illustrated in **Figure 5**. All samples were analyzed using both RP and HILIC chromatographic separations, coupled with ESI ionization in both negative and positive ion modes. RP separation was performed using a Zorbax Eclipse RRHD XDB-C18 column (2.1 × 100 mm, 1.8 µm, Agilent Technologies). The mobile phases consisted of ultra-pure $H_2O$ (A) and MeOH (B) both containing 0.1 % (v/v) of formic acid. The gradient profile was as follows: 0–

10.0 min, 2 % B → 100 % B; 10.0–14.5, 100 % B; 14.51–16.5, 2 % B at the flow rate of 0.4 mL/min. HILIC separation used an Acquity UPLC BEH Amide column (2.1 × 100 mm, 1.7 μm, Waters Corporation). The mobile phases were 20 mM ammonium formate in the final volume of 50 % aqueous acetonitrile (A) and 20 mM ammonium formate in the final volume of 90 % aqueous acetonitrile (B). The gradient profile was as follows: 0–2.50 min, 100 % B; 2.50–10.0, 100 % B → 0 % B; 10.01–12.5, 100 % B at the flow rate of 0.6 mL/min.

Prior to analysis, all instruments were calibrated, and mass-axis recalibration was performed throughout the sequences to maintain high mass accuracy (< 2 ppm). Experimental samples were analyzed in randomized order. Each sequence began with blank injections followed by 10–20 QC injections to condition the analytical platform. QC samples were also injected after every 12 experimental samples to monitor instrument performance and support downstream data processing. MS/MS data were acquired from QC samples in a data-dependent manner, both before and after the experimental sample injections.

Table 1. Analytical platforms and parameters applied in data acquisition for studies included in this PhD work.

| Parameter | Agilent UHD 6540 Q-ToF | Bruker Impact II Q-ToF | Thermo Q Exactive Focus Orbitrap MS |
|---|---|---|---|
| LC unit | 1290 Infinity Binary UHPLC | Elute HPG 1300 UHPLC | Vanquish UHPLC+ Focus |
| Resolution | Up to 40,000 | Up to 50,000 | Up to 70,000 |
| Mass calibration | Continuous mass axis calibration by monitoring reference ions, mass accuracy < 2 ppm | Calibration data acquired at the beginning of each injection and mass axis recalibrated post-analysis, | Continuous mass axis calibration by monitoring reference ions, mass accuracy < 2 ppm |
| Source settings | Capillary voltage 3500V; nozzle voltage 1000V, skimmer 45V, fragmentor 100V,,sheath gas flow 11 L/min and T 350 °C, nebulizer pressure 45 psi, dry gas flow 10 L/min and T 325 °C | Capillary voltage 3500V; End plate offset 500V, nebulizer pressure 45 psi, dry gas flow 10 L/min, gas T 325 °C | Spray voltage 3500V (+), 2500V (-); Capillary T 300 °C; Sheath gas 40 AU (+), 50 AU (-); auxiliary gas 10 AU (+), 12.5 AU (-); auxiliary T 425 °C |
| Mass range | MS: 50–1600 *m/z*, MS/MS: 50–1600 *m/z* | MS: 50–1600 *m/z*, MS/MS: 50–1600 *m/z* | MS: 50–1200 *m/z*, MS/MS: 120–1200 *m/z* |
| Scan time | MS: 1.67 Hz; MS/MS: 3.31 Hz | MS: 1.67 Hz; MS/MS: 1.67 Hz | MS: max. ion time 200 millisecond, 1 microscan; MS/MS: max. ion time 100 millisecond, 1 microscan |
| Precursor selection (MS/MS) | DDA, threshold 200 amu, target 20,000 counts, 4 precursors selected, excluded after 2 spectra for 0.25 min | DDA, threshold 150 amu, 4 precursors selected, excluded after 2 spectra for 0.25 min | DDA, AGC target 8,000 amu, 5 precursors selected, exclusion for 10 s |
| CID energies | Separate runs for 10, 20 and 40 eV | Separate runs for 10, 20 and 40 eV | Normalized collision energies at 20, 30, and 40 eV |

Abbreviations: AU, arbitrary units; CID, collision-induced dissociation; DDA, data-dependent acquisition; LC, liquid chromatography; MS, mass spectrum; ppm, parts per million; UHPLC, ultra-high pressucre liquid chromatography.

### 4.2.4 Data preprocessing

Peak-picking and alignment were performed using MS-DIAL software, utilizing either raw instrumental files or the .abf files converted via the Reifycs Abf Converter (https://www.reifycs.com/abfconverter/)[280]. Detailed parameters for peak detection and alignment, including peak height, peak width scan, MS1 and MS2 tolerances, selected adducts and retention time windows, are provided in the original publications[153, 273, 276, 278, 279]. Each dataset, corresponding to a specific chromatographic and ionization mode, was processed independently. The resulting spectral peak areas (in arbitrary units) were exported in tabular format. Subsequent data processing was conducted in R software using the "notame" R package, following a published workflow[277]. Briefly, the molecular features were flagged for low detection based on their presence in both QC and experimental samples. All features were log-transformed, and a regularized cubic spline regression line was fitted to each feature against the QC samples to correct for signal drift. An interval between 0.5 and 1.5 using leave-one-out cross validation was applied for the smoothing parameter to prevent overfitting. After drift correction, log-transformation was reversed and features with RSD > 0.2 and D-ratio > 0.4 were flagged as low-quality. QC samples were removed, and missing values were imputed using random forest imputation first on the non-flagged features and then on all features. Finally, datasets from different analytical modes were merged into a single data matrix and exported in table format.

### 4.2.5 Metabolite identification

Molecular features were prioritized for manual inspection based on parameters such as peak area, signal-to-noise ratio, availability of MS/MS spectra, statistical significance, and their ability to differentiate between study groups. For compound identification, exact masses, retention times, MS/MS fragment ions, and their intensities were compared against entries in an in-house database of chemical standards. Features with confirmed matches were assigned identification level 1, in accordance with established reporting standards for chemical analysis[281]. Putative annotations (identification level 2) were made by matching feature characteristics to publicly available spectral databases, including Human Metabolome DataBase[94], METLIN[282], LipidMaps[283], and MassBank of North America (https://massbank.us/). For unknown compounds, cheminformatic tools MS-FINDER[284] and SIRIUS[285] were used to predict the molecular formulas and chemical classes. These tools compared experimental MS/MS spectra to *in silico*-generated spectra, and resulting annotations were assigned identification level 3. Spectral data, both raw and processed, were

explored using MS-DIAL and vendor software Data Analysis (Bruker Daltonik), MassHunter Qualitative Analysis (Agilent Technologies) and FreeStyle (Thermo Fischer Scientific).

## 4.3 Targeted fecal SCFA analysis

### 4.3.1 Sample treatment

In study **II**, fecal samples were thawed on wet ice and suspended in ultra-pure $H_2O$ at 1:3 ratio (w/v) by vortexing in batches of twenty. For each sample, 0.5 g of $NaH_2PO_4$ was mixed in ultra-pure $H_2O$ in a 10 mL vial. The prepared fecal-water mixture was then added to the vial to reach a total liquid volume of 1.5 mL. Vials were sealed and kept at + 4°C until analysis. Analytical blanks consisted of 0.5 g of $NaH_2PO_4$ mixed in 1.5 mL of $H_2O$, without fecal material. Standard samples were prepared using analytical-grade standards of acetic acid, propionic acid and butyric acid (Sigma Aldrich). Each standard sample was made by adding 25 µL from stock solutions of acetic acid (2,500 ppm), propionic acid (2,500 ppm), and butyric acid (500 ppm) to a vial containing 0.5 g of $NaH_2PO_4$ and 1.5 mL of $H_2O$.

### 4.3.2 Data acquisition

The analysis sequence began with injections of a blank, a standard mix and a second blank. This combination was injected after every 26 samples to monitor analyte retention time reproducibility and potential carryover. SCFAs were analyzed using an established solid-phase microextraction coupled to GC-MS analysis method[286]. The analytical platform consisted of an Thermo Trace 1310 – TSQ 7000 Evo system equipped with a Triplus RSH autosampler (Thermo Fischer Scientific) with samples maintained at + 4°C. SCFA extraction was performed using a 75 µm CAR/PDMS, Fused Silica solid-phase microextraction fiber (Supelco), conditioned according to the manufacturer's instructions. Prior to extraction, samples were incubated at + 40 °C for 10 minutes, followed by a 40-minute extraction at the same temperature. Volatile compounds were separated using a Supelco-fused silica capillary column SPB-624 (60 m × 0.25 mm × 1.4 µm) with helium as carrier gas at flow rate of 1.40 mL/min. The GC oven program lasted 48 minutes where the temperature profile was as follows: + 40 °C hold for 10 minutes, ramp 5 °C/min to + 200 °C and hold for 10 minutes. The MS was set at 240 °C, with an electron impact voltage of 70 eV and a scan range to 30–300 amu. The instrument was operated through the Chromeleon 7.2.10 software (Thermo Fischer Scientific).

### 4.3.3 Data processing

Semi-quantitative data were processed using Chromeleon 7.2.10 software (Thermo Fischer Scientific). Identification of acetic acid, propanoic acid and butyric acid was based on the comparisons of retention times and peak intensities with those of external standards. Other compounds were identified by matching spectral peaks and their intensities against entries in the NIST20 v. 2.3 library (National Institute of Standards and Technology). Spectral peak areas were manually integrated and exported in .csv format for subsequent statistical analysis.

## 4.4 Statistical analysis

In study **I**, both univariate and multivariate analysis were performed using R software used to identify differential metabolites between study groups. Principal component analysis and sparse Partial Least-Squares Discriminant Analysis (sPLS-DA) were conducted using the 'mixOmics' R package to explore differences in the plasma metabolome between AUD and Control groups. The classification performance of the sPLS-DA model was evaluated using 10-fold cross-validation repeated 50 times and features were ranked by their Variable Importance in Projection (VIP) scores. For plasma, CSF and frontal cortex features, a feature-wise Welch's *t*-test was used to compare AUD/Alcohol and Control groups, with Cohen's D calculated to assess effect sizes. To evaluate the impact of alcohol withdrawal, feature-wise paired *t*-test were conducted within the AUD group between timepoints T1 and T2. Associations between the annotated significantly different plasma metabolites and psychological test scores were assessed using Spearman's rank correlation. All *p*-values were adjusted for multiple testing using the Benjamini-Hochberg false discovery rate, and results were reported as *q*-value. Statistical significance was defined as *p*- and *q*-values below 0.05.

In study **II**, discriminant plasma and fecal metabolomic features between inulin and placebo groups at T2 were identified by PLS-DA, model performance was assessed by 10-fold cross-validation and features ranked by VIP scores. Features with VIP >1.5 were further analyzed using the nonparametric Mann-Whitney U test. Feature meeting both criteria (VIP > 1.5, $p < 0.05$) were subjected to Spearman rank correlation to evaluate associations with inulin-modulated markers of gut microbiota, sociability, inflammation and hepatic function as previously described[274, 287]. Differences in fecal levels of identified SCFAs at T2 between groups were also assessed using the nonparametric Mann-Whitney U test, with $p < 0.05$ considered statistically significant. Analyses were conducted using R software, GraphPad Prism and MetaboAnalyst 4.0[288].

In study **III**, the associations between annotated fecal and plasma metabolites were assessed using the cor.test function in R software to calculate Spearman's correlation coefficients ($r_s$) and corresponding *p*-values. Multiple testing correction was applied using false discovery rate (*q*). Metabolite set enrichment analysis was performed using Metaboanalyst 6.0 platform to identify enriched chemical classes among annotated metabolites in the *Gut2Brain* and *Food4Gut* inulin trials[288]. Statistical significance for both the correlation and enrichment analyses was defined as *p*-value and *q*-value < 0.05.

# 5 RESULTS AND DISCUSSION

## 5.1 Effect of excessive alcohol use on the plasma metabolic profile

In study **I**, the impact of chronic, excessive alcohol use on plasma metabolome was assessed by combining baseline (T1) plasma samples from individuals with AUD and Controls across *AlcoholBis* and *Gut2Brain* cohorts to maximize sample size. Baseline characteristics of the AUD participants are summarized in **Table 2**. No significant differences were observed between the cohorts for the AUD groups in terms of mean age, biological sex distribution, smoking status, daily alcohol consumption, years of active drinking or psychological symptom scores for obsession, depression and anxiety. Although the *Gut2Brain* cohort showed higher scores of alcohol craving and the compulsion subscore, participants in the *AlcoholBis* cohort also exhibited elevated scores in these domains, indicating comparable symptom profiles. These baseline similarities justified pooling the AUD samples from both cohorts into a single group.

Table 2. Baseline characteristics of the AlcoholBis and Gut2Brain AUD groups. Data shown as mean ± standard deviation. Table modified from Leclercq, Ahmed, et al. (2024)[273].

| | AlcoholBis | Gut2Brain | Total | *p*[a] |
|---|---|---|---|---|
| n | 48 | 48 | 96 | |
| Age | 46 ± 10 | 48 ± 9 | 47 ± 10 | 0.24 |
| Biological sex | | | | 0.39 |
| Men (%) | 34 (71) | 34 (62.5) | 64 (67) | |
| Women (%) | 14 (29) | 18 (37.5) | 32 (33) | |
| Active smokers (%) | 37 (77) | 38 (79) | 37.5 (78) | 0.83 |
| Alcohol consumption g/day | 151 ± 112 | 139 ± 73 | 145 ± 94 | 0.54 |
| Years of drinking habit | 17 ± 10 | 16 ± 11 | 16 ± 11 | 0.76 |
| Alcohol craving score[b] | 20 ± 7 | 25 ± 6 | 22 ± 7 | < 0.01 |
| Obsession score[b] | 9 ± 5 | 11 ± 4 | 10 ± 4 | 0.26 |
| Compulsion score[b] | 11 ± 3 | 14 ± 3 | 13 ± 3 | 0.00 |
| Depression score[c] | 23 ± 11 | 26 ± 12 | 25 ± 12 | 0.26 |
| Anxiety score[d] | 44 ± 11 | 46 ± 15 | 45 ± 13 | 0.27 |

[a]Statistical difference between AlcoholBis and Gut2Brain AUD groups. Numerical variables compared using independent sample *t*-test and categorical variables using chi-square test.
[b]Scoring based on self-reported questionnaire using the Obsessive-Compulsive Drinking Scale (OCDS). Alcohol craving score calculated as the sum of Obsession and Compulsion sub-scores.
[c]Scoring based on self-reported questionnaire using the validated French translation of the 2nd version of the Beck Depression Inventory (BDI-II).
[d]Scoring based on self-reported questionnaire using the State-Trait Anxiety Inventory (STAI).

Principal component analysis of the plasma metabolic profiles revealed no clear separation between the AUD T1 group and Control when considering all detected molecular features (**Figure 6**). Component 1 and Component 2 accounted for 6 % and 5 % of the total variance, respectively. While the Control group tended to cluster more on toward the positive ends of both components, suggesting some group-specific patterns, distinct group separation was not observed. This outcome is not unexpected, given that the dataset included 11,651 molecular features, many of which likely represent background noise, redundant signal, and artifacts sample preparation, solvents, or in-source fragmentation, in addition to true biological features. As anticipated, the pooled QC samples clustered tightly at the center of plot, reflecting their role as representative 'mean' samples and indicating high data quality[289].

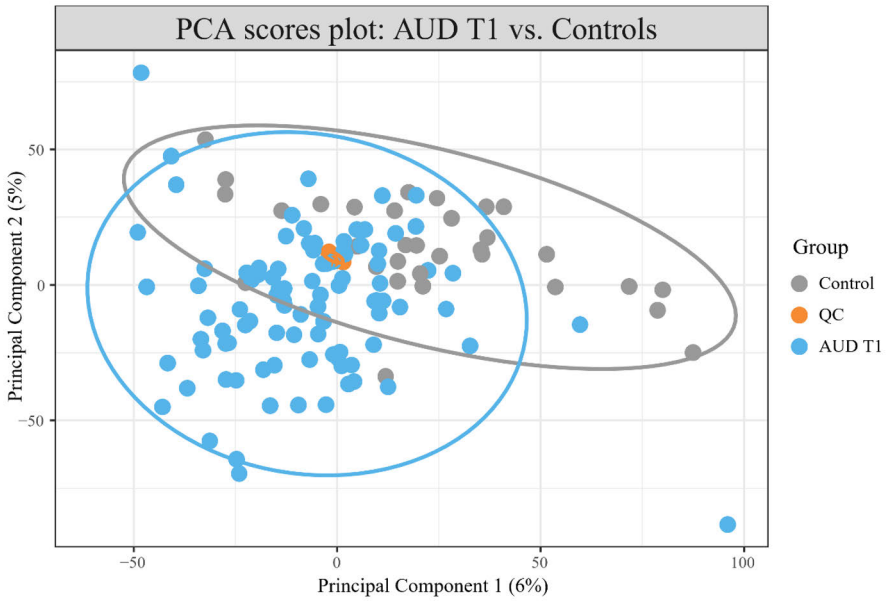


Figure 6. Principal component analysis score plot of the plasma molecular features between controls (grey) and individuals with AUD at T1 (blue). Ellipses indicate the 95 % confidence lever around sample groups. AUD, alcohol use disorder; QC, quality control. Figure reprinted from Leclercq, Ahmed, et al. (2024)[273].

Univariate analysis comparing the AUD group at T1 to Control identified 1,798 significantly altered plasma molecular features ($q < 0.05$). These features, shown in **Figure 7a**, were visualized after annotation and the removal of redundant signals and features lacking MS/MS spectra. Complementing these findings, sPLS-DA analysis confirmed the discriminatory power (overall classification accuracy of 0.91, balanced error rate of 0.09 and area under ROC curve of 1.0 for the two component sPLS-DA model based on 10-fold cross-

validation) of the annotated features, with the majority receiving VIP scores greater than 2.0 (**Figure 7b**).

Overall, the AUD metabolome differed markedly from that of Control, particularly in lipid-related metabolites. Notable alterations were observed in fatty acyls, phosphocholines, steroid hormones, bile acids, pharmaceuticals and xanthine derivatives. Specifically, circulating levels of monounsaturated fatty acids with 16- or 18-carbon chains and polyunsaturated with 20- or 22-carbon chains were elevated in the AUD group. These fatty acids were commonly incorporated into PCs, LPCs, and lysophosphatidylethanolamines (LPE). The pronounced impact of AUD on lipid species is consistent with previous studies, which have repeatedly reported changes in lipid metabolites, particularly those containing monounsaturated and polysaturated fatty acids, in alcohol-related metabolic profiling studies[255]. Alcohol consumption rapidly disrupts hepatic lipid metabolism, leading to significant shifts in circulating PCs, LPCs, sphingomyelins and phospatidylethanolamines[290].

Palmitic acid (16:0) which constitutes roughly one-quarter of the saturated fatty acids in the phospholipids and triglycerides, is tightly regulated through homeostatic control and *de novo* lipogenesis[291]. Its overrepresentation, along with palmitoleic acid (16:1), in the AUD metabolome is expected as excessive alcohol intake stimulated *de novo* lipogenesis. This results in increased palmitic acid production, which is subsequently desaturated to palmitoleic acid or elongated into longer-chain fatty acid. These synthesized fatty acids are incorporated into various lipid classes, including LPCs, PCs and sphingolipids, many of which have been suggested as biomarkers of chronic alcohol intake[292-294]. Such metabolic alterations reflect a range of biological pathways disrupted by alcohol, including dysregulation of lipid synthesis and oxidation, fatty acid deposition, and immune regulation.

The AUD group also exhibited elevated levels of both primary and secondary bile acids, particularly glycine-conjugated forms, as well as increased levels of the steroid hormone cortisol and various sulfated steroid metabolites. These findings are consistent with the interconnected nature of bile acid and steroid biosynthesis, both of which derive from cholesterol. Alcohol consumption is known to stimulate cholesterol production and upregulate enzymes involved in the downstream metabolic pathways[295, 296]. Moreover, alcohol disrupts enterohepatic circulation by modulating nuclear receptors such as the farnesoid X receptor and peroxisome proliferator-activated receptor alpha, while also altering gut microbiota composition. These combined effects accelerate bile acid synthesis[297]. The increased presence of benzodiazepines and antidepressants in the AUD group reflects the high prevalence of psychiatric comorbidities and their pharmacological treatment as well as medications used during withdrawal treatment. Similarly, elevated levels of cotinine, a nicotine metabolite, indicate

the high rate of active smoking within this population. The detection of 4-pyridoxic acid, a metabolite of vitamin $B_6$, corresponds to B-vitamin supplementation administered upon withdrawal.

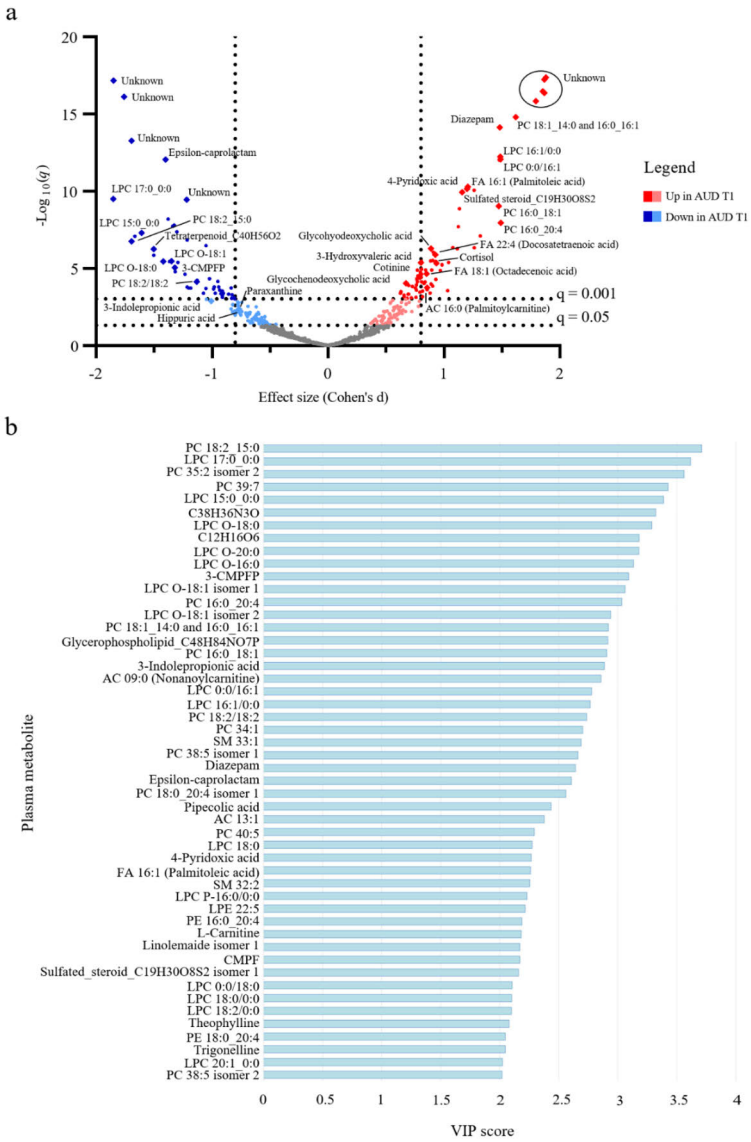


Figure 7. Plasma metabolic features altered by chronic alcohol intake. A) Volcano plot of the effect sizes (Cohen's d) of the differential plasma metabolic features derived from Welch's *t*-test analysis between AUD group at baseline and control group. Colored dots represent features with $q < 0.05$. B) Variable importance in projections (VIP) scores of the top 50 annotated metabolites discriminating AUD T1 from control group in an sPLS-DA model. 3-CMPFP, 3-carboxy-4-methyl-5-pentyl-2-furanpropionic acid; AC, acylcarnitine; FA, fatty acid; LPC, lysophosphatidylcholine; PC, phosphatidylcholine; PE, phosphatidylethanolamine; SM, sphingomyelin. Figure modified from Leclercq, Ahmed, et al. (2024)[273].

Although many fatty acids and their lipid intermediates were elevated in the AUD group, certain lipid subclasses showed the opposite trend. Notably, (L)PCs containing polyunsaturated 18-carbon chains or ether-bonds, as well as odd-chain LPCs (15:0 and 17:0) were consistently decreased. These patterns suggest alcohol-induced upregulation of 16- and 18-carbon fatty acid biosynthesis, alongside a downregulation of ether lipid production. This lipid profile shift was accompanied by reduced levels of several microbiota-associated metabolites, includings IPA, hippuric acid and *p*-cresol sulfate. Given the proposed link between gut microbiota and the synthesis of odd-chain LPCs, alcohol-induced dysbiosis could explain these reductions[259]. Fatty acids 15:0 and 17:0 have also been associated with dairy product intake, suggesting that dietary factors may contribute to the observed changes[292]. Several of the decreased metabolites, such as 3-carboxy-4-methyl-5-propyl-2-furanpropionic acid (CMPF), LPC 15:0, paraxanthine and trigonelline, have been linked to the consumption of fish, milk, or coffee[298, 299]. However, CMPF has also been correlated with total alcohol intake[299]. Importantly, individuals with AUD often have poor dietary habits, with alcohol contributing a substantial proportion of daily caloric intake, potentially leading to nutritional deficiencies.

To assess the impact of abstinence, a subset of AUD participants underwent a 3-week withdrawal period. This intervention confirmed that most of the observed metabolic alterations were attributable to chronic alcohol use in study **I**. Metabolites significantly altered in the AUD group ($q < 0.05$, VIP > 2.0) showed marked shifts, often in the opposite direction of those observed at baseline (**Figure 8**). For example, circulating levels of LPCs and PCs with odd-chain fatty acid (15:0 and 17:0), ether-linked LPCs, xanthine metabolites and indole derivatives such as IPA increased, as shown in **Figure 8a**. Conversely, abstinence led to decreased levels of heme metabolites bilirubin and biliverdin, saturated or monounsaturated LPCs and PCs (16- or 18-carbon chains), sulfated steroids, 3-hydroxyvaleric acid and retinol. In line with the findings, these metabolites have been associated with alcohol consumption[292, 299, 300]. These findings suggest that alcohol's disruptive effects on lipid metabolism are, at least in part, reversible. The reduction in heme metabolites, retinol and steroid-related compounds further indicates that metabolic pathways entwined with alcohol metabolism are downregulated in the absence of alcohol[296, 297].

Additionally, increased consumption of coffee, tea and chocolate during withdrawal, was reflected in elevated levels of caffeine metabolites such as theophylline, theobromine and paraxanthine. The rise in microbiota-associated tryptophan metabolites, especially IPA and 3-indolelactic acid, suggests enhanced microbial activity and improved nutritional status[145, 301]. Overall, **Figure 8b** illustrates a rebound-like effect, with many of the metabolic alterations distinguishing AUD T1 from Control shifting in the opposite direction following abstinence.

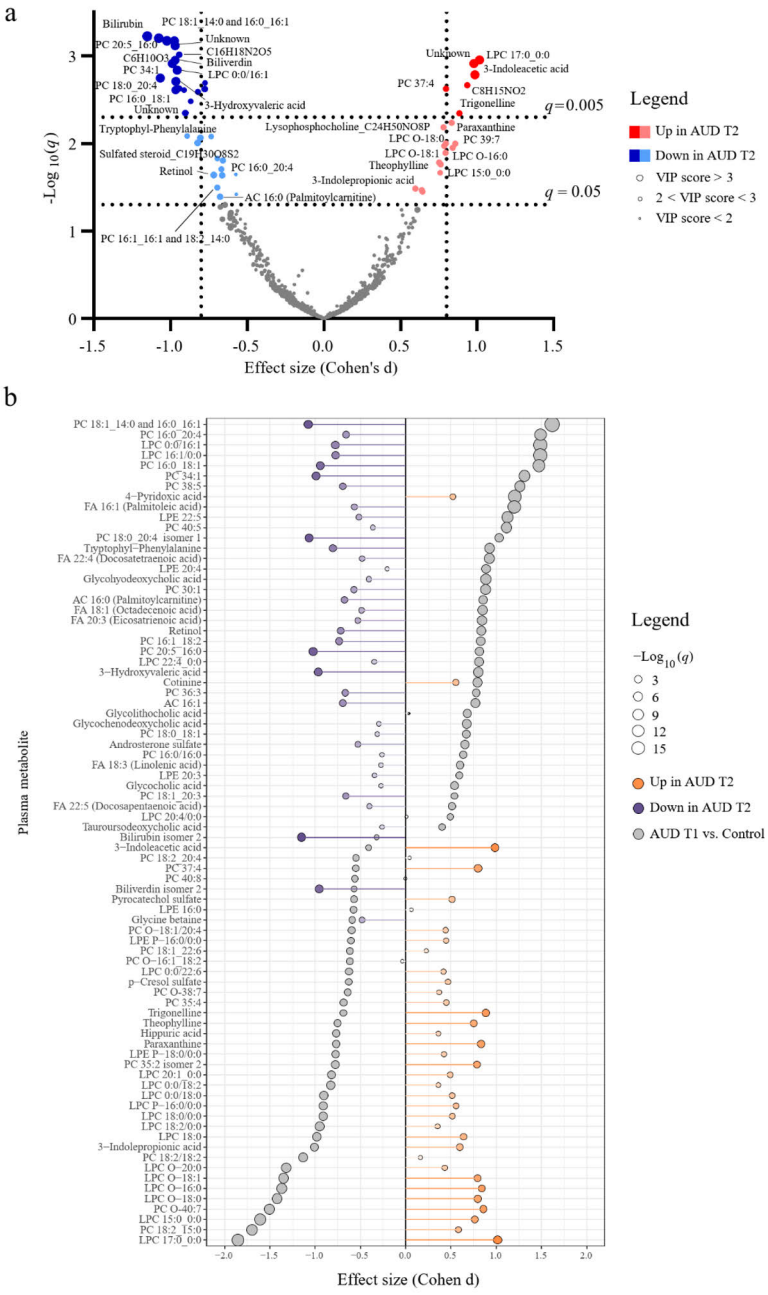


Figure 8. Effect of a 3-week alcohol withdrawal on the plasma metabolome. A) Volcano plot of the effect sizes (Cohen's d) of the differential plasma metabolic features derived from paired *t*-test analysis between AUD group at baseline and after alcohol withdrawal. Colored dots represent features with $q < 0.05$ and their size the variable importance in projections scores. B) Lollipop plot of the effect sizes (Cohen's D) of selected significantly ($q < 0.05$) altered annotated metabolites influenced by alcohol intake and alcohol withdrawal. Circle size reflects the -Log10 transformed $q$ values derived from

Welch's *t*-test comparing AUD T1 and control group or paired *t*-test comparing AUD T1 and AUD T2 groups. Grey dots indicate the results of comparison between AUD T1 and control while orange color shows the relative increase and violet color the relative decrease after withdrawal (T2). 3-CMPFP, 3-carboxy-4-methyl-5-pentyl-2-furanpropionic acid; AC, acylcarnitine; FA, fatty acid; LPC, lysophosphatidylcholine; PC, phosphatidylcholine; PE, phosphatidylethanolamine; SM, sphingomyelin. Figure reprinted from Leclercq, Ahmed, et al. (2024)[273].

## 5.2 Identification of potentially neuroactive plasma metabolites

Patients with AUD frequently exhibit one or more psychological symptoms such as anxiety or obsessive behavior[256]. To identify metabolites with potential neuroactive properties in AUD, study **I** assessed correlations between significantly altered metabolites at T1 and psychological symptom scores, as well as alcohol (**Figure 9).** Consistent with alcohol-induced metabolic changes, alcohol intake showed nominally significant, moderate positive correlations with several compound classes including pharmaceuticals, steroid-like metabolites, phosphocholines containing 16:1 or 18:1 fatty acid chains, 3-hydroxyvaleric acid, 4-hydroxyisoleucine, threonine, glycine betaine and an unknown phenylsulfate. These findings align with previous reports of elevated steroids, lipids, and amino acids in association with excessive alcohol consumption[255, 292, 293,294]. Conversely, metabolites negatively correlated with alcohol intake included xanthine derivatives, microbiota-associated metabolites, LPCs with odd-chain (15:0 or 17:0) or ether-linked fatty acids, PCs with polyunsaturated fatty acids, sphingomyelins and 3-carboxy-4-methyl-5-propyl-2-furanpropionic acid.

Correlation analysis also revealed that alcohol craving and its subscores, obsession and compulsion, were positively correlated with lysophosphatidylethanolamines (LPE), LPCs, benzodiazepines, 16- and 18-carbon fatty acids, steroids and glycine-conjugated bile acids (**Figure 9**). Additionally, individual metabolites such as 3-indoleacetic acid, epsilon-caprolactam, and 3-hydroxyvaleric acid were directly linked to alcohol craving and at least one of its subscores. In contrast, several metabolites were inversely correlated with craving and its components. These included xanthine metabolites, a pentose sugar (mannose/fructose), hippuric acid, pyrocatechol, 4-ethylphenylsulfate, and 1-methyl-pyridone-carboxamide.

There is a notable lack of research exploring the relationship between peripheral metabolic products and the pathophysiology of obsessive or compulsive traits, particularly in the context of alcohol craving. To date, only limited preliminary evidence from human studies has linked plasma amino acids[302], albeit weakly, as well as eicosanoids and palmitoylethanolamide[303], with alcohol craving in individuals with AUD. Other studies have focused on

neurotransmitter-related amino acids, such as glutamate and glutamine, due to their involvement in reward process and dopaminergic signaling, which are central to addictive behavior[304]. More recently, few metabolomics studies have investigated circulating metabolites in individuals with obsessive-compulsive disorder, identifying alterations in (L)PCs, LPEs, saturated and unsaturated fatty acids, and acylcarnitines as characteristic of the disorder[305, 306]. In the current study, circulating amino acids did not emerge as significantly altered; however, several lipid species were correlated with the craving component of psychological symptoms. These findings, along with prior research suggest that lipid metabolism may play a role in the neurobiology of craving, potentially through mechanism involving altered neurotransmitter signaling[307, 308], and the activation of inflammatory pathways[309, 310].

Many of the metabolites significantly correlated with alcohol intake and craving also showed similar patterns in relation to anxiety or depression scores (**Figure 9**). For example, acylcarnitine 09:0, 1-methyl-pyridone-carboxamide, hippuric acid, pyrocatechol sulfate, and xanthine metabolites were negatively correlated with both anxiety and depression. Additional metabolites inversely associated with anxiety included urea, LPC O-18:0, an unknown LPC, an unknown fatty acid and kynurenine. In contrast, creatinine, acylcarnitines 05:0 and 10:3, 4-ethylphenylsulfate, and a pentose sugar were inversely correlated with depression score. On the other hand, glycin-conjugated bile acids, antidepressants, fatty acids 16:0 and 16:1 and (L)PCs containing these fatty acid chains were consistently positively correlated with anxiety and/or depression scores.

Microbiota-associated metabolites such as hippuric acid, pyrocatechol sulfate and kynurenine were all decreased in the AUD group and showed negative correlations with anxiety score. Additionally, hippuric acid and 4-ethylphenylsulfate were inversely associated with depression score. Kynurenine is the first downstream product of microbiota-influenced tryptophan metabolism via the indoleamine-2,3-dioxygenase and tryptophan-2,3-dioxygenase pathways, which generate both neuroprotective and neurotoxic metabolites[181]. Kynurenine has been implicated in the pathophysiology of cognitive function in clinically diagnosed depression[83, 149] while favoring serotonin production over kynurenine pathway activation has been shown to alleviate anxiety[27]. Thus, the current finding appears to contradict previous reports. However, it may reflect alternative mechanisms, such as anti-inflammatory effects mediated by the aryl hydrocarbon receptor[184, 311], downregulation of neuroprotective kynurenic acid[312], or reduced tryptophan intake leading to suppressed tryptophan metabolism[144]. Pyrocatechol sulfate, a phenolic compound, has been linked to synapse formation and fear extinction learning in mice[108], and is also found at reduced levels in individuals with Parkinson's disease[313]. Interestingly, 4-

ethylphenylsulfate, a microbial metabolite, has been shown to induce anxiety-like behavior and neurodevelopmental alterations in animal models[19, 86]. Hippuric acid is a liver-conjugated product of benzoate, which is generated by gut microbial metabolism of dietary polyphenols in the colon[314]. Recent studies suggest that low levels of hippuric acid may contribute causally to depression[315], consistent with reduced intake of polyphenol-rich food among individuals with depression. Moreover, while decreased hippuric levels have been associated with alcohol use, they are also observed in individuals with depression independently of alcohol consumption[316].

The consistent inverse correlation between xanthine metabolites and psychological symptom scores warrant attention. These metabolites, biomarkers of caffeine intake[298, 300], are produced via the cytochrome-P450-dependent metabolism in the liver. Theobromine has been shown to improve mood[317], while paraxanthine can stimulate dopamine release and act as a psychostimulant[318]. Moreover, dietary sources of caffeine such as coffee, tea and cocoa have been associated with mood-enhancing and depression-alleviating effects[319]. Although still debated, these benefits are often attributed to the rich polyphenol content of these beverages and the neuromodulatory properties caffeine.

In contrast, metabolites positively associated with anxiety and/or depression scores were characterized by bile acids or saturated or monounsaturated fatty acids with 16-carbon chain, including LPC 16:0 which induces a pro-inflammatory signaling by increasing reactive oxygen species and chemokine secretion[320] Bile acids have been reported to exert both beneficial[162] and detrimental[161] effects on the BBB. In the context of neurodevelopmental disorders, several studies have found elevated brain bile acid levels associated with impaired cognition[81, 154, 155].

In pathological conditions such as obesity or AUD, the dysregulated *de novo* lipogenesis leads to excess palmitic acid production, which promotes the release of pro-inflammatory mediators and cellular stress[291]. Accumulation of fatty acids, particularly palmitic acid, has been shown to negatively affect brain cells and may increase susceptibility to neurological disorders[321]. In contrast, palmitoleic acid has demonstrated protective effects against palmitic acid-induced lipotoxicity[322]. Thus, the observed positive correlations may reflect the

detrimental impact of the dysregulated lipid metabolism on systemic inflammation, a process increasingly linked to psychological symptoms[323].

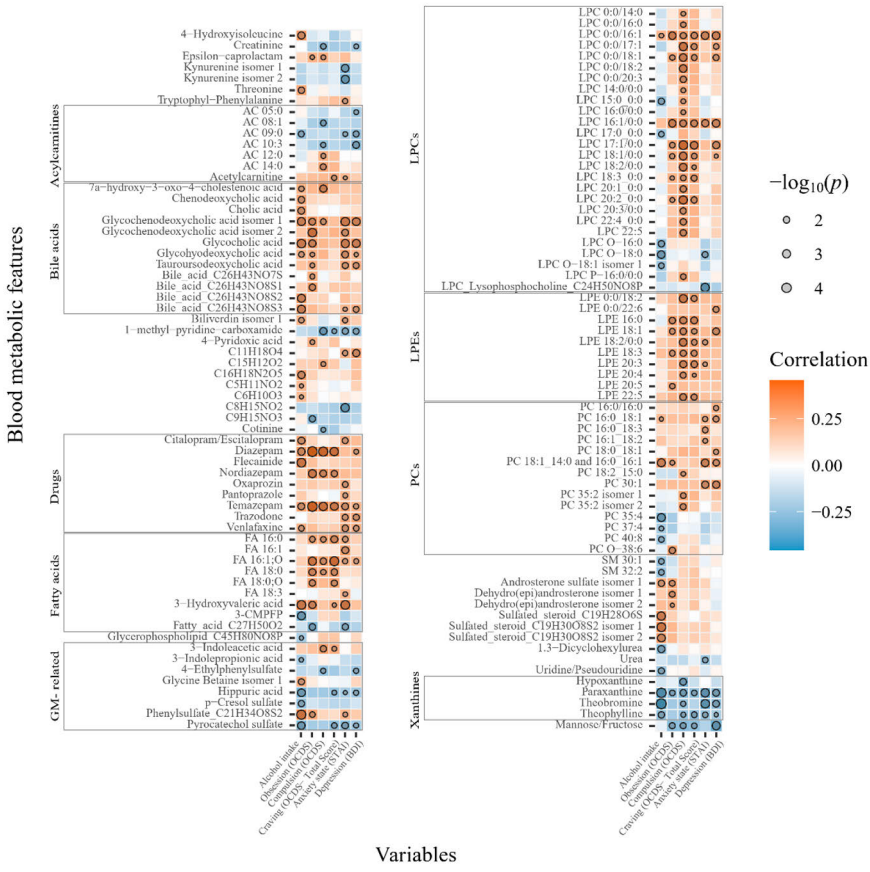


Figure 9. Heatmap of plasma metabolites correlated with alcohol intake and psychological symptom scores. Associations analyzed by Spearman rank correlation between plasma metabolites and alcohol intake or psychological symptom score of obsession, compulsion, alcohol craving, anxiety state or depression. Circle size refers to the level of significance, blue gradient color to the strength of negative while red to the strength of positive correlation coefficients. AC, acylcarnitine; FA, fatty acid; GM, gut microbiota; LPC, lysophosphatidylcholine; LPE, lysophosphatidylethanolamine; PC, phosphatidylcholine. Figure modified from Leclercq, Ahmed, et al. (2024)[273].

Another key factor that may facilitate the neuroactivity of peripheral metabolites is their ability to cross BBB and reach the CNS. To explore this, existing nontargeted metabolomics datasets from the frontal cortex and CSF of deceased individuals with a medical history of heavy alcohol use were utilized[153]. A targeted search based on the previously annotated plasma metabolites identified 79 and 74 matches from the CSF and frontal cortex, respectively.

Focusing on metabolites that correlated with at least one or more psychological symptom score, a total of 8 metabolites in the frontal cortex and 15 in the CSF were found to differ significantly ($q$ or $p < 0.05$) between individuals with and without a history of alcohol misuse (**Figure 10**).

The relative differences in metabolite levels largely mirrored those observed in plasma. For example, 3-hydroxyvaleric acid and cotinine were elevated, while paraxanthine and theobromine were decreased in both frontal cortex and CSF of the Alcohol group (**Figure 10**). Similarly, hippuric acid and pyrocatechol sulfate were reduced in the CSF (**Figure 10b**). However, some discrepancies between plasma and CNS trends were noted. For instance, LPE 20:3 and PC 16:0_18:1 were decreased in the frontal cortex of the Alcohol group, despite being elevated in plasma. Interestingly, all LPEs altered in the CSF followed the same direction as in plasma, as did LPCs, which were significantly increased in the Alcohol group.

It is important to note that the presence of a metabolite in the CNS does not necessarily imply neuroactivity or causality in relation to brain-related symptoms. Many of the overlapping metabolites belonged to lipid classes, which is expected given the brain's lipid-rich composition and tightly regulated lipid homeostasis[321]. Nonetheless, dysregulated lipid metabolism or chronic overconsumption of dietary fat is reflected in the brain lipid profile. This aligns with the current findings of increased phospholipids and fatty acids containing 16- and 18-carbon chains in the brains of individuals with history of heavy alcohol use.

The detection of hippuric acid and pyrocatechol sulfate in the brain further highlights the potential of microbiota-derived metabolites to cross the BBB and exert local neuromodulatory effects. Notably, 3-hydroxyvaleric acid, a five-carbon ketone body, was positively correlated with multiple psychological symptom scores, elevated in plasma, and responsive to alcohol withdrawal. While hydroxyvalerates have previously been linked to alcohol consumption, their origin and physiological roles remain unclear[253]. Some isolated reports suggest that this anaplerotic carbon source can be rapidly utilized in the citric acid cycle to support brain energetics and neurotransmission, particularly in inherited metabolic conditions[324].

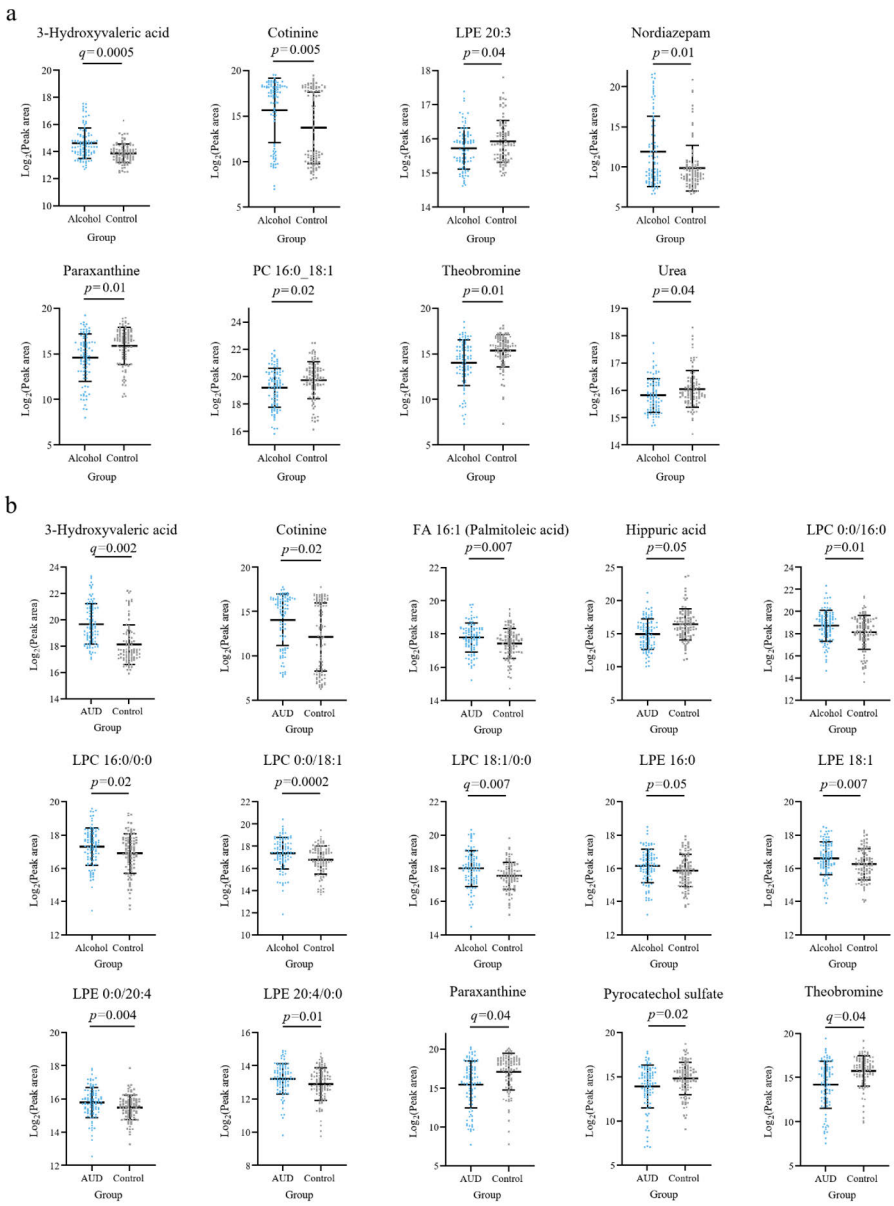


Figure 10. CNS metabolites linked with history of heavy alcohol use selected based on a corresponding plasma metabolite displaying association with psychological symptoms in persons with AUD. A) frontal cortex metabolites significantly altered ($p < 0.05$) between alcohol and control group B) cerebrospinal fluid metabolite significantly altered ($p < 0.05$) between alcohol and control group. Data expressed as $Log_2$-transformed mean peak area ± SD with individual values shown. The approximate threshold for an observed peak is a $Log_2$-transformed value > 12. Differences between groups analyzed by Welch's *t*-test comparing metabolite levels between control and alcohol groups. Figure reprinted from Leclercq, Ahmed, et al. (2024)[273].

## 5.3 Modulatory effect of inulin supplementation on neuroactive plasma and fecal metabolites

The preceding chapters demonstrated that both AUD and alcohol withdrawal significantly impact the circulating metabolome. This metabolite pool includes microbiota-associated compounds and lipid intermediates with potential neuroactive properties. Given the concurrent findings of dietary deficiencies and disrupted gut microbiota composition and function in individuals with AUD[259, 274], targeting the gut microbiota through nutritional interventions during alcohol withdrawal may offer adjunctive benefits by modulating neuroactive circulating metabolites. In study **II**, the effects of inulin fiber supplementation over a 3-week alcohol withdrawal period in individuals with AUD were investigated by analyzing changes in the plasma and fecal metabolomes, and their associations with gut microbiota composition, biological markers, and psychological symptoms[273, 279]. Clinical characteristics of the study participants are presented in **Table 3**.

Table 3. Baseline characteristics of individuals with AUD randomized to receive either inulin or placebo supplementation during a 3-week alcohol withdrawal program. Values shown as mean ± standard deviation. Table modified from Amadieu, Ahmed, Leclercq, et al. (2025)[279].

| | Inulin | Placebo | $p^a$ |
|---|---|---|---|
| n | 22 | 21 | 0.88 |
| Age | 48.3 ± 9.8 | 48.8 ± 8.8 | |
| Biological sex | | | 0.08 |
| Male (%) | 11 (50.0) | 16 (76.2) | |
| Female (%) | 11 (50.0) | 5 (23.8) | |
| Weight | 73.4 ± 14.6 | 70.8 ± 10.2 | 0.51 |
| BMI | 24.4 ± 3.1 | 23.2 ± 3.5 | 0.23 |
| MMSE | 27.7 ± 2.8 | 28.7 ± 1.2 | 0.14 |
| Active smokers (%) | 16 (72.7) | 17 (80.9) | 0.52 |
| Alcohol consumption g/day | 152.7 ± 90.7 | 134.1 ± 54.7 | 0.42 |
| Years of drinking habit | 16.5 ± 11.9 | 16.9 ± 10.3 | 0.90 |
| DSM-5 AUD score | 9.3 ± 1.3 | 8.0 ± 1.9 | 0.01 |

[a]Statistical difference between inulin and placebo groups. Numerical variables compared using independent sample *t*-test or Mann Whitney U test and categorical variables using chi-square test or Fisher's test for categorical values.
Abbreviations: AUD, Alcohol Use Disorder; BMI, Body Mass Index; DSM-5, Diagnostic and Statistical Manual of Mental Disorders fifth edition; MMSE, Mini Mental State Examination.

The effect of inulin supplementation on plasma and fecal metabolomes was evaluated using both univariate and multivariate analyses. The performance of the two component PLS-DA models showed that the model with fecal

metabolome had an accurary of 0.66, R2 of 0.68 and Q2 of 0.10 while the model with plasma metabolome had the accuracy of 0.58, R2 of 0.86 and Q2 of -0.14 indicating lack of classification ability of the models. Nevertheless, metabolic features meeting the criteria of $p < 0.05$ in the Mann–Whitney U test and a VIP score > 1.5 in the PLS-DA models were selected for further inspection. Following annotation, 13 plasma and 14 fecal metabolites were identified as significantly differing between the inulin and placebo groups at the end of the withdrawal (**Figure 11**). As shown in **Figure 11a**, most of the altered plasma metabolites were elevated in the Inulin group and primarily belonged to various lipid classes. Although the fold changes were modest (approximately 0.5), increases were observed in long-chain fatty acids, specifically 16:0, 18:2, 18:3, 20:3;O, 22:5, and 22:6, as well as in PCs containing these fatty acid chains. Additional increases were noted in sphingomyelin 36:2, acylcarnitine 10:2, cortisol, and an unidentified metabolite with the molecular formula $C_8H_{15}NO_2$. Only one annotated metabolite, 3-methylhistidine, was found to be decreased compared to Placebo.

These findings suggest that inulin's influence during withdrawal on plasma metabolome is relatively minor and primarily affects polyunsaturated lipid species. Importantly, these changes could not be attributed to differences in dietary intake[274]. Except for palmitic acid (16:0), none of the altered metabolites had previously shown neuroactive potential in correlation analyses (**Figure 9**). Moreover, inulin supplementation appeared to induce a modest increase in symptom-associated metabolites. While dietary fibers are generally known for their hypolipidemic effects, which influence various circulating lipid classes, long-chain inulin supplementation has also been reported to increase circulating lipids[325] and fecal fatty acids[266]. Notably, inulin also exhibits cholesterol-lowering properties[241]. Preclinical studies have shown that gut microbial metabolism of polyunsaturated acids can influence colonic lipid content, and that inulin may modulate hepatic expression of desaturases and elongase[326, 327]. However, the relevance of these mechanisms in humans remains to be fully established.

In contrast to plasma metabolome, the annotated fecal metabolites exhibited an opposite trend, with the majority showing decreased levels in the inulin group compared to placebo (**Figure 11b**). Moreover, the altered fecal metabolites belonged to distinctly different chemical classes than the lipid-rich profile observed in plasma. The decreases, though modest (fold change ~ -0.5), were primarily seen in secondary bile acids, including ketodeoxycholic, nutriacholic, lithocholic, and deoxycholic acids, as well as in amines such as aniline, 4-aminophenol, and dimethylphenylamine. Additional decreased metabolites included hydroxy fatty acid 18:1, indole-3-butyric acid, 5-AVAB, methylimidazoleacetic acid, and zeatin. Only two annotated metabolites were

elevated: N8-acetylspermidine and an unidentified compound with the molecular formula $C_6H_{11}NO$.

Notably, there was no overlap between the altered fecal metabolites and those observed in plasma, neither in study **I** nor study **II**, including gut microbiota-associated compounds. This suggests that the plasma and fecal metabolic pools are spatially distinct, or that inulin modulates metabolic pathways in a location-specific manner. The fecal metabolome primarily reflects the functional capacity of the gut microbiota and is largely shaped by microbial composition[14]. The consistent reduction in multiple secondary bile acids suggests that inulin may influence microbial pathways involved in bile acid deconjugation or dehydroxylation or promote the growth of microbial taxa not engaged in bile acid transformation[328]. The observed decrease in amines and aniline derivatives may reflect reduced exposure to dietary or environmental xenobiotics, or enhanced biotransformation of these compounds[329]. The decline in indole-3-butyric acid and zeatin, both plant-derived metabolites, coincided with a reported reduction in root vegetable intake in the Inulin group[274]. Meanwhile, the increase in N8-acetylspermidine may indicate shifts in polyamine metabolism, potentially reflecting improved gut health[330] and stress-ameliorating effects that could extend to the brain[331].

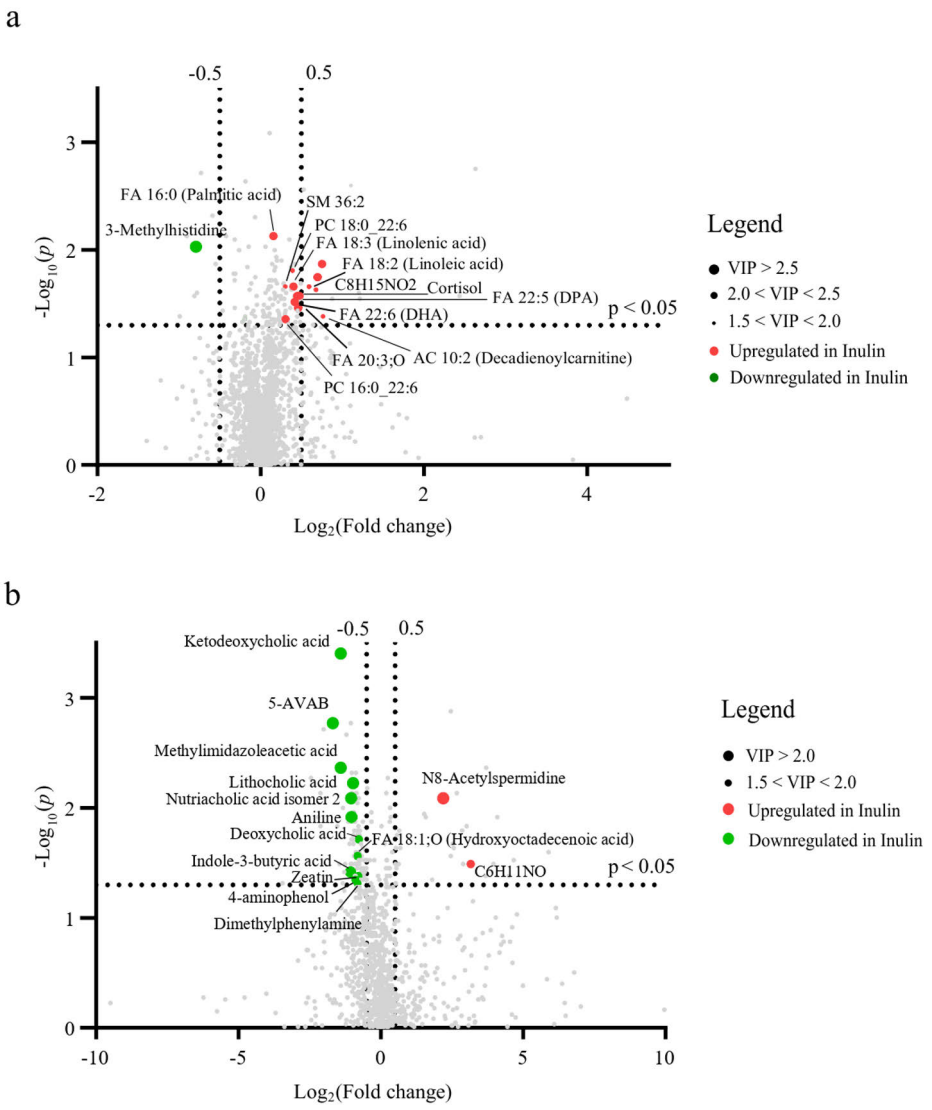


Figure 11. Volcano plot illustrating the differential plasma and fecal metabolic features between inulin and placebo groups after a 3-week alcohol withdrawal period. X-axis depicts the features' $Log_2$-transformed fold changes and y-axis their statistical significance in Mann-Whitney U test. Colored dots represent features with $p < 0.05$ and their size the variable importance in projections scores. A) Plasma metabolic features. B) Fecal metabolic features. 5-AVAB, 5-aminovaleric acid betaine; AC, acylcarnitine; DHA, docosahexaenoic acid; DPA, docosapentaenoic acid; FA, fatty acid; PC, phosphatidylcholine; SM, sphingomyelin. Figure reprinted from Amadieu, Ahmed & Leclercq, et al. (2025)[279].

Correlation analysis between inulin-altered plasma metabolites and AUD-associated gut microbiota composition revealed several nominally significant

associations (**Figure 12a**). Fatty acids were consistently positively correlated with the *Flavonifractor* genus and the *Ruminococcus torques* group, while *Butyricicoccus* showed inverse correlations with fatty acids 20:3;O and 22:5. Additionally, sphingomyelin 36:2 was positively associated with *Ruminococcus* torques and *Bacteroides*, and negatively correlated with liver function markers, including aspartate aminotransferase, alanine aminotransferase, and cell death biomarker M65. Plasma cortisol levels were positively correlated with *Lachnoclostridium* and *Flavonifractor* genera.

Among the inulin-associated fecal metabolites, several nominally significant correlations with gut microbiota composition were also observed (**Figure 12b**). Lithocholic acid was negatively correlated with *Butyricoccus, Bacteroides* and *Flavonifractor* genuses while ketodeoxycholic acid was negatively associated with *Lachnoclostridium* and positively with *Dorea*. Both lithocolic and ketodeoxycholic acids showed positive correlations with *Desulfovibrio*. Similarly, nutriacholic and deoxycholic acids were positively correlated with *Dorea*. Amine metabolites and indole-3-butyric acid were negatively correlated with *Bacteroides*. *Bifidobacterium* and *Lachnoclostridium* were positively associated with N8-acetylspermidine and an unknown metabolite (C6H11NO). Conversely, 5-AVAB was inversely correlated with *Lachnoclostridium* but positively associated with *Desulfovibrio* and social activity score. Finally, liver function markers alanine aminotransferase and cell death biomarker M65 were positively correlated with 4-aminophenol, nutriacholic acid and indole-3-butyric acid.

Correlation analysis between AUD-related gut microbiota composition and metabolites revealed moderate associations with limited statistical significance; however, several notable patterns emerged. For instance, plasma fatty acids were positively correlated with the *R. torques* group and the *Flavonifractor* genus. Although preliminary, a member of the *Flavonifractor* genus, *F. plautii*, has been suggested to influence liver metabolism through its metabolic products, which may modulate gene expression pathways involved in glucose and lipid metabolism[332]. Interestingly, while inulin is known for its bifidogenic effect, no significant correlations were observed between *Bifidobacterium* plasma metabolites. However, fecal N8-acetylspermidine was positively associated with *Bifdobacterium*, suggesting a localized metabolic interaction. Fecal secondary bile acids showed correlations with several gut microbial taxa, including *Lachnoclostridium* and *Dorea*, both members of the Lachnospiraceae family, which is known for its capacity to biotransform bile acids[328]. Among these, only *Dorea* has been previously implicated in the bile acid modulation[333]. Similarly, *Desulfovibrio* has also been linked to bile acid cycling within the colon, reinforcing its potential role in shaping the fecal bile acid profile.

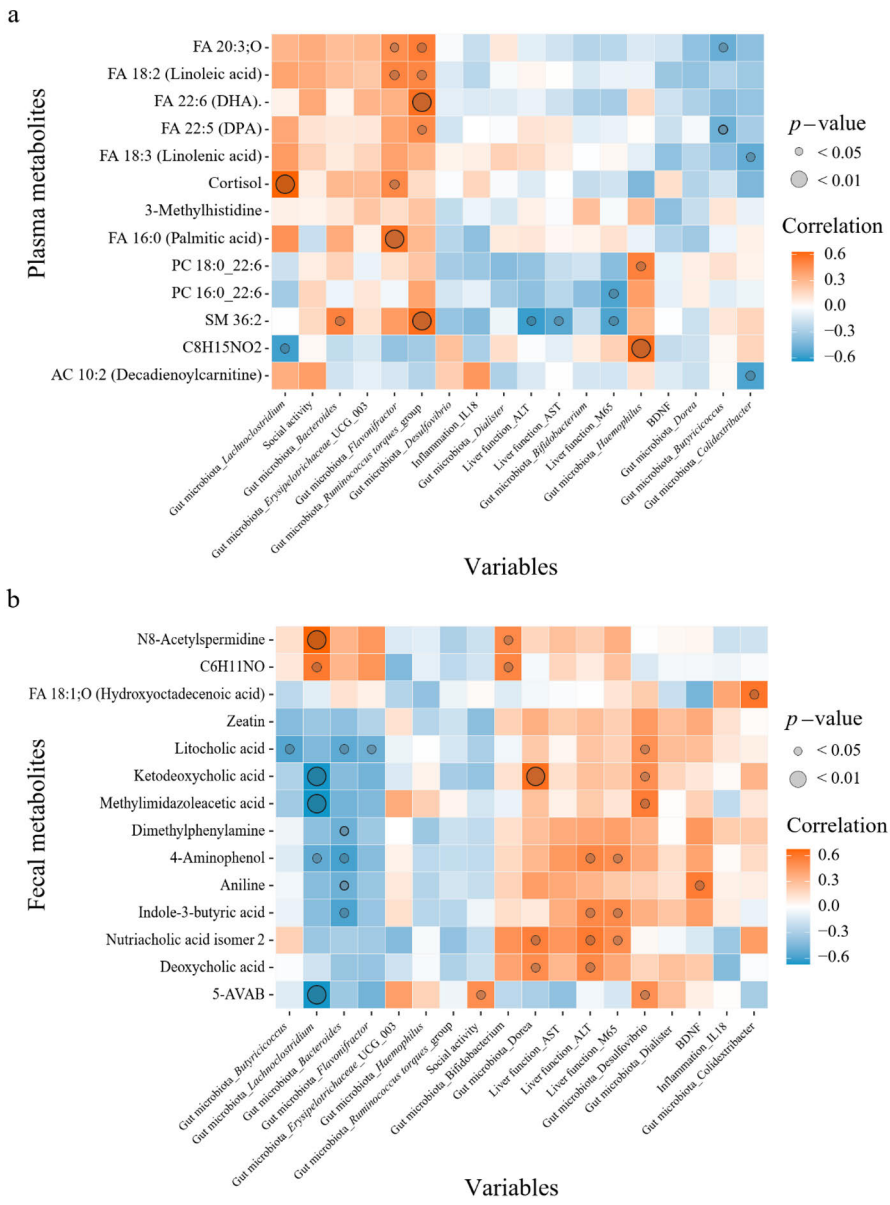


Figure 12. Correlations between inulin-associated metabolites and microbial, biological and psychological parameters after a three-week alcohol withdrawal period. Heatmaps of the Spearman rank correlations between metabolites and variables where blue color indicates negative and red positive correlation coefficient while the size of the dot is proportional to the level of significance. A) plasma metabolites and their correlations with biological and psychological parameters. B) Fecal metabolites and their correlations with biological and psychological parameters. 5-AVAB, 5-aminovaleric acid betaine; AC, acylcarnitine; BDNF, brain-derived neurotrophic; DHA, docosahexaenoic acid; DPA, docosapentaenoic acid; FA, fatty acid; PC, phosphatidylcholine; SM, sphingomyelin. Figure modified from Amadieu, Ahmed, Leclercq, et al. (2025)[279].

Inulin's prebiotic effect is known to stimulate the growth of *Bifidobacterium* and *Lactobacillus*, genera recognized for their fermentation capacity to produce SCFAs[334]. To assess this, fecal samples were analyzed for SCFAs content using a semi-targeted approach. **Figure 13** presents the relative differences between the inulin and placebo groups for the three most abundant SCFAs, acetic, propionic, and butyric acids, as well as for butyric acid isomers (isobutyric and 2-methylbutyric acid), valeric acid, isovaleric acid, and hexanoic acid. None of the measured SCFAs reached statistical significance between the groups. These findings are consistent with previous studies, which have reported mixed results regarding fecal SCFA levels following inulin supplementation. For example, 2- or 4-week inulin interventions in healthy adults, and a 6-week intervention in individuals with overweight or obesity, showed no significant changes in individual fecal SCFAs[264, 265]. In contrast, a 12-week supplementation with an inulin/oligofructose mixture in women with obesity led to decreased levels of acetic, propionic, and total SCFAs[267]. Conversely, other studies have reported increases in total fecal SCFAs after 2 weeks in healthy adults and increases in acetic and propionic acids after 4 weeks in patients with type 2 diabetes. This variability may reflect differences in the type of inulin used (e.g., short- vs. long-chain), dosage, dietary background, and study population. Moreover, while SCFAs are abundant in the colon, over 90% are absorbed in the intestine, meaning that fecal SCFA levels may not accurately reflect total SCFA production[335]. As a result, measuring circulating SCFAs may prove to be a more representative indicator of SCFA production and systemic availability.

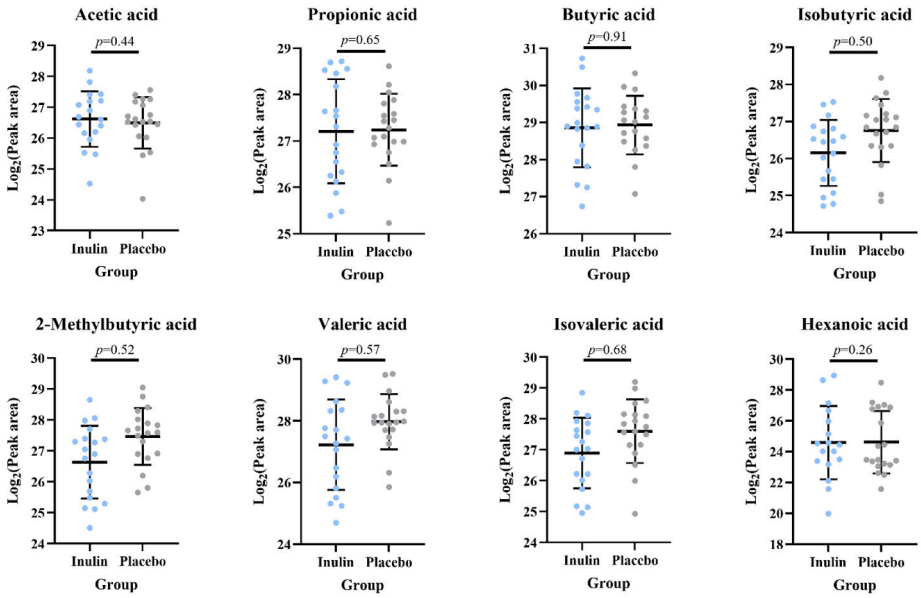


Figure 13. The effect of a 3-week inulin or placebo supplementation on the levels of identified fecal short-chain fatty acids (SCFAs). SCFAs were measured at the end of the alcohol withdrawal. Plots display individual values of $Log_2$-transformed arbitrary peak areas and group means ± standard deviation. Groups were compared using the Mann-Whitney U test on raw arbitrary peak areas. Figure modified from Amadieu, Ahmed, Leclercq, et al. (2025)[279].

## 5.4 Relationship between plasma and fecal metabolites

As observed in study **II** and illustrated in **Figure 11**, relatively few metabolites were altered in plasma and fecal metabolome following inulin supplementation in the individuals with AUD. More importantly, these changes and their associations with gut microbiota composition did not exhibit consistent or overlapping patterns (**Figure 12**). Therefore, the objective of study **III** was to investigate the associations between fecal and plasma metabolomes, identify shared patterns, and assess their reproducibility across two lifestyle intervention cohorts utilizing inulin supplementation and due to data availability, explore whether findings extend to another lifestyle factor, exercise training. To achieve this, available untargeted metabolomics data from three distinct lifestyle interventions were utilized. To maximize overlap, all annotated features were manually cross-checked across studies. The interventions included: (1) the 3-week inulin supplementation during alcohol withdrawal in individuals with AUD (*Gut2Brain*), (2) a 3-month inulin-enriched dietary intervention in individuals with obesity (*Food4Gut*), and (3) a 3-month high-intensity interval training program in individuals with MASLD (*BestTreat*). Following manual cross-checking, the number of annotated plasma metabolites was 286 in *Gut2Brain*,

239 in *Food4Gut* and 234 in *BestTreat* (**Figure 14**). For fecal metabolites, the corresponding numbers were 90, 173 and 195, respectively. All annotated metabolites were in the range of 60 to 900 *m/z* and listed in the **Supplementary table S1**. Across all three studies, 111 plasma metabolites and 46 fecal metabolites were shared. The differences in total annotations reflect study-specific metabolite coverage; however, approximately 50 % of plasma and 45 % of fecal metabolites were commonly observed across cohorts. The plasma metabolome reflects a combination of dietary and environmental exposures, microbial activity, host genetics, and clinical status, whereas the fecal metabolome is primarily shaped by gut microbiota composition[14, 336, 337]. Previous comparisons across five population-based studies have shown that approximately 66 % of plasma metabolome can be considered common [338]. Although the fecal metabolome tends to be more variable, many annotated metabolites—such as bile acids, heme derivatives, and fatty acids—are consistently enriched in industrialized populations, regardless of individual microbiome composition[339].

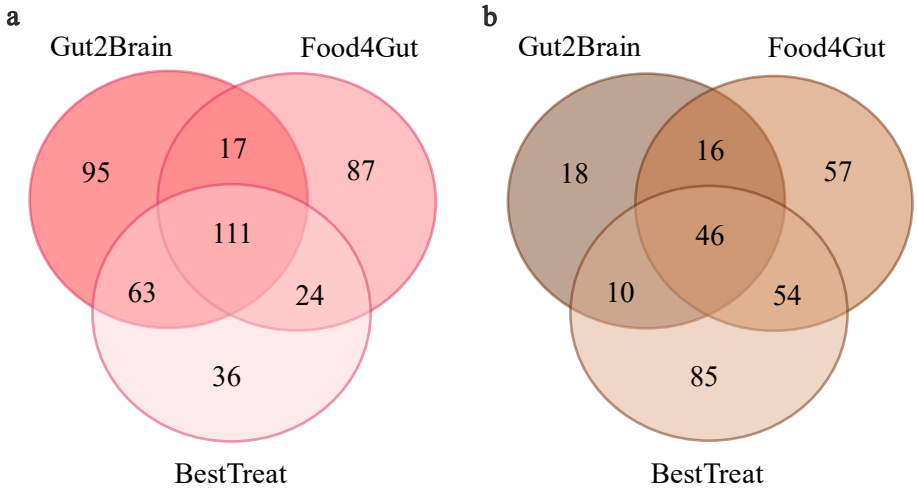


Figure 14. Number of cross-checked annotated metabolites from the Gut2Brain, Food4Gut and BestTreat metabolomes. A) Annotated plasma metabolites. B) Annotated fecal metabolites.

Fecal–plasma metabolite correlations were first assessed within each study, and the results are presented in **Figure 15**. Notably, no correlations remained statistically significant after false discovery rate correction ($q < 0.05$). Therefore, **Figure 15** displays all nominally significant correlations ($p < 0.05$), categorized by the direction of the correlation coefficient (positive or negative Spearman $r_s$). The highest number of nominally significant correlations was observed in the

*BestTreat* study, with 2,089, 2,172, and 2,720 correlations identified in the baseline, exercise, and control groups, respectively. However, only three correlations were shared across all three groups, and these involved metabolites from the lipid class—specifically phosphocholines and fatty acids. In contrast, the inulin-based trials (*Gut2Brain* and *Food4Gut*) showed no overlapping significant fecal–plasma metabolite pairs between their respective groups. Moreover, the study-specific heterogeneity of plasma and fecal metabolomes was also supported by the enrichment analysis. The *Gut2Brain* study exhibited the lowest number of correlations, with 1,177, 1,376, and 1,697 pairs in the baseline, inulin, and placebo groups, respectively. In the *Food4Gut* study, the number of significant pairs was 2,112 at baseline, 1,604 in the inulin group, and 2,185 in the placebo group. Importantly, the proportion of shared metabolite pairs between any two groups within each study remained below 2%, indicating that the observed fecal–plasma correlations were largely group- and time-specific, with limited reproducibility across conditions.

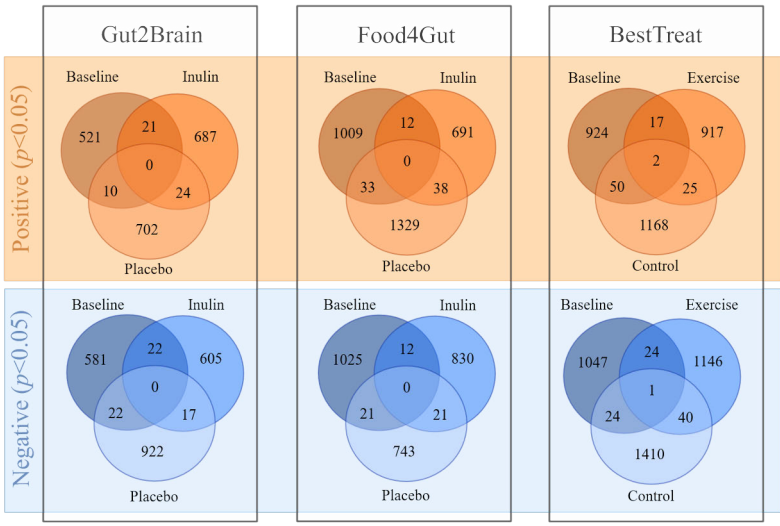


Figure 15. Statistically significant ($p$ < 0.05) fecal-plasma metabolite correlations within the Gut2Brain, Food4Gut or BestTreat studies. The common correlations were compared between baseline, treatment and control groups within studies. Red color indicates correlations with Spearman rank correlation coefficient values > 0 and blue color coefficient values < 0.

Despite inconsistencies in fecal–plasma metabolite correlations within individual studies, comparing these correlations across different baseline and treatment groups may offer deeper insights into microbiota–host interactions. To explore this, overlapping fecal–plasma metabolite pairs were assessed across

studies by comparing baseline, treatment, and control groups. However, the relatively small sample sizes posed a limitation: *Gut2Brain* had the largest cohort with 44 participants, followed by *BestTreat* with 40, and *Food4Gut* with only 27. These were further divided into treatment and control arms, reducing statistical power, despite some metabolite pairs showing strong correlation coefficients ($r_s$) even in the smallest groups. To address this, metabolite pairs were also selected for comparison based on a correlation coefficient threshold of $r_s > 0.3$ or $< -0.3$, provided they reached nominal significance ($p < 0.05$) in the group with the largest sample size. Results from both the statistical and $r_s$-based thresholds are presented in **Figure 16**. As expected, applying the $r_s$ threshold increased the number of metabolite pairs available for comparison to several thousand per group. However, this did not reveal substantial overlap: only one metabolite pair was shared at baseline, 16 in the treatment groups, and 23 in the control groups. When using the stricter statistical threshold, only a single correlation—between plasma acylcarnitine 16:1 and fecal trigonelline at baseline—was common across studies. Furthermore, the relative proportion of correlations meeting the $r_s$ threshold between any two studies remained below 4%. When applying the nominal significance threshold, this proportion dropped to below 1%, highlighting the limited reproducibility of fecal–plasma metabolite correlations across different interventions and populations.

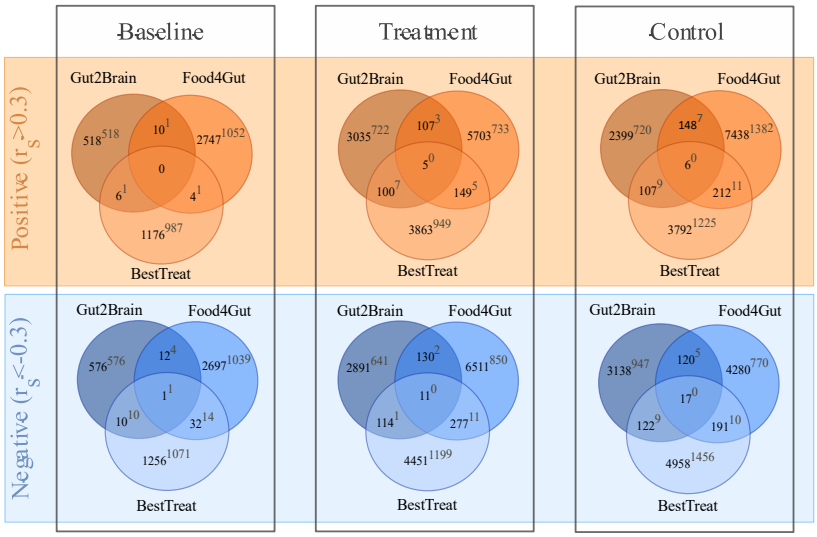


Figure 16. Fecal-plasma metabolite correlations displaying Spearman rank correlation coefficient ($r_s$) of > 0.3 or < -0.3 between the baseline, treatment or control groups across the Gut2Brain, Food4Gut or BestTreat studies. Superscript expresses the number of statistically significant ($p < 0.05$) correlations among the ones passing the $r_s$ threshold. Red color indicates correlations with Spearman rank correlation coefficient values > 0 and blue color coefficient values < 0.

These results suggest that while fecal–plasma metabolite correlations do exist, their consistency is limited. Previous studies across various populations have similarly reported correlations between fecal and plasma metabolites, but both their statistical significance and correlation strength ($r_s$) vary widely. For instance, in a cohort of 1,370 individuals with metabolic syndrome, only two metabolite pairs showed significant correlations ($q < 0.05$), and both had $r_s$ values below 0.3[340]. In another study involving over 1,000 middle-aged and elderly individuals, a set of 132 paired metabolites, detected in both feces and plasma, yielded an average $r_s$ of $0.05 \pm 0.12$, with only eight pairs exceeding $r_s > 0.3$[341]. In a pediatric population, fecal–plasma metabolite correlations have ranged from $r_s = -0.4$ to 0.4[342] while in endurance athletes, 12 fecal metabolites correlated with 70 plasma metabolites, producing nominally significant $r_s$ values between -0.7 and 0.7 similar to the exercise group in the present study[343]. What stands out across all these studies, including the current one, is the remarkably low number of consistently observed correlations. Although speculative, this variability may stem from both biological and methodological factors. Feces, as a waste product, have a distinct metabolic composition compared to the luminal environment, let alone the upper gastrointestinal tract[344]. Within the lumen, nutrient absorption and microbial metabolism continuously reshape the chemical landscape. Microbial communities form complex metabolic networks, including cross-feeding interactions[345]. Furthermore, biologically active metabolites produced in the gut are often utilized locally by host cells or processed by the liver before entering systemic circulation, limiting their detectability in plasma[346]. Lastly, results likely reflect the unique outcomes of metabolic alterations in AUD, obesity and MASLD challenged with fiber supplementation or intensive exercise.

## 5.5 Limitations and strengths

The overarching methodological approach used in this work, nontargeted LC-MS-based metabolomics, offers both strengths and limitations. Given that studies **I** and **II** were hypothesis-free explorations aimed at identifying biomarkers and assessing the metabolic effects of specific interventions, and study **III** focused on uncovering associations between fecal and plasma metabolites, LC-MS-based metabolomics was well suited to these objectives due to its high sensitivity and broad analytical coverage. Importantly, methodological consistency across studies, including similar metabolite extraction protocols, chromatographic separation techniques (RP and HILIC), analytical platforms, data preprocessing, and annotation workflows, supports the comparability of results. Nevertheless, each analytical technique introduces its own biases, and no single method can comprehensively capture the entire metabolome. For example, the fecal metabolome is rich in volatile compounds such as esters and alcohols,

which are not well detected by the LC-MS approaches used here, with the exception of the SCFA analysis in study **II**. Additionally, nontargeted metabolomics remains constrained by its reliance on existing spectral databases and chemical standards for metabolite identification, meaning that typically part of the observed metabolites remain unidentified, as was the case in these studies. The vast volume of data generated also requires compromises in the data analysis depth and necessitates rigorous curation to distinguish true biological signals from noise. In this context, the use of *in silico* and bioinformatics tools, many of which were applied during the annotation steps in this work, is essential for managing omics-scale data and ensuring the reliability of reported findings.

Although beyond the control of this work, it is worth acknowledging the limitations inherent to clinical research, particularly regarding group selection and the challenge of minimizing unwanted variation. In studies **I** and **II**, the individuals with AUD were enrolled in standardized manner and their alcohol consumption and abstinence were carefully verified in a clinical, longitudinal setting, all factors that should be considered as strengths. The inclusion of a matched control group enabled the investigation of alcohol-related metabolic profiles. However, dietary intake could not be matched, and since AUD is often accompanied by malnutrition, the influence of alcohol abstinence *per se* from those of improved nutritional status. Dietary factors are known to significantly influence both plasma and fecal metabolomes, likely confounding the results[5, 14]. Moreover, the subtle metabolic effects of inulin treatment observed in study **II** reflect the interplay between AUD, withdrawal and inulin. However, the absence of an inulin-treated control group limits the ability to reveal such effects. Across studies **I**, **II** and **III**, sample sizes ranged from 27 to 96 participant, representing small to moderate cohorts. This limits statistical power, particularly given that subtle metabolic changes often require large-scale metabolomics studies to detect. Additionally, clinical samples were collected at different times and locations using varying protocols, introducing potential sources of technical and biological variation that may be reflected in the metabolite profiles. Notably, prolonged storage may be reflected as potential shifts in the fecal polar metabolome, plasma lipids and hormones halting the comparability between studies as clinical samples for this work were collected across 2015 and 2020[347, 348]. In study **III**, the lifestyle interventions and health statuses of participating populations were heterogeneous. While this diversity may be viewed as a limitation, it also offers a strength by enabling the identification of underlying metabolic commonalities across different health contexts.

Finally, all three studies report semi-quantitative metabolomics data, which are valuable for identifying metabolic phenotypes and associations but do not establish causality. For example, while study **I** demonstrated that alcohol use alters specific circulating and brain metabolites associated with psychological

symptoms, the observed associations require follow-up *in vitro* or *in vivo* studies to provide mechanistic insights. Similarly, in study **II**, associations between microbial genera and metabolites may oversimplify the complexity of microbiota–host interactions. As discussed in study **III**, feces represent only a fraction of the intestinal chemical landscape, and the circulating metabolome is tightly regulated by homeostatic mechanisms. Therefore, the observed associations likely represent only a narrow snapshot of the broader, dynamic microbiota–host crosstalk.

## 5.6 Relevance and significance of the research

The findings presented in this thesis both reinforce existing knowledge and offer novel insights into alcohol-induced metabolic alterations, their associations with psychological symptoms, and the potential role of gut microbiota metabolism. While alcohol's impact on lipid metabolism is well established, this work demonstrated that specific lipid classes and fatty acids are distinctly modulated, alongside consistent changes in gut microbiota- and diet-associated metabolites during periods of alcohol intake and abstinence. The originality of these findings is underscored by the inverse associations between psychological symptoms and gut- or diet-derived metabolites, many of which were downregulated in individuals with AUD. Notably, several of these metabolites were also detected in the CNS and have previously been linked to beneficial neuroactive properties[144, 313, 315, 319]. This opens avenues for future proof-of-concept studies exploring their mechanistic roles.

Although inulin has been studied in various contexts, its application during alcohol withdrawal in individuals with AUD had not been previously explored. This thesis presents the first plasma and fecal metabolic profiling of such an intervention, offering a detailed view of its metabolic impact. While the overall effects were modest, consistent with earlier reports, an increase in plasma polyunsaturated fatty acids and their correlation with gut microbiota composition is noteworthy, particularly given inulin's proposed links to lipid metabolism[266, 325, 327].

The fecal metabolome provides a valuable window into microbial metabolism, while the plasma metabolome reflects both host and microbial influences. Although previous studies have reported correlations between fecal and plasma metabolites, this thesis systematically mapped such relationships across three distinct lifestyle interventions. The lack of consistent correlation patterns across studies raises questions about the generalizability of these findings. Moreover, the distinct chemical landscapes of fecal and plasma metabolomes highlight the complexity of microbial cross-feeding, intestinal metabolism, and hepatic processing before metabolites reach systemic circulation. These results

underscore the need for caution when linking fecal metabolite profiles to health outcomes beyond the gastrointestinal tract.

## 5.7 Future prospects

The findings from this work raise several questions that set the stage for subsequent works in the context of AUD. Considering the range of diet-linked metabolites altered in the AUD before and after withdrawal, and their associations with psychological symptoms, the independent effects of intensive nutritional therapy during alcohol withdrawal should be investigated. Such approaches could focus on supporting the intake of polyunsaturated fats, complex carbohydrates, fruits, vegetables and caffeine beverages. In the light of accumulating evidence on the detrimental effects of certain saturated and monounsaturated fatty acids and their associations with negative psychological symptoms, lipidomics could offer deeper insight into these observed alterations and support the design of mechanistic experiments. It is also important to determine whether these associations between lipid species and psychological symptoms are specific to chronic alcohol abuse or extend to other populations with lipid dysregulation. Similarly, the modest effect of inulin treatment, primarily observed in plasma lipids, raise the question of whether these changes result from interactions with AUD-altered physiology or reflect a general feature of inulin's influence on the gut–brain axis. Finally, although no consistent associations were found between fecal–plasma metabolites, future studies utilizing intestinal content may better capture the metabolic interaction between gut microbiota and host, offering more accurate insights into their health implications.

# 6 SUMMARY AND CONCLUSION

This doctoral thesis employed a nontargeted LC-MS-based metabolomics approach to characterize plasma and fecal metabolic profiles in humans. The aim was to identify microbiota-derived metabolites with neuroactive potential, examine the effects of gut microbiota-targeted fiber supplementation, and explore relationship between distinct metabolite pools. The studies included in this thesis analyzed biological samples from several clinical interventions conducted in Belgium and Finland, involving individuals with AUD, obesity or MASLD. Study **I** investigated the impact of excessive alcohol consumption and a three-week withdrawal period on plasma metabolome. Metabolite correlations with psychological symptoms and their presence in the CNS were used to assess neuroactive potential. Study **II** introduced inulin supplementation targeting gut microbiota during alcohol withdrawal. Changes in fecal and plasma metabolites were mapped and correlated with gut microbiota composition, as well as biological and psychological markers. Study **III** compared fecal and plasma metabolites identified across three separate lifestyle interventions to uncover common patterns of fecal–plasma metabolic crosstalk.

Study **I** revealed that individuals with AUD exhibited elevated plasma levels of PCs, saturated or monounsaturated fatty acids with 16- or 18-carbon chains, bile acids and steroids. These metabolites significantly decreased following alcohol abstinence. Notably, they showed consistent positive correlations with psychological symptoms, and several phosphocholines were also detected in the CNS of deceased individuals with history of heavy alcohol use. Conversely, LPCs containing ether bonds or saturated 15- or 17-carbon fatty acid chains, along with gut microbiota-derived or caffeine-related metabolites, were reduced in AUD but increased after withdrawal. These metabolites were negatively associated with psychological symptoms, and many were also present in CNS of the deceased individuals. Collectively, these findings highlight that chronic alcohol consumption disrupts liver lipid and steroid metabolism, leading to class-specific metabolic alterations. Additionally, the results underscore alcohol's impact on gut microbiota metabolism, either directly or via dietary deficiencies, which may contribute to broader physiological and psychological harm. These insights support the exploration of nutritional interventions, such as fiber or polyphenol supplementation, as adjunct therapies alongside standard treatment for substance use disorders.

Building on the findings from study **I**, study **II** examined the effects of restoring dietary fiber intake through inulin supplementation during alcohol withdrawal. The intervention had a relatively modest impact on both plasma and fecal metabolite profiles. In fecal samples, inulin primarily reduced levels of secondary

bile acids, amines, amino acid-derived metabolites and the fatty acid 18:1, while increased a single polyamine metabolite. In plasma, the supplementation led to increases in saturated and polyunsaturated fatty acids, phosphocholines, and select metabolites from other classes. However, correlation analysis yielded mostly sporadic associations, with the exception of multiple links between secondary bile acids, amines or fatty acids and gut microbiota taxa. Notably, none of the metabolites previously identified as potentially neuroactive, including those derived from microbiota, were significantly altered by inulin supplementation. While the correlations suggest that gut microbiota may influence plasma fatty acid levels to some extent, the underlying mechanism remains unclear and warrant further investigation. It is important to recognize that dietary fibers exert both general and fiber-specific effects, which are further modulated by individual metabolic differences. Given this complexity, the modest impact observed is not unexpected, especially considering the mixed evidence surrounding inulin's influence on various metabolic profiles.

The main finding of study **III** was that the fecal–plasma metabolite correlations are abundant but highly specific to group and time, lacking reproducibility within or across studies. This was demonstrated by analyzing correlations in at baseline and during treatment and control phases across three distinct intervention studies. Despite longitudinal monitoring of the participants, there was virtually no overlap in statistically significant metabolite pairs across conditions. This lack of consistency persisted even when comparing baseline, treatment, or control group between different studies. Adjusting for unequal group sizes by applying a correlation coefficient threshold yielded only minor changes, reinforcing the conclusion that consistent directly observable relationships between fecal and plasma metabolites are rare. Given the fundamentally different nature and function of fecal material and plasma, reflected in their distinct metabolic composition, it is unsurprising that direct links are limited. While fecal samples are valuable for assessing microbial activity, they should not be considered comprehensive indicators of the colonic environment or the health relevance of the metabolites they contain.

This thesis identified a group of circulating metabolites that may play a role in gut–brain axis communication, emphasizing the importance of dietary components and highlighting the distinct relevance of fecal versus circulating metabolites. The findings contribute to the growing body of knowledge on how the gut microbiota and lifestyle factors, particularly nutrition, affect psychological symptoms linked to mental health vulnerability. At the same time, the results underscore the necessity of carefully controlling lifestyle variables such as diet and physical activity in studies focused on the gut–brain axis. Such considerations enhance the ability of metabolomics to uncover novel insights into the complex microbiota–host relationship.

# ACKNOWLEDGEMENTS

This thesis was primarily conducted at the Unit of Food Sciences, Department of Life Technologies, University of Turku. The metabolomics data used were acquired at the core LC-MS laboratory facility of the School of Pharmacy, University of Eastern Finland, and at the Unit of Food Sciences, University of Turku. The studies were part of the "Gut2Behave" project, initiated from the ERA-NET NEURON network (Joint Transnational Call 2019), and funded by the Academy of Finland, the French National Research Agency and the Fonds de la Recherche scientifique. I am grateful to the Gut2Behave project, the Doctoral Programme in Technology, and the Jane and Aatos Erkko foundation for their financial support, which enabled me to focus on my research. I also thank the Doctoral Programme in Technology, the Nordic Metabolomics Society, the Finnish Foundation for Drug Research, and the Finnish Food Research Foundation for supporting my participation in academic events held in Marseille, Copenhagen, Niagara Falls, Trondheim, Brussel, Osaka and Turku.

My deepest gratitude goes to my supervisors Professor Kati Hanhineva, Docent Ville Koistinen and PhD Olli Kärkkäinen, for their guidance, expertise and support. Thank you for your trust and encouraging the autonomy that allowed me to grow both professionally and personally. I am also thankful to my advisory committee, Professor Kaisa Linderborg, Professor Baoru Yang and Professor Marjukka Kolehmainen, for their insights and support. Heartfelt thanks to my colleagues and co-authors in the Gut2Behave project: Professor Nathalie Delzenne, Professor Sophie Layé, PhD Audrey Neyrinck, PhD Sophie Leclercq, PhD Camille Amadieu and PhD Quentin Leyrolle. Finally, I am especially grateful to Associate Professor Nicholas Rattray and Associate Professor Tiina Sikanen for their time and effort in pre-examining this work and providing insightful comments further improving the thesis.

To Heli, Anu, Tapio and Leena, thank you for your invaluable help with administrative and practical matters. To my senior and junior colleagues and fellow doctoral researchers at the Food Sciences unit, Mikael, Niina, Tanja, Ella, Annelie, Marika, Priscilla, Eija, Gabriele, Kang, Mohammed, Anna, Enni, Sari, Ye, Yuqing, Ying, Qizai, Qizhu, Timo, Henri and Cong, thank you for the countless discussions and shared laughter that brightened my workdays. Special thanks to Alex, Mikael and Annelie for their training and endless knowledge of LC- and GC-MS instruments. To the metabolomics team, Topi, Retu, Sara, Jasmin, Shania, Iman, Ambrin, Artur, Anna and Ville, thank you for the camaraderie, shared frustrations, and humor, both in and out of the office. To my longtime friends, Heikki, Perttu, Esko, Aapeli, Juha, Timo, Henri, I'm deeply

grateful for your friendship and the good times we have shared. To Noora, Ville and the kids, thank you for the energy, support and warmth throughout the years.

To my parents, thank you for your unconditional love and support. Your belief in me has been a constant source of strength. You have taught me the values of perseverance, integrity, and kindness, which have shaped who I am today.

Finally, my colleague, friend, and life partner, Veera. You are my inspiration. Your love keeps me motivated and brings comfort in moments of hardship. Thank you for being there and sharing this path with me.

Turku, August 2025

# DISCLOSURE OF THE USE OF AI TOOLS

During the finalization of this doctoral thesis, Microsoft Copilot powered by OpenAI's GPT-4-turbo model, was used to improve grammar, flow and overall clarity of the text with the following prompt: "Act as a proofreading expert. Your task is to improve the clarity and conciseness of a given [text]. Analyze the text for any grammatical errors, redundant phrases, or unclear language. Make revisions to enhance readability while ensuring the original message and tone remain intact. Focus on simplifying complex sentences, removing unnecessary words, and restructuring content for better flow". Corrections were closely reviewed, and editing was made solely for linguistic refinement and not to generate content, conduct analysis or interpretate results. All intellectual contributions, research findings, and interpretations presented in this thesis are my own, and I remain fully responsible for the content.

# REFERENCES


1. Johnson, C.H.;Ivanisevic, J.&Siuzdak, G. Metabolomics: beyond biomarkers and towards mechanisms. *Nat. Rev. Mol. Cell Biol.* 2016;17(7):451-459. https://doi.org/10.1038/nrm.2016.25
2. Wishart, D.S. Emerging applications of metabolomics in drug discovery and precision medicine. *Nat. Rev. Drug Discov.* 2016;15(7):473-484. https://doi.org/10.1038/nrd.2016.32
3. Bar, N.;Korem, T.;Weissbrod, O.;Slieker, R.;Rutters, F.;Beulens, J., et al. A reference map of potential determinants for the human serum metabolome. *Nature*. 2020;588(7836):135-140. https://doi.org/10.1038/s41586-020-2896-2
4. Zmora, N.;Suez, J.&Elinav, E. You are what you eat: diet, health and the gut microbiota. *Nat. Rev. Gastroenterol. Hepatol.* 2018;16(1):35-56. https://doi.org/10.1038/s41575-018-0061-2
5. Chen, L.;Zhernakova, D.V.;Kurilshikov, A.;Andreu-Sanchez, S.;Wang, D.;Augustijn, H.E., et al. Influence of the microbiome, diet and genetics on inter-individual variation in the human plasma metabolome. *Nat Med*. 2022;28(11):2333-2343. https://doi.org/10.1038/s41591-022-02014-8
6. Dekkers, K.F.;Sayols-Baixeras, S.;Baldanzi, G.;Nowak, C.;Hammar, U.;Nguyen, D., et al. An online atlas of human plasma metabolite signatures of gut microbiome composition. *Nat. Commun.* 2022;13(1):5370. https://doi.org/10.1038/s41467-022-33050-0
7. Kortesniemi, M.;Noerman, S.;Karlund, A.;Raita, J.;Meuronen, T.;Koistinen, V., et al. Nutritional metabolomics: Recent developments and future needs. *Curr. Opin. Chem. Biol.* 2023;77:102400. https://doi.org/10.1016/j.cbpa.2023.102400
8. Chung, S.J.;Rim, J.H.;Ji, D.;Lee, S.;Yoo, H.S.;Jung, J.H., et al. Gut microbiota-derived metabolite trimethylamine N-oxide as a biomarker in early Parkinson's disease. *Nutrition*. 2021;83:111090. https://doi.org/10.1016/j.nut.2020.111090
9. Gao, B.;Zeng, S.;Maccioni, L.;Shi, X.;Armando, A.;Quehenberger, O., et al. Lipidomics for the Prediction of Progressive Liver Disease in Patients with Alcohol Use Disorder. *Metabolites*. 2022;12(5). https://doi.org/10.3390/metabo12050433
10. Geijsen, A.;Brezina, S.;Keski-Rahkonen, P.;Baierl, A.;Bachleitner-Hofmann, T.;Bergmann, M.M., et al. Plasma metabolites associated with colorectal cancer: A discovery-replication strategy. *Int. J. Cancer*. 2019;145(5):1221-1231. https://doi.org/10.1002/ijc.32146
11. Julkunen, H.;Cichonska, A.;Tiainen, M.;Koskela, H.;Nybo, K.;Makela, V., et al. Atlas of plasma NMR biomarkers for health and disease in 118,461 individuals from the UK Biobank. *Nat. Commun.* 2023;14(1):604. https://doi.org/10.1038/s41467-023-36231-7
12. Karagiannidis, E.;Moysidis, D.V.;Papazoglou, A.S.;Panteris, E.;Deda, O.;Stalikas, N., et al. Prognostic significance of metabolomic biomarkers in patients with diabetes mellitus and coronary artery disease. *Cardiovasc. Diabetol.* 2022;21(1):70. https://doi.org/10.1186/s12933-022-01494-9
13. Nho, K.;Kueider-Paisley, A.;Arnold, M.;MahmoudianDehkordi, S.;Risacher, S.L.;Louie, G., et al. Serum metabolites associated with brain amyloid beta deposition, cognition and dementia progression. *Brain Commun*. 2021;3(3):fcab139. https://doi.org/10.1093/braincomms/fcab139
14. Zierer, J.;Jackson, M.A.;Kastenmuller, G.;Mangino, M.;Long, T.;Telenti, A., et al. The fecal metabolome as a functional readout of the gut microbiome. *Nat. Genet*. 2018;50(6):790-795. https://doi.org/10.1038/s41588-018-0135-7
15. Ose, J.;Gigic, B.;Brezina, S.;Lin, T.;Baierl, A.;Geijsen, A., et al. Targeted Plasma Metabolic Profiles and Risk of Recurrence in Stage II and III Colorectal Cancer Patients: Results from an International Cohort Consortium. *Metabolites*. 2021;11(3). https://doi.org/10.3390/metabo11030129
16. Cryan, J.F.;O'Riordan, K.J.;Cowan, C.S.M.;Sandhu, K.V.;Bastiaanssen, T.F.S.;Boehme, M., et al. The Microbiota-Gut-Brain Axis. *Physiol. Rev*. 2019;99(4):1877-2013. https://doi.org/10.1152/physrev.00018.2018
17. Hsiao, Elaine Y.;McBride, Sara W.;Hsien, S.;Sharon, G.;Hyde, Embriette R.;McCue, T., et al. Microbiota Modulate Behavioral and Physiological Abnormalities Associated with Neurodevelopmental Disorders. *Cell*. 2013;155(7):1451-1463. https://doi.org/10.1016/j.cell.2013.11.024
18. Vuong, H.E.;Pronovost, G.N.;Williams, D.W.;Coley, E.J.L.;Siegler, E.L.;Qiu, A., et

al. The maternal microbiome modulates fetal neurodevelopment in mice. *Nature*. 2020;586(7828):281-283. https://doi.org/10.1038/s41586-020-2745-3

19. Needham, B.D.;Funabashi, M.;Adame, M.D.;Wang, Z.;Boktor, J.C.;Haney, J., et al. A gut-derived metabolite alters brain activity and anxiety behaviour in mice. *Nature*. 2022;602(7898):647-653. https://doi.org/10.1038/s41586-022-04396-8
20. Wu, W.-L.;Adame, M.D.;Liou, C.-W.;Barlow, J.T.;Lai, T.-T.;Sharon, G., et al. Microbiota regulate social behaviour via stress response neurons in the brain. *Nature*. 2021;595(7867):409-414. https://doi.org/10.1038/s41586-021-03669-y
21. Bercik, P.;Denou, E.;Collins, J.;Jackson, W.;Lu, J.;Jury, J., et al. The Intestinal Microbiota Affect Central Levels of Brain-Derived Neurotropic Factor and Behavior in Mice. *Gastroenterology*. 2011;141(2):599-609.e593. https://doi.org/10.1053/j.gastro.2011.04.052
22. Arpaia, N.;Campbell, C.;Fan, X.;Dikiy, S.;van der Veeken, J.;deRoos, P., et al. Metabolites produced by commensal bacteria promote peripheral regulatory T-cell generation. *Nature*. 2013;504(7480):451-455. https://doi.org/10.1038/nature12726
23. Asano, Y.;Hiramoto, T.;Nishino, R.;Aiba, Y.;Kimura, T.;Yoshihara, K., et al. Critical role of gut microbiota in the production of biologically active, free catecholamines in the gut lumen of mice. *Am. J. Physiol. Gastrointest Liver Physiol*. 2012;303(11):G1288-G1295. https://doi.org/10.1152/ajpgi.00341.2012
24. Barrett, E.;Ross, R.P.;O'Toole, P.W.;Fitzgerald, G.F.&Stanton, C. γ-Aminobutyric acid production by culturable bacteria from the human intestine. *J. Appl.. Microbiol*. 2012;113(2):411-417. https://doi.org/10.1111/j.1365-2672.2012.05344.x
25. Colombo, A.V.;Sadler, R.K.;Llovera, G.;Singh, V.;Roth, S.;Heindl, S., et al. Microbiota-derived short chain fatty acids modulate microglia and promote Aβ plaque deposition. *eLife*. 2021;10:e59826. https://doi.org/10.7554/eLife.59826
26. Jameson, K.G.;Kazmi, S.A.;Ohara, T.E.;Son, C.;Yu, K.B.;Mazdeyasnan, D., et al. Select microbial metabolites in the small intestinal lumen regulates vagal activity via receptor-mediated signaling. *iScience*. 2025;28(2):111699. https://doi.org/10.1016/j.isci.2024.111699
27. Chong, H.X.;Yusoff, N.A.A.;Hor, Y.Y.;Lew, L.C.;Jaafar, M.H.;Choi, S.B., et al. Lactobacillus plantarum DR7 alleviates stress and anxiety in adults: a randomised, double-blind, placebo-controlled study. *Benef. Microbes*. 2019;10(4):355-373. https://doi.org/10.3920/BM2018.0135
28. Heidarzadeh-Rad, N.;Gökmen-Özel, H.;Kazemi, A.;Almasi, N.&Djafarian, K. Effects of a Psychobiotic Supplement on Serum Brain-derived Neurotrophic Factor Levels in Depressive Patients: A Post Hoc Analysis of a Randomized Clinical Trial. *J. Neurogastroenterol. Motil*. 2020;26(4):486-495. https://doi.org/10.5056/jnm20079
29. Liu, R.T.;Walsh, R.F.L.&Sheehan, A.E. Prebiotics and probiotics for depression and anxiety: A systematic review and meta-analysis of controlled clinical trials. *Neurosci. Biobehav. Rev*. 2019;102:13-23. https://doi.org/10.1016/j.neubiorev.2019.03.023
30. Messaoudi, M.;Lalonde, R.;Violle, N.;Javelot, H.;Desor, D.;Nejdi, A., et al. Assessment of psychotropic-like properties of a probiotic formulation (Lactobacillus helveticus R0052 and Bifidobacterium longum R0175) in rats and human subjects. *Br. J. Nutr.* 2011;105(5):755-764. https://doi.org/10.1017/S0007114510004319
31. Sommer, F.&Backhed, F. The gut microbiota--masters of host development and physiology. *Nat. Rev. Microbiol*. 2013;11(4):227-238. https://doi.org/10.1038/nrmicro2974
32. Zheng, D.;Liwinski, T.&Elinav, E. Interaction between microbiota and immunity in health and disease. *Cell Res*. 2020;30(6):492-506. https://doi.org/10.1038/s41422-020-0332-7
33. Fan, Y.&Pedersen, O. Gut microbiota in human metabolic health and disease. *Nat. Rev. Microbiol*. 2021;19(1):55-71. https://doi.org/10.1038/s41579-020-0433-9
34. Chen, H.;Nwe, P.-K.;Yang, Y.;Rosen, C.E.;Bielecka, A.A.;Kuchroo, M., et al. A Forward Chemical Genetic Screen Reveals Gut Microbiota Metabolites That Modulate Host Physiology. *Cell*. 2019;177(5):1217-1231.e1218. https://doi.org/10.1016/j.cell.2019.03.036
35. Gacias, M.;Gaspari, S.;Santos, P.-M.G.;Tamburini, S.;Andrade, M.;Zhang, F.,

et al. Microbiota-driven transcriptional changes in prefrontal cortex override genetic differences in social behavior. *eLife*. 2016;5:e13442. https://doi.org/10.7554/elife.13442

36. Adesso, S.;Magnus, T.;Cuzzocrea, S.;Campolo, M.;Rissiek, B.;Paciello, O., et al. Indoxyl Sulfate Affects Glial Function Increasing Oxidative Stress and Neuroinflammation in Chronic Kidney Disease: Interaction between Astrocytes and Microglia. *Front. Pharmacol*. 2017;8:370. https://doi.org/10.3389/fphar.2017.00370
37. Ren, Z.;Zhang, R.;Li, Y.;Li, Y.;Yang, Z.&Yang, H. Ferulic acid exerts neuroprotective effects against cerebral ischemia/reperfusion-induced injury via antioxidant and anti-apoptotic mechanisms in vitro and in vivo. *Int. J. Mol. Med*. 2017;40(5):1444-1456. https://doi.org/10.3892/ijmm.2017.3127
38. Verzelloni, E.;Pellacani, C.;Tagliazucchi, D.;Tagliaferri, S.;Calani, L.;Costa, L.G., et al. Antiglycative and neuroprotective activity of colon-derived polyphenol catabolites. *Mol. Nutr. Food Res*. 2011;55(S1):S35-S43. https://doi.org/10.1002/mnfr.201000525
39. Dalile, B.;Van Oudenhove, L.;Vervliet, B.&Verbeke, K. The role of short-chain fatty acids in microbiota–gut–brain communication. *Nat. Rev. Gastroenterol. Hepatol*. 2019;16(8):461-478. https://doi.org/10.1038/s41575-019-0157-3
40. Dinan, T.G.&Cryan, J.F. Gut-brain axis in 2016: Brain-gut-microbiota axis - mood, metabolism and behaviour. *Nat. Rev. Gastroenterol. Hepatol*. 2017;14(2):69-70. https://doi.org/10.1038/nrgastro.2016.200
41. Thion, M.S.;Ginhoux, F.&Garel, S. Microglia and early brain development: An intimate journey. *Science*. 2018;362(6411):185-189. https://doi.org/10.1126/science.aat0474
42. Muller, P.A.;Schneeberger, M.;Matheis, F.;Wang, P.;Kerner, Z.;Ilanges, A., et al. Microbiota modulate sympathetic neurons via a gut-brain circuit. *Nature*. 2020;583(7816):441-446. https://doi.org/10.1038/s41586-020-2474-7
43. Bravo, J.A.;Forsythe, P.;Chew, M.V.;Escaravage, E.;Savignac, H.M.;Dinan, T.G., et al. Ingestion of Lactobacillus strain regulates emotional behavior and central GABA receptor expression in a mouse via the vagus nerve. *Proc. Natl. Acad. Sci. USA*. 2011;108(38):16050-16055. https://doi.org/10.1073/pnas.1102999108
44. Yano, Jessica M.;Yu, K.;Donaldson, Gregory P.;Shastri, Gauri G.;Ann, P.;Ma, L., et al. Indigenous bacteria from the gut microbiota regulate host serotonin biosynthesis. *Cell*. 2015;163(1):258. https://doi.org/10.1016/j.cell.2015.02.047
45. Christiansen, C.B.;Gabe, M.B.N.;Svendsen, B.;Dragsted, L.O.;Rosenkilde, M.M.&Holst, J.J. The impact of short-chain fatty acids on GLP-1 and PYY secretion from the isolated perfused rat colon. *Am. J. Physiol. Gastrointest. Liver Physiol*. 2018;315(1):G53-G65. https://doi.org/10.1152/ajpgi.00346.2017
46. Samuel, B.S.;Shaito, A.;Motoike, T.;Rey, F.E.;Backhed, F.;Manchester, J.K., et al. Effects of the gut microbiota on host adiposity are modulated by the short-chain fatty-acid binding G protein-coupled receptor, Gpr41. *Proc. Natl Acad. Sci. USA*. 2008;105(43):16767-16772. https://doi.org/10.1073/pnas.0808567105
47. de Goffau, M.C.;Lager, S.;Sovio, U.;Gaccioli, F.;Cook, E.;Peacock, S.J., et al. Human placenta has no microbiome but can contain potential pathogens. *Nature*. 2019;572(7769):329-334. https://doi.org/10.1038/s41586-019-1451-5
48. Gomez de Agüero, M.;Ganal-Vonarburg, S.C.;Fuhrer, T.;Rupp, S.;Uchimura, Y.;Li, H., et al. The maternal microbiota drives early postnatal innate immune development. *Science*. 2016;351(6279):1296-1302. https://doi.org/10.1126/science.aad2571
49. Sudo, N.;Chida, Y.;Aiba, Y.;Sonoda, J.;Oyama, N.;Yu, X.N., et al. Postnatal microbial colonization programs the hypothalamic–pituitary–adrenal system for stress response in mice. *J. Physiol*. 2004;558(1):263-275. https://doi.org/10.1113/jphysiol.2004.063388
50. Heijtz, R.D.;Wang, S.;Anuar, F.;Qian, Y.;Bjorkholm, B.;Samuelsson, A., et al. Normal gut microbiota modulates brain development and behavior. *Proc. Natl. Acad. Sci. USA*. 2011;108(7):3047-3052. https://doi.org/10.1073/pnas.1010529108
51. Li, Y.;Toothaker, J.M.;Ben-Simon, S.;Ozeri, L.;Schweitzer, R.;McCourt, B.T., et al. In utero human intestine harbors unique metabolome, including bacterial metabolites. *JCI Insight*. 2020;5(21). https://doi.org/10.1172/jci.insight.138751
52. Donald, K.&Finlay, B.B. Early-life interactions between the microbiota and immune system: impact on immune system

development and atopic disease. *Nat. Rev. Immunol*. 2023;23(11):735-748. https://doi.org/10.1038/s41577-023-00874-w

53. Desbonnet, L.;Clarke, G.;Traplin, A.;O'Sullivan, O.;Crispie, F.;Moloney, R.D., et al. Gut microbiota depletion from early adolescence in mice: Implications for brain and behaviour. *Brain. Behav. Immun*. 2015;48:165-173. https://doi.org/10.1016/j.bbi.2015.04.004
54. Ghosh, T.S.;Shanahan, F.&O'Toole, P.W. The gut microbiome as a modulator of healthy ageing. *Nat. Rev. Gastroenterol. Hepatol*. 2022;19(9):565-584. https://doi.org/10.1038/s41575-022-00605-x
55. Morais, L.H.;Schreiber, H.L.&Mazmanian, S.K. The gut microbiota-brain axis in behaviour and brain disorders. *Nat. Rev. Microbiol*. 2021;19(4):241-255. https://doi.org/10.1038/s41579-020-00460-0
56. Sampson, T.R.;Debelius, J.W.;Thron, T.;Janssen, S.;Shastri, G.G.;Ilhan, Z.E., et al. Gut Microbiota Regulate Motor Deficits and Neuroinflammation in a Model of Parkinson's Disease. *Cell*. 2016;167(6):1469-1480.e1412. https://doi.org/10.1016/j.cell.2016.11.018
57. Rao, M.&Gershon, M.D. The bowel and beyond: the enteric nervous system in neurological disorders. *Nat. Rev. Gastroenterol. Hepatol*. 2016;13(9):517-528. https://doi.org/10.1038/nrgastro.2016.107
58. Ye, L.;Bae, M.;Cassilly, C.D.;Jabba, S.V.;Thorpe, D.W.;Martin, A.M., et al. Enteroendocrine cells sense bacterial tryptophan catabolites to activate enteric and vagal neuronal pathways. *Cell Host Microbe*. 2021;29(2):179-196.e179. https://doi.org/10.1016/j.chom.2020.11.011
59. Kaelberer, M.M.;Buchanan, K.L.;Klein, M.E.;Barth, B.B.;Montoya, M.M.;Shen, X., et al. A gut-brain neural circuit for nutrient sensory transduction. *Science*. 2018;361(6408). https://doi.org/10.1126/science.aat5236
60. Siopi, E.;Galerne, M.;Rivagorda, M.;Saha, S.;Moigneu, C.;Moriceau, S., et al. Gut microbiota changes require vagus nerve integrity to promote depressive-like behaviors in mice. *Mol. Psychiatry*. 2023;28(7):3002-3012. https://doi.org/10.1038/s41380-023-02071-6
61. Hosoi, T.;Okuma, Y.&Nomura, Y. Electrical stimulation of afferent vagus nerve induces IL-1beta expression in the brain and activates HPA axis. *Am. J. Physiol. Regul. Integr. Comp. Physiol*. 2000;279(1):R141-147. https://doi.org/10.1152/ajpregu.2000.279.1.R141
62. Clarke, G.;Stilling, R.M.;Kennedy, P.J.;Stanton, C.;Cryan, J.F.&Dinan, T.G. Minireview: Gut Microbiota: The Neglected Endocrine Organ. *Mol. Endocrinol*. 2014;28(8):1221-1238. https://doi.org/10.1210/me.2014-1108
63. De Vadder, F.;Grasset, E.;Manneras Holm, L.;Karsenty, G.;Macpherson, A.J.;Olofsson, L.E., et al. Gut microbiota regulates maturation of the adult enteric nervous system via enteric serotonin networks. *Proc. Natl. Acad. Sci. USA*. 2018;115(25):6458-6463. https://doi.org/10.1073/pnas.1720017115
64. Batterham, R.L.;Cowley, M.A.;Small, C.J.;Herzog, H.;Cohen, M.A.;Dakin, C.L., et al. Gut hormone PYY(3-36) physiologically inhibits food intake. *Nature*. 2002;418(6898):650-654. https://doi.org/10.1038/nature00887
65. Batterham, R.L.;ffytche, D.H.;Rosenthal, J.M.;Zelaya, F.O.;Barker, G.J.;Withers, D.J., et al. PYY modulation of cortical and hypothalamic brain areas predicts feeding behaviour in humans. *Nature*. 2007;450(7166):106-109. https://doi.org/10.1038/nature06212
66. Trapp, S.&Brierley, D.I. Brain GLP-1 and the regulation of food intake: GLP-1 action in the brain and its implications for GLP-1 receptor agonists in obesity treatment. *Br. J. Pharmacol*. 2022;179(4):557-570. https://doi.org/10.1111/bph.15638
67. Hyland, N.P.&Cryan, J.F. Microbe-host interactions: Influence of the gut microbiota on the enteric nervous system. *Dev. Biol*. 2016;417(2):182-187. https://doi.org/10.1016/j.ydbio.2016.06.027
68. Anitha, M.;Vijay-Kumar, M.;Sitaraman, S.V.;Gewirtz, A.T.&Srinivasan, S. Gut microbial products regulate murine gastrointestinal motility via Toll-like receptor 4 signaling. *Gastroenterology*. 2012;143(4):1006-1016 e1004. https://doi.org/10.1053/j.gastro.2012.06.034
69. Yarandi, S.S.;Kulkarni, S.;Saha, M.;Sylvia, K.E.;Sears, C.L.&Pasricha, P.J. Intestinal Bacteria Maintain Adult Enteric Nervous

System and Nitrergic Neurons via Toll-like Receptor 2-induced Neurogenesis in Mice. *Gastroenterology*. 2020;159(1):200-213 e208. https://doi.org/10.1053/j.gastro.2020.03.050

70. Gensollen, T.;Iyer, S.S.;Kasper, D.L.&Blumberg, R.S. How colonization by microbiota in early life shapes the immune system. *Science*. 2016;352(6285):539-544. https://doi.org/10.1126/science.aad9378
71. Thion, M.S.;Low, D.;Silvin, A.;Chen, J.;Grisel, P.;Schulte-Schrepping, J., et al. Microbiome Influences Prenatal and Adult Microglia in a Sex-Specific Manner. *Cell*. 2018;172(3):500-516.e516. https://doi.org/10.1016/j.cell.2017.11.042
72. Brachman, R.A.;Lehmann, M.L.;Maric, D.&Herkenham, M. Lymphocytes from chronically stressed mice confer antidepressant-like effects to naive mice. *J. Neurosci*. 2015;35(4):1530-1538. https://doi.org/10.1523/JNEUROSCI.2278-14.2015
73. Smith, P.M.;Howitt, M.R.;Panikov, N.;Michaud, M.;Gallini, C.A.;Bohlooly, Y.M., et al. The microbial metabolites, short-chain fatty acids, regulate colonic Treg cell homeostasis. *Science*. 2013;341(6145):569-573. https://doi.org/10.1126/science.1241165
74. Bilbo, S.D.&Schwarz, J.M. The immune system and developmental programming of brain and behavior. *Front. Neuroendocrinol*. 2012;33(3):267-286. https://doi.org/10.1016/j.yfrne.2012.08.006
75. Da Mesquita, S.;Fu, Z.&Kipnis, J. The Meningeal Lymphatic System: A New Player in Neurophysiology. *Neuron*. 2018;100(2):375-388. https://doi.org/10.1016/j.neuron.2018.09.022
76. Kern, L.;Mastandrea, I.;Melekhova, A.&Elinav, E. Mechanisms by which microbiome-derived metabolites exert their impacts on neurodegeneration. *Cell Chem. Biol*. 2025;32(1):25-45. https://doi.org/10.1016/j.chembiol.2024.08.014
77. Erny, D.;Hrabě de Angelis, A.L.;Jaitin, D.;Wieghofer, P.;Staszewski, O.;David, E., et al. Host microbiota constantly control maturation and function of microglia in the CNS. *Nat. Neurosci*. 2015;18(7):965-977. https://doi.org/10.1038/nn.4030
78. Worheide, M.A.;Krumsiek, J.;Kastenmuller, G.&Arnold, M. Multi-omics integration in biomedical research - A metabolomics-centric review. *Anal. Chim. Acta*. 2021;1141:144-162. https://doi.org/10.1016/j.aca.2020.10.038
79. Lamichhane, S.;Sen, P.;Dickens, A.M.;Oresic, M.&Bertram, H.C. Gut metabolome meets microbiome: A methodological perspective to understand the relationship between host and microbe. *Methods*. 2018;149:3-12. https://doi.org/10.1016/j.ymeth.2018.04.029
80. Fraga-Corral, M.;Carpena, M.;Garcia-Oliveira, P.;Pereira, A.G.;Prieto, M.A.&Simal-Gandara, J. Analytical Metabolomics and Applications in Health, Environmental and Food Science. *Crit. Rev. Anal. Chem*. 2022;52(4):712-734. https://doi.org/10.1080/10408347.2020.1823811
81. MahmoudianDehkordi, S.;Arnold, M.;Nho, K.;Ahmad, S.;Jia, W.;Xie, G., et al. Altered bile acid profile associates with cognitive impairment in Alzheimer's disease-An emerging role for gut microbiome. *Alzheimers Dement*. 2019;15(1):76-92. https://doi.org/10.1016/j.jalz.2018.07.217
82. St John-Williams, L.;Blach, C.;Toledo, J.B.;Rotroff, D.M.;Kim, S.;Klavins, K., et al. Targeted metabolomics and medication classification data from participants in the ADNI1 cohort. *Sci. Data*. 2017;4:170140. https://doi.org/10.1038/sdata.2017.140
83. Zhou, Y.;Zheng, W.;Liu, W.;Wang, C.;Zhan, Y.;Li, H., et al. Cross-sectional relationship between kynurenine pathway metabolites and cognitive function in major depressive disorder. *Psychoneuroendocrinology*. 2019;101:72-79. https://doi.org/10.1016/j.psyneuen.2018.11.001
84. Caspani, G.;Harvey, M.&Swann, J.R. Metabolomics and the Gut–Brain Axis. In: Hyland NP, Stanton C, editors. The Gut-Brain Axis: Dietary, Probiotic, and Prebiotic Interventions on the Microbiota: Elsevier; 2023. p. 455-484.
85. Pessa-Morikawa, T.;Husso, A.;Kärkkäinen, O.;Koistinen, V.;Hanhineva, K.;Iivanainen, A., et al. Maternal microbiota-derived metabolic profile in fetal murine intestine, brain and placenta. *BMC Microbiol*. 2021;22(1):46. https://doi.org/https://doi.org/10.1186/s12866-022-02457-6
86. Needham, B.D.;Adame, M.D.;Serena, G.;Rose, D.R.;Preston, G.M.;Conrad, M.C., et al. Plasma and Fecal Metabolite Profiles in Autism Spectrum Disorder. *Biol. Psychiatry*. 2021;89(5):451-462.

https://doi.org/10.1016/j.biopsych.2020.09.025
87. Zarei, I.;Koistinen, V.M.;Kokla, M.;Klavus, A.;Babu, A.F.;Lehtonen, M., et al. Tissue-wide metabolomics reveals wide impact of gut microbiota on mice metabolite composition. *Sci. Rep*. 2022;12(1):15018. https://doi.org/10.1038/s41598-022-19327-w
88. Hulme, H.;Meikle, L.M.;Strittmatter, N.;Hooft, v.d.J.J.J.;Swales, J.;Bragg, R.A., et al. Microbiome-derived carnitine mimics as previously unknown mediators of gut-brain axis communication. *Sci. Adv*. 2020;6(11):eaax6328. https://doi.org/10.1126/sciadv.aax6328
89. Wishart, D.S.;Cheng, L.L.;Copie, V.;Edison, A.S.;Eghbalnia, H.R.;Hoch, J.C., et al. NMR and Metabolomics-A Roadmap for the Future. *Metabolites*. 2022;12(8). https://doi.org/10.3390/metabo12080678
90. Deda, O.;Gika, H.G.;Wilson, I.D.&Theodoridis, G.A. An overview of fecal sample preparation for global metabolic profiling. *J. Pharm. Biomed. Anal*. 2015;113:137-150. https://doi.org/10.1016/j.jpba.2015.02.006
91. Chaleckis, R.;Meister, I.;Zhang, P.&Wheelock, C.E. Challenges, progress and promises of metabolite annotation for LC-MS-based metabolomics. *Curr. Opin. Biotechnol*. 2019;55:44-50. https://doi.org/10.1016/j.copbio.2018.07.010
92. Brunius, C.;Shi, L.&Landberg, R. Large-scale untargeted LC-MS metabolomics data correction using between-batch feature alignment and cluster-based within-batch signal intensity drift correction. *Metabolomics*. 2016;12(11):173. https://doi.org/10.1007/s11306-016-1124-4
93. Kokla, M.;Virtanen, J.;Kolehmainen, M.;Paananen, J.&Hanhineva, K. Random forest-based imputation outperforms other methods for imputing LC-MS metabolomics data: a comparative study. *BMC Bioinformatics*. 2019;20(1):492. https://doi.org/10.1186/s12859-019-3110-0
94. Wishart, D.S.;Guo, A.;Oler, E.;Wang, F.;Anjum, A.;Peters, H., et al. HMDB 5.0: the Human Metabolome Database for 2022. *Nucleic Acids Res*. 2022;50(D1):D622-D631. https://doi.org/10.1093/nar/gkab1062
95. Wikoff, W.R.;Anfora, A.T.;Liu, J.;Schultz, P.G.;Lesley, S.A.;Peters, E.C., et al. Metabolomics analysis reveals large effects of gut microflora on mammalian blood metabolites. *Proc. Natl. Acad. Sci. USA*. 2009;106(10):3698-3703.
96. Jansen, R.;Milaneschi, Y.;Schranner, D.;Kastenmuller, G.;Arnold, M.;Han, X., et al. The metabolome-wide signature of major depressive disorder. *Mol. Psychiatry*. 2024;29(12):3722-3733. https://doi.org/10.1038/s41380-024-02613-6
97. van der Velpen, V.;Teav, T.;Gallart-Ayala, H.;Mehl, F.;Konz, I.;Clark, C., et al. Systemic and central nervous system metabolic alterations in Alzheimer's disease. *Alzheimers Res. Ther*. 2019;11(1):93. https://doi.org/10.1186/s13195-019-0551-7
98. Ahrens, A.P.;Hyotylainen, T.;Petrone, J.R.;Igelstrom, K.;George, C.D.;Garrett, T.J., et al. Infant microbes and metabolites point to childhood neurodevelopmental disorders. *Cell*. 2024;187(8):1853-1873 e1815. https://doi.org/10.1016/j.cell.2024.02.035
99. Zuffa, S.;Schmid, R.;Bauermeister, A.;PW, P.G.;Caraballo-Rodriguez, A.M.;El Abiead, Y., et al. microbeMASST: a taxonomically informed mass spectrometry search tool for microbial metabolomics data. *Nat. Microbiol*. 2024;9(2):336-345. https://doi.org/10.1038/s41564-023-01575-9
100. Mohanty, I.;Mannochio-Russo, H.;Schweer, J.V.;El Abiead, Y.;Bittremieux, W.;Xing, S., et al. The underappreciated diversity of bile acid modifications. *Cell*. 2024;187(7):1801-1818 e1820. https://doi.org/10.1016/j.cell.2024.02.019
101. Gentry, E.C.;Collins, S.L.;Panitchpakdi, M.;Belda-Ferre, P.;Stewart, A.K.;Carrillo Terrazas, M., et al. Reverse metabolomics for the discovery of chemical structures from humans. *Nature*. 2024;626(7998):419-426. https://doi.org/10.1038/s41586-023-06906-8
102. Dougherty, M.W.;Kudin, O.;Mühlbauer, M.;Neu, J.;Gharaibeh, R.Z.&Jobin, C. Gut microbiota maturation during early human life induces enterocyte proliferation via microbial metabolites. *BMC Microbiol*. 2020;20(1):205. https://doi.org/10.1186/s12866-020-01892-7
103. Kaiko, G.E.;Ryu, S.H.;Koues, O.I.;Collins, P.L.;Solnica-Krezel, L.;Pearce, E.J., et al. The Colonic Crypt Protects Stem Cells from Microbiota-Derived Metabolites. *Cell*. 2016;165(7):1708-1720. https://doi.org/10.1016/j.cell.2016.05.018

104. De Angelis, M.;Piccolo, M.;Vannini, L.;Siragusa, S.;De Giacomo, A.;Serrazzanetti, D.I., et al. Fecal microbiota and metabolome of children with autism and pervasive developmental disorder not otherwise specified. *PLoS One*. 2013;8(10):e76993. https://doi.org/10.1371/journal.pone.0076993
105. Altieri, L.;Neri, C.;Sacco, R.;Curatolo, P.;Benvenuto, A.;Muratori, F., et al. Urinary p-cresol is elevated in small children with severe autism spectrum disorder. *Biomarkers*. 2011;16(3):252-260. https://doi.org/10.3109/1354750X.2010.548010
106. Sharon, G.;Cruz, N.J.;Kang, D.-W.;Gandal, M.J.;Wang, B.;Kim, Y.-M., et al. Human Gut Microbiota from Autism Spectrum Disorder Promote Behavioral Symptoms in Mice. *Cell*. 2019;177(6):1600-1618.e1617. https://doi.org/10.1016/j.cell.2019.05.004
107. Liu, X.;Li, X.;Xia, B.;Jin, X.;Zou, Q.;Zeng, Z., et al. High-fiber diet mitigates maternal obesity-induced cognitive and social dysfunction in the offspring via gut-brain axis. *Cell Metab*. 2021;33(5):923-938.e926. https://doi.org/10.1016/j.cmet.2021.02.002
108. Chu, C.;Murdock, M.H.;Jing, D.;Won, T.H.;Chung, H.;Kressel, A.M., et al. The microbiota regulate neuronal function and fear extinction learning. *Nature*. 2019;574(7779):543-548. https://doi.org/10.1038/s41586-019-1644-y
109. Matsumoto, M.;Kibe, R.;Ooga, T.;Aiba, Y.;Sawaki, E.;Koga, Y., et al. Cerebral Low-Molecular Metabolites Influenced by Intestinal Microbiota: A Pilot Study. *Front. Syst. Neurosci*. 2013;7:9. https://doi.org/10.3389/fnsys.2013.00009
110. Serger, E.;Luengo-Gutierrez, L.;Chadwick, J.S.;Kong, G.;Zhou, L.;Crawford, G., et al. The gut metabolite indole-3 propionate promotes nerve regeneration and repair. *Nature*. 2022;607(7919):585-592. https://doi.org/10.1038/s41586-022-04884-x
111. Wei, G.Z.;Martin, K.A.;Xing, P.Y.;Agrawal, R.;Whiley, L.;Wood, T.K., et al. Tryptophan-metabolizing gut microbes regulate adult neurogenesis via the aryl hydrocarbon receptor. *Proc. Natl. Acad. Sci. USA*. 2021;118(27):e2021091118. https://doi.org/10.1073/pnas.2021091118
112. Dodd, D.;Spitzer, M.H.;Van Treuren, W.;Merrill, B.D.;Hryckowian, A.J.;Higginbottom, S.K., et al. A gut bacterial pathway metabolizes aromatic amino acids into nine circulating metabolites. *Nature*. 2017;551(7682):648-652. https://doi.org/10.1038/nature24661
113. Özoğul, F.;Kuley, E.;Özoğul, Y.&Özoğul, İ. The Function of Lactic Acid Bacteria on Biogenic Amines Production by Food-Borne Pathogens in Arginine Decarboxylase Broth. *Food Sci. Technol. Res*. 2012;18(6):795-804. https://doi.org/10.3136/fstr.18.795
114. Valles-Colomer, M.;Falony, G.;Darzi, Y.;Tigchelaar, E.F.;Wang, J.;Tito, R.Y., et al. The neuroactive potential of the human gut microbiota in quality of life and depression. *Nat. Microbiol*. 2019;4(4):623-632. https://doi.org/10.1038/s41564-018-0337-x
115. Bhattarai, Y.;Williams, B.B.;Battaglioli, E.J.;Whitaker, W.R.;Till, L.;Grover, M., et al. Gut Microbiota-Produced Tryptamine Activates an Epithelial G-Protein-Coupled Receptor to Increase Colonic Secretion. *Cell Host Microbe*. 2018;23(6):775-785.e775. https://doi.org/10.1016/j.chom.2018.05.004
116. Reigstad, C.S.;Salmonson, C.E.;Rainey, J.F.;Szurszewski, J.H.;Linden, D.R.;Sonnenburg, J.L., et al. Gut microbes promote colonic serotonin production through an effect of short-chain fatty acids on enterochromaffin cells. *FASEB J*. 2015;29(4):1395-1403. https://doi.org/10.1096/fj.14-259598
117. Bellono, N.W.;Bayrer, J.R.;Leitch, D.B.;Castro, J.;Zhang, C.;O'Donnell, T.A., et al. Enterochromaffin Cells Are Gut Chemosensors that Couple to Sensory Neural Pathways. *Cell*. 2017;170(1):185-198.e116. https://doi.org/10.1016/j.cell.2017.05.034
118. Chimerel, C.;Emery, E.;Summers, David K.;Keyser, U.;Gribble, Fiona M.&Reimann, F. Bacterial Metabolite Indole Modulates Incretin Secretion from Intestinal Enteroendocrine L Cells. *Cell Rep*. 2014;9(4):1202-1208. https://doi.org/10.1016/j.celrep.2014.10.032
119. Nøhr, M.K.;Egerod, K.L.;Christiansen, S.H.;Gille, A.;Offermanns, S.;Schwartz, T.W., et al. Expression of the short chain fatty acid receptor GPR41/FFAR3 in autonomic and somatic sensory ganglia. *Neuroscience*. 2015;290:126-137. https://doi.org/10.1016/j.neuroscience.2015.01.040
120. Tolhurst, G.;Heffron, H.;Lam, Y.S.;Parker, H.E.;Habib, A.M.;Diakogiannaki, E., et al.

Short-Chain Fatty Acids Stimulate Glucagon-Like Peptide-1 Secretion via the G-Protein-Coupled Receptor FFAR2. *Diabetes*. 2012;61(2):364-371. https://doi.org/10.2337/db11-1019

121. Jaglin, M.;Rhimi, M.;Philippe, C.;Pons, N.;Bruneau, A.;Goustard, B., et al. Indole, a Signaling Molecule Produced by the Gut Microbiota, Negatively Impacts Emotional Behaviors in Rats. *Front. Neurosci*. 2018;12:216. https://doi.org/10.3389/fnins.2018.00216
122. Constante, M.;De Palma, G.;Lu, J.;Jury, J.;Rondeau, L.;Caminero, A., et al. Saccharomyces boulardii CNCM I-745 modulates the microbiota-gut-brain axis in a humanized mouse model of Irritable Bowel Syndrome. *Neurogastroenterol. Motil*. 2020;33(3):e13985. https://doi.org/10.1111/nmo.13985
123. Yu, W.;Xiao, Y.;Jayaraman, A.;Yen, Y.C.;Lee, H.U.;Pettersson, S., et al. Microbial metabolites tune amygdala neuronal hyperexcitability and anxiety-linked behaviors. *EMBO Mol. Med*. 2025;17(2):249-264. https://doi.org/10.1038/s44321-024-00179-y
124. Barandouzi, Z.A.;Lee, J.;Del Carmen Rosas, M.;Chen, J.;Henderson, W.A.;Starkweather, A.R., et al. Associations of neurotransmitters and the gut microbiome with emotional distress in mixed type of irritable bowel syndrome. *Sci. Rep*. 2022;12(1):1648. https://doi.org/10.1038/s41598-022-05756-0
125. van de Wouw, M.;Boehme, M.;Lyte, J.M.;Wiley, N.;Strain, C.;O'Sullivan, O., et al. Short-chain fatty acids: microbial metabolites that alleviate stress-induced brain-gut axis alterations. *J. Physiol*. 2018;596(20):4923-4944. https://doi.org/10.1113/jp276431
126. Matsumoto, M.;Kibe, R.;Ooga, T.;Aiba, Y.;Kurihara, S.;Sawaki, E., et al. Impact of Intestinal Microbiota on Intestinal Luminal Metabolome. *Sci. Rep*. 2012;2(1):233. https://doi.org/10.1038/srep00233
127. Potter, M.C.;Elmer, G.I.;Bergeron, R.;Albuquerque, E.X.;Guidetti, P.;Wu, H.-Q., et al. Reduction of Endogenous Kynurenic Acid Formation Enhances Extracellular Glutamate, Hippocampal Plasticity, and Cognitive Behavior. *Neuropsychopharmacology*. 2010;35(8):1734-1742. https://doi.org/10.1038/npp.2010.39
128. Pocivavsek, A.;Wu, H.-Q.;Potter, M.C.;Elmer, G.I.;Pellicciari, R.&Schwarcz, R. Fluctuations in Endogenous Kynurenic Acid Control Hippocampal Glutamate and Memory. *Neuropsychopharmacology*. 2011;36(11):2357-2367. https://doi.org/10.1038/npp.2011.127
129. Chess, A.C.;Simoni, M.K.;Alling, T.E.&Bucci, D.J. Elevations of Endogenous Kynurenic Acid Produce Spatial Working Memory Deficits. *Schizophr. Bull*. 2007;33(3):797-804. https://doi.org/10.1093/schbul/sbl033
130. Zheng, P.;Zeng, B.;Liu, M.;Chen, J.;Pan, J.;Han, Y., et al. The gut microbiome from patients with schizophrenia modulates the glutamate-glutamine-GABA cycle and schizophrenia-relevant behaviors in mice. *Sci. Adv*. 2019;5(2):eaau8317. https://doi.org/10.1126/sciadv.aau8317
131. Takahama, K.;Hashimoto, T.;Wang, M.W.;Akaike, N.;Hitoshi, T.;Okano, Y., et al. Pipecolic acid enhancement of GABA response in single neurons of rat brain. *Neuropharmacology*. 1986;25(3):339-342. https://doi.org/10.1016/0028-3908(86)90263-7
132. Bernasconi, R.;Jones, R.S.;Bittiger, H.;Olpe, H.R.;Heid, J.;Martin, P., et al. Dose pipecolic acid interact with the central GABA-ergic system? *J. Neural Transm*. 1986;67(3-4):175.
133. Mao, J.-H.;Kim, Y.-M.;Zhou, Y.-X.;Hu, D.;Zhong, C.;Chang, H., et al. Genetic and metabolic links between the murine microbiome and memory. *Microbiome*. 2020;8(1):53. https://doi.org/10.1186/s40168-020-00817-w
134. O'Hagan, C.;Li, J.V.;Marchesi, J.R.;Plummer, S.;Garaiova, I.&Good, M.A. Long-term multi-species Lactobacillus and Bifidobacterium dietary supplement enhances memory and changes regional brain metabolites in middle-aged rats. *Neurobiol. Learn Mem*. 2017;144:36-47. https://doi.org/10.1016/j.nlm.2017.05.015
135. El Hayek, L.;Khalifeh, M.;Zibara, V.;Abi Assaad, R.;Emmanuel, N.;Karnib, N., et al. Lactate Mediates the Effects of Exercise on Learning and Memory through SIRT1-Dependent Activation of Hippocampal Brain-Derived Neurotrophic Factor (BDNF). *J. Neurosci*. 2019;39(13):2369-2382. https://doi.org/10.1523/JNEUROSCI.1661-18.2019

136. Tevzadze, G.;Tevzadze, G.;Oniani, N.;Oniani, N.;Zhuravliova, E.;Zhuravliova, E., et al. Effects of a Gut Microbiome Toxin, p-Cresol, on the Indices of Social Behavior in Rats. *Neurophysiology*. 2018;50(5):372-377. https://doi.org/10.1007/s11062-019-09764-1
137. Pascucci, T.;Colamartino, M.;Fiori, E.;Sacco, R.;Coviello, A.;Ventura, R., et al. P-cresol Alters Brain Dopamine Metabolism and Exacerbates Autism-Like Behaviors in the BTBR Mouse. *Brain Sci*. 2020;10(4):233. https://doi.org/10.3390/brainsci10040233
138. Bermudez-Martin, P.;Becker, J.A.J.;Caramello, N.;Fernandez, S.P.;Costa-Campos, R.;Canaguier, J., et al. The microbial metabolite p-Cresol induces autistic-like behaviors in mice by remodeling the gut microbiota. *Microbiome*. 2021;9(1):157. https://doi.org/10.1186/s40168-021-01103-z
139. Laudani, S.;Torrisi, S.A.;Alboni, S.;Bastiaanssen, T.F.S.;Benatti, C.;Rivi, V., et al. Gut microbiota alterations promote traumatic stress susceptibility associated with p-cresol-induced dopaminergic dysfunctions. *Brain Behav. Immun*. 2023;107:385-396. https://doi.org/10.1016/j.bbi.2022.11.004
140. Dell'Osso, L.;Carmassi, C.;Mucci, F.&Marazziti, D. Depression, Serotonin and Tryptophan. *Curr. Pharm. Des*. 2016;22(8):949-954. https://doi.org/10.2174/1381612822666151214104826
141. Marcinkiewcz, C.A.;Lowery-Gionta, E.G.&Kash, T.L. Serotonin's Complex Role in Alcoholism: Implications for Treatment and Future Research. *Alcohol Clin. Exp. Res*. 2016;40(6):1192-1201. https://doi.org/10.1111/acer.13076
142. Wong, A.C.;Devason, A.S.;Umana, I.C.;Cox, T.O.;Dohnalova, L.;Litichevskiy, L., et al. Serotonin reduction in post-acute sequelae of viral infection. *Cell*. 2023;186(22):4851-4867 e4820. https://doi.org/10.1016/j.cell.2023.09.013
143. Keski-Rahkonen, P.;Kolehmainen, M.;Lappi, J.;Micard, V.;Jokkala, J.;Rosa-Sibakov, N., et al. Decreased plasma serotonin and other metabolite changes in healthy adults after consumption of wholegrain rye: an untargeted metabolomics study. *Am. J. Clin. Nutr*. 2019;109(6):1630-1639. https://doi.org/10.1093/ajcn/nqy394
144. Pu, J.;Liu, Y.;Zhang, H.;Tian, L.;Gui, S.;Yu, Y., et al. An integrated meta-analysis of peripheral blood metabolites and biological functions in major depressive disorder. *Mol. Psychiatry*. 2020;26(8):4265-4276. https://doi.org/10.1038/s41380-020-0645-4
145. Gao, K.;Mu, C.-l.;Farzi, A.&Zhu, W.-y. Tryptophan Metabolism: A Link Between the Gut Microbiota and Brain. *Adv. Nutr*. 2020;11(3):709-723. https://doi.org/10.1093/advances/nmz127
146. Arnoriaga-Rodríguez, M.;Mayneris-Perxachs, J.;Burokas, A.;Contreras-Rodríguez, O.;Blasco, G.;Coll, C., et al. Obesity Impairs Short-Term and Working Memory through Gut Microbial Metabolism of Aromatic Amino Acids. *Cell Metab*. 2020;32(4):548-560.e547. https://doi.org/10.1016/j.cmet.2020.09.002
147. Philippe, C.;Szabo de Edelenyi, F.;Naudon, L.;Druesne-Pecollo, N.;Hercberg, S.;Kesse-Guyot, E., et al. Relation between Mood and the Host-Microbiome Co-Metabolite 3-Indoxylsulfate: Results from the Observational Prospective NutriNet-Santé Study. *Microorganisms*. 2021;9(4):716. https://doi.org/10.3390/microorganisms9040716
148. Brydges, C.R.;Fiehn, O.;Mayberg, H.S.;Schreiber, H.;Dehkordi, S.M.;Bhattacharyya, S., et al. Indoxyl sulfate, a gut microbiome-derived uremic toxin, is associated with psychic anxiety and its functional magnetic resonance imaging-based neurologic signature. *Sci. Rep*. 2021;11(1):21011. https://doi.org/10.1038/s41598-021-99845-1
149. Rudzki, L.;Ostrowska, L.;Pawlak, D.;Małus, A.;Pawlak, K.;Waszkiewicz, N., et al. Probiotic Lactobacillus Plantarum 299v decreases kynurenine concentration and improves cognitive functions in patients with major depression: A double-blind, randomized, placebo controlled study. *Psychoneuroendocrinology*. 2019;100:213-222. https://doi.org/10.1016/j.psyneuen.2018.10.010
150. Xu, R.&Wang, Q. Towards understanding brain-gut-microbiome connections in Alzheimer's disease. *BMC Syst. Biol*. 2016;10(Suppl 3):63. https://doi.org/10.1186/s12918-016-0307-y
151. Obermeier, B.;Daneman, R.&Ransohoff, R.M. Development, maintenance and disruption of the blood-brain barrier. *Nat.*

*Med*. 2013;19(12):1584-1596. https://doi.org/10.1038/nm.3407

152. Aburto, M.R.&Cryan, J.F. Gastrointestinal and brain barriers: unlocking gates of communication across the microbiota-gut-brain axis. *Nat. Rev. Gastroenterol. Hepatol*. 2024;21(4):222-247. https://doi.org/10.1038/s41575-023-00890-0
153. Kärkkäinen, O.;Kokla, M.;Lehtonen, M.;Auriola, S.;Martiskainen, M.;Tiihonen, J., et al. Changes in the metabolic profile of human male postmortem frontal cortex and cerebrospinal fluid samples associated with heavy alcohol use. *Addict. Biol*. 2021;26(6):e13035. https://doi.org/10.1111/adb.13035
154. Baloni, P.;Funk, C.C.;Yan, J.;Yurkovich, J.T.;Kueider-Paisley, A.;Nho, K., et al. Metabolic Network Analysis Reveals Altered Bile Acid Synthesis and Metabolism in Alzheimer's Disease. *Cell Rep. Med*. 2020;1(8):100138. https://doi.org/10.1016/j.xcrm.2020.100138
155. Marksteiner, J.;Blasko, I.;Kemmler, G.;Koal, T.&Humpel, C. Bile acid quantification of 20 plasma metabolites identifies lithocholic acid as a putative biomarker in Alzheimer's disease. *Metabolomics*. 2018;14(1):1-10. https://doi.org/10.1007/s11306-017-1297-5
156. Heinken, A.;Ravcheev, D.A.;Baldini, F.;Heirendt, L.;Fleming, R.M.T.&Thiele, I. Systematic assessment of secondary bile acid metabolism in gut microbes reveals distinct metabolic capabilities in inflammatory bowel disease. *Microbiome*. 2019;7(1):75. https://doi.org/10.1186/s40168-019-0689-3
157. Braniste, V.;Al-Asmakh, M.;Kowal, C.;Anuar, F.;Abbaspour, A.;Toth, M., et al. The gut microbiota influences blood-brain barrier permeability in mice. *Sci. Transl. Med*. 2014;6(263):263ra158. https://doi.org/10.1126/scitranslmed.3009759
158. Li, H.;Sun, J.;Wang, F.;Ding, G.;Chen, W.;Fang, R., et al. Sodium butyrate exerts neuroprotective effects by restoring the blood–brain barrier in traumatic brain injury mice. *Brain Res*. 2016;1642:70-78. https://doi.org/10.1016/j.brainres.2016.03.031
159. Hoyles, L.;Snelling, T.;Umlai, U.-K.;Nicholson, J.K.;Carding, S.R.;Glen, R.C., et al. Microbiome-host systems interactions: protective effects of propionate upon the blood-brain barrier. *Microbiome*. 2018;6(1):55. https://doi.org/10.1186/s40168-018-0439-y
160. Xie, J.;Bruggeman, A.;De Nolf, C.;Vandendriessche, C.;Van Imschoot, G.;Van Wonterghem, E., et al. Gut microbiota regulates blood-cerebrospinal fluid barrier function and Abeta pathology. *EMBO J*. 2023;42(17):e111515. https://doi.org/10.15252/embj.2022111515
161. Quinn, M.;McMillin, M.;Galindo, C.;Frampton, G.;Pae, H.Y.&DeMorrow, S. Bile acids permeabilize the blood brain barrier after bile duct ligation in rats via Rac1-dependent mechanisms. *Dig. Liver. Dis*. 2014;46(6):527-534. https://doi.org/10.1016/j.dld.2014.01.159
162. Palmela, I.;Correia, L.;Silva, R.F.M.;Sasaki, H.;Kim, K.S.;Brites, D., et al. Hydrophilic bile acids protect human blood-brain barrier endothelial cells from disruption by unconjugated bilirubin: an in vitro study. *Front. Neurosci*. 2015;9:80. https://doi.org/10.3389/fnins.2015.00080
163. Hoyles, L.;Pontifex, M.G.;Rodriguez-Ramiro, I.;Anis-Alavi, M.A.;Jelane, K.S.;Snelling, T., et al. Regulation of blood–brain barrier integrity by microbiome-associated methylamines and cognition by trimethylamine N-oxide. *Microbiome*. 2021;9(1):235. https://doi.org/10.1186/s40168-021-01181-z
164. Stachulski, A.V.;Knausenberger, T.B.;Shah, S.N.;Hoyles, L.&McArthur, S. A host-gut microbial amino acid co-metabolite, p-cresol glucuronide, promotes blood-brain barrier integrity in vivo. *Tissue Barriers*. 2023;11(1):2073175. https://doi.org/10.1080/21688370.2022.2073175
165. Zhao, Q.;Chen, T.;Ni, C.;Hu, Y.;Nan, Y.;Lin, W., et al. Indole-3-propionic Acid Attenuates HI-Related Blood-Brain Barrier Injury in Neonatal Rats by Modulating the PXR Signaling Pathway. *ACS Chem. Neurosci*. 2022;13(19):2897-2912. https://doi.org/10.1021/acschemneuro.2c00418
166. Bobot, M.;Thomas, L.;Moyon, A.;Fernandez, S.;McKay, N.;Balasse, L., et al. Uremic Toxic Blood-Brain Barrier Disruption Mediated by AhR Activation Leads to Cognitive Impairment during Experimental Renal Dysfunction. *J. Am. Soc. Nephrol*. 2020;31(7):1509-1521. https://doi.org/10.1681/ASN.2019070728

167. Matcovitch-Natan, O.;Winter, D.R.;Giladi, A.;Vargas Aguilar, S.;Spinrad, A.;Sarrazin, S., et al. Microglia development follows a stepwise program to regulate brain homeostasis. *Science*. 2016;353(6301):aad8670. https://doi.org/10.1126/science.aad8670
168. Levy, M.;Thaiss, Christoph A.;Zeevi, D.;Dohnalová, L.;Zilberman-Schapira, G.;Mahdi, Jemal A., et al. Microbiota-Modulated Metabolites Shape the Intestinal Microenvironment by Regulating NLRP6 Inflammasome Signaling. *Cell*. 2015;163(6):1428-1443. https://doi.org/10.1016/j.cell.2015.10.048
169. Heneka, M.T.;Carson, M.J.;Khoury, J.E.;Landreth, G.E.;Brosseron, F.;Feinstein, D.L., et al. Neuroinflammation in Alzheimer's disease. *Lancet Neurol*. 2015;14(4):388-405. https://doi.org/https://doi.org/10.1016/S1474-4422(15)70016-5
170. Ransohoff, R.M. How neuroinflammation contributes to neurodegeneration. *Science*. 2016;353(6301):777-783. https://doi.org/10.1126/science.aag2590
171. Salter, M.W.&Stevens, B. Microglia emerge as central players in brain disease. *Nat. Med*. 2017;23(9):1018-1027. https://doi.org/10.1038/nm.4397
172. Haghikia, A.;Jörg, S.;Duscha, A.;Berg, J.;Manzel, A.;Waschbisch, A., et al. Dietary Fatty Acids Directly Impact Central Nervous System Autoimmunity via the Small Intestine. *Immunity*. 2016;44(4):951-953. https://doi.org/10.1016/j.immuni.2016.04.006
173. Shultz, S.R.;Aziz, N.A.B.;Yang, L.;Sun, M.;MacFabe, D.F.&O'Brien, T.J. Intracerebroventricular injection of propionic acid, an enteric metabolite implicated in autism, induces social abnormalities that do not differ between seizure-prone (FAST) and seizure-resistant (SLOW) rats. *Behav. Brain Res*. 2015;278:542-548. https://doi.org/10.1016/j.bbr.2014.10.050
174. Shultz, S.R.;MacFabe, D.F.;Ossenkopp, K.-P.;Scratch, S.;Whelan, J.;Taylor, R., et al. Intracerebroventricular injection of propionic acid, an enteric bacterial metabolic end-product, impairs social behavior in the rat: Implications for an animal model of autism. *Neuropharmacology*. 2008;54(6):901-911. https://doi.org/10.1016/j.neuropharm.2008.01.013
175. MacFabe, D.;Cain, D.;Rodriguez-Capote, K.;Franklin, A.;Hoffman, J.;Boon, F., et al. Neurobiological effects of intraventricular propionic acid in rats: Possible role of short chain fatty acids on the pathogenesis and characteristics of autism spectrum disorders. *Behav. Brain Res*. 2007;176(1):149-169. https://doi.org/10.1016/j.bbr.2006.07.025
176. MacFabe, D.F.;Cain, N.E.;Boon, F.;Ossenkopp, K.-P.&Cain, D.P. Effects of the enteric bacterial metabolic product propionic acid on object-directed behavior, social behavior, cognition, and neuroinflammation in adolescent rats: Relevance to autism spectrum disorder. *Behav. Brain Res*. 2011;217(1):47-54. https://doi.org/10.1016/j.bbr.2010.10.005
177. Erny, D.;Dokalis, N.;Mezö, C.;Castoldi, A.;Mossad, O.;Staszewski, O., et al. Microbiota-derived acetate enables the metabolic fitness of the brain innate immune system during health and disease. *Cell Metab*. 2021;33(11):2260-2276.e2267. https://doi.org/10.1016/j.cmet.2021.10.010
178. Marizzoni, M.;Cattaneo, A.;Mirabelli, P.;Festari, C.;Lopizzo, N.;Nicolosi, V., et al. Short-Chain Fatty Acids and Lipopolysaccharide as Mediators Between Gut Dysbiosis and Amyloid Pathology in Alzheimer's Disease. *J. Alzheimers Dis*. 2020;78(2):683-697. https://doi.org/10.3233/JAD-200306
179. McLoughlin, R.F.;Berthon, B.S.;Jensen, M.E.;Baines, K.J.&Wood, L.G. Short-chain fatty acids, prebiotics, synbiotics, and systemic inflammation: a systematic review and meta-analysis. *Am. J. Clin. Nutr*. 2017;106(3):930-945. https://doi.org/10.3945/ajcn.117.156265
180. Barroso, A.;Mahler, J.V.;Fonseca-Castro, P.H.&Quintana, F.J. The aryl hydrocarbon receptor and the gut-brain axis. *Cell Mol. Immunol*. 2021;18(2):259-268. https://doi.org/10.1038/s41423-020-00585-5
181. Kennedy, P.J.;Cryan, J.F.;Dinan, T.G.&Clarke, G. Kynurenine pathway metabolism and the microbiota-gut-brain axis. *Neuropharmacology*. 2017;112(Pt B):399-412. https://doi.org/10.1016/j.neuropharm.2016.07.002
182. Karbowska, M.;Hermanowicz, J.M.;Tankiewicz-Kwedlo, A.;Kalaska, B.;Kaminski, T.W.;Nosek, K., et al. Neurobehavioral effects of uremic toxin–indoxyl sulfate in the rat model. *Sci. Rep*. 2020;10(1):9483.

https://doi.org/10.1038/s41598-020-66421-y
183. Rothhammer, V.;Borucki, D.M.;Tjon, E.C.;Takenaka, M.C.;Chao, C.-C.;Ardura-Fabregat, A., et al. Microglial control of astrocytes in response to microbial metabolites. *Nature*. 2018;557(7707):724-728. https://doi.org/10.1038/s41586-018-0119-x
184. Rothhammer, V.;Mascanfroni, I.D.;Bunse, L.;Takenaka, M.C.;Kenison, J.E.;Mayo, L., et al. Type I interferons and microbial metabolites of tryptophan modulate astrocyte activity and CNS inflammation via the aryl hydrocarbon receptor. *Nat. Med*. 2016;22(6):586-597. https://doi.org/10.1038/nm.4106
185. Sankowski, B.;Księżarczyk, K.;Raćkowska, E.;Szlufik, S.;Koziorowski, D.&Giebułtowicz, J. Higher cerebrospinal fluid to plasma ratio of p-cresol sulfate and indoxyl sulfate in patients with Parkinson's disease. *Clin. Chim. Acta*. 2020;501:165-173. https://doi.org/10.1016/j.cca.2019.10.038
186. Toney, A.M.;Albusharif, M.;Works, D.;Polenz, L.;Schlange, S.;Chaidez, V., et al. Differential Effects of Whole Red Raspberry Polyphenols and Their Gut Metabolite Urolithin A on Neuroinflammation in BV-2 Microglia. *Int. J. Environ. Res. Public Health*. 2020;18(1):68. https://doi.org/10.3390/ijerph18010068
187. Shen, P.-X.;Li, X.;Deng, S.-Y.;Zhao, L.;Zhang, Y.-Y.;Deng, X., et al. Urolithin A ameliorates experimental autoimmune encephalomyelitis by targeting aryl hydrocarbon receptor. *EBioMedicine*. 2021;64:103227. https://doi.org/10.1016/j.ebiom.2021.103227
188. Lin, X.H.;Ye, X.J.;Li, Q.F.;Gong, Z.;Cao, X.;Li, J.H., et al. Urolithin A Prevents Focal Cerebral Ischemic Injury via Attenuating Apoptosis and Neuroinflammation in Mice. *Neuroscience*. 2020;448:94-106. https://doi.org/10.1016/j.neuroscience.2020.09.027
189. Li, S.;Cai, Y.;Guan, T.;Zhang, Y.;Huang, K.;Zhang, Z., et al. Quinic acid alleviates high-fat diet-induced neuroinflammation by inhibiting DR3/IKK/NF-kappaB signaling via gut microbial tryptophan metabolites. *Gut Microbes*. 2024;16(1):2374608. https://doi.org/10.1080/19490976.2024.2374608
190. Wang, J.;Hodes, G.E.;Zhang, H.;Zhang, S.;Zhao, W.;Golden, S.A., et al. Epigenetic modulation of inflammation and synaptic plasticity promotes resilience against stress in mice. *Nat. Commun*. 2018;9(1):477-414. https://doi.org/10.1038/s41467-017-02794-5
191. Mossad, O.;Batut, B.;Yilmaz, B.;Dokalis, N.;Mezo, C.;Nent, E., et al. Gut microbiota drives age-related oxidative stress and mitochondrial damage in microglia via the metabolite N(6)-carboxymethyllysine. *Nat. Neurosci*. 2022;25(3):295-305. https://doi.org/10.1038/s41593-022-01027-3
192. Brunt, V.E.;LaRocca, T.J.;Bazzoni, A.E.;Sapinsley, Z.J.;Miyamoto-Ditmon, J.;Gioscia-Ryan, R.A., et al. The gut microbiome–derived metabolite trimethylamine N-oxide modulates neuroinflammation and cognitive function with aging. *GeroScience*. 2020;43(1):377-394. https://doi.org/10.1007/s11357-020-00257-2
193. Meng, F.;Li, N.;Li, D.;Song, B.&Li, L. The presence of elevated circulating trimethylamine N-oxide exaggerates postoperative cognitive dysfunction in aged rats. *Behav. Brain. Res*. 2019;368:111902. https://doi.org/10.1016/j.bbr.2019.111902
194. Quan, W.;Qiao, C.M.;Niu, G.Y.;Wu, J.;Zhao, L.P.;Cui, C., et al. Trimethylamine N-Oxide Exacerbates Neuroinflammation and Motor Dysfunction in an Acute MPTP Mice Model of Parkinson's Disease. *Brain Sci*. 2023;13(5). https://doi.org/10.3390/brainsci13050790
195. Li, D.;Ke, Y.;Zhan, R.;Liu, C.;Zhao, M.;Zeng, A., et al. Trimethylamine-N-oxide promotes brain aging and cognitive impairment in mice. *Aging Cell*. 2018;17(4):e12768. https://doi.org/10.1111/acel.12768
196. Vogt, N.M.;Romano, K.A.;Darst, B.F.;Engelman, C.D.;Johnson, S.C.;Carlsson, C.M., et al. The gut microbiota-derived metabolite trimethylamine N-oxide is elevated in Alzheimer's disease. *Alzheimers Res. Ther*. 2018;10(1):124. https://doi.org/10.1186/s13195-018-0451-2
197. Girones, X.;Guimera, A.;Cruz-Sanchez, C.Z.;Ortega, A.;Sasaki, N.;Makita, Z., et al. N epsilon-carboxymethyllysine in brain aging, diabetes mellitus, and Alzheimer's disease. *Free Radic. Biol. Med*. 2004;36(10):1241-1247.

https://doi.org/10.1016/j.freeradbiomed.2004.02.006
198. Wong, A.;Luth, H.J.;Deuther-Conrad, W.;Dukic-Stefanovic, S.;Gasic-Milenkovic, J.;Arendt, T., et al. Advanced glycation endproducts co-localize with inducible nitric oxide synthase in Alzheimer's disease. *Brain Res*. 2001;920(1-2):32-40. https://doi.org/10.1016/s0006-8993(01)02872-4
199. Magistretti, Pierre J.&Allaman, I. A Cellular Perspective on Brain Energy Metabolism and Functional Imaging. *Neuron*. 2015;86(4):883-901. https://doi.org/10.1016/j.neuron.2015.03.035
200. Suzuki, A.;Stern, Sarah A.;Bozdagi, O.;Huntley, George W.;Walker, Ruth H.;Magistretti, Pierre J., et al. Astrocyte-Neuron Lactate Transport Is Required for Long-Term Memory Formation. *Cell*. 2011;144(5):810-823. https://doi.org/10.1016/j.cell.2011.02.018
201. Gibbs, M.E.;Lloyd, H.G.E.;Santa, T.&Hertz, L. Glycogen is a preferred glutamate precursor during learning in 1-day-old chick: Biochemical and behavioral evidence. *J. Neurosci Res*. 2007;85(15):3326-3333. https://doi.org/10.1002/jnr.21307
202. Wideman, C.E.;Jardine, K.H.&Winters, B.D. Involvement of classical neurotransmitter systems in memory reconsolidation: Focus on destabilization. *Neurobiol. Learn. Mem*. 2018;156:68-79. https://doi.org/10.1016/j.nlm.2018.11.001
203. Han, Y.M.;Ramprasath, T.&Zou, M.H. beta-hydroxybutyrate and its metabolic effects on age-associated pathology. *Exp. Mol. Med*. 2020;52(4):548-555. https://doi.org/10.1038/s12276-020-0415-z
204. Ota, M.;Matsuo, J.;Ishida, I.;Hattori, K.;Teraishi, T.;Tonouchi, H., et al. Effect of a ketogenic meal on cognitive function in elderly adults: potential for cognitive enhancement. *Psychopharmacology*. 2016;233(21):3797-3802. https://doi.org/10.1007/s00213-016-4414-7
205. Jensen, N.J.;Nilsson, M.;Ingerslev, J.S.;Olsen, D.A.;Fenger, M.;Svart, M., et al. Effects of β-hydroxybutyrate on cognition in patients with type 2 diabetes. *Eur. J. Endocrinol*. 2020;182(2). https://doi.org/10.1530/EJE-19-0710
206. Lund, T.M.;Obel, L.F.;Risa, Ø.&Sonnewald, U. β-Hydroxybutyrate is the preferred substrate for GABA and glutamate synthesis while glucose is indispensable during depolarization in cultured GABAergic neurons. *Neurochem. Int*. 2011;59(2):309-318. https://doi.org/10.1016/j.neuint.2011.06.002
207. Leclercq, S.;Le Roy, T.;Furgiuele, S.;Coste, V.;Bindels, L.B.;Leyrolle, Q., et al. Gut Microbiota-Induced Changes in β-Hydroxybutyrate Metabolism Are Linked to Altered Sociability and Depression in Alcohol Use Disorder. *Cell Rep*. 2020;33(2):108238. https://doi.org/10.1016/j.celrep.2020.108238
208. Liu, Z.;Dai, X.;Zhang, H.;Shi, R.;Hui, Y.;Jin, X., et al. Gut microbiota mediates intermittent-fasting alleviation of diabetes-induced cognitive impairment. *Nat. Commun*. 2020;11(1):855. https://doi.org/10.1038/s41467-020-14676-4
209. Poeggeler, B.;Sambamurti, K.;Siedlak, S.L.;Perry, G.;Smith, M.A.&Pappolla, M.A. A novel endogenous indole protects rodent mitochondria and extends rotifer lifespan. *PLoS One*. 2010;5(4):e10206. https://doi.org/10.1371/journal.pone.0010206
210. Dragicevic, N.;Copes, N.;O'Neal-Moffitt, G.;Jin, J.;Buzzeo, R.;Mamcarz, M., et al. Melatonin treatment restores mitochondrial function in Alzheimer's mice: a mitochondrial protective role of melatonin membrane receptor signaling. *J. Pineal. Res*. 2011;51(1):75-86. https://doi.org/10.1111/j.1600-079X.2011.00864.x
211. Rossignol, D.A.&Frye, R.E. Mitochondrial dysfunction in autism spectrum disorders: a systematic review and meta-analysis. *Mol. Psychiatry*. 2012;17(3):290-314. https://doi.org/10.1038/mp.2010.136
212. Rose, S.;Bennuri, S.C.;Davis, J.E.;Wynne, R.;Slattery, J.C.;Tippett, M., et al. Butyrate enhances mitochondrial function during oxidative stress in cell lines from boys with autism. *Transl. Psychiatry*. 2018;8(1):42-17. https://doi.org/10.1038/s41398-017-0089-z
213. Thomas, R.H.;Foley, K.A.;Mepham, J.R.;Tichenoff, L.J.;Possmayer, F.&MacFabe, D.F. Altered brain phospholipid and acylcarnitine profiles in propionic acid infused rodents: further development of a potential model of autism spectrum disorders. *J. Neurochem*. 2010;113(2):515-529. https://doi.org/10.1111/j.1471-4159.2010.06614.x

214. Kärkkäinen, O.;Tuomainen, T.;Koistinen, V.;Tuomainen, M.;Leppänen, J.;Laitinen, T., et al. Whole grain intake associated molecule 5-aminovaleric acid betaine decreases β-oxidation of fatty acids in mouse cardiomyocytes. *Sci. Rep*. 2018;8(1):13036-13037. https://doi.org/10.1038/s41598-018-31484-5
215. Mithul Aravind, S.;Wichienchot, S.;Tsao, R.;Ramakrishnan, S.&Chakkaravarthi, S. Role of dietary polyphenols on gut microbiota, their metabolites and health benefits. *Food Res. Int*. 2021;142:110189. https://doi.org/10.1016/j.foodres.2021.110189
216. Sanchez-Martinez, J.D.;Valdes, A.;Gallego, R.;Suarez-Montenegro, Z.J.;Alarcon, M.;Ibanez, E., et al. Blood-Brain Barrier Permeability Study of Potential Neuroprotective Compounds Recovered From Plants and Agri-Food by-Products. *Front. Nutr*. 2022;9:924596. https://doi.org/10.3389/fnut.2022.924596
217. Wang, D.;Ho, L.;Faith, J.;Ono, K.;Janle, E.M.;Lachcik, P.J., et al. Role of intestinal microbiota in the generation of polyphenol-derived phenolic acid mediated attenuation of Alzheimer's disease β-amyloid oligomerization. *Mol. Nutr. Food. Res*. 2015;59(6):1025-1040. https://doi.org/10.1002/mnfr.201400544
218. Matsuda, Y.;Ozawa, N.;Shinozaki, T.;Wakabayashi, K.-I.;Suzuki, K.;Kawano, Y., et al. Ergothioneine, a metabolite of the gut bacterium Lactobacillus reuteri, protects against stress-induced sleep disturbances. *Transl. Psychiatry*. 2020;10(1):170. https://doi.org/10.1038/s41398-020-0855-1
219. Halliwell, B.;Cheah, I.K.&Tang, R.M.Y. Ergothioneine – a diet-derived antioxidant with therapeutic potential. *FEBS Lett*. 2018;592(20):3357-3366. https://doi.org/10.1002/1873-3468.13123
220. Mori, T.;Koyama, N.;Guillot-Sestier, M.-V.;Tan, J.&Town, T. Ferulic acid Is a nutraceutical β-secretase modulator that improves behavioral impairment and Alzheimer-like pathology in transgenic mice. *PLoS One*. 2013;8(2):e55774. https://doi.org/10.1371/journal.pone.0055774
221. Beaver, L.M.;Jamieson, P.E.;Wong, C.P.;Hosseinikia, M.;Stevens, J.F.&Ho, E. Promotion of Healthy Aging Through the Nexus of Gut Microbiota and Dietary Phytochemicals. *Adv. Nutr*. 2025;16(3):100376. https://doi.org/10.1016/j.advnut.2025.100376
222. Chyan, Y.-J.;Poeggeler, B.;Omar, R.A.;Chain, D.G.;Frangione, B.;Ghiso, J., et al. Potent Neuroprotective Properties against the Alzheimer β-Amyloid by an Endogenous Melatonin-related Indole Structure, Indole-3-propionic Acid. *J. Biol. Chem*. 1999;274(31):21937-21942. https://doi.org/10.1074/jbc.274.31.21937
223. Nunes, A.;Amaral, J.;Lo, A.;Fonseca, M.;Viana, R.;Callaerts-Vegh, Z., et al. TUDCA, a Bile Acid, Attenuates Amyloid Precursor Protein Processing and Amyloid-β Deposition in APP/PS1 Mice. *Mol. Neurobiol*. 2012;45(3):440-454. https://doi.org/10.1007/s12035-012-8256-y
224. Mertens, K.L.;Kalsbeek, A.;Soeters, M.R.&Eggink, H.M. Bile Acid Signaling Pathways from the Enterohepatic Circulation to the Central Nervous System. *Front. Neurosci*. 2017;11. https://doi.org/10.3389/fnins.2017.00617
225. Zeni, A.L.B.;Camargo, A.&Dalmagro, A.P. Ferulic acid reverses depression-like behavior and oxidative stress induced by chronic corticosterone treatment in mice. *Steroids*. 2017;125:131-136. https://doi.org/10.1016/j.steroids.2017.07.006
226. Zhang, M.;Tang, X.;Mao, B.;Zhang, Q.;Zhao, J.;Chen, W., et al. Inhibition of the NF-kappaB and mTOR targets by urolithin A attenuates D-galactose-induced aging in mice. *Food Funct*. 2023;14(23):10375-10386. https://doi.org/10.1039/d3fo03847e
227. Westfall, S.&Pasinetti, G.M. The Gut Microbiota Links Dietary Polyphenols With Management of Psychiatric Mood Disorders. *Front. Neurosci*. 2019;13:1196. https://doi.org/10.3389/fnins.2019.01196
228. Berding, K.;Vlckova, K.;Marx, W.;Schellekens, H.;Stanton, C.;Clarke, G., et al. Diet and the Microbiota-Gut-Brain Axis: Sowing the Seeds of Good Mental Health. *Adv. Nutr.* 2021;12(4):1239-1285. https://doi.org/10.1093/advances/nmaa181
229. Donoso, F.;Cryan, J.F.;Olavarria-Ramirez, L.;Nolan, Y.M.&Clarke, G. Inflammation, Lifestyle Factors, and the Microbiome-Gut-Brain Axis: Relevance to Depression and Antidepressant Action. *Clin. Pharmacol. Ther*. 2023;113(2):246-259. https://doi.org/10.1002/cpt.2581
230. Dalton, A.;Mermier, C.&Zuhl, M. Exercise influence on the microbiome-gut-brain axis. *Gut Microbes*. 2019;10(5):555-568.

https://doi.org/10.1080/19490976.2018.1562268
231. Rohm, T.V.;Meier, D.T.;Olefsky, J.M.&Donath, M.Y. Inflammation in obesity, diabetes, and related disorders. *Immunity*. 2022;55(1):31-55. https://doi.org/10.1016/j.immuni.2021.12.013
232. Choi, B.S.;Daoust, L.;Pilon, G.;Marette, A.&Tremblay, A. Potential therapeutic applications of the gut microbiome in obesity: from brain function to body detoxification. *Int. J. Obes*. 2020;44(9):1818-1831. https://doi.org/10.1038/s41366-020-0618-3
233. Bruce-Keller, A.J.;Salbaum, J.M.;Luo, M.;Blanchard, E.t.;Taylor, C.M.;Welsh, D.A., et al. Obese-type gut microbiota induce neurobehavioral changes in the absence of obesity. *Biol. Psychiatry*. 2015;77(7):607-615. https://doi.org/10.1016/j.biopsych.2014.07.012
234. Zheng, P.;Zeng, B.;Zhou, C.;Liu, M.;Fang, Z.;Xu, X., et al. Gut microbiome remodeling induces depressive-like behaviors through a pathway mediated by the host's metabolism. *Mol. Psychiatry*. 2016;21(6):786-796. https://doi.org/10.1038/mp.2016.44
235. Moreno-Navarrete, J.M.;Blasco, G.;Puig, J.;Biarnes, C.;Rivero, M.;Gich, J., et al. Neuroinflammation in obesity: circulating lipopolysaccharide-binding protein associates with brain structure and cognitive performance. *Int. J. Obes*. 2017;41(11):1627-1635. https://doi.org/10.1038/ijo.2017.162
236. Dyer, A.H.;McKenna, L.;Batten, I.;Jones, K.;Widdowson, M.;Dunne, J., et al. Peripheral Inflammation and Cognitive Performance in Middle-Aged Adults With and Without Type 2 Diabetes: Results From the ENBIND Study. *Front. Aging Neurosci*. 2020;12:605878. https://doi.org/10.3389/fnagi.2020.605878
237. Charisis, S.;Yannakoulia, M.&Scarmeas, N. Diets to promote healthy brain ageing. *Nat. Rev. Neurol*. 2025;21(1):5-16. https://doi.org/10.1038/s41582-024-01036-9
238. Sandhu, K.V.;Sherwin, E.;Schellekens, H.;Stanton, C.;Dinan, T.G.&Cryan, J.F. Feeding the microbiota-gut-brain axis: diet, microbiome, and neuropsychiatry. *Transl. Res*. 2017;179:223-244. https://doi.org/10.1016/j.trsl.2016.10.002
239. Gibson, G.R.;Hutkins, R.;Sanders, M.E.;Prescott, S.L.;Reimer, R.A.;Salminen, S.J., et al. Expert consensus document: The International Scientific Association for Probiotics and Prebiotics (ISAPP) consensus statement on the definition and scope of prebiotics. *Nat. Rev. Gastroenterol. Hepatol*. 2017;14(8):491-502. https://doi.org/10.1038/nrgastro.2017.75
240. Mekhora, C.;Lamport, D.J.&Spencer, J.P.E. An overview of the relationship between inflammation and cognitive function in humans, molecular pathways and the impact of nutraceuticals. *Neurochem. Int*. 2024;181:105900. https://doi.org/10.1016/j.neuint.2024.105900
241. Delzenne, N.M.;Bindels, L.B.;Neyrinck, A.M.&Walter, J. The gut microbiome and dietary fibres: implications in obesity, cardiometabolic diseases and cancer. *Nat. Rev. Microbiol*. 2024. https://doi.org/10.1038/s41579-024-01108-z
242. Desmedt, O.;Broers, V.J.V.;Zamariola, G.;Pachikian, B.;Delzenne, N.&Luminet, O. Effects of prebiotics on affect and cognition in human intervention studies. *Nutr. Rev*. 2019;77(2):81-95. https://doi.org/10.1093/nutrit/nuy052
243. Ni Lochlainn, M.;Bowyer, R.C.E.;Moll, J.M.;Garcia, M.P.;Wadge, S.;Baleanu, A.F., et al. Effect of gut microbiome modulation on muscle function and cognition: the PROMOTe randomised controlled trial. *Nat. Commun*. 2024;15(1):1859. https://doi.org/10.1038/s41467-024-46116-y
244. Gubert, C.;Kong, G.;Renoir, T.&Hannan, A.J. Exercise, diet and stress as modulators of gut microbiota: Implications for neurodegenerative diseases. *Neurobiol. Dis*. 2020;134:104621. https://doi.org/10.1016/j.nbd.2019.104621
245. Garcia-Cabrerizo, R.&Cryan, J.F. A gut (microbiome) feeling about addiction: Interactions with stress and social systems. *Neurobiol. Stress*. 2024;30:100629. https://doi.org/10.1016/j.ynstr.2024.100629
246. Garcia-Cabrerizo, R.;Carbia, C.;KJ, O.R.;Schellekens, H.&Cryan, J.F. Microbiota-gut-brain axis as a regulator of reward processes. *J. Neurochem*. 2021;157(5):1495-1524. https://doi.org/10.1111/jnc.15284
247. Cuesta, S.;Burdisso, P.;Segev, A.;Kourrich, S.&Sperandio, V. Gut colonization by Proteobacteria alters host metabolism and modulates cocaine neurobehavioral responses. *Cell Host Microbe*.

2022;30(11):1615-1629 e1615. https://doi.org/10.1016/j.chom.2022.09.014

248. Kiraly, D.D.;Walker, D.M.;Calipari, E.S.;Labonte, B.;Issler, O.;Pena, C.J., et al. Alterations of the Host Microbiome Affect Behavioral Responses to Cocaine. *Sci. Rep*. 2016;6:35455. https://doi.org/10.1038/srep35455
249. Meckel, K.R.;Simpson, S.S.;Godino, A.;Peck, E.G.;Sens, J.P.;Leonard, M.Z., et al. Microbial short-chain fatty acids regulate drug seeking and transcriptional control in a model of cocaine seeking. *Neuropsychopharmacology*. 2024;49(2):386-395. https://doi.org/10.1038/s41386-023-01661-w
250. Hofford, R.S.;Mervosh, N.L.;Euston, T.J.;Meckel, K.R.;Orr, A.T.&Kiraly, D.D. Alterations in microbiome composition and metabolic byproducts drive behavioral and transcriptional responses to morphine. *Neuropsychopharmacology*. 2021;46(12):2062-2072. https://doi.org/10.1038/s41386-021-01043-0
251. Yang, J.;Zhang, Z.;Xie, Z.;Bai, L.;Xiong, P.;Chen, F., et al. Metformin modulates microbiota-derived inosine and ameliorates methamphetamine-induced anxiety and depression-like withdrawal symptoms in mice. *Biomed. Pharmacother*. 2022;149:112837. https://doi.org/10.1016/j.biopha.2022.112837
252. Anderson, B.O.;Berdzuli, N.;Ilbawi, A.;Kestel, D.;Kluge, H.P.;Krech, R., et al. Health and cancer risks associated with low levels of alcohol consumption. *Lancet Public Health*. 2023;8(1):e6-e7. https://doi.org/10.1016/S2468-2667(22)00317-6
253. Trius-Soler, M.;Pratico, G.;Gurdeniz, G.;Garcia-Aloy, M.;Canali, R.;Fausta, N., et al. Biomarkers of moderate alcohol intake and alcoholic beverages: a systematic literature review. *Genes Nutr*. 2023;18(1):7. https://doi.org/10.1186/s12263-023-00726-1
254. Wilson, D.F.&Matschinsky, F.M. Ethanol metabolism: The good, the bad, and the ugly. *Med. Hypotheses*. 2020;140:109638. https://doi.org/10.1016/j.mehy.2020.109638
255. Voutilainen, T.&Karkkainen, O. Changes in the Human Metabolome Associated With Alcohol Use: A Review. *Alcohol*. 2019;54(3):225-234. https://doi.org/10.1093/alcalc/agz030
256. Carbia, C.;Lannoy, S.;Maurage, P.;Lopez-Caneda, E.;O'Riordan, K.J.;Dinan, T.G., et al. A biological framework for emotional dysregulation in alcohol misuse: from gut to brain. *Mol. Psychiatry*. 2021;26(4):1098-1118. https://doi.org/10.1038/s41380-020-00970-6
257. Bajaj, J.S. Alcohol, liver disease and the gut microbiota. *Nat. Rev. Gastroenterol. Hepatol*. 2019;16(4):235-246. https://doi.org/10.1038/s41575-018-0099-1
258. Meijnikman, A.S.;Nieuwdorp, M.&Schnabl, B. Endogenous ethanol production in health and disease. *Nat. Rev. Gastroenterol. Hepatol*. 2024;21(8):556-571. https://doi.org/10.1038/s41575-024-00937-w
259. Leclercq, S.;Matamoros, S.;Cani, P.D.;Neyrinck, A.M.;Jamar, F.;Stärkel, P., et al. Intestinal permeability, gut-bacterial dysbiosis, and behavioral markers of alcohol-dependence severity. *PNAS Plus*. 2014;111(42):E4485-E4493. https://doi.org/10.1073/pnas.1415174111
260. Ahmed, W.&Rashid, S. Functional and therapeutic potential of inulin: A comprehensive review. *Crit. Rev. Food Sci. Nutr*. 2019;59(1):1-13. https://doi.org/10.1080/10408398.2017.1355775
261. So, D.;Whelan, K.;Rossi, M.;Morrison, M.;Holtmann, G.;Kelly, J.T., et al. Dietary fiber intervention on gut microbiota composition in healthy adults: a systematic review and meta-analysis. *Am. J. Clin. Nutr*. 2018;107(6):965-983. https://doi.org/10.1093/ajcn/nqy041
262. Nakajima, H.;Nakanishi, N.;Miyoshi, T.;Okamura, T.;Hashimoto, Y.;Senmaru, T., et al. Inulin reduces visceral adipose tissue mass and improves glucose tolerance through altering gut metabolites. *Nutr. Metab.* 2022;19(1):50. https://doi.org/10.1186/s12986-022-00685-1
263. Wu, Z.;Du, Z.;Tian, Y.;Liu, M.;Zhu, K.;Zhao, Y., et al. Inulin accelerates weight loss in obese mice by regulating gut microbiota and serum metabolites. *Front. Nutr*. 2022;9:980382. https://doi.org/10.3389/fnut.2022.980382
264. Vandeputte, D.;Falony, G.;Vieira-Silva, S.;Wang, J.;Sailer, M.;Theis, S., et al. Prebiotic inulin-type fructans induce specific changes in the human gut

microbiota. *Gut*. 2017;66(11):1968-1974. https://doi.org/10.1136/gutjnl-2016-313271

265. Chambers, E.S.;Byrne, C.S.;Morrison, D.J.;Murphy, K.G.;Preston, T.;Tedford, C., et al. Dietary supplementation with inulin-propionate ester or inulin improves insulin sensitivity in adults with overweight and obesity with distinct effects on the gut microbiota, plasma metabolome and systemic inflammatory responses: a randomised cross-over trial. *Gut*. 2019;68(8):1430-1438. https://doi.org/10.1136/gutjnl-2019-318424
266. Neyrinck, A.M.;Rodriguez, J.;Zhang, Z.;Seethaler, B.;Sanchez, C.R.;Roumain, M., et al. Prebiotic dietary fibre intervention improves fecal markers related to inflammation in obese patients: results from the Food4Gut randomized placebo-controlled trial. *Eur. J. Nutr*. 2021;60(6):3159-3170. https://doi.org/10.1007/s00394-021-02484-5
267. Salazar, N.;Dewulf, E.M.;Neyrinck, A.M.;Bindels, L.B.;Cani, P.D.;Mahillon, J., et al. Inulin-type fructans modulate intestinal Bifidobacterium species populations and decrease fecal short-chain fatty acids in obese women. *Clin. Nutr*. 2015;34(3):501-507. https://doi.org/10.1016/j.clnu.2014.06.001
268. Chen, P.;Li, X.;Yu, Y.;Zhang, J.;Zhang, Y.;Li, C., et al. Administration Time and Dietary Patterns Modified the Effect of Inulin on CUMS-Induced Anxiety and Depression. *Mol. Nutr. Food Res*. 2023;67(8):e2200566. https://doi.org/10.1002/mnfr.202200566
269. Yanckello, L.M.;Fanelli, B.;McCulloch, S.;Xing, X.;Sun, M.;Hammond, T.C., et al. Inulin Supplementation Mitigates Gut Dysbiosis and Brain Impairment Induced by Mild Traumatic Brain Injury during Chronic Phase. *J. Cell. Immunol*. 2022;4(2):50-64. https://doi.org/10.33696/immunology.4.132
270. Reimer, R.A.;Willis, H.J.;Tunnicliffe, J.M.;Park, H.;Madsen, K.L.&Soto-Vaca, A. Inulin-type fructans and whey protein both modulate appetite but only fructans alter gut microbiota in adults with overweight/obesity: A randomized controlled trial. *Mol. Nutr. Food Res*. 2017;61(11). https://doi.org/10.1002/mnfr.201700484
271. Medawar, E.;Beyer, F.;Thieleking, R.;Haange, S.B.;Rolle-Kampczyk, U.;Reinicke, M., et al. Prebiotic diet changes neural correlates of food decision-making in overweight adults: a randomised controlled within-subject cross-over trial. *Gut*. 2024;73(2):298-310. https://doi.org/10.1136/gutjnl-2023-330365
272. Benitez-Paez, A.;Hess, A.L.;Krautbauer, S.;Liebisch, G.;Christensen, L.;Hjorth, M.F., et al. Sex, Food, and the Gut Microbiota: Disparate Response to Caloric Restriction Diet with Fiber Supplementation in Women and Men. *Mol. Nutr. Food Res*. 2021;65(8):e2000996. https://doi.org/10.1002/mnfr.202000996
273. Leclercq S, A.H., Amadieu C, Petit G, Koistinen V, Leyrolle Q, Poncin M, Stärkel P, Kok E, Karhunen PJ, de Timary P, Laye S, Neyrinck AM, Kärkkäinen OK, Hanhineva K, Delzenne N. Blood metabolomic profiling reveals new targets in the management of psychological symptoms associated with severe alcohol use disorder. *Elife*. 2024;13:RP96937. https://doi.org/10.7554/eLife.96937
274. Amadieu, C.;Coste, V.;Neyrinck, A.M.;Thijssen, V.;Leyrolle, Q.;Bindels, L.B., et al. Restoring an adequate dietary fiber intake by inulin supplementation: a pilot study showing an impact on gut microbiota and sociability in alcohol use disorder patients. *Gut Microbes*. 2022;14(1):2007042. https://doi.org/10.1080/19490976.2021.2007042
275. Hiel, S.;Gianfrancesco, M.A.;Rodriguez, J.;Portheault, D.;Leyrolle, Q.;Bindels, L.B., et al. Link between gut microbiota and health outcomes in inulin -treated obese patients: Lessons from the Food4Gut multicenter randomized placebo-controlled trial. *Clin. Nutr*. 2020;39(12):3618-3628. https://doi.org/10.1016/j.clnu.2020.04.005
276. Babu, A.F.;Csader, S.;Mannisto, V.;Tauriainen, M.M.;Pentikainen, H.;Savonen, K., et al. Effects of exercise on NAFLD using non-targeted metabolomics in adipose tissue, plasma, urine, and stool. *Sci. Rep*. 2022;12(1):6485. https://doi.org/10.1038/s41598-022-10481-9
277. Klåvus, A.;Kokla, M.;Noerman, S.;Koistinen, V.M.;Tuomainen, M.;Zarei, I., et al. "notame": Workflow for Non-Targeted LC-MS Metabolic Profiling. *Metabolites*. 2020;10(4):135. https://doi.org/10.3390/metabo10040135

278. Leyrolle, Q.;Cserjesi, R.;Demeure, R.;Neyrinck, A.M.;Amadieu, C.;Rodriguez, J., et al. Microbiota and Metabolite Profiling as Markers of Mood Disorders: A Cross-Sectional Study in Obese Patients. *Nutrients*. 2021;14(1). https://doi.org/10.3390/nu14010147
279. Amadieu, C.;Ahmed, H.;Leclercq, S.;Koistinen, V.;Leyrolle, Q.;Starkel, P., et al. Effect of inulin supplementation on fecal and blood metabolome in alcohol use disorder patients: A randomised, controlled dietary intervention. *Clin. Nutr. ESPEN*. 2025. https://doi.org/10.1016/j.clnesp.2025.01.046
280. Tsugawa, H.;Cajka, T.;Kind, T.;Ma, Y.;Higgins, B.;Ikeda, K., et al. MS-DIAL: data-independent MS/MS deconvolution for comprehensive metabolome analysis. *Nat. Methods*. 2015;12(6):523-526. https://doi.org/10.1038/nmeth.3393
281. Sumner, L.W.;Amberg, A.;Barrett, D.;Beale, M.H.;Beger, R.;Daykin, C.A., et al. Proposed minimum reporting standards for chemical analysis Chemical Analysis Working Group (CAWG) Metabolomics Standards Initiative (MSI). *Metabolomics*. 2007;3(3):211-221. https://doi.org/10.1007/s11306-007-0082-2
282. Guijas, C.;Montenegro-Burke, J.R.;Domingo-Almenara, X.;Palermo, A.;Warth, B.;Hermann, G., et al. METLIN: A Technology Platform for Identifying Knowns and Unknowns. *Anal. Chem*. 2018;90(5):3156-3164. https://doi.org/10.1021/acs.analchem.7b04424
283. Conroy, M.J.;Andrews, R.M.;Andrews, S.;Cockayne, L.;Dennis, E.A.;Fahy, E., et al. LIPID MAPS: update to databases and tools for the lipidomics community. *Nucleic Acids Res*. 2024;52(D1):D1677-D1682. https://doi.org/10.1093/nar/gkad896
284. Lai, Z.;Tsugawa, H.;Wohlgemuth, G.;Mehta, S.;Mueller, M.;Zheng, Y., et al. Identifying metabolites by integrating metabolome databases with mass spectrometry cheminformatics. *Nat. Methods*. 2018;15(1):53-56. https://doi.org/10.1038/nmeth.4512
285. Duhrkop, K.;Fleischauer, M.;Ludwig, M.;Aksenov, A.A.;Melnik, A.V.;Meusel, M., et al. SIRIUS 4: a rapid tool for turning tandem mass spectra into metabolite structure information. *Nat. Methods*. 2019;16(4):299-302. https://doi.org/10.1038/s41592-019-0344-8
286. Nylund, L.;Hakkola, S.;Lahti, L.;Salminen, S.;Kalliomaki, M.;Yang, B., et al. Diet, Perceived Intestinal Well-Being and Compositions of Fecal Microbiota and Short Chain Fatty Acids in Oat-Using Subjects with Celiac Disease or Gluten Sensitivity. *Nutrients*. 2020;12(9). https://doi.org/10.3390/nu12092570
287. Amadieu, C.;Maccioni, L.;Leclercq, S.;Neyrinck, A.M.;Delzenne, N.M.;de Timary, P., et al. Liver alterations are not improved by inulin supplementation in alcohol use disorder patients during alcohol withdrawal: A pilot randomized, double-blind, placebo-controlled study. *EBioMedicine*. 2022;80:104033. https://doi.org/10.1016/j.ebiom.2022.104033
288. Pang, Z.;Lu, Y.;Zhou, G.;Hui, F.;Xu, L.;Viau, C., et al. MetaboAnalyst 6.0: towards a unified platform for metabolomics data processing, analysis and interpretation. *Nucleic Acids Res*. 2024;52(W1):W398-W406. https://doi.org/10.1093/nar/gkae253
289. Broadhurst, D.;Goodacre, R.;Reinke, S.N.;Kuligowski, J.;Wilson, I.D.;Lewis, M.R., et al. Guidelines and considerations for the use of system suitability and quality control samples in mass spectrometry assays applied in untargeted clinical metabolomic studies. *Metabolomics*. 2018;14(6):72. https://doi.org/10.1007/s11306-018-1367-3
290. Thiele, M.;Suvitaival, T.;Trost, K.;Kim, M.;de Zawadzki, A.;Kjaergaard, M., et al. Sphingolipids Are Depleted in Alcohol-Related Liver Fibrosis. *Gastroenterology*. 2023;164(7):1248-1260. https://doi.org/10.1053/j.gastro.2023.02.023
291. Carta, G.;Murru, E.;Banni, S.&Manca, C. Palmitic Acid: Physiological Role, Metabolism and Nutritional Implications. *Front. Physiol*. 2017;8:902. https://doi.org/10.3389/fphys.2017.00902
292. Jaremek, M.;Yu, Z.;Mangino, M.;Mittelstrass, K.;Prehn, C.;Singmann, P., et al. Alcohol-induced metabolomic differences in humans. *Transl. Psychiatry*. 2013;3(7):e276. https://doi.org/10.1038/tp.2013.55
293. Liu, D.;Yang, Z.;Chandler, K.;Oshodi, A.;Zhang, T.;Ma, J., et al. Serum metabolomic analysis reveals several novel metabolites in association with excessive alcohol use - an exploratory study. *Transl.*

*Res*. 2022;240:87-98. https://doi.org/10.1016/j.trsl.2021.10.008
294. Li, Y.;Wang, M.;Liu, X.;Rong, J.;Miller, P.E.;Joehanes, R., et al. Circulating metabolites may illustrate relationship of alcohol consumption with cardiovascular disease. *BMC Med*. 2023;21(1):443. https://doi.org/10.1186/s12916-023-03149-2
295. Ridlon, J.M.;Kang, D.J.;Hylemon, P.B.&Bajaj, J.S. Gut microbiota, cirrhosis, and alcohol regulate bile acid metabolism in the gut. *Dig. Dis*. 2015;33(3):338-345. https://doi.org/10.1159/000371678
296. Kumari, S.;Mittal, A.&Dabur, R. Moderate alcohol consumption in chronic form enhances the synthesis of cholesterol and C-21 steroid hormones, while treatment with Tinospora cordifolia modulate these events in men. *Steroids*. 2016;114:68-77. https://doi.org/10.1016/j.steroids.2016.03.016
297. Manley, S.&Ding, W. Role of farnesoid X receptor and bile acids in alcoholic liver disease. *Acta Pharm. Sin. B*. 2015;5(2):158-167. https://doi.org/10.1016/j.apsb.2014.12.011
298. Guertin, K.A.;Moore, S.C.;Sampson, J.N.;Huang, W.Y.;Xiao, Q.;Stolzenberg-Solomon, R.Z., et al. Metabolomics in nutritional epidemiology: identifying metabolites associated with diet and quantifying their potential to uncover diet-disease relations in populations. *Am. J. Clin. Nutr*. 2014;100(1):208-217. https://doi.org/10.3945/ajcn.113.078758
299. Wang, Y.;Gapstur, S.M.;Carter, B.D.;Hartman, T.J.;Stevens, V.L.;Gaudet, M.M., et al. Untargeted Metabolomics Identifies Novel Potential Biomarkers of Habitual Food Intake in a Cross-Sectional Study of Postmenopausal Women. *J. Nutr*. 2018;148(6):932-943. https://doi.org/10.1093/jn/nxy027
300. Langenau, J.;Oluwagbemigun, K.;Brachem, C.;Lieb, W.;Giuseppe, R.D.;Artati, A., et al. Blood Metabolomic Profiling Confirms and Identifies Biomarkers of Food Intake. *Metabolites*. 2020;10(11). https://doi.org/10.3390/metabo10110468
301. Huang, Z.;Boekhorst, J.;Fogliano, V.;Capuano, E.&Wells, J.M. Impact of High-Fiber or High-Protein Diet on the Capacity of Human Gut Microbiota To Produce Tryptophan Catabolites. *J. Agric. Food Chem*. 2023;71(18):6956-6966. https://doi.org/10.1021/acs.jafc.2c08953
302. Ho, M.F.;Zhang, C.;Wei, L.;Zhang, L.;Moon, I.;Geske, J.R., et al. Genetic variants associated with acamprosate treatment response in alcohol use disorder patients: A multiple omics study. *Br. J. Pharmacol*. 2022;179(13):3330-3345. https://doi.org/10.1111/bph.15795
303. Miliano, C.;Natividad, L.A.;Quello, S.;Stoolmiller, M.;Gregus, A.M.;Buczynski, M.W., et al. The Predictive Value of Plasma Bioactive Lipids on Craving in Human Volunteers With Alcohol Use Disorder. *Biol. Psychiatry Glob. Open. Sci*. 2024;4(6):100368. https://doi.org/10.1016/j.bpsgos.2024.100368
304. Bauer, J.;Pedersen, A.;Scherbaum, N.;Bening, J.;Patschke, J.;Kugel, H., et al. Craving in alcohol-dependent patients after detoxification is related to glutamatergic dysfunction in the nucleus accumbens and the anterior cingulate cortex. *Neuropsychopharmacology*. 2013;38(8):1401-1408. https://doi.org/10.1038/npp.2013.45
305. Chen, G.;Zhao, X.;Xie, M.;Chen, H.;Shao, C.;Zhang, X., et al. Serum metabolites and inflammation predict brain functional connectivity changes in Obsessive-Compulsive disorder. *Brain Behav. Immun*. 2025;126:113-125. https://doi.org/10.1016/j.bbi.2025.01.013
306. Li, Z.;Gao, J.;Lin, L.;Zheng, Z.;Yan, S.;Wang, W., et al. Untargeted metabolomics analysis in drug-naive patients with severe obsessive-compulsive disorder. *Front. Neurosci*. 2023;17:1148971. https://doi.org/10.3389/fnins.2023.1148971
307. Martens, C.;Shekhar, M.;Borysik, A.J.;Lau, A.M.;Reading, E.;Tajkhorshid, E., et al. Direct protein-lipid interactions shape the conformational landscape of secondary transporters. *Nat. Commun*. 2018;9(1):4151. https://doi.org/10.1038/s41467-018-06704-1
308. Xu, P.;Huang, S.;Zhang, H.;Mao, C.;Zhou, X.E.;Cheng, X., et al. Structural insights into the lipid and ligand regulation of serotonin receptors. *Nature*. 2021;592(7854):469-473. https://doi.org/10.1038/s41586-021-03376-8
309. Li, Z.;Agellon, L.B.;Allen, T.M.;Umeda, M.;Jewell, L.;Mason, A., et al. The ratio of phosphatidylcholine to phosphatidylethanolamine influences membrane integrity and steatohepatitis. *Cell. Metab*. 2006;3(5):321-331. https://doi.org/10.1016/j.cmet.2006.03.007

310. Sabogal-Guaqueta, A.M.;Villamil-Ortiz, J.G.;Arias-Londono, J.D.&Cardona-Gomez, G.P. Inverse Phosphatidylcholine/Phosphatidylinositol Levels as Peripheral Biomarkers and Phosphatidylcholine/Lysophosphatidylethanolamine-Phosphatidylserine as Hippocampal Indicator of Postischemic Cognitive Impairment in Rats. *Front. Neurosci*. 2018;12:989. https://doi.org/10.3389/fnins.2018.00989
311. Opitz, C.A.;Litzenburger, U.M.;Sahm, F.;Ott, M.;Tritschler, I.;Trump, S., et al. An endogenous tumour-promoting ligand of the human aryl hydrocarbon receptor. *Nature*. 2011;478(7368):197-203. https://doi.org/10.1038/nature10491
312. Desbonnet, L.;Garrett, L.;Clarke, G.;Bienenstock, J.&Dinan, T.G. The probiotic Bifidobacteria infantis: An assessment of potential antidepressant properties in the rat. *J. Psychiatr. Res*. 2008;43(2):164-174. https://doi.org/10.1016/j.jpsychires.2008.03.009
313. Chen, S.J.&Lin, C.H. Gut microenvironmental changes as a potential trigger in Parkinson's disease through the gut-brain axis. *J. Biomed. Sci*. 2022;29(1):54. https://doi.org/10.1186/s12929-022-00839-6
314. Pruss, K.M.;Chen, H.;Liu, Y.;Van Treuren, W.;Higginbottom, S.K.;Jarman, J.B., et al. Host-microbe co-metabolism via MCAD generates circulating metabolites including hippuric acid. *Nat. Commun*. 2023;14(1):512. https://doi.org/10.1038/s41467-023-36138-3
315. van der Spek, A.;Stewart, I.D.;Kuhnel, B.;Pietzner, M.;Alshehri, T.;Gauss, F., et al. Circulating metabolites modulated by diet are associated with depression. *Mol. Psychiatry*. 2023;28(9):3874-3887. https://doi.org/10.1038/s41380-023-02180-2
316. Karkkainen, O.;Tolmunen, T.;Kivimaki, P.;Kurkinen, K.;Ali-Sisto, T.;Mantyselka, P., et al. Alcohol use-associated alterations in the circulating metabolite profile in the general population and in individuals with major depressive disorder. *Alcohol*. 2024;120:161-167. https://doi.org/10.1016/j.alcohol.2024.01.005
317. Franco, R.&Martinez-Pinilla, E. One-way or two-way sweet link between theobromine and depression? *BMC Psychiatry*. 2023;23(1):411. https://doi.org/10.1186/s12888-023-04662-7
318. Orru, M.;Guitart, X.;Karcz-Kubicha, M.;Solinas, M.;Justinova, Z.;Barodia, S.K., et al. Psychostimulant pharmacological profile of paraxanthine, the main metabolite of caffeine in humans. *Neuropharmacology*. 2013;67:476-484. https://doi.org/10.1016/j.neuropharm.2012.11.029
319. Garcia-Blanco, T.;Davalos, A.&Visioli, F. Tea, cocoa, coffee, and affective disorders: vicious or virtuous cycle? *J. Affect. Disord*. 2017;224:61-68. https://doi.org/10.1016/j.jad.2016.11.033
320. Tan, S.T.;Ramesh, T.;Toh, X.R.&Nguyen, L.N. Emerging roles of lysophospholipids in health and disease. *Prog. Lipid Res*. 2020;80:101068. https://doi.org/10.1016/j.plipres.2020.101068
321. Vesga-Jimenez, D.J.;Martin, C.;Barreto, G.E.;Aristizabal-Pachon, A.F.;Pinzon, A.&Gonzalez, J. Fatty Acids: An Insight into the Pathogenesis of Neurodegenerative Diseases and Therapeutic Potential. *Int. J. Mol. Sci*. 2022;23(5). https://doi.org/10.3390/ijms23052577
322. Yu, Q.;Yang, Y.;Xu, T.;Cai, Y.;Yang, Z.&Yuan, F. Palmitoleic acid protects microglia from palmitate-induced neurotoxicity in vitro. *PLoS One*. 2024;19(1):e0297031. https://doi.org/10.1371/journal.pone.0297031
323. Frank, P.;Jokela, M.;Batty, G.D.;Cadar, D.;Steptoe, A.&Kivimaki, M. Association Between Systemic Inflammation and Individual Symptoms of Depression: A Pooled Analysis of 15 Population-Based Cohort Studies. *Am. J. Psychiatry*. 2021;178(12):1107-1118. https://doi.org/10.1176/appi.ajp.2021.20121776
324. Mochel, F.;DeLonlay, P.;Touati, G.;Brunengraber, H.;Kinman, R.P.;Rabier, D., et al. Pyruvate carboxylase deficiency: clinical and biochemical response to anaplerotic diet therapy. *Mol. Genet. Metab*. 2005;84(4):305-312. https://doi.org/10.1016/j.ymgme.2004.09.007
325. Lancaster, S.M.;Lee-McMullen, B.;Abbott, C.W.;Quijada, J.V.;Hornburg, D.;Park, H., et al. Global, distinctive, and personal changes in molecular and microbial profiles

by specific fibers in humans. *Cell Host Microbe*. 2022;30(6):848-862 e847. https://doi.org/10.1016/j.chom.2022.03.036

326. Druart, C.;Bindels, L.B.;Schmaltz, R.;Neyrinck, A.M.;Cani, P.D.;Walter, J., et al. Ability of the gut microbiota to produce PUFA-derived bacterial metabolites: Proof of concept in germ-free versus conventionalized mice. *Mol. Nutr. Food Res*. 2015;59(8):1603-1613. https://doi.org/10.1002/mnfr.201500014
327. Albouery, M.;Bretin, A.;Buteau, B.;Gregoire, S.;Martine, L.;Gambert, S., et al. Soluble Fiber Inulin Consumption Limits Alterations of the Gut Microbiota and Hepatic Fatty Acid Metabolism Caused by High-Fat Diet. *Nutrients*. 2021;13(3). https://doi.org/10.3390/nu13031037
328. Ridlon, J.M.&Gaskins, H.R. Another renaissance for bile acid gastrointestinal microbiology. *Nat. Rev. Gastroenterol. Hepatol*. 2024;21(5):348-364. https://doi.org/10.1038/s41575-024-00896-2
329. Koppel, N.;Maini Rekdal, V.&Balskus, E.P. Chemical transformation of xenobiotics by the human gut microbiota. *Science*. 2017;356(6344). https://doi.org/10.1126/science.aag2770
330. Ma, L.;Ni, Y.;Wang, Z.;Tu, W.;Ni, L.;Zhuge, F., et al. Spermidine improves gut barrier integrity and gut microbiota function in diet-induced obese mice. *Gut Microbes*. 2020;12(1):1-19. https://doi.org/10.1080/19490976.2020.1832857
331. Cruz-Pereira, J.S.;Moloney, G.M.;Bastiaanssen, T.F.S.;Boscaini, S.;Tofani, G.;Borras-Bisa, J., et al. Prebiotic supplementation modulates selective effects of stress on behavior and brain metabolome in aged mice. *Neurobiol. Stress*. 2022;21:100501. https://doi.org/10.1016/j.ynstr.2022.100501
332. Li, L.;Li, T.;Liang, X.;Zhu, L.;Fang, Y.;Dong, L., et al. A decrease in Flavonifractor plautii and its product, phytosphingosine, predisposes individuals with phlegm-dampness constitution to metabolic disorders. *Cell. Discov*. 2025;11(1):25. https://doi.org/10.1038/s41421-025-00789-x
333. Martin, G.;Kolida, S.;Marchesi, J.R.;Want, E.;Sidaway, J.E.&Swann, J.R. In Vitro Modeling of Bile Acid Processing by the Human Fecal Microbiota. *Front. Microbiol*. 2018;9:1153. https://doi.org/10.3389/fmicb.2018.01153
334. Le Bastard, Q.;Chapelet, G.;Javaudin, F.;Lepelletier, D.;Batard, E.&Montassier, E. The effects of inulin on gut microbial composition: a systematic review of evidence from human studies. *Eur. J. Clin. Microbiol. Infect. Dis*. 2020;39(3):403-413. https://doi.org/10.1007/s10096-019-03721-w
335. Mukhopadhya, I.&Louis, P. Gut microbiota-derived short-chain fatty acids and their role in human health and disease. *Nat. Rev. Microbiol*. 2025. https://doi.org/10.1038/s41579-025-01183-w
336. Pietzner, M.;Stewart, I.D.;Raffler, J.;Khaw, K.T.;Michelotti, G.A.;Kastenmuller, G., et al. Plasma metabolites to profile pathways in noncommunicable disease multimorbidity. *Nat. Med*. 2021;27(3):471-479. https://doi.org/10.1038/s41591-021-01266-0
337. Tang, Z.Z.;Chen, G.;Hong, Q.;Huang, S.;Smith, H.M.;Shah, R.D., et al. Multi-Omic Analysis of the Microbiome and Metabolome in Healthy Subjects Reveals Microbiome-Dependent Relationships Between Diet and Metabolites. *Front. Genet*. 2019;10:454. https://doi.org/10.3389/fgene.2019.00454
338. Ghosh, N.;Lejonberg, C.;Czuba, T.;Dekkers, K.;Robinson, R.;Arnlov, J., et al. Analysis of plasma metabolomes from 11 309 subjects in five population-based cohorts. *Sci. Rep*. 2024;14(1):8933. https://doi.org/10.1038/s41598-024-59388-7
339. Haffner, J.J.;Katemauswa, M.;Kagone, T.S.;Hossain, E.;Jacobson, D.;Flores, K., et al. Untargeted Fecal Metabolomic Analyses across an Industrialization Gradient Reveal Shared Metabolites and Impact of Industrialization on Fecal Microbiome-Metabolome Interactions. *mSystems*. 2022;7(6):e0071022. https://doi.org/10.1128/msystems.00710-22
340. Ponce-de-Leon, M.;Wang-Sattler, R.;Peters, A.;Rathmann, W.;Grallert, H.;Artati, A., et al. Stool and blood metabolomics in the metabolic syndrome: a cross-sectional study. *Metabolomics*. 2024;20(5):105. https://doi.org/10.1007/s11306-024-02166-3
341. Deng, K.;Xu, J.J.;Shen, L.;Zhao, H.;Gou, W.;Xu, F., et al. Comparison of fecal and blood metabolome reveals inconsistent associations of the gut microbiota with

cardiometabolic diseases. *Nat. Commun*. 2023;14(1):571. https://doi.org/10.1038/s41467-023-36256-y

342. Yang, Y.;Chen, J.;Gao, H.;Cui, M.;Zhu, M.;Xiang, X., et al. Characterization of the gut microbiota and fecal and blood metabolomes under various factors in urban children from Northwest China. *Front. Cell Infect. Microbiol*. 2024;14:1374544. https://doi.org/10.3389/fcimb.2024.1374544
343. Tabone, M.;Bressa, C.;Garcia-Merino, J.A.;Moreno-Perez, D.;Van, E.C.;Castelli, F.A., et al. The effect of acute moderate-intensity exercise on the serum and fecal metabolomes and the gut microbiota of cross-country endurance athletes. *Sci. Rep*. 2021;11(1):3558. https://doi.org/10.1038/s41598-021-82947-1
344. Folz, J.;Culver, R.N.;Morales, J.M.;Grembi, J.;Triadafilopoulos, G.;Relman, D.A., et al. Human metabolome variation along the upper intestinal tract. *Nat. Metab*. 2023;5(5):777-788. https://doi.org/10.1038/s42255-023-00777-z
345. Culp, E.J.&Goodman, A.L. Cross-feeding in the gut microbiome: Ecology and mechanisms. *Cell Host Microbe*. 2023;31(4):485-499. https://doi.org/10.1016/j.chom.2023.03.016
346. Koh, A.;De Vadder, F.;Kovatcheva-Datchary, P.&Backhed, F. From Dietary Fiber to Host Physiology: Short-Chain Fatty Acids as Key Bacterial Metabolites. *Cell*. 2016;165(6):1332-1345. https://doi.org/10.1016/j.cell.2016.05.041
347. Wagner-Golbs, A.;Neuber, S.;Kamlage, B.;Christiansen, N.;Bethan, B.;Rennefahrt, U., et al. Effects of Long-Term Storage at -80 degrees C on the Human Plasma Metabolome. *Metabolites*. 2019;9(5). https://doi.org/10.3390/metabo9050099
348. De Spiegeleer, M.;De Graeve, M.;Huysman, S.;Vanderbeke, A.;Van Meulebroek, L.&Vanhaecke, L. Impact of storage conditions on the human stool metabolome and lipidome: Preserving the most accurate fingerprint. *Anal. Chim. Acta*. 2020;1108:79-88. https://doi.org/10.1016/j.aca.2020.02.046

Supplementary table S1. Molecular characteristics of the annotated features,across studies, level of identifications and annotation sources.

| Annotation | Sample matrix & study | Molecular formula | Column | Retention time | ESI | *m/z* | Adduct type | MS/MS fragments (%) | ID level | Annotation source |
|---|---|---|---|---|---|---|---|---|---|---|
| 4-Trimethylammoniobutanoic acid | Feces: G2B | C7H15NO | HILIC | 3.37 | Pos | 146.1175 | [M+H]+ | 146.116 (100), 87.043 (9) | 2 | HMDB |
| .alpha.-Pinene oxide | Plasma: F4G | C10H16O | RP | 8.64 | Pos | 135.1194 | [M+H-H2O]+ | 91.054 (100), 77.038 (53), 102.925 (44), 105.071 (44), 117.071 (35), 107.049 (28), 70.982 (27), 119.085 (26), 69.07 (23), 107.087 (19) | 2 | NIST MS Data Center |
| .beta.-D-Glucose | Plasma: F4G | C6H12O6 | HILIC | 5.29 | Pos | 383.1172 | [2M+Na]+ | 203.053 (100) | 2 | NIST MS Data Center |
| 1,2-Diamino-2-methylpropane | Plasma: F4G | C4H12N2 | HILIC | 4.96 | Pos | 72.0804 | [M-H-NH3]+ | 55.054 (100), 72.081 (43), 57.057 (41), 42.033 (9), 56.049 (6), 53.041 (4) | 2 | NIST MS Data Center |
| 1,3-Dicyclohexylurea | Plasma: G2B/AlcoholBis, BestTreat<br>Feces: G2B, BestTreat | C13H24N2O | RP | 7.97 | Pos | 225.1957 | [M+H]+ | 225.194 (100), 100.112 (32), 225.204 (30) | 2 | HMDB |
| 1,3-Dihydro-(2H)-indole-2-one | Plasma: BestTreat<br>Feces: F4G, BestTreat | C8H7NO | RP | 4.49 | Pos | 134.0602 | [M+H]+ | 134.06 (100), 106.065 (7) | 2 | NIST MS Data Center |
| 1,3-Dimethylurate | Plasma: F4G<br>Feces: G2B, F4G, BestTreat | C7H8N4O3 | HILIC | 1.05 | Neg | 195.0525 | [M-H]- | 195.052 (100), 180.028 (62), 137.024 (40), 110.035 (7), 63.63 (6), 56.5 (6), 121.496 (6), 20.267 (5), 89.684 (5), 67.357 (5) | 2 | HMDB |
| 1,5-Pentanediamine | Plasma: F4G | C5H14N2 | HILIC | 4.35 | Pos | 86.0967 | [M+H-NH3]+ | 69.07 (100), 57.057 (72), 86.096 (62), 44.049 (51), 42.033 (44), 41.038 (43), 39.022 (14), 56.048 (13), 43.055 (12), 41.39 (6) | 2 | NIST MS Data Center |
| 10-hydroxydecanoic acid | Plasma: F4G | C10H20O3 | RP | 6.74 | Pos | 171.1390 | [M+H]+ | 41.039 (100), 55.054 (94), 69.069 (50), 63.022 (42), 44.014 (42), 60.987 (30), 104.956 (27), 53.938 (26), 154.937 (20), 79.054 (17) | 1 | In-house library |
| 13-Docosenamide | Plasma: G2B/AlcoholBis, F4G, BestTreat<br>Feces: G2B, F4G, BestTreat | C22H43NO | RP | 11.66 | Pos | 338.3414 | [M-H]+ | 338.342 (100), 83.086 (71), 69.071 (69), 97.102 (64), 57.071 (50) | 2 | HMDB |
| 1-Hexadecanoyl-sn-glycerol | Plasma: F4G, BestTreat<br>Feces: F4G, BestTreat | C19H38O4 | RP | 10.55 | Pos | 331.2861 | [M+H]+ | 313.274 (100), 239.237 (40), 57.07 (17), 85.102 (15), 95.086 (15), 109.101 (14), 71.086 (13), 257.249 (12), 97.101 (10), 81.07 (9) | 2 | LipidMaps |
| 1-Hexadecylamine | Plasma: F4G | C16H35N | RP | 7.60 | Pos | 242.2898 | [M+H]+ | 242.288 (100), 57.072 (10), 182.95 (5), 207.179 (5), 242.107 (4), 134.954 (4), 71.087 (4), 242.208 (4), 161.137 (4) | 2 | NIST MS Data Center |
| 1-Hydroxybenzotriazole | Plasma: F4G | C6H5N3O | HILIC | 3.59 | Pos | 136.0507 | [M-H]+ | 91.042 (100), 136.049 (44), 119.046 (32), 53.038 (12), 80.048 (11), 78.047 (9), 64.028 (8), 54.032 (6) | 2 | HMDB |
| 1-Methylhistidine | Plasma: G2B/AlcoholBis, F4G, BestTreat<br>Feces: F4G, BestTreat | C7H11N3O2 | HILIC | 6.43 | Pos | 170.0925 | [M+H]+ | 124.086 (100), 170.092 (31), 109.078 (10), 83.057 (5), 79.053 (4) | 1 | In-house library |
| 1-Methylnicotinamide | Plasma: G2B/AlcoholBis, F4G, BestTreat<br>Feces: F4G, BestTreat | C7H9N2O | HILIC | 2.37 | Pos | 137.0707 | [M+H]+ | 137.071 (100), 94.066 (51), 78.034 (14), 120.045 (9), 67.055 (7), 87.494 (4) | 1 | In-house library |
| 1-methyl-pyridone-carboxamide | Plasma: G2B/AlcoholBis | C7H8N2O2 | RP | 1.67 | Pos | 153.0659 | [M+H]+ | 153.065 (100), 106.964 (19), 104.948 (11) | 2 | Metlin |
| 2,4,7,9-Tetramethyl-5-decyne-4,7-diol | Plasma: F4G | C14H26O2 | RP | 8.64 | Pos | 209.1931 | [M-H-H2O]+ | 209.191 (100), 153.128 (20), 83.085 (14), 135.119 (10), 95.086 (9), 153.054 (8), 105.069 (8), 209.153 (7), 85.064 (7), 209.123 (7) | 2 | MassBank |
| 2,6-Di-tert-butylphenol | Plasma: F4G | C14H22O | RP | 9.53 | Neg | 205.1598 | [M-H]- | 205.16 (100) | 2 | MassBank |
| 2,x-Dimethylpyridine | Feces: G2B, F4G | C7H9N | HILIC | 1.13 | Pos | 108.0809 | [M+H]+ | 108.0816 (100), 67.0512 (22), 93.0549 (14), 94.0666 (6) | 3 | MS-FINDER/SIRIUS |
| 2-Aminoisobutyric acid | Plasma: F4G | C4H9NO2 | HILIC | 5.30 | Pos | 104.0708 | [M+H]+ | 86.061 (100), 30.033 (71), 104.069 (36), 57.034 (36), 87.043 (28), 104.108 (27), 44.048 (12), 48.252 (8), 29.113 (4), 70.735 (4) | 1 | In-house library |
| 2-Hydroxybenzyl alcohol | Plasma: F4G | C7H8O2 | RP | 8.25 | Pos | 107.0493 | [M+H-H2O]+ | 107.05 (100), 77.039 (34), 79.054 (7), 79.017 (5), 51.023 (4) | 2 | MassBank |
| 2-hydroxy-butanoic acid | Plasma: F4G | C4H8O3 | RP | 1.53 | Neg | 103.0400 | [M-H]- | 57.034 (100), 44.998 (42), 34.97 (30), 103.041 (25), 23.017 (14), 102.896 (12), 59.011 (11), 20.053 (9), 20.683 (8), 68.36 (8) | 2 | MassBank |
| 2-Mercaptobenzothiazole | Plasma: G2B/AlcoholBis | C7H5NS2 | RP | 6.13 | Pos/Neg | 167.9936 | [M+H]+ | Pos: 167.994 (100), 108.96 (6)<br>Neg: 165.98 (100), 134.008 (10) | 2 | HMDB |
| 3-(?,?-dimethoxyphenyl)propanoic acid | Plasma: G2B/AlcoholBis, BestTreat<br>Feces: BestTreat | C11H14O3 | RP | 6.46 | Pos | 211.0969 | [M+H]+ | 165.091 (100), 151.075 (95), 193.087 (80) | 3 | MS-FINDER/SIRIUS |
| 3-(3-Hydroxyphenyl)propionic acid | Plasma: G2B/AlcoholBis, BestTreat<br>Feces: G2B, BestTreat | C9H10O3 | RP | 4.67 | Neg | 165.0557 | [M-H]- | 147.0454 (100), 164.8958 (30), 165.056 (25), 119.0505 (23), 72.9926 (21) | 1 | In-house library |
| 3,4-Methylenedioxyamphetamine | Plasma: F4G | C10H13NO2 | RP | 7.14 | Pos | 163.0777 | [M-H-NH3]+ | 105.034 (100), 163.075 (28), 41.039 (25), 84.961 (24), 100.975 (20), 133.047 (14), 147.08 (12), 163.112 (9), 112.004 (8), 96.959 (5) | 2 | MassBank |
| 3-CMPFP | Plasma: G2B/AlcoholBis, BestTreat<br>Feces: F4G, BestTreat | C15H14N4O | RP | 8.82 | Neg | 267.1242 | [M-H]- | 223.134 (100), 179.145 (46), 267.124 (23) | 2 | HMDB |
| 3-Hydroxyoctanoic acid | Plasma: G2B/AlcoholBis | C8H16O3 | RP | 6.50 | Neg | 159.1027 | [M-H]- | 59.013 (100), 159.103 (15), 130.984 (12) | 2 | HMDB |
| 3-Hydroxyvaleric acid | Plasma: G2B/AlcoholBis | C5H10O3 | HILIC | 0.79 | Neg | 117.0554 | [M-H]- | 71.05 (100), 117.055 (44), 32.031 (10), 36.105 (8), 51.807 (5), 72.996 (5) | 2 | HMDB |
| 3-Indoleacetic acid | Plasma: G2B/AlcoholBis, F4G, BestTreat<br>Feces: G2B, F4G, BestTreat | C10H9NO2 | RP | 5.29 | Pos | 176.0707 | [M+H]+ | 130.065 (100), 176.071 (11) | 1 | In-house library |
| 3-Indolepropionic acid | Plasma: G2B/AlcoholBis, F4G, BestTreat<br>Feces: BestTreat | C11H11NO2 | RP | 6.03 | Pos | 190.0863 | [M-H]+ | 130.065 (100), 172.075 (21), 190.086 (15) | 1 | In-house library |
| 3-Methylhistamine | Feces: F4G | C6H11N3 | HILIC | 4.78 | Pos | 126.1032 | [M+H]+ | 126.102 (100), 109.075 (67), 124.086 (31), 125.089 (10), 125.07 (7), 110.077 (4) | 1 | In-house library |
| 3-Methylhistidine | Plasma: G2B/AlcoholBis, F4G, BestTreat<br>Feces: F4G, BestTreat | C7H11N3O2 | HILIC | 7.01 | Pos | 170.0927 | [M-H]+ | 170.093 (100), 96.069 (40), 126.103 (32), 109.077 (30), 97.077 (14), 125.072 (4) | 2 | HMDB |
| 3-Pyridinecarboxamide, 1,6-dihydro-1-methyl-6- | Plasma: F4G | C7H8N2O2 | HILIC | 0.79 | Pos | 153.0663 | [M+H]+ | 136.039 (100), 92.049 (48), 108.044 (11), 110.058 (6), 153.064 (6), 95.012 (5), 82.064 (4) | 3 | MS-FINDER/SIRIUS |
| 4-amino-5-aminomethyl-2-methylpyrimidine | Feces: G2B | C6H10N4 | HILIC | 5.21 | Pos | 139.0988 | [M-H]+ | 81.044 (100), 139.098 (89), 122.071 (82), 49.589 (6), 83.047 (6), 77.888 (6), 82.047 (6), 122.023 (5), 138.102 (5), 123.056 (5) | 2 | Metlin |
| 4-amino-5-formamidomethyl-2-methylpyrimidin | Feces: G2B | C7H10N4O | HILIC | 1.12 | Pos | 167.0929 | [M-H]+ | 124.087 (100), 167.093 (68), 139.098 (52), 122.072 (49), 166.097 (38), 81.044 (31), 152.072 (19), 166.085 (17), 89.058 (8) | 3 | MS-FINDER/SIRIUS |
| 4-Amino-5-hydroxymethyl-2-methylpyrimidine | Feces: G2B | C6H9N3O | HILIC | 1.22 | Pos | 140.0818 | [M+H]+ | 81.045 (100), 140.082 (60), 122.071 (18), 97.308 (4), 82.046 (4), 93.071 (4) | 2 | Metlin |
| 4-aminophenol | Feces: G2B, F4G | C6H7NO | HILIC | 1.70 | Pos | 110.0601 | [M+H]+ | 110.06 (100) | 2 | HMDB |
| 4-Ethylphenylsulfate | Plasma: G2B/AlcoholBis, BestTreat | C8H10O4S | RP | 5.09 | Neg | 201.0230 | [M-H]- | 121.065 (100), 201.023 (92) | 2 | HMDB |
| 4-Guanidinobutanoic acid | Feces: F4G | C5H11N3O2 | HILIC | 4.12 | Pos | 146.0930 | [M-H]+ | 146.093 (100), 87.045 (61), 86.061 (37), 104.071 (14), 128.082 (13), 146.117 (11), 111.055 (11), 121.967 (5), 98.097 (4) | 1 | In-house library |
| 4-Hydroxybenzoic acid isomer 1 | Plasma: BestTreat<br>Feces: BestTreat, F4G | C7H6O3 | RP | 3.27 | Neg | 137.0237 | [M-H]- | 93.033 (100), 137.023 (14), 94.037 (4) | 2 | HMDB |
| 4-Hydroxybenzoic acid isomer 2 | Plasma: F4G | C7H6O3 | RP | 5.25 | Neg | 137.0244 | [M-H]- | 93.035 (100), 118.938 (8), 65.041 (7), 31.261 (5), 137.025 (4), 78.288 (4) | 2 | HMDB |
| 4-Hydroxybenzoylcholine | Feces: G2B | C12H18NO3 | HILIC | 0.90 | Pos | 224.1266 | [M]+ | 121.027 (100), 122.031 (9), 165.054 (8) | 2 | HMDB |
| 4-Hydroxyisoleucine | Plasma: G2B/AlcoholBis | C19H22N2O | RP | 0.67 | Pos | 148.0969 | [M+H]+ | 74.024 (100), 102.092 (49) | 2 | Metlin |
| 4-Methyl-1H-pyrazole | Plasma: F4G | C4H6N2 | HILIC | 5.77 | Pos | 83.0606 | [M+H]+ | 83.06 (100), 56.05 (50), 66.034 (23), 43.041 (20), 42.034 (6) | 2 | MassBank |
| 4-Nitrobenzylamine | Plasma: F4G | C7H8N2O2 | RP | 1.51 | Pos | 153.0667 | [M+H]+ | 153.067 (100), 136.039 (9), 72.987 (5), 103.003 (5), 135.023 (5) | 2 | NIST MS Data Center |
| 4-Pyridoxic acid | Plasma: G2B/AlcoholBis, BestTreat<br>Feces: G2B, F4G, BestTreat | C8H9NO4 | RP | 1.72 | Pos/Neg | 184.0605 | [M+H]+ | Pos: 166.051 (100), 148.04 (38), 184.061 (16), 167.054 (15), 149.044 (5)<br>Neg: 138.053 (100), 108.043 (46), 182.042 (42), 139.056 (6), 181.034 (5) | 2 | HMDB |

| Annotation | Sample matrix & study | Molecular formula | Column | Retention time | ESI | m/z | Adduct type | MS/MS fragments (%) | ID level | Annotation source |
|---|---|---|---|---|---|---|---|---|---|---|
| 4-Trimethylammoniobutanoic acid | Plasma: G2B/AlcoholBis, F4G, BestTreat<br>Feces: BestTreat | C7H15NO2 | HILIC | 3.57 | Pos | 146.1178 | [M+H]+ | 146.118 (100), 87.044 (61), 60.081 (30), 43.018 (6) | 1 | In-house library |
| 5-(2-Hydroxyethyl)-4-methylthiazole | Feces: G2B | C6H9NOS | RP | 1.94 | Pos | 144.0483 | [M+H]+ | 144.047 (100), 84.959 (82), 113.029 (68), 126.037 (26), 143.035 (15), 127.039 (9), 100.934 (8), 86.019 (7), 66.934 (7), 128.936 (6) | 2 | HMDB |
| 5-Aminovaleric acid | Plasma: F4G<br>Feces: F4G | C5H11NO2 | RP | 2.08 | Pos | 100.0761 | [M+H-H2O]+ | 100.075 (100), 56.049 (16), 55.054 (7), 82.065 (7) | 2 | HMDB |
| 5-AVAB | Plasma: G2B/AlcoholBis, F4G, BestTreat<br>Feces: G2B, F4G, BestTreat | C8H17NO2 | HILIC | 2.23 | Pos | 160.1330 | [M+H]+ | 55.054 (100), 83.05 (56), 60.082 (51), 101.06 (39), 160.136 (38), 59.05 (37), 43.017 (14), 58.065 (8) | 1 | In-house library |
| 7a-hydroxy-3-oxo-4-cholestenoic acid | Plasma: G2B/AlcoholBis, BestTreat<br>Feces: BestTreat | C27H42O4 | RP | 9.95 | Pos/Neg | 431.3156 | [M+H]+ | Pos: 395.292 (100), 97.065 (92), 431.316 (73)<br>Neg: 429.305 (100), 411.289 (24) | 1 | In-house library |
| 7-Methylguanine | Plasma: F4G<br>Feces: F4G | C6H7N5O | HILIC | 1.56 | Pos | 166.0725 | [M+H]+ | 166.074 (100), 166.129 (7), 124.051 (5) | 2 | MassBank |
| AC 03:0 (Propionylcarnitine) | Plasma: F4G, BestTreat | C10H19NO4 | HILIC | 2.13 | Pos | 218.1396 | [M+H]+ | 218.14 (100), 85.029 (54), 159.066 (15), 60.082 (11), 144.103 (6) | 1 | In-house library |
| AC 04:0 (Butanoylcarnitine) | Plasma: G2B/AlcoholBis, F4G, BestTreat<br>Feces: BestTreat | C11H21NO4 | RP | 1.75 | Pos | 232.1543 | [M+H]+ | 85.028 (100), 232.154 (93), 71.047 (21), 60.079 (14), 232.059 (8), 232.313 (7), 58.189 (6), 36.406 (5), 173.079 (5) | 1 | In-house library |
| AC 05:0 (Isovalerylcarnitine) | Plasma: G2B/AlcoholBis, F4G, BestTreat | C12H23NO4 | HILIC | 1.39 | Pos | 246.1714 | [M-H]+ | 85.029 (100), 246.173 (71), 60.082 (34), 187.095 (30), 144.106 (17), 44.996 (12), 57.071 (11) | 1 | In-house library |
| AC 06:0 (Hexanoylcarnitine) | Plasma: G2B/AlcoholBis, F4G | C13H25NO4 | RP | 4.21 | Pos | 260.1855 | [M-H]+ | 85.029 (100), 260.186 (44), 260.194 (20) | 1 | In-house library |
| AC 08:0 (Octanoylcarnitine) | Plasma: G2B/AlcoholBis, F4G, BestTreat<br>Feces: BestTreat | C15H29NO4 | RP | 6.01 | Pos | 288.2168 | [M-H]+ | 85.029 (100), 288.217 (44) | 1 | In-house library |
| AC 08:1 (Octenoyl-L-carnitine) | Plasma: G2B/AlcoholBis, F4G, BestTreat | C15H27NO4 | RP | 5.20 | Pos | 286.2012 | [M+H]+ | 85.029 (100), 286.199 (48) | 1 | In-house library |
| AC 09:0 (Nonanoylcarnitine) | Plasma: G2B/AlcoholBis, BestTreat<br>Feces: BestTreat | C16H31NO4 | RP | 6.37 | Pos | 302.2324 | [M+H]+ | 85.029 (100), 302.233 (52) | 1 | In-house library |
| AC 10:0 (Decanoylcarnitine) | Plasma: G2B/AlcoholBis, F4G | C17H33NO4 | RP | 7.27 | Pos | 316.2481 | [M+H]+ | 316.249 (100), 85.029 (17), 257.176 (6) | 1 | In-house library |
| AC 10:1 (Decenoylcarnitine) | Plasma: G2B/AlcoholBis, F4G, BestTreat | C17H31NO4 | RP | 6.95 | Pos | 314.2324 | [M-H]+ | 85.029 (100), 314.233 (43) | 2 | LipidMaps |
| AC 10:2 (Decadienoylcarnitine) | Plasma: G2B/AlcoholBis, BestTreat | C17H29NO4 | RP | 6.21 | Pos | 312.2168 | [M-H]+ | 85.029 (100), 312.218 (50) | 2 | LipidMaps |
| AC 10:3 (Decatrienoylcarnitine) | Plasma: G2B/AlcoholBis | C17H27NO4 | RP | 5.95 | Pos | 310.2011 | [M-H]+ | 85.029 (100), 310.203 (34) | 2 | LipidMaps |
| AC 11:1 (Undecenoylcarnitine) | Plasma: G2B/AlcoholBis, F4G, BestTreat | C18H33NO4 | RP | 7.15 | Pos | 328.2487 | [M+H]+ | 328.249 (100), 85.028 (20), 269.177 (13), 133.081 (4) | 2 | LipidMaps |
| AC 12:0 (Dodecanoylcarnitine) | Plasma: G2B/AlcoholBis, F4G, BestTreat<br>Feces: BestTreat | C19H37NO4 | RP | 8.15 | Pos | 344.2795 | [M-H]+ | 344.281 (100), 85.029 (17), 285.209 (9) | 1 | In-house library |
| AC 12:1 (Dodecenoylcarnitine) | Plasma: G2B/AlcoholBis, F4G, BestTreat<br>Feces: BestTreat | C19H35NO4 | RP | 7.74 | Pos | 342.2638 | [M+H]+ | 85.029 (100), 342.264 (24), 60.082 (14), 163.146 (11), 283.188 (10), 121.098 (10), 157.048 (8), 95.085 (7), 181.161 (7), 83.083 (6) | 1 | In-house library |
| AC 13:0 | Plasma: G2B/AlcoholBis | C20H40NO4 | RP | 8.40 | Pos | 358.2950 | [M+H]+ | 85.029 (100), 358.293 (61) | 2 | LipidMaps |
| AC 13:1 (Tridecenoylcarnitine) | Plasma: G2B/AlcoholBis, BestTreat<br>Feces: BestTreat | C20H38NO4 | RP | 8.12 | Pos | 356.2793 | [M+H]+ | 85.029 (100), 356.281 (61) | 2 | LipidMaps |
| AC 14:0 (Tetradecanoyl-L-carnitine) | Plasma: G2B/AlcoholBis, F4G, BestTreat<br>Feces: F4G, BestTreat | C21H41NO4 | RP | 8.81 | Pos | 372.3107 | [M+H]+ | 372.312 (100), 46.064 (19), 372.363 (13), 85.026 (9), 60.079 (7), 272.155 (5), 75.025 (5), 111.078 (5), 327.963 (4) | 1 | In-house library |
| AC 14:1 (Tetradecenoylcarnitine) | Plasma: G2B/AlcoholBis, F4G, BestTreat<br>Feces: F4G, BestTreat | C21H39NO4 | RP | 8.49 | Pos | 370.2951 | [M+H]+ | 85.022 (100), 370.29 (71), 60.075 (33), 311.215 (19), 144.093 (12), 191.171 (10), 209.182 (8), 69.063 (8), 109.094 (7), 121.094 (7) | 1 | In-house library |
| AC 14:2 (Tetradecadienoylcarnitine) | Plasma: G2B/AlcoholBis, F4G, BestTreat<br>Feces: BestTreat | C21H37NO4 | RP | 8.11 | Pos | 368.2795 | [M+H]+ | 85.029 (100), 368.282 (55) | 2 | LipidMaps |
| AC 15:OH (Hydroxyoctanoylcarnitine) | Plasma: G2B/AlcoholBis | C15H26NO5 | RP | 4.85 | Pos | 304.2117 | [M+H]+ | 85.029 (100), 304.208 (66) | 2 | LipidMaps |
| AC 16:0 (Palmitoylcarnitine) | Plasma: G2B/AlcoholBis, F4G, BestTreat<br>Feces: F4G, BestTreat | C23H45NO4 | RP | 9.32 | Pos | 400.3416 | [M-H]+ | 85.029 (100), 400.343 (53), 400.358 (26) | 1 | In-house library |
| AC 16:1 (O-Palmitoleoylcarnitine) | Plasma: G2B/AlcoholBis, F4G, BestTreat<br>Feces: F4G, BestTreat | C23H43NO4 | RP | 8.99 | Pos | 398.3264 | [M+H]+ | 85.029 (100), 398.329 (61), 398.314 (35) | 2 | LipidMaps |
| AC 17:OH (Hydroxydecanoylcarnitine) | Plasma: G2B/AlcoholBis | C19H37NO5 | RP | 6.31 | Pos | 332.2430 | [M+H]+ | 85.029 (100), 332.245 (67), 288.036 (27) | 2 | LipidMaps |
| AC 18:1 (Oleylcarnitine) | Plasma: G2B/AlcoholBis, F4G, BestTreat<br>Feces: F4G, BestTreat | C25H47NO4 | RP | 9.44 | Pos | 426.3570 | [M+H]+ | 426.358 (100), 85.028 (74), 60.08 (16), 57.068 (5), 241.139 (4), 144.102 (4), 367.287 (4), 255.16 (4), 265.254 (4) | 1 | In-house library |
| AC 18:2 (Linoleylcarnitine) | Plasma: G2B/AlcoholBis, F4G, BestTreat<br>Feces: F4G, BestTreat | C25H45NO4 | RP | 9.17 | Pos | 424.3420 | [M+H]+ | 424.343 (100), 69.07 (6), 424.392 (5), 281.542 (4), 363.898 (4) | 1 | In-house library |
| Acesulfame-K | Feces: F4G | C4H5NO4S | RP | 1.46 | Neg | 161.9856 | [M-H]- | 77.966 (100), 82.029 (66), 144.889 (15), 64.138 (22), 79.960 (12), 45.209 (6) | 2 | HMDB |
| Acetylcarnitine | Plasma: G2B/AlcoholBis, F4G, BestTreat<br>Feces: F4G, BestTreat | C9H17NO4 | HILIC | 3.20 | Pos | 204.1239 | [M+H]+ | 85.028 (100), 43.018 (37), 57.033 (28), 58.064 (18), 60.08 (16), 84.08 (11), 41.038 (5), 45.057 (4) | 1 | In-house library |
| Ala-Ala-Lys | Feces: F4G | C12H24N4O4 | HILIC | 7.23 | Pos | 289.1887 | [M+H]+ | 84.08 (100), 130.084 (36), 129.101 (10), 115.085 (8), 147.109 (6), 82.064 (5) | 2 | NIST MS Data Center |
| Ala-Lys | Feces: F4G | C9H19N3O3 | HILIC | 7.26 | Pos | 218.1496 | [M+H]+ | 147.113 (100), 130.087 (67), 129.103 (58), 84.081 (54), 218.151 (46), 131.091 (7), 101.107 (7), 148.116 (5), 155.118 (5), 201.123 (5) | 2 | NIST MS Data Center |
| Alanine | Plasma: F4G | C3H7NO2 | HILIC | 5.72 | Pos | 90.0552 | [M+H]+ | 44.049 (100), 90.054 (17), 90.093 (10) | 1 | In-house library |
| Alanine betaine/beta-alanine betaine | Plasma: F4G, BestTreat<br>Feces: BestTreat | C6H13NO2 | HILIC | 3.60 | Pos | 132.1023 | [M+H]+ | 132.102 (100), 59.073 (9), 58.066 (9), 103.955 (5) | 1 | In-house library |
| Alanylleucine | Feces: BestTreat, | C9H18N2O3 | RP | 2.15 | Pos | 203.1391 | [M-H]+ | 132.102 (100), 86.097 (85), 157.133 (30) | 2 | HMDB |
| Alanylleucine | Feces: F4G | C9H18N2O3 | RP | 1.63 | Pos | 203.1393 | [M+H]+ | 132.101 (100), 203.139 (97), 157.132 (63), 147.112 (23), 158.118 (19), 186.075 (18), 133.106 (17), 86.096 (16), 202.144 (14), 175.096 (12) | 2 | NIST MS Data Center |
| Allocholic acid | Plasma: BestTreat<br>Feces: BestTreat | C24H40O5 | RP | 9.25 | Neg | 407.2811 | [M-H]- | 407.279 (100) | 1 | In-house library |
| alpha-Tocopherol | Plasma: F4G<br>Feces: F4G | C29H50O2 | RP | 12.27 | Pos | 430.3824 | [M+H]+ | 430.377 (100), 165.09 (33), 164.083 (17), 166.091 (6), 163.111 (5), 57.069 (5), 175.111 (5), 43.053 (4), 109.1 (4), 430.261 (4) | 1 | In-house library |
| Anandamide (18:2, n-6) | Feces: F4G | C20H37NO2 | RP | 10.23 | Pos | 324.2885 | [M+H]+ | 324.288 (100), 323.254 (4), 307.261 (1), 306.277 (1), 263.235 (1), 162.059 (1) | 2 | MassBank |
| Androsterone sulfate isomer 1 | Plasma: G2B/AlcoholBis, F4G<br>Feces: F4G | C19H30O5S | RP | 7.16 | Neg | 369.1744 | [M-H]- | 96.96 (100), 369.172 (13), 98.957 (6), 212.994 (4) | 2 | HMDB |
| Androsterone sulfate isomer 2 | Plasma: G2B/AlcoholBis, F4G, BestTreat<br>Feces: F4G, BestTreat | C19H30O5S | RP | 7.85 | Neg | 369.1741 | [M-H]- | 369.173 (100), 96.96 (30) | 2 | HMDB |
| Androsterone sulfate isomer 3 | Plasma: G2B/AlcoholBis | C19H30O5S | RP | 8.99 | Neg | 369.1746 | [M-H]- | 369.173 (100), 96.96 (34) | 2 | HMDB |
| Aniline | Feces: G2B, F4G | C6H7N | HILIC | 1.34 | Pos | 94.0649 | [M+H]+ | 94.064 (100) | 2 | HMDB |

| Annotation | Sample matrix & study | Molecular formula | Column | Retention time | ESI | *m/z* | Adduct type | MS/MS fragments (%) | ID level | Annotation source |
|---|---|---|---|---|---|---|---|---|---|---|
| Arachidic acid | Feces: F4G | C20H40O2 | RP | 11.42 | Neg | 311.2969 | [M-H]- | 183.012 (100), 311.169 (31), 197.027 (26), 184.015 (14), 186.013 (7), 225.059 (6), 119.052 (5), 198.033 (4), 108.396 (4), 130.966 (4) | 2 | HMDB |
| Arginine | Plasma: G2B/AlcoholBis, F4G, BestTreat<br>Feces: G2B, F4G, BestTreat | C6H14N4O2 | HILIC | 7.10 | Pos | 175.1194 | [M+H]+ | 175.119 (100), 70.065 (57), 60.056 (46), 116.07 (43), 158.092 (17), 130.099 (10), 114.103 (6), 112.087 (4), 72.08 (4), 43.029 (4) | 1 | In-house library |
| Asparagine | Plasma: F4G | C4H8N2O3 | HILIC | 6.30 | Pos | 133.0611 | [M+H]+ | 74.024 (100), 87.055 (35), 133.061 (23), 88.039 (18), 44.05 (14), 46.028 (9), 43.017 (7), 116.037 (7), 45.047 (6), 60.043 (4) | 1 | In-house library |
| Azelaic acid | Plasma: G2B/AlcoholBis, F4G, BestTreat<br>Feces: G2B, F4G, BestTreat | C9H16O4 | RP | 5.97 | Neg | 187.0976 | [M-H]- | 125.097 (100), 187.098 (52), 123.081 (14), 97.066 (10), 57.034 (10), 169.087 (6), 143.107 (5), 95.05 (4) | 2 | MassBank |
| BA @ 9.04 | Feces: G2B | C24H40O5 | RP | 9.06 | Neg/Pos | 407.2791 | [M-H]- | Neg: 407.283 (100)<br>Pos: 355.2642 (100), 356.2678 (38), 373.2748 (17), 309.2588 (10), 337.252 (10), 339.2683 (8), 245.1552 (7), 213.1647 (4), 319.2448 (3) | 3 | MS-FINDER/SIRIUS |
| BA@7.85 | Feces: G2B, F4G, BestTreat | C24H40O5 | RP | 7.85 | Pos/Neg | 407.2799 | [M-H]- | Neg: 407.283 (100), 112.987 (4)<br>Pos: 355.264 (100), 356.268 (22), 373.274 (18), 372.205 (7), 247.17 (6), 245.155 (5), 264.242 (5), 93.07 (4), 227.179 (4) | 3 | MS-FINDER/SIRIUS |
| Bestatin | Plasma: F4G | C16H24N2O4 | RP | 5.15 | Pos | 309.1834 | [M+H]+ | 120.081 (100), 103.054 (25), 91.054 (13), 133.064 (10), 77.038 (7), 30.033 (7), 86.096 (6), 65.038 (6), 88.04 (5), 96.08 (5) | 2 | MassBank |
| Bile acid_C26H43NO7S | Plasma: G2B/AlcoholBis | C26H42ClN3O3S | RP | 9.47 | Neg | 512.2688 | [M-H]- | 432.316 (100), 512.272 (70), 74.024 (62) | 3 | MS-FINDER/SIRIUS |
| Bile acid_C26H43NO8S isomer 1 | Plasma: G2B/AlcoholBis | C29H39NO8 | RP | 8.94 | Neg | 528.2645 | [M-H]- | 448.304 (100), 528.263 (57), 74.024 (43) | 3 | MS-FINDER/SIRIUS |
| Bile acid_C26H43NO8S isomer 2 | Plasma: G2B/AlcoholBis | C29H39NO8 | RP | 7.56 | Neg | 528.2644 | [M-H]- | 448.305 (100), 74.024 (77), 528.264 (76) | 3 | MS-FINDER/SIRIUS |
| Bile acid_C26H43NO8S isomer 3 | Plasma: G2B/AlcoholBis | C29H39NO8 | RP | 8.76 | Neg | 528.2645 | [M-H]- | 448.304 (100), 74.024 (65), 528.261 (61) | 3 | MS-FINDER/SIRIUS |
| Bilirubin isomer 1 | Plasma: G2B/AlcoholBis | C33H36N4O6 | RP | 7.16 | Pos/Neg | 585.2709 | [M+H]+ | Pos: 299.138 (100), 285.123 (72), 585.276 (62), 568.237 (50)<br>Neg: 227.12 (100), 299.142 (69), 253.135 (61), 239.119 (57) | 2 | HMDB |
| Bilirubin isomer 2 | Plasma: G2B/AlcoholBis | C33H36N4O6 | RP | 5.91 | Pos/Neg | 585.2710 | [M+H]+ | Pos: 299.138 (100), 285.123 (48), 568.25 (41)<br>Neg: 227.12 (100), 299.143 (83), 285.125 (75), 239.12 (70) | 2 | HMDB |
| Bilirubin isomer 3 | Plasma: BestTreat<br>Feces: F4G, BestTreat | C33H36N4O6 | RP | 11.69 | Pos | 585.2698 | [M+H]+ | 299.138 (100), 299.152 (20), 299.123 (13), 299.157 (6), 300.141 (4), 299.118 (4) | 2 | HMDB |
| Biliverdin isomer 1 | Plasma: G2B/AlcoholBis, F4G, BestTreat<br>Feces: F4G, BestTreat | C33H34N4O6 | RP | 8.24 | Pos | 583.2551 | [M+H]+ | 583.255 (100), 297.124 (5), 243.109 (4) | 2 | HMDB |
| Biliverdin isomer 2 | Plasma: G2B/AlcoholBis, F4G, BestTreat<br>Feces: F4G | C33H34N4O6 | RP | 11.83 | Pos | 583.2552 | [M+H]+ | 297.121 (100), 583.267 (56) | 2 | HMDB |
| C10H10O2 | Plasma: G2B/AlcoholBis, BestTreat<br>Feces: BestTreat | C10H10O2 | RP | 6.12 | Pos | 163.0755 | [M+H]+ | 145.065 (100), 117.07 (51), 163.075 (21) | 3 | MS-FINDER/SIRIUS |
| C12H16O6 | Plasma: G2B/AlcoholBis, BestTreat<br>Feces: BestTreat | C12H16O6 | RP | 5.55 | Neg/Pos | 255.0877 | [M-H]- | Neg: 211.097 (100), 255.088 (18), 167.107 (17)<br>Pos: 193.087 (100), 179.069 (86), 239.092 (31) | 3 | MS-FINDER/SIRIUS |
| C14H22O3 | Plasma: G2B/AlcoholBis, BestTreat<br>Feces: BestTreat | C14H22O3 | RP | 9.66 | Pos | 239.1640 | [M+H]+ | 179.142 (100), 239.162 (35) | 3 | MS-FINDER/SIRIUS |
| C15H12O2 | Plasma: G2B/AlcoholBis | C15H12O2 | RP | 8.41 | Pos | 225.0909 | [M+H]+ | 197.096 (100), 105.034 (39), 225.091 (34) | 3 | MS-FINDER/SIRIUS |
| C16H18N2O5 | Plasma: G2B/AlcoholBis | C16H18N2O5 | RP | 5.86 | Pos | 301.1182 | [M+H-H2O]+ | 255.113 (100), 241.096 (59), 283.106 (46) | 3 | MS-FINDER/SIRIUS |
| C18H33NO2 | Plasma: G2B/AlcoholBis | C18H33NO2 | RP | 9.27 | Pos | 278.2478 | [M+H-H2O]+ | 81.071 (100), 95.086 (85), 261.219 (59), 109.102 (47) | 3 | MS-FINDER/SIRIUS |
| C18H35NO2 | Plasma: G2B/AlcoholBis | C18H35NO2 | RP | 9.45 | Pos | 280.2635 | [M+H-H2O]+ | 81.071 (100), 95.086 (92), 109.102 (73), 280.263 (67) | 3 | MS-FINDER/SIRIUS |
| C24H32O7 | Feces: G2B | C24H32O7 | RP | 8.44 | Pos | 415.2124 | [M+H-H2O]+ | 119.085 (100), 120.089 (11), 91.054 (4) | 3 | MS-FINDER/SIRIUS |
| C24H38O4 | Plasma: BestTreat<br>Feces: BestTreat | C24H38O4 | RP | 9.18 | Pos | 391.2844 | [M+H]+ | 355.264 (100), 309.256 (92), 373.273 (45) | 3 | MS-FINDER/SIRIUS |
| C29H48O3 | Plasma: G2B/AlcoholBis | C29H48O3 | RP | 11.95 | Pos | 445.3676 | [M+H]+ | 139.075 (100), 445.292 (57), 69.071 (51), 81.071 (43) | 3 | MS-FINDER/SIRIUS |
| C29H50O4 | Plasma: G2B/AlcoholBis | C29H50O4 | RP | 12.43 | Pos | 445.3671 | [M+H-H2O]+ | 139.075 (100), 69.071 (76), 445.288 (63),83.086 (49 | 3 | MS-FINDER/SIRIUS |
| C38H36N3O | Plasma: G2B/AlcoholBis | C38H36N3O | RP | 11.43 | Pos | 568.4274 | [M+H]+ | 119.086 (100), 145.102 (84), 133.102 (69), 159.117 (58) | 3 | MS-FINDER/SIRIUS |
| C5H11NO2 | Plasma: BestTreat<br>Feces: F4G, BestTreat | C5H11NO2 | HILIC | 4.16 | Pos | 118.0869 | [M+H]+ | 72.081 (100), 118.087 (25) | 3 | MS-FINDER/SIRIUS |
| C6H10O3 | Plasma: G2B/AlcoholBis | C6H10O3 | RP | 3.64 | Neg | 129.0559 | [M-H]- | 129.055 (100), 113.926 (10) | 3 | MS-FINDER/SIRIUS |
| C6H11NO | Feces: G2B | C6H11NO | HILIC | 3.54 | Pos | 114.0911 | [M+H]+ | 113.107 (100), 70.065 (38), 84.078 (37), 86.098 (25), 114.091 (24) | 3 | MS-FINDER/SIRIUS |
| C7H16N2O | Feces: G2B, F4G, BestTreat | C7H16N2O | HILIC | 2.89 | Pos | 145.1330 | [M+H]+ | 145.132 (100), 128.106 (29), 86.095 (16), 121.964 (5) | 3 | MS-FINDER/SIRIUS |
| C8H15NO2 | Plasma: G2B/AlcoholBis, BestTreat<br>Feces: BestTreat | C8H15NO2 | RP | 3.34 | Pos | 158.1176 | [M+H]+ | 141.001 (100), 53.04 (76), 95.05 (63), 105.045 (56) | 3 | MS-FINDER/SIRIUS |
| C8H17NO3 | Plasma: G2B/AlcoholBis | C8H17NO3 | RP | 0.60 | Pos | 176.1282 | [M+H]+ | 176.128 (100), 102.056 (54) | 3 | MS-FINDER/SIRIUS |
| C8H9NO2 | Plasma: G2B/AlcoholBis, BestTreat<br>Feces: BestTreat | C8H9NO2 | RP | 2.51 | Pos | 152.0707 | [M+H]+ | 152.071 (100), 110.061 (73), 106.964 (35) | 3 | MS-FINDER/SIRIUS |
| C8H9NO5S | Plasma: G2B/AlcoholBis | C8H9NO5S | RP | 2.02 | Neg | 230.0130 | [M-H]- | 150.055 (100), 230.013 (40) | 3 | MS-FINDER/SIRIUS |
| C9H15NO3 | Plasma: G2B/AlcoholBis | C9H15NO3 | RP | 0.67 | Pos | 186.1131 | [M+H]+ | 186.112 (100), 168.103 (9), 126.092 (7) | 3 | MS-FINDER/SIRIUS |
| C9H16N2O2 isomer 1 | Plasma: G2B/AlcoholBis, BestTreat<br>Feces: BestTreat | C9H16N2O2 | RP | 2.77 | Pos | 185.1285 | [M+H]+ | 126.092 (100), 185.129 (24), 126.088 (23) | 3 | MS-FINDER/SIRIUS |
| C9H16N2O2 isomer 2 | Plasma: G2B/AlcoholBis | C9H16N2O2 | RP | 2.38 | Pos | 185.1284 | [M+H]+ | 126.092 (100), 185.129 (22), 125.108 (20) | 3 | MS-FINDER/SIRIUS |
| Caffeine | Plasma: G2B/AlcoholBis, F4G, BestTreat<br>Feces: G2B, F4G, BestTreat | C8H10N4O2 | RP | 3.81 | Pos | 195.0878 | [M+H]+ | 195.088 (100), 138.066 (30) | 1 | In-house library |
| Catechin | Feces: F4G | C15H14O6 | HILIC | 7.94 | Pos | 291.0878 | [M+H]+ | 123.045 (100), 135.044 (99), 139.038 (61), 89.04 (44), 106.063 (44), 147.044 (34), 124.048 (30), 111.045 (30), 119.05 (29), 166.087 (25) | 2 | MassBank |
| Chenodeoxycholic acid | Plasma: G2B/AlcoholBis, BestTreat<br>Feces: G2B, F4G, BestTreat | C24H40O4 | RP | 9.82 | Neg/Pos | 437.2910 | [M-HCOO]- | Neg: 391.284 (100), 416.9821 (3), 254.9873 (2)<br>Pos: 91.787 (100), 431.256 (96), 106.258 (72), 62.73 (70), 151.61 (69), 111.625 (68), 120.995 (68) | 1 | In-house library |
| Cholesterol isomer 1 | Plasma: F4G | C27H46O | RP | 12.38 | Pos | 369.3526 | [M+H-H2O]+ | 369.352 (100), 147.118 (52), 109.101 (50), 135.117 (44), 161.132 (35), 69.069 (32), 175.147 (26), 111.115 (24), 83.085 (23), 215.181 (21) | 1 | In-house library |
| Cholesterol isomer 2 | Plasma: BestTreat<br>Feces: BestTreat | C27H46O | RP | 13.54 | Pos | 369.3517 | [M+H-H2O]+ | 369.35 (100), 147.117 (45), 95.086 (42), 135.116 (40), 109.101 (38) | 1 | In-house library |
| Cholesterol sulfate | Plasma: F4G | C27H46O4S | RP | 10.51 | Neg | 465.3038 | [M-H]- | 465.303 (100), 96.96 (12), 146.937 (4) | 2 | MassBank |
| Cholic acid | Plasma: G2B/AlcoholBis, BestTreat<br>Feces: G2B, F4G, BestTreat | C24H40O5 | RP | 9.29 | Pos | 373.2736 | [M+H-2H2O]+ | 355.262 (100), 373.273 (11), 213.164 (11), 245.152 (10) | 1 | In-house library |

| Annotation | Sample matrix & study | Molecular formula | Column | Retention time | ESI | *m/z* | Adduct type | MS/MS fragments (%) | ID level | Annotation source |
|---|---|---|---|---|---|---|---|---|---|---|
| Choline | Plasma: F4G<br>Feces: G2B, F4G | C5H14NO | HILIC | 1.54 | Pos | 104.1071 | [M]+ | 58.065 (100), 44.049 (54), 45.033 (18), 42.033 (16), 45.056 (15), 43.041 (10), 60.08 (8), 43.017 (5) | 2 | HMDB |
| Citalopram/Escitalopram | Plasma: G2B/AlcoholBis | C20H21FN2O | RP | 5.61 | Pos | 325.1710 | [M+H]+ | 325.173 (100), 109.045 (64), 262.103 (49) | 2 | MassBank |
| Citric acid | Feces: G2B, F4G | C6H8O7 | HILIC | 6.82 | Neg | 191.0216 | [M-H]- | 111.01 (100), 87.011 (47), 85.031 (41), 191.022 (38), 129.022 (21), 55.991 (11), 88.832 (11), 65.944 (8), 61.12 (8) | 2 | HMDB |
| Citrulline | Plasma: G2B/AlcoholBis, F4G, BestTreat<br>Feces: F4G, BestTreat | C6H13N3O3 | HILIC | 6.51 | Pos | 176.1034 | [M+H]+ | 159.076 (100), 113.071 (47), 70.065 (33), 115.086 (12), 116.071 (11), 176.105 (7), 114.056 (6), 133.094 (4) | 1 | In-house library |
| CMPF | Plasma: G2B/AlcoholBis, F4G, BestTreat | C12H16O5 | RP | 7.79 | Neg/Pos | 239.0926 | [M-H]- | Neg: 195.102 (100), 151.112 (51)<br>Pos: 181.086 (100), 163.075 (20), 139.039 (15) | 2 | HMDB |
| Coprocholic Acid | Feces: F4G | C27H46O5 | RP | 9.84 | Neg | 449.3274 | [M-H]- | 449.33 (100), 253.219 (11), 96.96 (5) | 2 | NIST MS Data Center |
| Cortisol | Plasma: G2B/AlcoholBis, F4G, BestTreat<br>Feces: BestTreat | C21H30O5 | RP | 6.99 | Pos/Neg | 363.2165 | [M+H]+ | Pos: 363.218 (100), 121.066 (70), 327.194 (33)<br>Neg: 331.191 (100), 329.176 (30) | 1 | In-house library |
| Cortisone | Plasma: G2B/AlcoholBis, BestTreat | C21H28O5 | RP | 6.74 | Neg/Pos | 405.1918 | [M-HCOO]- | Neg: 329.177 (100), 254.986 (23), 301.179 (21)<br>Pos: 361.199 (100), 163.112 (60) | 1 | In-house library |
| Cotinine | Plasma: G2B/AlcoholBis | C10H12N2O | RP | 1.37 | Pos | 177.1023 | [M+H]+ | 177.101 (100), 80.05 (17), 102.055 (12) | 2 | HMDB |
| Creatine | Plasma: F4G, BestTreat<br>Feces: F4G, BestTreat | C4H9N3O2 | HILIC | 5.65 | Pos | 132.0763 | [M+H]+ | 90.055 (100), 132.077 (96), 44.049 (57), 43.029 (6), 114.065 (5), 87.057 (4) | 1 | In-house library |
| Creatinine | Plasma: G2B/AlcoholBis, F4G, BestTreat<br>Feces: G2B, F4G, BestTreat | C4H7N3O | HILIC | 1.35 | Pos | 114.0659 | [M+H]+ | 44.049 (100), 114.067 (84), 86.071 (11) | 1 | In-house library |
| Cyclo(Pro-Val) | Plasma: F4G, BestTreat<br>Feces: BestTreat | C10H16N2O2 | RP | 3.51 | Pos | 197.1293 | [M+H]+ | 197.128 (100), 70.064 (10), 72.081 (9), 69.07 (7), 55.053 (6), 84.079 (6), 154.074 (5), 169.134 (4) | 2 | HMDB |
| Cyclohexylamine | Plasma: G2B/AlcoholBis | C6H13N | HILIC | 1.18 | Pos | 100.1124 | [M+H]+ | 55.054 (100), 83.085 (73), 100.111 (30) | 2 | HMDB |
| Cysteine S-sulfate | Plasma: F4G | C3H7NO5S2 | HILIC | 5.74 | Neg | 199.9696 | [M-H]- | 80.965 (100), 120.012 (26), 55.611 (24), 191.347 (22), 74.007 (21), 168.795 (16), 75.425 (14), 167.899 (9), 166.248 (8), 24.316 (8) | 2 | HMDB |
| Dehydro(epi)androsterone sulfate isomer 1 | Plasma: F4G, BestTreat<br>Feces: BestTreat | C19H28O5S | RP | 7.03 | Neg | 367.1587 | [M-H]- | 367.158 (100), 96.96 (34) | 2 | HMDB |
| Dehydro(epi)androsterone sulfate isomer 2 | Plasma: G2B/AlcoholBis | C19H28O5S | RP | 8.00 | Neg | 367.1586 | [M-H]- | 96.96 (100), 367.156 (94) | 2 | HMDB |
| Dehydro(epi)androsterone sulfate isomer 3 | Feces: F4G | C19H28O5S | RP | 7.37 | Neg | 367.1605 | [M-H]- | 367.16 (100), 96.96 (6), 367.181 (4) | 2 | HMDB |
| Dehydroandrosterone | Plasma: G2B/AlcoholBis, F4G, BestTreat<br>Feces: BestTreat | C19H28O2 | RP | 7.59 | Pos | 271.2056 | [M+H-H2O]+ | 271.205 (100), 253.195 (87), 213.164 (54) | 2 | HMDB |
| Dehydrophytosphingosine | Feces: BestTreat, | C18H37NO3 | RP | 8.76 | Pos | 316.2846 | [M+H]+ | 60.045 (100), 316.286 (56) | 2 | MassBank |
| Dehydrophytosphingosine | Feces: F4G | C18H37NO3 | RP | 8.47 | Pos | 316.2837 | [M+H]+ | 316.283 (100), 314.323 (7), 297.242 (2), 280.266 (2), 271.2028 (1), 219.213 (1) | 2 | ReSpect |
| Deoxycholic acid | Plasma: G2B/AlcoholBis, F4G, BestTreat<br>Feces: G2B, F4G, BestTreat | C24H40O4 | RP | 9.90 | Pos/Neg | 410.3264 | [M+NH4]+ | Pos: 357.278 (100), 221.155 (9), 339.265 (9)<br>Neg: 391.285 (100), 345.279 (5) | 1 | In-house library |
| Diazepam | Plasma: G2B/AlcoholBis | C16H13ClN2O | RP | 7.98 | Pos | 285.0789 | [M+H]+ | 285.078 (100), 257.085 (9), 154.042 (7) | 2 | HMDB |
| Dimethylglycine | Plasma: F4G | C4H9NO2 | HILIC | 4.82 | Pos | 104.0714 | [M+H]+ | 58.065 (100), 104.071 (26), 104.107 (6) | 2 | MassBank |
| Dimethylphenylamine | Plasma: BestTreat<br>Feces: G2B, F4G, BestTreat | C8H11N | HILIC | 0.82 | Pos | 122.0960 | [M+H]+ | 122.096 (100), 107.072 (36) | 2 | HMDB |
| EDTA | Plasma: G2B/AlcoholBis | C10H16N2O8 | HILIC | 7.93 | Pos | 293.0987 | [M+H]+ | 132.066 (100), 160.061 (67), 114.055 (13), 86.06 (12), 88.039 (9), 74.06 (7), 60.044 (5), 102.055 (5) | 2 | HMDB |
| Enterodiol | Feces: F4G, BestTreat | C18H22O4 | RP | 6.05 | Neg | 301.1448 | [M-H]- | 301.145 (100), 253.123 (32), 271.135 (12), 257.131 (11) | 2 | HMDB |
| Enterolactone | Feces: G2B, F4G, BestTreat | C18H18O4 | RP | 6.27 | Neg | 297.1136 | [M-H]- | 297.1158 (100), 253.1263 (8), 107.0521 (6), 165.0549 (4), 251.1114 (4), 254.1295 (4), 133.0618 (2), 132.0599 (2), 189.0567 (2) | 2 | HMDB |
| Epsilon-caprolactam | Plasma: G2B/AlcoholBis, F4G | C6H11NO | HILIC | 0.59 | Pos | 114.0921 | [M+H]+ | 44.013 (100), 114.091 (67), 69.07 (66), 41.038 (58), 55.054 (57), 43.054 (55), 79.054 (41), 55.018 (21), 96.082 (17), 97.065 (8) | 2 | HMDB |
| Ethyl imidazole-2-carboxylate | Plasma: F4G | C6H8N2O2 | HILIC | 5.39 | Pos | 141.0661 | [M+H]+ | 141.065 (100), 95.059 (10), 96.069 (8) | 2 | MassBank |
| FA 12:0 (Hydroxydodecanoid acid) | Plasma: G2B/AlcoholBis, BestTreat<br>Feces: F4G, BestTreat | C12H24O3 | RP | 9.12 | Neg | 215.1655 | [M-H]- | 59.013 (100), 115.921 (31), 215.167 (24) | 2 | NIST MS Data Center |
| FA 14:0 (Myristic acid) | Plasma: F4G, BestTreat<br>Feces: BestTreat | C14H28O2 | RP | 10.42 | Neg | 227.2018 | [M-H]- | 227.201 (100), 209.157 (8), 92.912 (6), 227.125 (6), 119.736 (5) | 2 | Agilent MassHunter PCDL |
| FA 16:0 (Palmitic acid) | Plasma: G2B/AlcoholBis, F4G, BestTreat<br>Feces: G2B, F4G, BestTreat | C16H30O2 | RP | 11.14 | Neg | 255.2335 | [M-H]- | 255.235 (100) | 2 | HMDB |
| FA 16:1 (Palmitoleic acid) | Plasma: G2B/AlcoholBis, F4G, BestTreat<br>Feces: F4G, BestTreat | C16H30O2 | RP | 10.80 | Neg | 253.2174 | [M-H]- | 253.216 (100) | 2 | HMDB |
| FA 16:1;O (Hydroxyhexadecanoic acid) | Plasma: BestTreat<br>Feces: F4G, BestTreat | C16H32O3 | RP | 10.60 | Neg | 271.2288 | [M-H]- | 271.228 (100), 225.223 (51) | 2 | LipidMaps |
| FA 16:1;O (Hydroxyhexadecenoic acid) | Plasma: G2B/AlcoholBis | C16H32O3 | RP | 10.64 | Pos/Neg | 271.2291 | [M-H]- | Neg: 271.23 (100), 270.98 (8)<br>Pos: 69.071 (100), 57.071 (93), 83.086 (84), 219.211 (80), 97.102 (71) | 2 | MassBank |
| FA 18:0 (Stearic acid) | Plasma: G2B/AlcoholBis, F4G, BestTreat<br>Feces: G2B, F4G, BestTreat | C18H36O2 | RP | 11.59 | Neg | 283.2645 | [M-H]- | 283.262 (100), 112.985 (5) | 2 | HMDB |
| FA 18:0;O (Hydroxyoctadecanoic acid) | Plasma: G2B/AlcoholBis, BestTreat<br>Feces: G2B, F4G, BestTreat | C18H36O3 | RP | 10.93 | Neg | 299.2597 | [M-H]- | 59.013 (100), 299.261 (29) | 2 | LipidMaps |
| FA 18:1 (Octadecenoic acid) | Plasma: G2B/AlcoholBis, F4G, BestTreat<br>Feces: G2B, F4G, BestTreat | C18H34O2 | RP | 11.24 | Neg/Pos | 281.2489 | [M-H]- | Neg: 281.247 (100), 112.986 (5)<br>Pos: 69.071 (100), 57.071 (98), 83.087 (87), 97.102 (78), 71.086 (74) | 2 | NIST MS Data Center |
| FA 18:1;O (Hydroxyoctadecenoic acid) | Feces: G2B | C18H34O3 | RP | 9.98 | Pos/Neg | 299.2594 | [M+H]+ | Pos: 141.128 (100), 253.253 (49), 123.118 (43), 71.086 (37), 97.102 (29), 245.226 (27), 95.086 (26), 235.243 (23), 109.101 (21), 81.07 (18)<br>Neg: 297.237 (100), 297.146 (7) | 2 | LipidMaps |
| FA 18:1;O2 (Octadecanedioic acid) | Plasma: G2B/AlcoholBis, BestTreat<br>Feces: BestTreat | C18H34O4 | RP | 10.13 | Neg | 313.2392 | [M-H]- | 313.24 (100), 251.237 (85), 295.227 (51) | 2 | Fiehn-HILIC |
| FA 18:2 (Linolcic acid) | Plasma: G2B/AlcoholBis, F4G, BestTreat<br>Feces: G2B, F4G, BestTreat | C18H32O2 | RP | 10.96 | Neg | 279.2333 | [M-H]- | 279.232 (100) | 2 | MassBank |
| FA 18:3 (Linolenic acid) | Plasma: G2B/AlcoholBis, BestTreat<br>Feces: F4G, BestTreat | C18H30O3 | RP | 10.71 | Neg | 277.2173 | [M-H]- | 277.216 (100), 192.99 (11) | 2 | ReSpect |
| FA 20:3 (Eicosatrienoic acid) | Plasma: G2B/AlcoholBis, BestTreat<br>Feces: F4G, BestTreat | C20H32O2 | RP | 11.11 | Neg | 305.2492 | [M-H]- | 305.251 (100), 304.985 (6) | 2 | NIST MS Data Center |

| Annotation | Sample matrix & study | Molecular formula | Column | Retention time | ESI | *m/z* | Adduct type | MS/MS fragments (%) | ID level | Annotation source |
|---|---|---|---|---|---|---|---|---|---|---|
| FA 20:3;O | Plasma: G2B/AlcoholBis, BestTreat<br>Feces: BestTreat | C20H34O3 | RP | 10.92 | Pos/Neg | 305.2474 | [M+H-H2O]+ | Pos: 305.246 (100), 121.101 (35), 95.086 (35), 81.071 (33)<br>Neg: 303.233 (100), 59.013 (17), 259.245 (15) | 2 | LipidMaps |
| FA 20:4 (Arachidonic acid) | Plasma: F4G, BestTreat<br>Feces: F4G, BestTreat | C20H32O2 | RP | 10.64 | Neg | 303.2332 | [M-H]- | 303.233 (100), 259.245 (20), 59.014 (9), 205.194 (4) | 1 | In-house library |
| FA 22:1 (Erucic acid) | Plasma: BestTreat<br>Feces: F4G, BestTreat | C22H42O2 | RP | 12.07 | Neg | 337.3124 | [M-H]- | 337.313 (100) | 1 | In-house library |
| FA 22:4 (Docosatetraenoic acid) | Plasma: G2B/AlcoholBis, BestTreat<br>Feces: F4G, BestTreat | C22H36O2 | RP | 11.26 | Neg | 331.2649 | [M-H]- | 331.267 (100), 330.98 (16) | 2 | NIST MS Data Center |
| FA 22:5 (Docosapentaenoic acid) | Plasma: G2B/AlcoholBis, F4G, BestTreat<br>Feces: F4G, BestTreat | C22H34O2 | RP | 11.03 | Neg/Pos | 329.2490 | [M-H]- | Neg: 329.25 (100), 285.258 (12), 242.985 (10)<br>Pos: 331.264 (100), 81.071 (35), 121.101 (30), 95.086 (27), 133.102 (27) | 2 | NIST MS Data Center |
| FA 22:6 (DHA) | Plasma: G2B/AlcoholBis, F4G, BestTreat<br>Feces: F4G, BestTreat | C22H32O2 | RP | 10.89 | Neg/Pos | 327.2333 | [M-H]- | Neg: 283.243 (100), 59.013 (83), 327.242 (64)<br>Pos: 329.248 (100), 119.086 (22), 93.071 (22) | 1 | In-house library |
| FA 28:7 | Plasma: F4G | C28H42O2 | RP | 11.16 | Neg | 409.3112 | [M-H]- | 409.31 (100) | 2 | LipidMaps |
| Fatty_acid_C27H50O2 | Plasma: G2B/AlcoholBis, BestTreat<br>Feces: BestTreat | C29H50O2 | RP | 13.14 | Pos | 429.3713 | [M+Na]– | 165.091 (100), 429.376 (39) | 3 | MS-FINDER/SIRIUS |
| Fenofibric acid | Plasma: F4G<br>Feces: BestTreat | C17H15ClO4 | RP | 8.56 | Neg | 317.0591 | [M-H]- | 231.021 (100) | 2 | MassBank |
| Flecainide | Plasma: G2B/AlcoholBis | C17H20F6N2O3 | RP | 5.67 | Pos | 415.1450 | [M+H]+ | 398.117 (100), 415.147 (78) | 2 | HMDB |
| Gabapentin | Plasma: F4G, BestTreat<br>Feces: BestTreat | C9H17NO2 | RP | 4.55 | Pos | 172.1331 | [M+H]+ | 109.102 (100), 67.054 (44), 155.108 (43), 84.959 (18), 97.063 (15), 96.959 (14), 119.085 (10), 69.069 (10), 172.13 (9), 137.096 (8) | 2 | MassBank |
| Gliclazide | Plasma: F4G | C15H21N3O3S | RP | 7.49 | Neg | 322.1236 | [M-H]- | 322.124 (100), 170.027 (100), 106.066 (8), 322.175 (5) | 2 | Agilent MassHunter PCDL |
| Glucoheptonic acid | Plasma: F4G | C7H14O8 | HILIC | 5.28 | Neg | 225.0615 | [M-H]- | 59.014 (100), 71.014 (34), 44.997 (14), 89.025 (12), 113.025 (9), 101.022 (8), 43.018 (5), 55.018 (5), 87.01 (4) | 2 | MassBank |
| Glutamic acid | Plasma: G2B/AlcoholBis, F4G, BestTreat<br>Feces: G2B, F4G, BestTreat | C5H9NO4 | HILIC | 6.51 | Pos | 148.0602 | [M+H]+ | 84.043 (100), 42.409 (3), 71.661 (2) | 1 | In-house library |
| Glutamine | Plasma: G2B/AlcoholBis, F4G, BestTreat<br>Feces: F4G, BestTreat | C5H10N2O3 | HILIC | 6.27 | Pos | 147.0767 | [M+H]+ | 130.05 (100), 84.044 (93), 101.071 (15), 147.076 (10), 41.038 (4) | 1 | In-house library |
| Glutaric acid | Plasma: BestTreat<br>Feces: G2B, F4G, BestTreat | C5H8O4 | RP | 1.89 | Neg | 131.0342 | [M-H]- | 87.044 (100), 131.034 (20), 113.024 (9), 69.033 (9) | 1 | In-house library |
| Glycerophosphocholine | Plasma: F4G, BestTreat<br>Feces: F4G, BestTreat | C8H20NO6P | HILIC | 6.28 | Pos | 258.1116 | [M+H]+ | 104.107 (100), 125 (15), 184.073 (15), 60.081 (8), 86.096 (8), 258.112 (7), 166.062 (4) | 2 | MassBank |
| Glycerophospholipid_C44H78NO7P | Plasma: G2B/AlcoholBis | C44H78NO7P | RP | 12.97 | Pos | 764.5584 | [M+H]+ | 184.073 (100), 623.505 (35) | 3 | MS-FINDER/SIRIUS |
| Glycerophospholipid_C45H80NO8P | Plasma: G2B/AlcoholBis | C45H80NO8P | RP | 12.92 | Pos | 832.5244 | [M+K]+ | 184.073 (100),86.097 (32), 773.44 (19) | 3 | MS-FINDER/SIRIUS |
| Glycerophospholipid_C48H84NO7P | Plasma: G2B/AlcoholBis | C48H84NO7P | RP | 13.61 | Pos | 856.5610 | [M+K]+ | 797.498 (100), 86.097 (95), 162.956 (78) | 3 | MS-FINDER/SIRIUS |
| Glycine Betaine | Plasma: G2B/AlcoholBis, F4G, BestTreat<br>Feces: BestTreat | C5H11NO2 | HILIC | 4.02 | Pos | 118.0871 | [M+H]+ | 58.065 (100), 59.073 (97), 118.087 (33) | 1 | In-house library |
| Glycochenodeoxycholic acid isomer 1 | Plasma: G2B/AlcoholBis, F4G, BestTreat<br>Feces: F4G, BestTreat | C26H43NO5 | RP | 9.24 | Pos/Neg | 432.3109 | [M+H-H2O]+ | Pos: 414.298 (100), 339.271 (38), 76.04 (34), 321.26 (27)<br>Neg: 74.024 (100), 448.307 (64) | 1 | In-house library |
| Glycochenodeoxycholic acid isomer 2 | Plasma: G2B/AlcoholBis | C26H43NO5 | RP | 9.38 | Neg | 448.3074 | [M-H]- | 74.024 (100), 448.307 (82), 242.989 (65), 192.99 (54) | 1 | In-house library |
| Glycocholic acid | Plasma: G2B/AlcoholBis, BestTreat<br>Feces: BestTreat | C26H43NO6 | RP | 8.75 | Neg/Pos | 464.3016 | [M-H]- | Neg: 464.306 (100), 74.024 (67)<br>Pos: 412.281 (100), 337.252 (60), 319.242 (33) | 1 | In-house library |
| Glycohyodeoxycholic acid | Plasma: G2B/AlcoholBis, BestTreat<br>Feces: BestTreat | C26H43NO5 | RP | 8.26 | Neg/Pos | 448.3076 | [M-H]- | Neg: 448.306 (100), 74.024 (68)<br>Pos: 414.298 (100), 76.04 (52), 269.451 (37), 201.163 (36), 237.234 (34) | 1 | In-house library |
| Glycolithocholic acid | Plasma: G2B/AlcoholBis | C26H43NO4 | RP | 9.43 | Pos | 416.3159 | [M+H-H2O]+ | 76.04 (100), 323.274 (69), 416.313 (67), 341.283 (48) | 1 | In-house library |
| Glycoursodeoxycholic acid | Plasma: F4G | C26H43NO5 | RP | 9.04 | Neg | 448.3070 | [M-H]- | 448.309 (100), 74.025 (21), 345.65 (5), 239.295 (5), 404.315 (4) | 1 | In-house library |
| Gly-Pro-Arg | Feces: F4G | C13H24N6O4 | HILIC | 7.08 | Pos | 329.1932 | [M+H]+ | 329.191 (100), 175.119 (19), 329.143 (12), 312.171 (8), 328.183 (6), 327.18 (5), 312.117 (5), 110.07 (5), 72.079 (4), 246.095 (4) | 2 | Metlin |
| Guanidineacetic acid | Plasma: F4G | C3H7N3O2 | HILIC | 5.79 | Pos | 118.0607 | [M+H]+ | 58.065 (100), 59.073 (47), 43.028 (18), 118.086 (16), 72.057 (6), 44.05 (5) | 2 | HMDB |
| Hippuric acid | Plasma: G2B/AlcoholBis, F4G, BestTreat<br>Feces: BestTreat | C9H9NO3 | RP | 3.55 | Pos | 180.0656 | [M+H]+ | 105.034 (100) | 1 | In-house library |
| Histamine | Feces: G2B, F4G, BestTreat | C5H9N3 | HILIC | 5.54 | Pos | 112.0872 | [M+H]+ | 95.0585 (100), 112.087 (95), 111.9247 (6), 93.6266 (6), 69.0675 (2), 95.6332 (2) | 1 | In-house library |
| Histidine | Plasma: F4G<br>Feces: F4G | C6H9N3O2 | HILIC | 6.84 | Pos | 156.0770 | [M+H]+ | 110.071 (100), 83.06 (34), 93.044 (22), 56.049 (12), 95.06 (10), 82.053 (8) | 1 | In-house library |
| Histidinol | Feces: G2B | C6H11N3O | HILIC | 0.57 | Pos | 124.0869 | [M+H-H2O]+ | 124.087 (100), 83.06 (10), 84.044 (5) | 2 | MassBank |
| Hydroxyoctanoic acid | Plasma: G2B/AlcoholBis | C8H16O3 | RP | 7.02 | Neg | 159.1027 | [M-H]- | 113.097 (100), 159.103 (62) | 2 | HMDB |
| Hydroxyphenyllactic acid | Plasma: G2B/AlcoholBis, BestTreat<br>Feces: BestTreat | C9H10O4 | RP | 3.03 | Neg | 181.0509 | [M-H]- | 163.04 (100), 135.045 (71), 181.05 (68), 136.984 (52) | 2 | HMDB |
| Hydroxysebacic acid | Feces: F4G | C10H18O5 | HILIC | 1.20 | Neg | 217.1078 | [M-H]- | 171.104 (100), 217.109 (87), 155.109 (46), 215.041 (15), 172.107 (12), 125.098 (10), 66.679 (8), 215.096 (8), 199.101 (8), 215.995 (6) | 2 | MassBank |
| Hypoxanthine | Plasma: G2B/AlcoholBis, F4G, BestTreat<br>Feces: G2B, BestTreat | C5H4N4O | HILIC | 1.53 | Pos | 137.0456 | [M+H]+ | 137.047 (100), 94.04 (42), 119.035 (28), 82.04 (8), 120.016 (7), 110.033 (4) | 1 | In-house library |
| Ile-Ala | Feces: F4G | C9H18N2O3 | HILIC | 4.42 | Pos | 203.1386 | [M+H]+ | 203.139 (100), 203.052 (17), 100.076 (9), 188.092 (6) | 2 | HMDB |
| Indole-3-butyric acid | Feces: G2B, BestTreat | C12H13NO2 | HILIC | 1.06 | Pos | 204.1023 | [M+H]+ | 204.101 (100), 107.071 (11), 198.674 (4), 204.051 (4), 106.065 (4), 102.067 (4) | 2 | HMDB |
| Indolelactic acid | Plasma: G2B/AlcoholBis, F4G, BestTreat<br>Feces: BestTreat | C11H11NO3 | RP | 4.82 | Pos/Neg | 206.0809 | [M+H]+ | Pos: 160.076 (100), 188.071 (99), 118.066 (86), 206.082 (76)<br>Neg: 204.066 (100), 158.061 (86) | 1 | In-house library |
| Indoxyl sulfate | Plasma: G2B/AlcoholBis, F4G, BestTreat<br>Feces: BestTreat | C8H7NO4S | RP | 2.73 | Neg | 212.0028 | [M-H]- | 212.002 (100), 79.957 (91), 80.964 (72), 212.078 (62) | 1 | In-house library |
| Isoleucine | Plasma: G2B/AlcoholBis, F4G, BestTreat<br>Feces: F4G, BestTreat | C6H13NO2 | HILIC | 4.51 | Pos | 132.1021 | [M+H]+ | 86.096 (100), 69.07 (17), 41.038 (9), 132.101 (6), 30.033 (5) | 1 | In-house library |
| Ketodeoxycholic acid | Feces: G2B, F4G, BestTreat | C24H38O4 | RP | 8.63 | Pos | 391.2867 | [M+H]+ | 355.264 (100), 373.275 (53), 327.269 (50), 337.254 (30), 356.268 (24), 309.259 (17), 374.278 (14), 328.273 (13), 215.18 (12), 319.241 (8) | 1 | In-house library |
| Kynurenic acid | Feces: F4G | C10H7NO3 | RP | 3.20 | Pos | 190.0506 | [M+H]+ | 162.055 (100), 144.043 (50), 190.049 (44), 172.038 (16), 163.06 (15), 145.017 (7), 145.049 (7), 148.036 (5), 188.969 (5), 143.404 (4) | 2 | ReSpect |
| Kynurenine | Plasma: G2B/AlcoholBis, F4G | C10H12N2O3 | RP | 1.91 | Pos | 209.0920 | [M+H]+ | 94.066 (100), 192.065 (73), 146.059 (64), 136.075 (52) | 1 | In-house library |

| Annotation | Sample matrix & study | Molecular formula | Column | Retention time | ESI | *m/z* | Adduct type | MS/MS fragments (%) | ID level | Annotation source |
|---|---|---|---|---|---|---|---|---|---|---|
| L,L-Cyclo(leucylprolyl) isomer 1 | Plasma: G2B/AlcoholBis, BestTreat<br>Feces: BestTreat | C11H18N2O2 | RP | 4.64 | Pos | 211.1446 | [M+H]+ | 211.144 (100), 70.066 (30), 183.15 (21), 141.001 (21) | 2 | HMDB |
| L,L-Cyclo(leucylprolyl) isomer 2 | Plasma: G2B/AlcoholBis | C11H18N2O2 | RP | 4.79 | Pos | 211.1445 | [M+H]+ | 211.144 (100), 70.066 (41), 141.001 (25) | 2 | HMDB |
| Lactic acid | Plasma: F4G | C3H6O3 | HILIC | 1.46 | Neg | 89.0246 | [M-H]- | 43.019 (100), 89.025 (64), 41.003 (9) | 1 | In-house library |
| L-alfa-Hydroxyisovaleric acid | Plasma: F4G | C5H10O3 | RP | 2.73 | Neg | 117.0558 | [M-H]- | 71.05 (100), 117.054 (46), 43.904 (25), 47.647 (21), 22.763 (14), 71.163 (13), 96.816 (11), 104.782 (11), 37.103 (10), 57.559 (8) | 2 | HMDB |
| Lauryl diethanolamide | Plasma: G2B/AlcoholBis | C16H33NO3 | RP | 9.32 | Pos | 288.2538 | [M+H]+ | 106.086 (100), 88.077 (59), 227.2 (31) | 2 | HMDB |
| L-Carnitine | Plasma: G2B/AlcoholBis, F4G, BestTreat<br>Feces: G2B, F4G, BestTreat | C7H15NO3 | HILIC | 5.10 | Pos | 162.1132 | [M+H]+ | 60.081 (100), 103.039 (89), 85.028 (68), 43.017 (67), 102.091 (47), 162.112 (45), 57.033 (23), 59.073 (9), 41.038 (4) | 1 | In-house library |
| Leucine | Plasma: G2B/AlcoholBis, F4G, BestTreat<br>Feces: G2B, F4G, BestTreat | C6H13NO2 | HILIC | 4.28 | Pos | 132.1019 | [M+H]+ | 44.049 (100), 86.096 (42), 43.054 (32), 30.033 (20), 41.037 (12), 55.054 (11), 55.017 (8), 73.065 (5) | 1 | In-house library |
| Leucine-Proline | Plasma: G2B/AlcoholBis<br>Feces: G2B, F4G | C11H20N2O3 | RP | 0.67 | Pos | 229.1546 | [M+H]+ | 229.155 (100), 142.085 (11) | 2 | HMDB |
| Linoleamide | Plasma: G2B/AlcoholBis, BestTreat<br>Feces: BestTreat | C18H33NO | RP | 10.57 | Pos | 280.2637 | [M+H]+ | 263.237 (100), 280.263 (96), 95.086 (94), 81.071 (88) | 2 | HMDB |
| Lithocholic acid | Feces: G2B, F4G, BestTreat | C24H40O3 | RP | 10.09 | Pos/Neg | 359.2965 | [M+H-H2O]+ | Pos: 95.085 (100), 81.07 (75), 121.101 (70), 109.101 (58), 107.085 (54), 93.07 (52), 135.117 (49), 149.133 (35), 67.054 (32), 133.101 (29)<br>Neg: 375.293 (100), 376.297 (27), 393.304 (8), 377.3 (4) | 1 | In-house library |
| Lysine | Plasma: F4G, BestTreat<br>Feces: F4G, BestTreat | C6H14N2O2 | HILIC | 7.17 | Pos | 147.1135 | [M+H]+ | 56.049 (100), 84.081 (73), 64.927 (30), 41.038 (13), 30.034 (12), 55.053 (9), 69.057 (9), 53.038 (6), 28.017 (5) | 1 | In-house library |
| LysoPC 0:0/14:0 | Plasma: G2B/AlcoholBis, F4G, BestTreat<br>Feces: BestTreat | C22H46NO7P | RP | 9.76 | Neg/Pos | 512.2994 | [M+HCOO]- | Neg: 227.201 (100), 192.989 (16)<br>Pos: 468.31 (100), 184.074 (70), 86.095 (5), 450.298 (5) | 2 | LipidMaps |
| LysoPC 0:0/16:0 | Plasma: G2B/AlcoholBis, F4G, BestTreat<br>Feces: F4G, BestTreat | C24H50NO7P | RP | 10.34 | Pos/Neg | 496.3399 | [M+H]+ | Pos: 184.075 (100), 86.097 (12)<br>Neg: 255.234 (100), 480.309 (8) | 2 | LipidMaps |
| LysoPC 0:0/16:1 | Plasma: G2B/AlcoholBis, F4G, BestTreat<br>Feces: BestTreat | C24H48NO7P | RP | 9.95 | Pos/Neg | 494.3243 | [M+H]+ | Pos: 184.072 (100), 86.097 (10)<br>Neg: 253.219 (100), 478.299 (8) | 2 | LipidMaps |
| LysoPC 0:0/17:1 | Plasma: G2B/AlcoholBis | C25H50NO7P | RP | 10.55 | Pos/Neg | 508.3398 | [M+H]+ | Pos: 184.075 (100), 104.108 (70), 508.336 (35)<br>Neg: 267.233 (100), 224.0708 (10), 96.3146 (5) | 2 | LipidMaps |
| LysoPC 0:0/18:0 | Plasma: G2B/AlcoholBis, F4G, BestTreat<br>Feces: BestTreat | C26H54NO7P | RP | 10.79 | Pos/Neg | 524.3713 | [M+H]+ | Pos: 184.072 (100), 86.097 (11)<br>Neg: 283.262 (100), 508.337 (5) | 2 | LipidMaps |
| LysoPC 0:0/18:1 | Plasma: G2B/AlcoholBis, BestTreat<br>Feces: BestTreat | C26H52NO7P | RP | 10.47 | Pos | 522.3556 | [M+H]+ | 184.075 (100), 86.097 (13) | 2 | LipidMaps |
| LysoPC 0:0/18:2 | Plasma: G2B/AlcoholBis, F4G, BestTreat | C26H50NO7P | RP | 10.16 | Pos/Neg | 520.3400 | [M+H]+ | Pos: 184.075 (100), 86.097 (13)<br>Neg: 279.232 (100), 504.306 (7) | 2 | LipidMaps |
| LysoPC 0:0/20:3 | Plasma: G2B/AlcoholBis | C28H52NO7P | RP | 10.37 | Neg | 590.3471 | [M+HCOO]- | 305.247 (100), 530.319 (7) | 2 | LipidMaps |
| LysoPC 0:0/20:4 | Plasma: G2B/AlcoholBis, F4G, BestTreat | C28H50NO7P | RP | 10.17 | Neg/Pos | 588.3318 | [M+HCOO]- | Neg: 303.233 (100), 528.311 (11)<br>Pos: 184.074 (100), 86.097 (9) | 2 | LipidMaps |
| LysoPC 0:0/20:5 | Plasma: G2B/AlcoholBis, F4G, BestTreat | C28H48NO7P | RP | 9.88 | Pos/Neg | 542.3242 | [M+H]+ | Pos: 184.073 (100), 86.097 (15)<br>Neg: 301.219 (100), 242.985 (14), 257.23 (14) | 2 | LipidMaps |
| LysoPC 0:0/22:6 | Plasma: G2B/AlcoholBis, F4G | C30H50NO7P | RP | 10.16 | Pos/Neg | 568.3397 | [M+H]+ | Pos: 184.073 (100), 86.097 (12)<br>Neg: 327.231 (100), 283.244 (46), 552.307 (21) | 2 | LipidMaps |
| LysoPC 14:0/0:0 | Plasma: G2B/AlcoholBis, F4G, BestTreat<br>Feces: BestTreat | C22H46NO7P | RP | 9.91 | Neg/Pos | 512.2998 | [M+HCOO]- | Neg: 227.201 (100), 452.275 (18)<br>Pos: 184.0733 (100), 104.1074 (84), 468.3082 (28), 86.097 (17) | 2 | LipidMaps |
| LysoPC 15:0 | Plasma: G2B/AlcoholBis, F4G, BestTreat<br>Feces: BestTreat | C23H48NO7P | RP | 10.21 | Pos/Neg | 482.3243 | [M+H]+ | Pos: 184.072 (100), 104.108 (80)<br>Neg: 241.216 (100), 466.295 (22), 168.99 (13) | 1 | In-house library |
| LysoPC 15:1 | Plasma: BestTreat<br>Feces: BestTreat | C23H46NO7P | RP | 10.65 | Pos | 480.3446 | [M+H]+ | 104.107 (100), 480.347 (94), 86.097 (43) | 2 | LipidMaps |
| LysoPC 16:0/0:0 | Plasma: G2B/AlcoholBis, F4G, BestTreat<br>Feces: G2B, F4G, BestTreat | C24H50NO7P | RP | 10.47 | Pos/Neg | 496.3399 | [M+H]+ | Pos: 184.073 (100), 104.108 (70), 496.336 (28)<br>Neg: 255.234 (100), 480.308 (17) | 2 | LipidMaps |
| LysoPC 16:1/0:0 | Plasma: G2B/AlcoholBis, F4G, BestTreat<br>Feces: BestTreat | C24H48NO7P | RP | 10.09 | Pos/Neg | 494.3243 | [M+H]+ | Pos: 184.073 (100), 104.108 (75)<br>Neg: 253.219 (100), 478.297 (17) | 2 | LipidMaps |
| LysoPC 17:0 | Plasma: G2B/AlcoholBis, F4G, BestTreat<br>Feces: BestTreat | C25H52NO7P | RP | 10.70 | Pos/Neg | 510.3556 | [M+H]+ | Pos: 184.072 (100), 104.108 (74)<br>Neg: 269.249 (100), 224.098 (15), 494.326 (10) | 1 | In-house library |
| LysoPC 17:1 | Plasma: BestTreat<br>Feces: BestTreat | C25H50NO7P | RP | 10.33 | Pos | 508.3398 | [M+H]+ | 184.074 (100), 104.108 (89) | 2 | LipidMaps |
| LysoPC 17:1/0:0 | Plasma: G2B/AlcoholBis | C25H50NO7P | RP | 10.36 | Pos/Neg | 508.3398 | [M+H]+ | Pos: 184.073 (100), 104.108 (71), 508.339 (31)<br>Neg: 267.232 (100), 492.308 (13), 224.07 (11) | 2 | LipidMaps |
| LysoPC 18:0 | Plasma: G2B/AlcoholBis | C26H54NO7P | RP | 11.14 | Pos | 524.3713 | [M+H]+ | 184.072 (100), 104.108 (68) | 2 | LipidMaps |
| LysoPC 18:0/0:0 | Plasma: G2B/AlcoholBis, F4G, BestTreat<br>Feces: F4G, BestTreat | C26H54NO7P | RP | 10.91 | Pos/Neg | 524.3713 | [M+H]+ | Pos: 184.072 (100), 104.108 (77), 524.374 (31)<br>Neg: 283.266 (100), 508.345 (15), 224.07 (12) | 2 | LipidMaps |
| LysoPC 18:1/0:0 | Plasma: G2B/AlcoholBis, F4G, BestTreat<br>Feces: F4G, BestTreat | C26H52NO7P | RP | 10.59 | Pos/Neg | 522.3557 | [M+H]+ | Pos: 184.073 (100), 104.108 (72), 522.353 (28)<br>Neg: 281.25 (100), 224.069 (10), 506.328 (10) | 2 | LipidMaps |
| LysoPC 18:2/0:0 | Plasma: G2B/AlcoholBis, F4G, BestTreat<br>Feces: G2B, F4G, BestTreat | C26H50NO7P | RP | 10.29 | Neg/Pos | 564.3312 | [M+HCOO]- | Neg: 279.236 (100), 224.07 (13), 504.306 (13)<br>Pos: 520.342 (100), 184.074 (90), 104.108 (56), 502.33 (16) | 2 | LipidMaps |
| LysoPC 18:3 | Plasma: G2B/AlcoholBis, F4G, BestTreat<br>Feces: BestTreat | C26H48NO7P | RP | 10.00 | Pos | 518.3246 | [M+H]+ | 184.073 (100), 104.108 (68) | 2 | LipidMaps |
| LysoPC 20:0 | Plasma: G2B/AlcoholBis | C28H58NO7P | RP | 11.30 | Pos | 552.4023 | [M+H]+ | 184.072 (100), 104.108 (79), 552.4 (28) | 2 | LipidMaps |
| LysoPC 20:1 | Plasma: G2B/AlcoholBis, BestTreat<br>Feces: BestTreat | C28H56NO7P | RP | 10.98 | Pos/Neg | 550.3867 | [M+H]+ | Pos: 184.073 (100), 104.108 (70), 550.63 (59)<br>Neg: 309.281 (100), 534.362 (12), 224.07 (11) | 2 | LipidMaps |
| LysoPC 20:2 | Plasma: G2B/AlcoholBis, F4G, BestTreat<br>Feces: BestTreat | C28H54NO7P | RP | 10.73 | Neg | 592.3629 | [M+HCOO]- | 307.264 (100), 532.34 (16), 224.069 (11) | 2 | LipidMaps |
| LysoPC 20:3 | Plasma: BestTreat | C28H52NO7P | RP | 10.34 | Neg | 590.3475 | [M+HCOO]- | 305.25 (100), 530.324 (20) | 2 | LipidMaps |
| LysoPC 20:3/0:0 | Plasma: G2B/AlcoholBis, F4G | C28H52NO7P | RP | 10.48 | Pos | 546.3555 | [M+H]+ | 546.356 (100), 184.073 (7), 104.106 (5), 528.346 (5) | 2 | LipidMaps |

| Annotation | Sample matrix & study | Molecular formula | Column | Retention time | ESI | *m/z* | Adduct type | MS/MS fragments (%) | ID level | Annotation source |
|---|---|---|---|---|---|---|---|---|---|---|
| LysoPC 20:4/0:0 | Plasma: G2B/AlcoholBis, F4G, BestTreat | C28H50NO7P | RP | 10.28 | Neg/Pos | 588.3320 | [M−HCOO]- | Neg: 303.233 (100), 528.312 (25), 224.07 (23)<br>Pos: 290.627 (100), 86.097 (62), 184.072 (52), 104.108 (41) | 2 | LipidMaps |
| LysoPC 20:5/0:0 | Plasma: G2B/AlcoholBis, F4G | C28H48NO7P | RP | 9.81 | Pos | 542.3174 | [M+H]+ | 542.326 (100), 104.108 (68), 184.075 (65), 524.312 (17), 86.099 (6), 199.036 (5) | 2 | LipidMaps |
| LysoPC 22:4 | Plasma: G2B/AlcoholBis | C30H54NO7P | RP | 10.65 | Neg | 616.3628 | [M−HCOO]- | 331.265 (100), 112.986 (40), 556.341 (22) | 2 | LipidMaps |
| LysoPC 22:5 | Plasma: G2B/AlcoholBis, F4G, BestTreat | C30H52NO7P | RP | 10.42 | Neg | 614.3473 | [M−HCOO]- | 329.251 (100), 554.329 (27), 224.07 (27) | 2 | LipidMaps |
| LysoPC 22:6/0:0 | Plasma: G2B/AlcoholBis, F4G, BestTreat<br>Feces: BestTreat | C33H51NO6S | RP | 10.26 | Neg/Pos | 612.3319 | [M−HCOO]- | Neg: 327.233 (100), 230.987 (43), 292.984 (32), 283.244 (30), 218.286 (30), 168.990 (27), 211.257 (27), 193.350 (25), 115.921 (25)<br>Pos: 568.333 (100), 184.061 (42), 104.097 (39), 550.32 (10), 86.087 (7) | 2 | LipidMaps |
| LysoPC O-16:0 | Plasma: G2B/AlcoholBis, F4G, BestTreat<br>Feces: F4G, BestTreat | C24H52NO6P | RP | 10.75 | Pos/Neg | 482.3606 | [M+H]+ | Pos: 104.108 (100), 482.361 (27), 184.072 (19)<br>Neg: 466.334 (100), 78.958 (60), 168.043 (29) | 2 | LipidMaps |
| LysoPC O-18:0 | Plasma: G2B/AlcoholBis, BestTreat<br>Feces: BestTreat | C26H56NO6P | RP | 11.16 | Pos | 510.3919 | [M+H]+ | 104.108 (100), 510.388 (34) | 2 | LipidMaps |
| LysoPC O-18:1 isomer 1 | Plasma: G2B/AlcoholBis, F4G, BestTreat<br>Feces: BestTreat | C26H54NO6P | RP | 10.84 | Pos/Neg | 508.3763 | [M+H]+ | Pos: 104.108 (100), 508.371 (29), 184.073 (21)<br>Neg: 78.958 (100), 168.043 (62), 492.342 (48) | 2 | LipidMaps |
| LysoPC O-18:1 isomer 2 | Plasma: G2B/AlcoholBis, BestTreat<br>Feces: BestTreat | C26H54NO6P | RP | 11.07 | Pos | 508.3763 | [M+H]+ | 104.108 (100), 508.381 (93), 184.072 (44), 86.097 (43) | 2 | LipidMaps |
| LysoPC P-16:0 | Plasma: F4G | C24H50NO6P | RP | 10.40 | Neg | 524.3353 | [M-H]- | 464.314 (100), 44.997 (13), 224.069 (12), 375.229 (4) | 2 | LipidMaps |
| LysoPE 0:0/16:0 | Feces: F4G | C21H44NO7P | RP | 10.10 | Neg | 452.2798 | [M-H]- | 255.233 (100), 452.28 (24), 256.238 (15), 214.05 (4) | 2 | LipidMaps |
| LysoPE 0:0/18:0 | Plasma: F4G, BestTreat<br>Feces: F4G, BestTreat | C23H48NO7P | RP | 10.76 | Neg | 480.3091 | [M-H]- | 283.265 (100), 480.311 (7) | 2 | LipidMaps |
| LysoPE 0:0/18:2 | Plasma: G2B/AlcoholBis, BestTreat<br>Feces: BestTreat | C23H44NO7P | RP | 10.18 | Neg/Pos | 476.2784 | [M-H]- | Neg: 279.235 (100)<br>Pos: 337.275 (100), 60.082 (18), 81.071 (15) | 2 | LipidMaps |
| LysoPE 14:0 | Feces: F4G, BestTreat | C19H40NO7P | RP | 9.72 | Neg | 424.2470 | [M-H]- | 424.247 (100), 227.201 (61), 196.037 (10), 228.205 (8) | 2 | LipidMaps |
| LysoPE 15:0 | Feces: G2B, F4G, BestTreat | C20H42NO7P | RP | 9.96 | Pos | 440.2803 | [M−H]+ | 299.258 (100), 439.277 (94), 439.781 (27), 300.259 (21), 440.283 (20), 165.091 (13), 268.263 (12), 438.782 (12), 155.011 (11), 239.15 (10) | 2 | LipidMaps |
| LysoPE 16:0 | Plasma: G2B/AlcoholBis, F4G, BestTreat<br>Feces: G2B, BestTreat | C21H44NO7P | RP | 10.47 | Neg | 452.2794 | [M-H]- | 452.279 (100), 255.232 (44), 196.038 (6), 44.996 (5) | 2 | LipidMaps |
| LysoPE 16:0/0:0 | Feces: F4G, BestTreat | C21H44NO7P | RP | 10.21 | Neg | 452.2798 | [M-H]- | 452.279 (100), 255.233 (37), 256.236 (7), 196.038 (4) | 2 | LipidMaps |
| LysoPE 18:0/0:0 | Plasma: F4G, BestTreat<br>Feces: BestTreat | C23H48NO7P | RP | 10.60 | Neg | 480.3098 | [M-H]- | 283.265 (100), 480.31 (34), 196.035 (5), 255.235 (4) | 2 | LipidMaps |
| LysoPE 18:1 | Plasma: G2B/AlcoholBis, F4G, BestTreat<br>Feces: F4G, BestTreat | C23H46NO7P | RP | 10.59 | Pos | 480.3088 | [M−H]+ | 339.289 (100), 62.061 (13), 308.296 (10) | 2 | LipidMaps |
| LysoPE 18:2/0:0 | Plasma: G2B/AlcoholBis, F4G<br>Feces: F4G | C23H43NO7P | RP | 10.30 | Neg | 476.2784 | [M-H]- | 279.231 (100), 192.99 (16), 392.978 (15) | 2 | LipidMaps |
| LysoPE 18:3 | Plasma: G2B/AlcoholBis, BestTreat<br>Feces: BestTreat | C23H42NO7P | RP | 10.01 | Neg/Pos | 474.2629 | [M-H]- | Neg: 277.219 (100), 454.978 (23)<br>Pos: 335.258 (100), 95.086 (19), 81.071 (19), 62.061 (19) | 2 | LipidMaps |
| LysoPE 20:3 | Plasma: G2B/AlcoholBis, BestTreat<br>Feces: BestTreat | C25H46NO7P | RP | 10.48 | Neg | 502.2945 | [M-H]- | 305.251 (100), 196.038 (13), 502.293 (12) | 2 | LipidMaps |
| LysoPE 20:4 | Plasma: G2B/AlcoholBis, F4G, BestTreat | C25H44NO7P | RP | 10.18 | Neg/Pos | 500.2787 | [M-H]- | Neg: 303.232 (100), 259.244 (11)<br>Pos: 361.277 (100), 91.055 (26), 81.071 (25), 95.086 (25), 67.055 (25) | 2 | LipidMaps |
| LysoPE 20:5 | Plasma: G2B/AlcoholBis, BestTreat | C25H42NO7P | RP | 10.01 | Neg | 498.2632 | [M-H]- | 301.219 (100), 196.038 (47), 257.229 (25) | 2 | LipidMaps |
| LysoPE 22:5 | Plasma: G2B/AlcoholBis, BestTreat | C27H46NO7P | RP | 10.42 | Neg | 526.2944 | [M-H]- | 329.25 (100), 526.291 (29), 196.038 (22), 140.01 (8), 78.958 (7), 214.048 (6), 59.012 (6), 285.261 (4), 361.516 (4), 230.94 (4) | 2 | LipidMaps |
| LysoPE 22:6 | Plasma: G2B/AlcoholBis, F4G, BestTreat | C27H44NO7P | RP | 10.18 | Pos/Neg | 526.2928 | [M−H]+ | Pos: 385.273 (100), 67.055 (21), 79.055 (19), 93.07 (18)<br>Neg: 327.233 (100), 524.279 (89), 283.243 (42), 196.038 (41), 214.048 (13), 59.014 (11), 229.195 (8), 140.009 (5), 249.186 (4), 191.178 (4) | 2 | LipidMaps |
| LysoPE P-16:0 | Plasma: G2B/AlcoholBis, BestTreat<br>Feces: F4G, BestTreat | C21H44NO6P | RP | 10.67 | Neg | 436.2823 | [M-H]- | 196.039 (100), 78.958 (100), 140.012 (88), 436.281 (79), 239.238 (70) | 2 | LipidMaps |
| LysoPE P-18:0 | Plasma: G2B/AlcoholBis, BestTreat<br>Feces: BestTreat | C23H48NO6P | RP | 11.06 | Neg | 464.3151 | [M-H]- | 78.958 (100), 196.038 (94), 464.316 (80), 140.012 (60) | 2 | LipidMaps |
| Lysophosphatidylcholine_C24H50NO8P | Plasma: G2B/AlcoholBis | C29H51NO8S | RP | 8.87 | Pos/Neg | 556.3262 | [M−HCOO]- | Neg: 271.228 (100), 224.07 (10)<br>Pos: 184.073 (100), 104.108 (71), 512.326 (32) | 3 | MS-FINDER/SIRIUS |
| Lysophosphocholine_512.3348@10.05 | Plasma: G2B/AlcoholBis | C23H48NO7P | RP | 10.05 | Pos/Neg | 512.3348 | [M−H]+ | Pos: 104.108 (100), 184.073 (88), 512.33 (41)<br>Neg: 271.229 (100), 225.223 (22), 224.07 (13) | 3 | MS-FINDER/SIRIUS |
| LysoPI 20:4 | Plasma: BestTreat | C29H49O12P | RP | 11.74 | Neg | 619.2902 | [M-H]- | 619.291 (100), 152.995 (67), 303.236 (65), 241.011 (58), 315.051 (26), 78.958 (20), 91.744 (17), 89.792 (7), 259.243 (7), 355.853 (6) | 2 | LipidMaps |
| Mesobilirubinogen | Plasma: BestTreat<br>Feces: G2B, F4G, BestTreat | C33H42N4O6 | RP | 6.17 | Pos | 593.3334 | [M+H]+ | 344.174 (100), 343.165 (45), 593.338 (43) | 2 | HMDB |
| Metformin | Plasma: F4G, BestTreat<br>Feces: G2B, F4G, BestTreat | C4H11N5 | HILIC | 1.55 | Pos | 130.1090 | [M+H]+ | 71.061 (100), 60.056 (66), 46.065 (25), 85.051 (20), 43.029 (20), 88.087 (13), 113.084 (5), 68.025 (5) | 2 | HMDB |
| Methionine | Plasma: G2B/AlcoholBis, F4G, BestTreat<br>Feces: G2B, F4G, BestTreat | C5H11NO2S | HILIC | 4.71 | Pos | 150.0585 | [M+H]+ | 56.05 (100), 104.053 (69), 150.061 (42), 133.03 (35), 61.008 (16), 87.026 (6), 74.024 (6), 102.065 (6), 47.22 (4) | 1 | In-house library |
| Methylimidazoleacetic acid | Feces: G2B | C6H8N2O2 | HILIC | 4.58 | Pos | 141.0664 | [M+H]+ | 141.065 (100), 95.06 (16), 96.067 (11) | 2 | MassBank |
| Metyrosine | Feces: F4G | C10H13NO3 | HILIC | 2.14 | Pos | 196.0962 | [M+H]+ | 196.096 (100), 195.112 (14), 196.133 (9), 195.086 (4) | 2 | MassBank |
| Monoeladidin | Feces: F4G | C21H40O4 | RP | 10.79 | Pos | 339.2853 | [M+H-H2O]− | 339.285 (100) | 2 | NIST MS Data Center |
| Monolinolenin (9c,12c,15c) | Plasma: F4G | C21H36O4 | RP | 10.55 | Pos | 353.2675 | [M−H]+ | 353.269 (100) | 2 | NIST MS Data Center |
| Monosaccharide | Plasma: G2B/AlcoholBis | C6H12O6 | RP | 0.53 | Neg | 179.0568 | [M-H]- | 59.013 (100), 71.013 (64), 143.866 (59), 89.024 (40) | 3 | MS-FINDER/SIRIUS |
| Myristamide | Plasma: G2B/AlcoholBis, BestTreat<br>Feces: BestTreat | C14H29NO | RP | 10.16 | Pos | 228.2315 | [M+H]+ | 228.234 (100),88.077 (9) | 1 | In-house library |
| Myrtenol | Plasma: F4G | C10H16O | RP | 8.73 | Pos | 135.1190 | [M−H-H2O]+ | 135.118 (100), 107.086 (53), 102.925 (29), 119.087 (28), 134.95 (19), 70.979 (13), 55.053 (12), 72.983 (9), 79.053 (8), 84.963 (8) | 2 | HMDB |
| N(6)-Methyllysine | Feces: F4G | C7H16N2O2 | HILIC | 6.81 | Pos | 161.1283 | [M+H]+ | 130.086 (100), 161.128 (83), 144.101 (23), 70.065 (19), 84.081 (10), 72.081 (5), 159.147 (5) | 2 | HMDB |

| Annotation | Sample matrix & study | Molecular formula | Column | Retention time | ESI | *m/z* | Adduct type | MS/MS fragments (%) | ID level | Annotation source |
|---|---|---|---|---|---|---|---|---|---|---|
| N,N-Dimethylarginine | Plasma: F4G, BestTreat<br>Feces: F4G, BestTreat | C8H18N4O2 | HILIC | 6.46 | Pos | 203.1505 | [M+H]+ | 70.065 (100), 116.07 (33), 71.06 (27), 88.085 (16), 158.126 (13), 115.088 (12), 172.103 (11), 126.105 (8), 71.048 (4), 72.079 (4) | 2 | Agilent MassHunter PCDL |
| N,O-Didesmethylvenlafaxine | Plasma: F4G | C15H23NO2 | RP | 7.58 | Pos | 250.1831 | [M+H]+ | 250.18 (100), 105.068 (6), 232.171 (4), 59.05 (4) | 2 | HMDB |
| N.alpha.-Acetyl-L-lysine | Feces: F4G, BestTreat | C8H16N2O3 | HILIC | 5.85 | Pos | 189.1232 | [M+H]+ | 189.122 (100), 129.101 (15), 130.085 (8), 84.08 (7), 147.112 (5), 172.096 (4), 171.112 (4), 126.09 (4), 188.174 (4) | 1 | In-house library |
| N1-Acetylspermidine | Feces: F4G | C9H21N3O | HILIC | 6.25 | Pos | 188.1759 | [M+H]+ | 188.175 (100), 171.148 (25), 72.081 (13), 100.075 (12), 117.102 (8) | 2 | Fiehn-HILIC |
| N2-Acetylornithine | Feces: F4G | C7H14N2O3 | HILIC | 5.99 | Pos | 175.1078 | [M+H]+ | 175.106 (100), 115.086 (89), 157.096 (66), 158.08 (31), 116.07 (22), 116.089 (9), 174.111 (8), 133.095 (7), 158.101 (7), 174.085 (6) | 2 | HMDB |
| N8-Acetylspermidine | Feces: G2B | C9H21N3O | HILIC | 6.17 | Pos | 188.1765 | [M+H]+ | 100.075 (100), 72.081 (35), 171.149 (28), 188.175 (16), 73.084 (10), 117.101 (8), 58.921 (5), 80.913 (5), 59.112 (5), 154.095 (5) | 2 | Fiehn-HILIC |
| N-a-Acetyl-L-arginine | Plasma: BestTreat<br>Feces: F4G, BestTreat | C8H16N4O3 | HILIC | 5.77 | Pos | 217.1303 | [M+H]+ | 70.066 (100), 71.05 (13), 72.08 (9), 60.055 (8), 43.018 (7), 43.054 (5), 55.03 (5), 43.029 (4), 55.054 (4) | 2 | NIST MS Data Center |
| Naringenin | Feces: F4G | C15H12O5 | RP | 6.27 | Neg | 271.0592 | [M-H]- | 271.063 (100), 151.005 (99), 139.114 (35), 119.051 (27), 115.04 (23), 271.158 (22), 253.148 (16), 177.02 (12), 107.016 (12), 270.914 (11) | 2 | HMDB |
| N-Desmethylvenlafaxine | Plasma: G2B/AlcoholBis | C16H25NO2 | RP | 5.34 | Pos | 264.1957 | [M+H]+ | 215.143 (100), 121.066 (93), 246.186 (88), 147.08 (68) | 2 | MassBank |
| Ne,Ne,Ne-Trimethyllysine | Plasma: F4G, BestTreat<br>Feces: G2B, F4G, BestTreat | C9H20N2O2 | HILIC | 6.83 | Pos | 189.1605 | [M+H]+ | 189.159 (100), 130.086 (91), 84.081 (48), 60.08 (33), 74.072 (10), 144.139 (4) | 1 | In-house library |
| Nervonic acid | Feces: F4G | C24H46O2 | RP | 11.90 | Neg | 365.3419 | [M-H]- | 365.342 (100), 160.976 (6), 297.153 (4) | 2 | HMDB |
| Niclosamide | Plasma: F4G | C13H8Cl2N2O4 | RP | 11.48 | Pos | 327.0092 | [M+H]+ | 98.972 (100), 174.979 (60), 250.987 (23), 327.064 (6), 326.998 (5) | 2 | HMDB |
| N-Methyl-2-pyrrolidone | Feces: G2B | C5H9NO | RP | 1.83 | Pos | 100.0759 | [M+H]+ | 100.076 (100), 72.081 (6), 98.984 (6), 60.291 (4) | 2 | MassBank |
| N-Methyl-lysine | Plasma: F4G | C7H15NO2 | HILIC | 4.24 | Pos | 144.1021 | [M+H]+ | 144.101 (100), 98.095 (64), 144.076 (7), 42.032 (5), 88.072 (4), 70.061 (4) | 2 | MassBank |
| N-methyl-proline | Plasma: G2B/AlcoholBis, F4G, BestTreat<br>Feces: G2B, F4G, BestTreat | C6H11NO2 | HILIC | 4.18 | Pos | 130.0866 | [M+H]+ | 84.081 (100), 130.088 (76), 57.07 (21), 130.159 (11) | 2 | MassBank |
| Nordiazepam | Plasma: G2B/AlcoholBis | C15H10O5 | RP | 7.68 | Pos | 271.0632 | [M+H]+ | 271.065 (100), 140.026 (6), 243.068 (5) | 2 | MassBank |
| Nutriacholic acid isomer 1 | Feces: G2B, F4G | C24H38O4 | RP | 9.01 | Pos | 391.2865 | [M+H]+ | 355.263 (100), 373.274 (63), 309.258 (61), 356.266 (24), 337.252 (22), 374.276 (17), 310.262 (12), 391.283 (7), 338.256 (6), 245.154 (6) | 2 | HMDB |
| Nutriacholic acid isomer 2 | Feces: G2B, F4G | C24H38O4 | RP | 9.38 | Neg | 389.2651 | [M-H]- | 389.272 (100), 343.266 (25), 345.282 (21), 327.271 (14), 353.249 (6), 363.293 (5), 311.240 (4), 328.277 (4), 309.226 (3) | 2 | HMDB |
| Octadecanamide | Plasma: G2B/AlcoholBis, BestTreat<br>Feces: BestTreat | C18H37NO | RP | 11.15 | Pos | 284.2951 | [M+H]+ | 284.294 (100), 88.077 (9) | 2 | HMDB |
| Oleamide | Plasma: G2B/AlcoholBis, BestTreat<br>Feces: BestTreat | C18H35NO | RP | 10.83 | Pos | 282.2786 | [M+H]+ | 282.281 (100), 69.071 (75), 83.086 (72), 97.102 (62) | 2 | HMDB |
| Omeprazole | Plasma: F4G | C17H19N3O3S | RP | 5.72 | Pos | 346.1255 | [M+H]+ | 198.06 (100), 149.072 (21), 151.101 (20), 168.103 (14), 180.048 (4) | 2 | Agilent MassHunter PCDL |
| Ornithine | Plasma: G2B/AlcoholBis, BestTreat<br>Feces: BestTreat | C5H12N2O2 | HILIC | 7.30 | Pos | 133.0977 | [M+H]+ | 70.065 (100), 116.071 (45), 115.086 (6), 133.096 (4) | 1 | In-house library |
| Oxindole-3-acetic acid | Feces: G2B, F4G, BestTreat | C10H9NO3 | RP | 3.98 | Neg | 190.0473 | [M-H]- | 146.064 (100), 131.04 (19), 128.053 (15), 144.048 (14), 190.053 (12), 147.067 (9), 102.951 (7) | 2 | HMDB |
| p-Acetamidophenyl glucuronide | Plasma: G2B/AlcoholBis | C14H17NO8 | RP | 0.70 | Neg | 326.0885 | [M-H]- | 150.055 (100), 113.025 (63), 85.029 (41) | 2 | HMDB |
| Palmitamide | Plasma: G2B/AlcoholBis, BestTreat<br>Feces: BestTreat | C16H33NO | RP | 10.71 | Pos | 256.2629 | [M+H]+ | 256.265 (100), 88.077 (9) | 2 | HMDB |
| Palmitoleamide | Plasma: G2B/AlcoholBis, BestTreat<br>Feces: BestTreat | C16H31NO | RP | 10.34 | Pos | 254.2474 | [M+H]+ | 254.246 (100), 83.087 (80), 69.071 (58), 97.102 (57) | 2 | HMDB |
| Palmitoylglycine | Feces: F4G | C18H33NO3 | RP | 10.34 | Neg | 312.2543 | [M+H]+ | 312.257 (100), 311.170 (26), 312.173 (5) | 2 | HMDB |
| Pantoprazole | Plasma: G2B/AlcoholBis | C16H15F2N3O4S | RP | 6.12 | Pos/Neg | 384.0823 | [M+H]+ | Pos: 138.055 (100), 200.036 (71), 153.077 (24)<br>Neg: 229.997 (100), 209.991 (5) | 2 | HMDB |
| Pantothenate | Plasma: F4G<br>Feces: G2B, F4G | C9H17NO5 | HILIC | 1.07 | Neg | 218.1033 | [M-H]- | 88.039 (100), 146.079 (59), 218.1 (38), 71.013 (20), 75.816 (20), 71.307 (19), 89.759 (19), 39.52 (15), 24.253 (13), 41.939 (13) | 2 | ReSpect |
| Paracetamol | Feces: F4G | C8H9NO2 | RP | 2.28 | Pos | 152.0701 | [M+H]+ | 152.069 (100), 110.058 (18) | 2 | HMDB |
| Paraxanthine | Plasma: G2B/AlcoholBis, F4G, BestTreat<br>Feces: F4G, BestTreat | C7H8N4O2 | RP | 2.61 | Pos | 181.0720 | [M+H]+ | 181.072 (100), 124.051 (11), 105.935 (10) | 1 | In-house library |
| PC 14:0_16:0 | Plasma: G2B/AlcoholBis, F4G, BestTreat | C38H76NO8P | RP | 12.87 | Pos/Neg | 706.5378 | [M+H]+ | Pos: 184.072 (100), 86.097 (11)<br>Neg: 227.203 (100), 255.233 (82) | 2 | LipidMaps |
| PC 14:0_18:2 | Plasma: F4G | C40H76NO8P | RP | 11.78 | Neg | 774.5293 | [M+HCOO]- | 714.508 (100), 774.528 (17), 279.232 (12), 715.508 (7), 227.202 (6), 44.998 (5) | 2 | LipidMaps |
| PC 14:0_20:4 | Plasma: F4G | C42H76NO8P | RP | 11.73 | Neg | 798.5292 | [M+HCOO]- | 798.528 (100), 738.507 (29), 753.264 (4) | 2 | LipidMaps |
| PC 14:0_22:6 | Plasma: F4G | C44H76NO8P | RP | 11.66 | Neg | 822.5290 | [M+HCOO]- | 822.529 (100), 762.507 (31), 301.213 (5), 823.003 (4), 822.466 (4), 100.932 (4) | 2 | LipidMaps |
| PC 15:0_18:2 | Plasma: F4G | C41H78NO8P | RP | 11.99 | Neg | 788.5449 | [M+HCOO]- | 728.524 (100), 788.543 (24), 279.232 (16), 729.524 (11), 241.216 (11), 44.998 (6), 729.475 (5) | 2 | LipidMaps |
| PC 15:0_20:4 | Plasma: F4G | C43H78NO8P | RP | 11.93 | Neg | 812.5441 | [M+HCOO]- | 303.232 (100), 241.216 (41), 224.068 (22), 304.236 (15), 466.293 (15), 537.769 (14), 59.897 (12), 752.522 (11), 289.213 (10), 166.923 (9) | 2 | LipidMaps |
| PC 16:0/16:0 | Plasma: G2B/AlcoholBis | C40H80NO8P | RP | 13.62 | Pos/Neg | 734.5693 | [M+H]+ | Pos: 184.073 (100), 86.097 (10)<br>Neg: 255.233 (100), 718.547 (4) | 2 | LipidMaps |
| PC 16:0_16:1 | Plasma: F4G | C40H78NO8P | RP | 12.09 | Neg | 776.5449 | [M+HCOO]- | 253.218 (100), 255.232 (39), 281.247 (28), 44.998 (10), 716.519 (6), 227.201 (6), 480.311 (5), 224.068 (5) | 2 | LipidMaps |
| PC 16:0_18:1 | Plasma: G2B/AlcoholBis, F4G, BestTreat | C42H82NO8P | RP | 13.76 | Pos/Neg | 760.5850 | [M+H]+ | Pos: 184.072 (100), 86.097 (11)<br>Neg: 281.248 (100), 255.234 (36) | 2 | LipidMaps |
| PC 16:0_18:2 | Plasma: G2B/AlcoholBis, F4G, BestTreat | C42H80NO8P | RP | 13.18 | Pos/Neg | 758.5718 | [M+H]+ | Pos: 184.072 (100), 86.097 (10)<br>Neg: 279.232 (100), 255.235 (42) | 2 | LipidMaps |
| PC 16:0_18:3 | Plasma: G2B/AlcoholBis | C42H78NO8P | RP | 12.79 | Pos/Neg | 756.5536 | [M+H]+ | Pos: 184.073 (100), 86.097 (13)<br>Neg: 277.22 (100), 255.234 (54) | 2 | LipidMaps |
| PC 16:0_20:3 | Plasma: G2B/AlcoholBis | C44H79O8P | RP | 13.44 | Pos/Neg | 784.5853 | [M+H]+ | Pos: 184.073 (100), 86.097 (12)<br>Neg: 305.251 (100), 255.234 (57) | 2 | LipidMaps |
| PC 16:0_20:4 | Plasma: G2B/AlcoholBis, BestTreat | C44H80NO8P | RP | 13.09 | Pos/Neg | 782.5694 | [M+H]+ | Pos: 184.072 (100), 86.097 (13)<br>Neg: 303.232 (100), 255.234 (78) | 2 | LipidMaps |
| PC 16:0_20:5 | Plasma: BestTreat | C44H78NO8P | RP | 12.60 | Neg | 824.5467 | [M+HCOO]- | 301.217 (100), 255.232 (78), 764.535 (35), 257.227 (16), 480.31 (9), 168.042 (8), 224.07 (6), 78.957 (5), 59.013 (4) | 2 | LipidMaps |
| PC 16:0_22:5 and 18:1_20:4 | Plasma: F4G | C46H82NO8P | RP | 12.25 | Pos/Neg | 852.5771 | [M+HCOO]- | Pos: 852.576 (100), 792.554 (27)<br>Neg: 792.554 (100), 852.575 (35), 329.248 (6), 303.232 (5), 255.233 (4), 281.248 (3) | 2 | LipidMaps |
| PC 16:0_22:6 | Plasma: G2B/AlcoholBis, BestTreat | C46H80NO8P | RP | 12.98 | Pos/Neg | 806.5693 | [M+H]+ | Pos: 184.072 (100), 86.097<br>Neg: 255.234 (100), 327.232 (64), 283.243 (29) | 2 | LipidMaps |

| Annotation | Sample matrix & study | Molecular formula | Column | Retention time | ESI | *m/z* | Adduct type | MS/MS fragments (%) | ID level | Annotation source |
|---|---|---|---|---|---|---|---|---|---|---|
| PC 16:1_16:1 and 18:2_14:0 | Plasma: G2B/AlcoholBis | C40H76NO8P | RP | 12.56 | Pos/Neg | 730.5379 | [M+H]+ | Pos: 184.072 (100), 86.097 (12)<br>Neg: 253.219 (100), 279.236 (5) | 2 | LipidMaps |
| PC 16:1_18:2 | Plasma: G2B/AlcoholBis, F4G | C42H78NO8P | RP | 12.68 | Pos/Neg | 756.5539 | [M+H]+ | Pos: 184.073 (100), 86.097 (11)<br>Neg: 279.231 (100), 253.219 (45) | 2 | LipidMaps |
| PC 16:1_20:4 and 16:0_20:5 | Plasma: F4G | C44H78NO8P | RP | 11.88 | Neg | 824.5452 | [M+HCOO]- | 764.524 (100), 824.541 (20), 303.234 (14), 765.526 (13) | 2 | LipidMaps |
| PC 16:1_22:6 | Plasma: F4G | C46H78NO8P | RP | 11.74 | Neg | 848.5440 | [M+HCOO]- | 788.5225 (100), 848.5443 (37), 253.2187 (8), 327.233 (7) | 2 | LipidMaps |
| PC 17:0_18:2 | Plasma: F4G | C43H82NO8P | RP | 12.51 | Neg | 816.5767 | [M+HCOO]- | 279.233 (100), 269.247 (44), 44.998 (11), 168.042 (10), 255.232 (8), 280.237 (7), 756.557 (7), 494.326 (6), 281.247 (5) | 2 | LipidMaps |
| PC 18:0_18:1 | Plasma: G2B/AlcoholBis, F4G, BestTreat | C44H86NO8P | RP | 14.84 | Pos/Neg | 788.6161 | [M+H]+ | Pos: 184.073 (100), 86.097 (12)<br>Neg: 281.247 (100), 283.266 (37) | 2 | LipidMaps |
| PC 18:0_20:3 | Plasma: G2B/AlcoholBis, F4G, BestTreat | C46H86NO8P | RP | 14.41 | Neg | 856.6088 | [M+HCOO]- | 305.249 (100), 283.265 (32), 796.586 (21), 303.233 (7), 508.343 (6) | 2 | LipidMaps |
| PC 18:0_20:4 | Plasma: G2B/AlcoholBis, F4G, BestTreat | C46H84NO8P | RP | 13.91 | Pos/Neg | 810.6010 | [M+H]+ | Pos: 184.073 (100), 86.097 (12)<br>Neg: 303.232 (100), 283.266 (62) | 2 | LipidMaps |
| PC 18:0_22:5 | Plasma: F4G | C48H86NO8P | RP | 12.86 | Neg | 880.6074 | [M+HCOO]- | 329.247 (100), 94.990 (68), 283.264 (42), 820.582 (31), 303.2291 (14), 508.342 (12) | 2 | LipidMaps |
| PC 18:0_22:6 | Plasma: G2B/AlcoholBis, F4G, BestTreat | C48H84NO8P | RP | 13.75 | Pos/Neg | 834.6004 | [M+H]+ | Pos: 184.072 (100), 86.097 (14)<br>Neg: 283.268, (100), 327.234 (70), 118.931 (14), 281.2495 (12), 168.0438 (12), 818.571 (10), 224.07 (9) | 2 | LipidMaps |
| PC 18:1_14:0 and 16:0_16:1 | Plasma: G2B/AlcoholBis, BestTreat | C40H78NO8P | RP | 12.99 | Pos/Neg | 732.5540 | [M+H]+ | Pos: 184.075 (100), 86.097 (12)<br>Neg: 253.219 (100), 255.234 (46), 281.247 (40) | 2 | LipidMaps |
| PC 18:1_18:1 | Plasma: F4G | C44H84NO8P | RP | 12.84 | Neg | 830.5932 | [M+HCOO]- | 770.571 (100), 830.592 (37), 771.573 (16), 281.248 (13), 44.998 (4) | 2 | LipidMaps |
| PC 18:1_18:2 | Plasma: F4G, BestTreat | C44H82NO8P | RP | 12.39 | Neg | 828.5761 | [M+HCOO]- | 279.233 (100), 281.249 (36), 768.556 (8), 44.998 (8), 280.235 (5), 506.326 (5), 305.249 (4), 168.043 (4) | 2 | LipidMaps |
| PC 18:1_20:3 | Plasma: G2B/AlcoholBis, BestTreat | C46H84NO8P | RP | 13.58 | Pos/Neg | 810.6003 | [M+H]+ | Pos: 184.072 (100), 86.097 (17)<br>Neg: 305.25 (100), 281.25 (47) | 2 | LipidMaps |
| PC 18:1_22:6 | Plasma: G2B/AlcoholBis, F4G | C48H82NO8P | RP | 13.10 | Pos/Neg | 832.5844 | [M+H]+ | Pos: 184.073 (100), 86.097 (14)<br>Neg: 281.251 (100), 327.231 (50) | 2 | LipidMaps |
| PC 18:2/18:2 | Plasma: G2B/AlcoholBis, F4G | C44H80NO8P | RP | 12.85 | Pos/Neg | 782.5695 | [M+H]+ | Pos: 184.072 (100), 86.097 (11)<br>Neg: 279.232 (100), 277.216 (14), 281.248 (11) | 2 | LipidMaps |
| PC 18:2_15:0 | Plasma: G2B/AlcoholBis | C41H78NO8P | RP | 12.87 | Pos/Neg | 788.5464 | [M+HCOO]- | Neg: 279.231 (100), 241.216 (40)<br>Pos: 184.073 (100), 86.097 (13) | 2 | LipidMaps |
| PC 18:2_20:4 | Plasma: G2B/AlcoholBis, F4G | C46H80NO8P | RP | 12.78 | Neg | 850.5618 | [M+HCOO]- | 790.539 (100), 850.559 (26), 791.543 (14), 303.234 (11), 279.233 (8) | 2 | LipidMaps |
| PC 20:4_14:0 | Plasma: G2B/AlcoholBis | C42H76NO8P | RP | 12.49 | Pos/Neg | 754.5378 | [M+H]+ | Pos: 184.073 (100), 86.097 (12)<br>Neg: 303.233 (100), 227.201 (86) | 2 | LipidMaps |
| PC 20:5_16:0 | Plasma: G2B/AlcoholBis | C44H78NO8P | RP | 12.71 | Pos/Neg | 780.5538 | [M+H]+ | Pos: 184.072 (100), 86.097 (13)<br>Neg: 301.218 (100), 255.233 (99) | 2 | LipidMaps |
| PC 30:1 | Plasma: G2B/AlcoholBis | C38H74NO8P | RP | 12.40 | Pos | 704.5222 | [M+H]+ | 184.073 (100), 86.097 (9) | 3 | MS-FINDER/SIRIUS |
| PC 32:0 isomer 1 | Plasma: BestTreat | C40H80NO8P | RP | 13.28 | Pos | 734.5696 | [M+H]+ | 184.074 (100), 86.097 (9) | 3 | MS-FINDER/SIRIUS |
| PC 32:0 isomer 2 | Plasma: BestTreat | C40H80NO8P | RP | 13.44 | Pos | 734.5696 | [M+H]+ | 184.074 (100), 86.097 (8) | 3 | MS-FINDER/SIRIUS |
| PC 32:2 | Plasma: BestTreat | C40H76NO8P | RP | 12.45 | Pos | 730.5377 | [M+H]+ | 184.074 (100), 86.097 (9) | 3 | MS-FINDER/SIRIUS |
| PC 34:1 | Plasma: G2B/AlcoholBis | C42H82NO8P | RP | 14.33 | Pos | 760.5861 | [M+H]+ | 184.072 (100), 86.097 (11) | 3 | MS-FINDER/SIRIUS |
| PC 34:2 | Plasma: G2B/AlcoholBis | C42H80NO8P | RP | 14.33 | Pos | 758.5701 | [M+H]+ | 184.075 (100), 86.097 (10) | 3 | MS-FINDER/SIRIUS |
| PC 34:3 isomer 1 | Plasma: BestTreat | C42H78NO8P | RP | 12.58 | Pos | 756.5533 | [M+H]+ | 184.074 (100), 86.097 (10) | 3 | MS-FINDER/SIRIUS |
| PC 34:3 isomer 2 | Plasma: BestTreat | C42H78NO8P | RP | 12.68 | Pos | 756.5534 | [M+H]+ | 184.074 (100), 86.097 (9) | 3 | MS-FINDER/SIRIUS |
| PC 35:2 isomer 1 | Plasma: G2B/AlcoholBis | C43H82NO8P | RP | 13.45 | Pos | 772.5847 | [M+H]+ | 184.073 (100), 86.097 (11) | 3 | MS-FINDER/SIRIUS |
| PC 35:2 isomer 2 | Plasma: G2B/AlcoholBis | C43H82NO8P | RP | 13.60 | Pos | 772.5844 | [M+H]+ | 184.073 (100), 86.097 (17) | 3 | MS-FINDER/SIRIUS |
| PC 35:4 | Plasma: G2B/AlcoholBis | C43H78NO8P | RP | 12.77 | Pos | 768.5531 | [M+H]+ | 184.073 (100), 86.097 (15) | 3 | MS-FINDER/SIRIUS |
| PC 36:1 isomer 1 | Plasma: BestTreat | C44H86NO8P | RP | 14.50 | Pos | 788.6162 | [M+H]+ | 184.074 (100), 86.097 (9) | 3 | MS-FINDER/SIRIUS |
| PC 36:1 isomer 2 | Plasma: BestTreat | C44H86NO8P | RP | 14.59 | Pos | 788.6160 | [M+H]+ | 184.074 (100), 86.097 (9) | 3 | MS-FINDER/SIRIUS |
| PC 36:2 | Plasma: F4G | C44H84NO8P | RP | 12.26 | Pos | 808.5877 | [M+Na]+ | 808.582 (100), 184.073 (63) | 3 | MS-FINDER/SIRIUS |
| PC 36:4 | Plasma: F4G | C44H80NO8P | RP | 12.15 | Pos | 782.5684 | [M+H]+ | 782.572 (100), 184.075 (12) | 3 | MS-FINDER/SIRIUS |
| PC 37:4 | Plasma: G2B/AlcoholBis | C45H82NO8P | RP | 13.47 | Pos | 796.5828 | [M+H]+ | 184.073 (100), 86.097 (37), 162.956 (37), 737.453 (37) | 3 | MS-FINDER/SIRIUS |
| PC 38:3 | Plasma: G2B/AlcoholBis | C46H86NO8P | RP | 14.35 | Pos | 812.6158 | [M+H]+ | 184.073 (100), 86.097 (11) | 3 | MS-FINDER/SIRIUS |
| PC 38:4 | Plasma: G2B/AlcoholBis, F4G, BestTreat | C46H84NO8P | RP | 13.71 | Pos | 810.6000 | [M+H]+ | 810.5984 (100), 184.0732 (75), 86.0969 (6), 271.187 (4), 161.1164 (2), 124.999 (2) | 3 | MS-FINDER/SIRIUS |
| PC 38:5 isomer 1 | Plasma: G2B/AlcoholBis | C46H82NO8P | RP | 13.24 | Neg | 852.5779 | [M+HCOO]- | 303.232 (100), 329.251 (78), 255.234 (67), 281.247 (65) | 3 | MS-FINDER/SIRIUS |
| PC 38:5 isomer 2 | Plasma: G2B/AlcoholBis | C46H82NO8P | RP | 13.42 | Neg | 852.5779 | [M+HCOO]- | 301.219 (100), 283.266 (87), 255.234 (53), 329.251 (46) | 3 | MS-FINDER/SIRIUS |
| PC 38:6 | Plasma: F4G, BestTreat | C46H80NO8P | RP | 12.08 | Pos | 806.5723 | [M+H]+ | 184.076 (100), 86.098 (7), 623.509 (5) | 3 | MS-FINDER/SIRIUS |
| PC 40:5 | Plasma: G2B/AlcoholBis | C48H86NO8P | RP | 14.07 | Pos | 836.6156 | [M+H]+ | 184.073 (100), 86.097 (14) | 3 | MS-FINDER/SIRIUS |
| PC 40:8 | Plasma: G2B/AlcoholBis | C48H80NO8P | RP | 12.66 | Pos | 830.5695 | [M+H]+ | 184.073 (100), 86.097 (16) | 3 | MS-FINDER/SIRIUS |
| PC O-16:0_20:4 | Plasma: G2B/AlcoholBis, F4G | C44H82NO7P | RP | 13.64 | Pos/Neg | 768.5900 | [M+H]+ | Pos: 184.073 (100), 86.097 (13)<br>Neg: 303.232 (100), 259.241 (9) | 2 | LipidMaps |
| PC O-16:1_18:2 | Plasma: G2B/AlcoholBis | C42H80NO7P | RP | 13.54 | Pos/Neg | 742.5742 | [M+H]+ | Pos: 184.073 (100), 86.097 (11)<br>Neg: 279.231 (100), 112.986 (5) | 2 | LipidMaps |
| PC O-16:1_20:4 | Plasma: G2B/AlcoholBis, BestTreat | C44H80NO7P | RP | 13.15 | Pos/Neg | 766.5740 | [M+H]+ | Pos: 184.073 (100), 86.097 (12)<br>Neg: 303.235 (100), 750.553 (28), 464.315 (14), 259.242 (7), 78.958 (7), 224.07 (4), 446.306 (4) | 2 | LipidMaps |
| PC O-18:1_20:4 | Plasma: G2B/AlcoholBis, F4G, BestTreat | C46H84NO7P | RP | 13.75 | Pos/Neg | 794.6055 | [M+H]+ | Pos: 184.075 (100), 86.097 (13)<br>Neg: 303.232 (100), 259.241 (11) | 2 | LipidMaps |
| PC O-18:2_20:4 | Plasma: F4G | C46H80NO8P | RP | 12.47 | Neg | 836.5814 | [M+HCOO]- | 836.579 (100), 776.558 (27), 777.561 (5), 697.675 (5), 303.231 (4) | 2 | LipidMaps |
| PC O-34:3 | Plasma: F4G | C42H80NO7P | RP | 12.48 | Pos | 742.5742 | [M+H]+ | 184.073 (100), 742.575 (82), 480.349 (4) | 3 | MS-FINDER/SIRIUS |
| PC O-36:4 | Plasma: F4G, BestTreat | C44H82NO7P | RP | 12.56 | Pos | 768.5918 | [M+H]+ | 184.073 (100), 86.095 (7) | 3 | MS-FINDER/SIRIUS |
| PC O-36:5 | Plasma: G2B/AlcoholBis, F4G | C44H80NO7P | RP | 13.41 | Pos | 766.5744 | [M+H]+ | 184.075 (100), 86.097 (12) | 3 | MS-FINDER/SIRIUS |
| PC O-38:6 | Plasma: G2B/AlcoholBis, F4G, BestTreat | C46H82NO7P | RP | 13.28 | Pos | 792.5891 | [M+H]+ | 184.072 (100), 86.097 (13) | 3 | MS-FINDER/SIRIUS |
| PC O-38:7 | Plasma: G2B/AlcoholBis | C46H80NO7P | RP | 13.27 | Pos | 790.5739 | [M+H]+ | 184.073 (100), 86.097 (14) | 3 | MS-FINDER/SIRIUS |
| PC O-40:7 | Plasma: G2B/AlcoholBis | C48H84NO7P | HILIC | 0.67 | Pos | 818.6073 | [M+H]+ | 818.609 (100), 184.073 (7) | 3 | MS-FINDER/SIRIUS |
| PC P-38:7 | Plasma: BestTreat | C46H80NO7P | RP | 13.44 | Pos | 790.5710 | [M+H]+ | 86.097 (100), 146.982 (99), 731.495 (83), 86.096 (68), 57.071 (60) | 3 | MS-FINDER/SIRIUS |
| p-Cresol sulfate | Plasma: G2B/AlcoholBis, F4G, BestTreat<br>Feces: BestTreat | C7H8O4S | RP | 3.85 | Neg | 187.0073 | [M-H]- | 107.05 (100), 187.007 (85) | 2 | HMDB |

| Annotation | Sample matrix & study | Molecular formula | Column | Retention time | ESI | *m/z* | Adduct type | MS/MS fragments (%) | ID level | Annotation source |
|---|---|---|---|---|---|---|---|---|---|---|
| PE 16:0_20:4 | Plasma: G2B/AlcoholBis, F4G, BestTreat | C41H74NO8P | RP | 13.06 | Pos/Neg | 740.5222 | [M+H]+ | Pos: 599.501 (100), 313.274 (61), 184.073 (35)<br>Neg: 303.233 (100), 255.234 (70) | 2 | LipidMaps |
| PE 16:0_22:6 | Plasma: G2B/AlcoholBis, F4G, BestTreat | C43H74NO8P | RP | 12.95 | Pos/Neg | 764.5225 | [M+H]+ | Pos: 184.073 (100), 623.505 (69)<br>Neg: 255.235 (100), 327.235 (80), 283.246 (27), 762.515 (21), 452.276 (13), 140.011 (12), 196.038 (8), 78.957 (6), 59.012 (5), 229.195 (4) | 2 | LipidMaps |
| PE 18:0_20:4 | Plasma: G2B/AlcoholBis, F4G, BestTreat | C43H78NO8P | RP | 13.86 | Pos/Neg | 768.5538 | [M+H]+ | Pos: 184.073 (100), 627.541 (49), 341.307 (32)<br>Neg: 303.233 (100), 283.266 (74) | 2 | LipidMaps |
| PE P-16:0_20:4 | Plasma: G2B/AlcoholBis, F4G, BestTreat | C41H74NO7P | RP | 13.38 | Pos/Neg | 724.5273 | [M+H]+ | Pos: 361.271 (100), 364.26 (47), 81.071 (32), 95.086 (30)<br>Neg: 303.232 (100), 78.958 (9), 436.283 (8) | 2 | LipidMaps |
| PE P-18:1_20:4 | Plasma: F4G, BestTreat | C43H76NO7P | RP | 12.45 | Neg | 748.5298 | [M-H]- | 303.233 (100), 329.25 (26), 462.298 (12), 444.29 (7), 205.197 (7), 259.241 (7), 304.238 (5), 196.039 (5), 140.01 (4), 168.042 (4) | 2 | LipidMaps |
| Phenylacetaldehyde | Plasma: F4G | C8H8O | RP | 1.49 | Pos | 103.0543 | [M+H-H2O]+ | 51.022 (100), 50.015 (36), 77.039 (25), 74.015 (13), 102.045 (12) | 2 | HMDB |
| Phenylacetylglutamine | Plasma: G2B/AlcoholBis, F4G, BestTreat<br>Feces: BestTreat | C13H16N2O4 | HILIC | 2.09 | Pos/Neg | 265.1188 | [M+H]+ | Pos: 130.05 (100), 91.055 (29), 129.064 (13), 265.116 (10), 136.075 (9), 84.043 (8), 147.078 (8), 83.059 (7), 247.109 (6) | 2 | HMDB |
| Phenylalanine | Plasma: G2B/AlcoholBis, F4G, BestTreat<br>Feces: G2B, F4G, BestTreat | C9H11NO2 | HILIC | 4.20 | Pos/Neg | 166.0865 | [M+H]+ | Pos: 77.038 (100), 103.053 (53), 91.054 (18), 79.053 (10), 51.021 (8), 102.044 (5), 120.08 (5), 47.012 (4)<br>Neg: 147.045 (100), 164.072 (53), 103.92 (30), 72.009 (29) | 1 | In-house library |
| Phenylalanylarginine | Feces: F4G | C15H23N5O3 | HILIC | 6.24 | Pos | 322.1874 | [M+H]+ | 322.188 (100), 175.119 (30), 120.081 (13), 305.161 (13), 190.098 (8), 158.093 (6) | 2 | HMDB |
| Phenylethanolamine | Plasma: F4G, BestTreat<br>Feces: F4G, BestTreat | C8H11NO | RP | 1.50 | Pos | 120.0806 | [M+H-H2O]+ | 51.022 (100), 77.038 (39), 65.038 (25), 91.055 (23), 74.012 (10), 78.044 (8), 60.985 (5) | 2 | Fiehn-HILIC |
| Phenylsulfate C21H34O8S2 | Plasma: G2B/AlcoholBis | C21H34O8S2 | RP | 6.15 | Neg | 238.0779 | [M-H2O-H]2- | 96.96 (100), 238.078 (92) | 3 | MS-FINDER/SIRIUS |
| Phosphoric acid | Plasma: F4G<br>Feces: G2B, F4G | H3O4P | HILIC | 7.30 | Neg | 96.9695 | [M-H]- | 78.96 (100), 69.926 (5) | 2 | Fiehn-HILIC |
| p-Hydroxyphenyllactate | Plasma: F4G | C9H10O4 | HILIC | 1.18 | Neg | 181.0503 | [M-H]- | 181.05 (100), 135.044 (71), 163.042 (61), 119.048 (48), 72.993 (24), 116.933 (23), 159.273 (21), 82.392 (17), 103.338 (17), 78.681 (14) | 2 | HMDB |
| Phytosphingosine | Plasma: BestTreat<br>Feces: F4G, BestTreat | C18H39NO3 | RP | 8.93 | Pos | 318.3003 | [M+H]+ | 60.045 (100), 318.301 (55) | 2 | Fiehn-HILIC |
| PI 32:3 | Feces: F4G | C41H73O13P | RP | 8.22 | Pos | 805.4850 | [M+H]+ | 805.483 (100), 513.305 (51), 501.304 (31), 514.309 (19), 803.466 (13), 397.163 (11), 805.24 (11), 502.308 (10), 804.462 (9), 805.759 (8) | 2 | LipidMaps |
| Pipecolic acid | Plasma: G2B/AlcoholBis, F4G, BestTreat<br>Feces: F4G, BestTreat | C6H11NO2 | RP | 0.67 | Pos | 130.0868 | [M+H]+ | 84.081 (100), 130.088 (76), 57.07 (21), 130.159 (11) | 1 | In-house library |
| Piperine | Plasma: G2B/AlcoholBis, F4G, BestTreat<br>Feces: F4G, BestTreat | C17H19NO3 | RP | 8.39 | Pos | 286.1437 | [M+H]+ | 201.055 (100), 286.144 (66) | 2 | HMDB |
| Piroxicam | Plasma: F4G | C15H13N3O4S | RP | 6.57 | Pos | 332.0813 | [M+H]+ | 95.06 (100), 332.072 (91), 332.215 (57), 332.158 (17), 164.083 (13), 121.039 (8), 259.135 (6), 122.042 (5) | 2 | HMDB |
| Pregabalin | Feces: F4G | C8H17NO2 | RP | 2.74 | Pos | 160.1326 | [M+H]+ | 144.079 (100), 160.131 (49), 142.12 (31), 143.105 (10), 145.083 (10), 97.099 (5), 125.094 (4) | 2 | HMDB |
| Proline | Plasma: G2B/AlcoholBis, F4G, BestTreat<br>Feces: G2B, F4G, BestTreat | C5H9NO2 | HILIC | 5.11 | Pos | 116.0707 | [M+H]+ | 70.065 (100), 116.071 (17), 43.054 (5) | 1 | In-house library |
| Proline betaine | Plasma: G2B/AlcoholBis, F4G, BestTreat<br>Feces: G2B, BestTreat | C7H13NO2 | HILIC | 3.83 | Pos | 144.1030 | [M+H]+ | 144.103 (100), 58.065 (52), 84.081 (37), 43.017 (15), 57.033 (11), 71.049 (10), 44.049 (10), 99.042 (8), 98.095 (8), 102.055 (6) | 1 | In-house library |
| Pseudouridine | Plasma: F4G, BestTreat | C9H12N2O6 | HILIC | 3.77 | Neg | 243.0623 | [M-H]- | 153.03 (100), 183.04 (11), 111.02 (9), 243.061 (7), 63.058 (7), 140.033 (7) | 2 | HMDB |
| Psicose | Plasma: F4G | C6H12O6 | HILIC | 5.27 | Neg | 215.0326 | [M+Cl]- | 34.969 (100), 215.032 (14), 59.014 (4) | 2 | MassBank |
| Putrescine | Feces: F4G | C4H12N2 | HILIC | 6.56 | Pos | 89.1078 | [M+H]+ | 72.081 (100), 73.083 (5), 89.106 (5) | 2 | HMDB |
| Pyridoxamine | Feces: G2B, F4G, BestTreat | C8H12N2O2 | HILIC | 5.30 | Pos | 169.0979 | [M+H]+ | 134.058 (100), 135.063 (45), 81.043 (34), 77.037 (30), 80.049 (30), 106.064 (22), 79.053 (20), 65.039 (11) | 2 | ReSpect |
| Pyridoxine | Plasma: G2B/AlcoholBis<br>Feces: G2B | C8H11NO3 | HILIC | 0.99 | Pos | 170.0817 | [M+H]+ | 152.071 (100), 170.081 (46), 134.061 (28) | 2 | HMDB |
| Pyrocatechol sulfate | Plasma: G2B/AlcoholBis, F4G, BestTreat<br>Feces: BestTreat | C6H6O5S | RP | 2.15 | Neg | 188.9864 | [M-H]- | 109.029 (100), 160.894 (53), 144.898 (51), 188.987 (45) | 2 | HMDB |
| Pyrophosphoric acid | Feces: G2B | H4O7P2 | HILIC | 6.76 | Neg | 176.9372 | [M-H]- | 78.96 (100), 158.929 (43), 176.934 (16), 159.29 (14), 159.198 (9) | 2 | NIST MS Data Center |
| Quinic acid | Plasma: F4G<br>Feces: G2B, F4G | C7H12O6 | HILIC | 5.86 | Neg | 191.0561 | [M-H]- | 85.032 (100), 191.054 (36), 71.013 (26), 111.043 (25), 37.622 (22), 170.823 (17), 180.292 (17), 107.069 (14), 185.963 (14), 44.999 (12) | 1 | In-house library |
| Quinine | Plasma: F4G | C20H24N2O2 | HILIC | 0.74 | Pos | 325.1923 | [M+H]+ | 325.191 (100), 172.075 (14), 160.076 (13), 253.125 (13), 81.069 (12), 111.1 (10), 307.18 (9), 264.134 (8), 184.076 (7), 110.099 (7) | 2 | HMDB |
| Quinoxalines | Feces: F4G | C12H18ClNO | HILIC | 5.27 | Pos | 228.1236 | [M+H]+ | 228.123 (100), 109.076 (6), 226.119 (4) | 3 | MS-FINDER/SIRIUS |
| Retinol | Plasma: G2B/AlcoholBis, F4G, BestTreat<br>Feces: BestTreat | C20H30O | RP | 10.83 | Pos | 269.2262 | [M+H-H2O]+ | 269.225 (100), 93.07 (94), 81.071 (62), 95.086 (62) | 2 | HMDB |
| Ricinoleic acid | Feces: F4G | C18H34O3 | RP | 9.99 | Pos | 299.2580 | [M+H]+ | 299.256 (100), 281.245 (34), 263.235 (8), 282.249 (8) | 2 | NIST MS Data Center |
| S-(5'-Adenosyl)-L-methionine cation | Feces: F4G, BestTreat | C15H23N6O5S | HILIC | 7.36 | Pos | 399.1451 | [M]+ | 250.092 (100), 298.094 (24), 136.061 (16), 251.094 (11), 102.054 (10), 264.089 (9), 399.141 (6) | 2 | NIST MS Data Center |
| Saccharopine | Feces: G2B, F4G | C11H20N2O6 | HILIC | 6.77 | Pos | 259.1283 | [M+H-H2O]+ | 213.123 (100), 84.08 (49), 259.127 (25), 214.122 (11), 195.111 (8) | 2 | NIST MS Data Center |
| Salicylic acid | Feces: F4G, BestTreat | C7H6O3 | RP | 2.76 | Neg | 137.0249 | [M-H]- | 137.025 (100), 93.035 (87), 94.038 (8), 137.042 (6), 74.447 (4) | 2 | NIST MS Data Center |
| Salicyluric acid | Plasma: F4G | C9H9NO4 | HILIC | 0.85 | Neg | 194.0462 | [M-H]- | 150.055 (100), 93.034 (69), 62.466 (10), 107.673 (8), 123.114 (7), 39.762 (6), 129.759 (6), 93.236 (6), 69.496 (5), 98.541 (5) | 2 | HMDB |
| Sebacic acid | Plasma: G2B/AlcoholBis, F4G, BestTreat<br>Feces: G2B, F4G, BestTreat | C10H18O4 | RP | 6.75 | Neg | 201.1140 | [M-H]- | 139.113 (100), 201.113 (77), 183.103 (43) | 2 | MassBank |
| Ser-Ile-Arg | Feces: F4G | C15H30N6O5 | HILIC | 6.78 | Pos | 375.2351 | [M+H]+ | 375.232 (100), 374.237 (36), 175.118 (12), 200.137 (5), 147.111 (4) | 2 | MassBank |
| Serine | Plasma: F4G | C3H7NO3 | HILIC | 6.24 | Pos | 106.0494 | [M+H]+ | 60.043 (100), 42.034 (22), 88.038 (16), 106.048 (11), 70.027 (6), 70.064 (4) | 1 | In-house library |
| Sinapyl alcohol | Plasma: F4G | C11H14O4 | RP | 6.22 | Pos | 211.0885 | [M+H]+ | 77.039 (100), 91.055 (79), 79.055 (37), 78.047 (33), 103.054 (29), 65.038 (18), 151.075 (17), 121.065 (16), 105.07 (14), 119.05 (11) | 2 | HMDB |
| SM 30:1 | Plasma: G2B/AlcoholBis, BestTreat | C35H71N2O6P | RP | 11.75 | Pos | 647.5120 | [M+H]+ | 184.073 (100), 86.097 (10) | 3 | MS-FINDER/SIRIUS |
| SM 32:1 | Plasma: G2B/AlcoholBis, F4G, BestTreat | C37H75N2O6P | RP | 12.12 | Pos | 675.5436 | [M+H]+ | 184.074 (100), 86.097 (8) | 3 | MS-FINDER/SIRIUS |
| SM 32:2 | Plasma: G2B/AlcoholBis, F4G, BestTreat | C37H73N2O6P | RP | 11.86 | Neg | 717.5203 | [M+HCOO]- | 657.496 (100), 168.043 (79), 176.95 (21), 169.048 (17), 59.235 (15), 451.077 (14), 176.546 (13), 517.158 (12), 63.629 (12), 522.206 (12) | 3 | MS-FINDER/SIRIUS |
| SM 33:1 | Plasma: G2B/AlcoholBis, F4G, BestTreat | C38H77N2O6P | RP | 12.48 | Pos/Neg | 733.5516 | [M+HCOO]- | Neg: 168.043 (100), 78.958 (94)<br>Pos: 184.0726, 689.5544, 71.0729 | 3 | MS-FINDER/SIRIUS |

| Annotation | Sample matrix & study | Molecular formula | Column | Retention time | ESI | *m/z* | Adduct type | MS/MS fragments (%) | ID level | Annotation source |
|---|---|---|---|---|---|---|---|---|---|---|
| SM 34:1 | Plasma: G2B/AlcoholBis, F4G, BestTreat | C39H79N2O6P | RP | 12.78 | Pos/Neg | 747.5668 | [M−HCOO]- | Neg: 168.043 (100), 78.958 (80)<br>Pos: 184.0724, 703.5742 | 3 | MS-FINDER/SIRIUS |
| SM 34:2 | Plasma: G2B/AlcoholBis, F4G, BestTreat | C39H77N2O6P | RP | 12.33 | Pos/Neg | 701.5593 | [M+H]+ | Pos: 184.075 (100), 86.097 (11)<br>Neg: 168.0436, 78.9584, 685.5359 | 3 | MS-FINDER/SIRIUS |
| SM 36:1 | Plasma: G2B/AlcoholBis, BestTreat | C41H83N2O6P | RP | 13.50 | Pos | 731.6058 | [M+H]+ | 184.073 (100), 86.097 (12) | 3 | MS-FINDER/SIRIUS |
| SM 36:2 | Plasma: G2B/AlcoholBis, F4G, BestTreat | C41H81N2O6P | RP | 12.94 | Neg | 773.5831 | [M−HCOO]- | 168.043 (100), 78.959 (83) | 3 | MS-FINDER/SIRIUS |
| SM 42:3 | Plasma: F4G, BestTreat | C47H91N2O6P | RP | 13.40 | Neg | 855.6594 | [M−HCOO]- | 855.661 (100), 795.641 (31), 855.593 (10), 112.487 (6), 361.789 (5), 796.58 (4), 855.483 (4) | 3 | MS-FINDER/SIRIUS |
| Solanidine | Plasma: BestTreat<br>Feces: G2B, F4G, BestTreat | C27H43NO | RP | 6.78 | Pos | 398.3419 | [M+H]+ | 398.341 (100),398.318 (14), 398.371 (5) | 2 | HMDB |
| Sphinganine | Feces: G2B | C18H39NO2 | RP | 10.80 | Pos | 284.2968 | [M−H-H2O]− | 284.295 (100) | 1 | In-house library |
| Stercobilin | Plasma: BestTreat<br>Feces: G2B, F4G, BestTreat | C33H46N4O6 | RP | 6.25 | Pos | 595.3492 | [M+H]+ | 345.181 (100), 470.263 (91), 595.345 (90) | 2 | HMDB |
| Stercobilinogen | Feces: F4G | C33H48N4O6 | RP | 8.59 | Pos | 597.3653 | [M-H]- | 597.361 (100), 305.185 (5), 595.347 (3), 596.351 (3), 180.101 (1) | 2 | HMDB |
| Suberic acid | Plasma: F4G<br>Feces: F4G, BestTreat | C8H14O4 | RP | 4.80 | Neg | 173.0817 | [M-H]- | 111.081 (100), 173.081 (68), 112.084 (22), 57.034 (21), 109.065 (13), 30.769 (7), 170.979 (7), 36.364 (7), 172.829 (7), 111.356 (6) | 2 | NIST MS Data Center |
| Succinic acid | Feces: F4G | C4H6O4 | HILIC | 1.44 | Neg | 117.0193 | [M-H]- | 117.021 (100), 99.009 (72), 73.029 (53), 52.54 (9), 49.749 (7), 73.018 (5), 75.032 (4) | 2 | HMDB |
| Sulfated steroid_C19H28O6S | Plasma: G2B/AlcoholBis | C19H28O6S | RP | 6.48 | Neg | 383.1539 | [M-H]- | 96.96 (100), 383.155 (74) | 3 | MS-FINDER/SIRIUS |
| Sulfated steroid_C19H30O6S | Plasma: G2B/AlcoholBis | C19H30O6S | RP | 7.46 | Neg | 385.1693 | [M-H]- | 385.168 (100), 96.96 (41) | 3 | MS-FINDER/SIRIUS |
| Sulfated steroid_C19H30O8S2 isomer 1 | Plasma: G2B/AlcoholBis, BestTreat<br>Feces: BestTreat | C19H30O8S2 | RP | 5.71 | Neg | 224.0622 | [M-H2O-H]2- | 224.061 (100), 96.96 (79) | 3 | MS-FINDER/SIRIUS |
| Sulfated steroid_C19H30O8S2 isomer 2 | Plasma: G2B/AlcoholBis, BestTreat<br>Feces: BestTreat | C19H30O8S2 | RP | 6.30 | Neg | 224.0622 | [M-H2O-H]2- | 96.96 (100), 224.061 (83) | 3 | MS-FINDER/SIRIUS |
| Taurine | Plasma: F4G<br>Feces: F4G | C2H7NO3S | HILIC | 5.45 | Neg | 124.0075 | [M-H]- | 79.958 (100), 124.008 (60), 32.199 (17), 41.395 (17), 98.78 (12), 124.03 (10), 101.015 (10), 93.824 (9), 103.999 (8), 56.357 (7) | 1 | In-house library |
| Taurochenodeoxycholic acid | Plasma: G2B/AlcoholBis, F4G<br>Feces: F4G | C26H45NO6S | RP | 9.64 | Pos | 464.2831 | [M−H-2H2O]+ | 464.285 (100), 126.022 (84), 215.18 (48) | 1 | In-house library |
| Taurursodeoxycholic acid | Feces: BestTreat, | C26H45NO6S | RP | 9.52 | Pos | 464.2831 | [M−H-2H2O]+ | 464.285 (100), 126.022 (75), 201.163 (40) | 1 | In-house library |
| Temazepam | Plasma: G2B/AlcoholBis | C16H13ClN2O2 | RP | 7.54 | Pos | 301.0738 | [M+H]+ | 255.067 (100), 283.061 (20), 301.077 (17) | 2 | MassBank |
| Tetrapyrrole derivative | Feces: G2B, F4G | C33H46N4O6 | RP | 8.55 | Pos | 595.3500 | [M−H]+ | 303.171 (100), 133.086 (55), 89.06 (55), 180.102 (48), 177.113 (31), 166.091 (27), 102.067 (22), 124.082 (22), 593.334 (21), 144.078 (19) | 3 | MS-FINDER/SIRIUS |
| Theobromine | Plasma: G2B/AlcoholBis, BestTreat<br>Feces: BestTreat | C7H8N4O2 | RP | 2.08 | Pos | 181.0721 | [M−H]+ | 181.072 (100),138.066 (6) | 1 | In-house library |
| Theophylline | Plasma: G2B/AlcoholBis, BestTreat<br>Feces: BestTreat | C7H8N4O2 | RP | 3.06 | Pos | 181.0720 | [M+H]+ | 181.072 (100), 124.051 (21) | 1 | In-house library |
| Thiamine isomer 1 | Feces: G2B, BestTreat | C12H17N4OS | HILIC | 3.37 | Pos | 265.1110 | [M]+ | 122.071 (100), 144.047 (27), 123.073 (7), 81.044 (5) | 2 | NIST MS Data Center |
| Thiamine isomer 2 | Feces: G2B, F4G | C12H17N4OS | HILIC | 3.82 | Pos | 265.1134 | [M]+ | 122.07 (100), 265.109 (53), 144.046 (28), 123.073 (7) | 2 | NIST MS Data Center |
| Threonic acid | Plasma: F4G | C4H8O5 | HILIC | 5.70 | Neg | 135.0299 | [M-H]- | 134.866 (100), 75.009 (64), 59.015 (16), 34.969 (14), 135.024 (7), 52.02 (6), 135.452 (6), 116.941 (5), 129.637 (5), 62.302 (5) | 2 | HMDB |
| Threonine | Plasma: G2B/AlcoholBis, F4G, BestTreat<br>Feces: BestTreat | C4H9NO3 | HILIC | 5.95 | Pos | 120.0655 | [M+H]+ | 56.05 (100), 57.033 (48), 74.059 (45) | 2 | HMDB |
| Thr-Gly-Arg | Feces: F4G | C12H24N6O5 | HILIC | 7.37 | Pos | 333.1881 | [M+H]+ | 333.186 (100), 175.119 (16), 316.159 (8), 215.11 (6), 332.194 (5), 289.161 (4), 204.132 (4), 159.073 (4), 112.085 (4), 176.12 (4) | 2 | MassBank |
| Thr-Leu | Feces: F4G | C10H20N2O4 | HILIC | 7.09 | Pos | 233.1493 | [M+H]+ | 233.148 (100), 174.076 (17), 232.164 (5), 217.107 (4) | 2 | MassBank |
| Trazodone | Plasma: G2B/AlcoholBis | C19H22ClN5O | RP | 5.01 | Pos | 372.1585 | [M−H]+ | 176.082 (100), 372.16 (80) | 2 | MassBank |
| Triacetin | Plasma: F4G, BestTreat<br>Feces: G2B, BestTreat | C9H14O6 | RP | 4.67 | Pos | 241.0699 | [M+Na]+ | 241.068 (100), 181.049 (59), 196.896 (7), 241.106 (6), 195.1 (5), 83.009 (4) | 2 | MassBank |
| Tricin | Feces: F4G | C17H14O7 | RP | 6.98 | Neg | 329.0679 | [M-H]- | 271.026 (100), 299.022 (87), 227.036 (20), 161.025 (18), 272.03 (14), 300.026 (13), 243.032 (13), 203.036 (10), 185.026 (6), 314.044 (6) | 2 | MassBank |
| Trigonelline | Plasma: G2B/AlcoholBis, F4G, BestTreat<br>Feces: G2B, F4G, BestTreat | C7H7NO2 | HILIC | 4.49 | Pos | 138.0549 | [M+H]+ | 92.049 (100), 94.064 (49), 53.036 (17), 67.054 (14), 78.032 (14), 138.054 (13), 77.036 (8), 65.039 (8), 93.057 (7) | 1 | In-house library |
| Trimethylamine-N-oxide | Plasma: G2B/AlcoholBis, F4G, BestTreat | C3H9NO | HILIC | 1.62 | Pos | 151.1443 | [2M+H]+ | 76.076 (100), 59.072 (33), 58.065 (26), 60.076 (5), 45.034 (4) | 2 | HMDB |
| Trimethyluric acid | Feces: G2B, F4G, BestTreat | C8H10N4O3 | RP | 3.16 | Neg | 209.0660 | [M-H]- | 209.0706 (100), 194.0465 (35), 137.0261 (29), 124.0533 (13), 66.0127 (10), | 2 | Fiehn-HILIC |
| Triterpenoid | Feces: F4G | C30H50O2 | RP | 10.80 | Pos | 465.3709 | [M−Na]+ | 465.368 (100) | 3 | MS-FINDER/SIRIUS |
| Tryptophan | Plasma: G2B/AlcoholBis, F4G, BestTreat<br>Feces: G2B, F4G, BestTreat | C11H12N2O2 | HILIC | 4.14 | Pos/Neg | 205.0982 | [M−H]+ | Pos: 146.06 (100), 118.065 (57), 144.081 (33), 188.071 (21), 159.092 (15), 132.08 (10), 170.06 (9), 143.07 (8), 142.064 (4), 74.024 (4) | 1 | In-house library |
| Tryptophan betaine | Plasma: G2B/AlcoholBis, BestTreat<br>Feces: BestTreat | C14H18N2O2 | RP | 3.00 | Pos | 247.1440 | [M+H]+ | 188.071 (100), 146.059 (53),60.082 (35), 60.082 (31) | 1 | In-house library |
| Tryptophyl-Phenylalanine | Plasma: G2B/AlcoholBis | C20H21N3O3 | RP | 4.69 | Pos | 352.1654 | [M+H]+ | 120.081 (100), 205.098 (25) | 2 | HMDB |
| Tyrosine | Plasma: G2B/AlcoholBis, F4G, BestTreat<br>Feces: BestTreat | C9H11NO3 | HILIC | 5.30 | Pos/Neg | 182.0822 | [M−H]+ | Pos: 91.054 (100), 119.049 (99), 136.076 (82), 95.048 (37), 121.06 (14), 123.042 (13), 147.046 (8), 107.047 (5)<br>Neg: 163.0403, 180.0678, 103.9206 | 1 | In-house library |
| Undecanedioic acid | Plasma: F4G | C11H20O4 | RP | 7.20 | Neg | 215.1288 | [M-H]- | 197.118 (100), 153.129 (72), 215.127 (16), 57.036 (4) | 2 | HMDB |
| Urea | Plasma: G2B/AlcoholBis, F4G | CH4N2O | HILIC | 1.04 | Pos | 61.0393 | [M−H]+ | 44.013 (100), 61.038 (5) | 2 | HMDB |
| Uridine | Plasma: F4G<br>Feces: F4G | C9H12N2O6 | HILIC | 1.55 | Neg | 243.0623 | [M-H]- | 110.024 (100), 243.063 (84), 152.035 (67), 200.055 (54), 140.034 (44), 61.987 (30), 41.999 (30), 100.294 (22), 108.046 (17), 20 (17) | 1 | In-house library |
| Uridine/Pseudouridine | Plasma: G2B/AlcoholBis | C9H12N2O6 | RP | 0.67 | Neg | 243.0617 | [M-H]- | 153.031 (100), 110.025 (40), 116.929 (33) | 2 | HMDB |
| Urobilin | Plasma: G2B/AlcoholBis<br>Feces: G2B, F4G | C33H42N4O6 | RP | 6.10 | Pos | 591.3176 | [M+H]+ | 343.165 (100), 591.318 (20), 466.235 (10), 445.373 (5), 198.227 (3), 127.830 (3), 55.822 (3) | 2 | HMDB |
| Urobilinogen | Feces: F4G | C33H42N4O6 | RP | 7.56 | Pos | 591.3187 | [M+H]+ | 591.32 (100), 466.234 (33), 589.305 (10), 467.238 (8), 465.227 (7), 590.307 (6), 343.165 (5), 464.218 (4) | 2 | HMDB |
| Urocanic acid | Plasma: BestTreat<br>Feces: G2B, F4G, BestTreat | C6H6N2O2 | HILIC | 1.10 | Pos | 139.0574 | [M−H]+ | 121.041 (100), 139.052 (74), 93.046 (37), 95.059 (17), 121.421 (4), 93.155 (4) | 2 | MassBank |
| Valine | Plasma: F4G<br>Feces: G2B | C5H11NO2 | HILIC | 4.96 | Pos | 118.0860 | [M−H]+ | 72.081 (100), 55.054 (22), 118.086 (7) | 1 | In-house library |
| Val-Lys | Feces: F4G | C11H23N3O3 | HILIC | 6.79 | Pos | 246.1807 | [M−H]+ | 147.113 (100), 246.182 (69), 130.087 (27), 72.082 (21), 129.102 (20), 84.082 (11), 100.076 (9), 148.116 (6), 206.129 (6), 228.171 (4) | 2 | NIST MS Data Center |

| Annotation | Sample matrix & study | Molecular formula | Column | Retention time | ESI | m/z | Adduct type | MS/MS fragments (%) | ID level | Annotation source |
|---|---|---|---|---|---|---|---|---|---|---|
| Valsartan | Feces: F4G, BestTreat | C24H29N5O3 | RP | 8.03 | Pos | 436.2344 | [M+H]+ | 235.098 (100), 291.15 (76), 207.092 (40), 306.172 (37), 352.178 (16), 292.154 (14), 236.102 (12), 362.224 (11), 307.176 (6), 208.096 (5) | 2 | MassBank |
| Venlafaxine | Plasma: G2B/AlcoholBis<br>Feces: G2B, F4G | C17H27NO2 | RP | 5.31 | Pos | 278.2114 | [M+H]+ | 277.106 (100), 149.024 (73), 260.205 (30), 278.214 (12), 215.143 (12), 208.886 (12), 121.065 (11) | 2 | MassBank |
| Xanthine | Plasma: F4G | C5H4N4O2 | HILIC | 1.80 | Neg | 151.0262 | [M-H]- | 108.021 (100), 151.027 (55), 130.139 (16), 104.918 (14), 76.644 (12), 23.55 (11), 115.398 (10), 69.862 (10), 144.578 (8), 104.357 (7) | 1 | In-house library |
| Zeatin | Feces: G2B, F4G, BestTreat | C10H13N5O | HILIC | 1.80 | Pos | 220.1189 | [M+H]+ | 220.117 (100), 148.06 (38), 160.061 (8), 136.061 (6), 140.07 (5), 202.109 (4) | 2 | MassBank |

Abbreviations: 3-CMPFP, 3-carboxy-4-methyl-5-pentyl-2-furanpropionic acid; 5-AVAB, 5-aminovaleric acid betaine; AC, acylcarnitine; CMPF, 3-carboxy-4-methyl-5-propyl-2-furanpropionic acid; FA, fatty acid; F4G. Food4Gut; G2B, Gut2Brain; ESI, electrospray ionization; HILIC, hydrophilic interaction chromatography; HMDB, Human metabolome database; LysoPC, lysophosphatidylcholine; LPE lysophosphatidylethanolamine; NIST, National Institute of Standards and Technology; PC, phosphatidylcholine; PE, phosphatidylethanolamine; RP, reversed-phase; SM, sphingomyelin.

# APPENDIX: ORIGINAL PUBLICATIONS

I. Reprinted from *eLife*, 2024, 13: RP96937. eLife Sciences Publication Ltd, an open access article published under the terms of the Creative Commons (CC-BY 4.0) license.

II. Reprinted from *Clin. Nutr. ESPEN*, 2025, 66, 361–371. Elsevier Ltd, an open access article published under the terms of the Creative Commons (CC-BY-NC-ND 4.0) license.

III. Submitted.

# DOCTORAL THESES IN FOOD SCIENCES AT THE UNIVERSITY OF TURKU

1. **REINO R. LINKO (1967)** Fatty acids and other components of Baltic herring flesh lipids. (Organic chemistry).
2. **HEIKKI KALLIO (1975)** Identification of volatile aroma compounds in arctic bramble, *Rubus arcticus* L. and their development during ripening of the berry, with special reference to *Rubus stellatus* SM.
3. **JUKKA KAITARANTA (1981)** Fish roe lipids and lipid hydrolysis in processed roe of certain *Salmonidae* fish as studied by novel chromatographic techniques.
4. **TIMO HIRVI (1983)** Aromas of some strawberry and blueberry species and varieties studied by gas liquid chromatographic and selected ion monitoring techniques.
5. **RAINER HUOPALAHTI (1985)** Composition and content of aroma compounds in the dill herb, *Anethum graveolens* L., affected by different factors.
6. **MARKKU HONKAVAARA (1989)** Effect of porcine stress on the development of PSE meat, its characteristics and influence on the economics of meat products manufacture.
7. **PÄIVI LAAKSO (1992)** Triacylglycerols – approaching the molecular composition of natural mixtures.
8. **MERJA LEINO (1993)** Application of the headspace gas chromatography complemented with sensory evaluation to analysis of various foods.
9. **KAISLI KERROLA (1994)** Essential oils from herbs and spices: isolation by carbon dioxide extraction and characterization by gas chromatography and sensory evaluation.
10. **ANJA LAPVETELÄINEN (1994)** Barley and oat protein products from wet processes: food use potential.
11. **RAIJA TAHVONEN (1995)** Contents of lead and cadmium in foods in Finland.
12. **MAIJA SAXELIN (1995)** Development of dietary probiotics: estimation of optimal *Lactobacillus* GG concentrations.
13. **PIRJO-LIISA PENTTILÄ (1995)** Estimation of food additive and pesticide intakes by means of a stepwise method.
14. **SIRKKA PLAAMI (1996)** Contents of dietary fiber and inositol phosphates in some foods consumed in Finland.
15. **SUSANNA EEROLA (1997)** Biologically active amines: analytics, occurrence and formation in dry sausages.
16. **PEKKA MANNINEN (1997)** Utilization of supercritical carbon dioxide in the analysis of triacylglycerols and isolation of berry oils.
17. **TUULA VESA (1997)** Symptoms of lactose intolerance: influence of milk composition, gastric emptying, and irritable bowel syndrome.
18. **EILA JÄRVENPÄÄ (1998)** Strategies for supercritical fluid extraction of analytes in trace amounts from food matrices.
19. **ELINA TUOMOLA (1999)** *In vitro* adhesion of probiotic lactic acid bacteria.
20. **ANU JOHANSSON (1999)** Availability of seed oils from Finnish berries with special reference to compositional, geographical and nutritional aspects.
21. **ANNE PIHLANTO-LEPPÄLÄ (1999)** Isolation and characteristics of milk-derived bioactive peptides.
22. **MIKA TUOMOLA (2000)** New methods for the measurement of androstenone and skatole – compounds associated with boar taint problem. (Biotechnology).
23. **LEEA PELTO (2000)** Milk hypersensitivity in adults: studies on diagnosis, prevalence and nutritional management.
24. **ANNE NYKÄNEN (2001)** Use of nisin and lactic acid/lactate to improve the microbial and sensory quality of rainbow trout products.
25. **BAORU YANG (2001)** Lipophilic components of sea buckthorn (*Hippophaë rhamnoides*) seeds and berries and physiological effects of sea buckthorn oils.
26. **MINNA KAHALA (2001)** Lactobacillar S-layers: Use of *Lactobacillus brevis* S-layer signals for heterologous protein production.
27. **OLLI SJÖVALL (2002)** Chromatographic and mass spectrometric analysis of non-volatile oxidation products of triacylglycerols with emphasis on core aldehydes.
28. **JUHA-PEKKA KURVINEN (2002)** Automatic data processing as an aid to mass spectrometry of dietary triacylglycerols and tissue glycerophospholipids.
29. **MARI HAKALA (2002)** Factors affecting the internal quality of strawberry (*Fragaria x ananassa* Duch.) fruit.
30. **PIRKKA KIRJAVAINEN (2003)** The intestinal microbiota – a target for treatment in infant atopic eczema?

31. **TARJA ARO (2003)** Chemical composition of Baltic herring: effects of processing and storage on fatty acids, mineral elements and volatile compounds.
32. **SAMI NIKOSKELAINEN (2003)** Innate immunity of rainbow trout: effects of opsonins, temperature and probiotics on phagocytic and complement activity as well as on disease resistance.
33. **KAISA YLI-JOKIPII (2004)** Effect of triacylglycerol fatty acid positional distribution on postprandial lipid metabolism.
34. **MARIKA JESTOI (2005)** Emerging *Fusarium*-mycotoxins in Finland.
35. **KATJA TIITINEN (2006)** Factors contributing to sea buckthorn (*Hippophaë rhamnoides* L.) flavour.
36. **SATU VESTERLUND (2006)** Methods to determine the safety and influence of probiotics on the adherence and viability of pathogens.
37. **FANDI FAWAZ ALI IBRAHIM (2006)** Lactic acid bacteria: an approach for heavy metal detoxification.
38. **JUKKA-PEKKA SUOMELA (2006)** Effects of dietary fat oxidation products and flavonols on lipoprotein oxidation.
39. **SAMPO LAHTINEN (2007)** New insights into the viability of probiotic bacteria.
40. **SASKA TUOMASJUKKA (2007)** Strategies for reducing postprandial triacylglycerolemia.
41. **HARRI MÄKIVUOKKO (2007)** Simulating the human colon microbiota: studies on polydextrose, lactose and cocoa mass.
42. **RENATA ADAMI (2007)** Micronization of pharmaceuticals and food ingredients using supercritical fluid techniques.
43. **TEEMU HALTTUNEN (2008)** Removal of cadmium, lead and arsenic from water by lactic acid bacteria.
44. **SUSANNA ROKKA (2008)** Bovine colostral antibodies and selected lactobacilli as means to control gastrointestinal infections.
45. **ANU LÄHTEENMÄKI-UUTELA (2009)** Foodstuffs and medicines as legal categories in the EU and China. Functional foods as a borderline case. (Law).
46. **TARJA SUOMALAINEN (2009)** Characterizing *Propionibacterium freudenreichii* ssp. *shermanii* JS and *Lactobacillus rhamnosus* LC705 as a new probiotic combination: basic properties of JS and pilot *in vivo* assessment of the combination.
47. **HEIDI LESKINEN (2010)** Positional distribution of fatty acids in plant triacylglycerols: contributing factors and chromatographic/mass spectrometric analysis.
48. **TERHI POHJANHEIMO (2010)** Sensory and non-sensory factors behind the liking and choice of healthy food products.
49. **RIIKKA JÄRVINEN (2010)** Cuticular and suberin polymers of edible plants – analysis by gas chromatographic-mass spectrometric and solid state spectroscopic methods.
50. **HENNA-MARIA LEHTONEN (2010)** Berry polyphenol absorption and the effect of northern berries on metabolism, ectopic fat accumulation, and associated diseases.
51. **PASI KANKAANPÄÄ (2010)** Interactions between polyunsaturated fatty acids and probiotics.
52. **PETRA LARMO (2011)** The health effects of sea buckthorn berries and oil.
53. **HENNA RÖYTIÖ (2011)** Identifying and characterizing new ingredients *in vitro* for prebiotic and synbiotic use.
54. **RITVA REPO-CARRASCO-VALENCIA (2011)** Andean indigenous food crops: nutritional value and bioactive compounds.
55. **OSKAR LAAKSONEN (2011)** Astringent food compounds and their interactions with taste properties.
56. **ŁUKASZ MARCIN GRZEŚKOWIAK (2012)** Gut microbiota in early infancy: effect of environment, diet and probiotics.
57. **PENGZHAN LIU (2012)** Composition of hawthorn (*Crataegus* spp.) fruits and leaves and emblic leafflower (*Phyllanthus emblica*) fruits.
58. **HEIKKI ARO (2012)** Fractionation of hen egg and oat lipids with supercritical fluids. Chemical and functional properties of fractions.
59. **SOILI ALANNE (2012)** An infant with food allergy and eczema in the family – the mental and economic burden of caring.
60. **MARKO TARVAINEN (2013)** Analysis of lipid oxidation during digestion by liquid chromatography-mass spectrometric and nuclear magnetic resonance spectroscopic techniques.
61. **JIE ZHENG (2013)** Sugars, acids and phenolic compounds in currants and sea buckthorn in relation to the effects of environmental factors.
62. **SARI MÄKINEN (2014)** Production, isolation and characterization of bioactive peptides with antihypertensive properties from potato and rapeseed proteins.
63. **MIKA KAIMAINEN (2014)** Stability of natural colorants of plant origin.

64. **LOTTA NYLUND (2015)** Early life intestinal microbiota in health and in atopic eczema.
65. **JAAKKO HIIDENHOVI (2015)** Isolation and characterization of ovomucin – a bioactive agent of egg white.
66. **HANNA-LEENA HIETARANTA-LUOMA (2016)** Promoting healthy lifestyles with personalized, *APOE* genotype based health information: The effects on psychological-, health behavioral and clinical factors.
67. **VELI HIETANIEMI (2016)** The *Fusarium* mycotoxins in Finnish cereal grains: How to control and manage the risk.
68. **MAARIA KORTESNIEMI (2016)** NMR metabolomics of foods – Investigating the influence of origin on sea buckthorn berries, *Brassica* oilseeds and honey.
69. **JUHANI AAKKO (2016)** New insights into human gut microbiota development in early infancy: influence of diet, environment and mother's microbiota.
*70.* **WEI YANG (2017)** Effects of genetic and environmental factors on proanthocyanidins in sea buckthorn (*Hippophaë rhamnoides*) and flavonol glycosides in leaves of currants (*Ribes* spp.).
71. **LEENAMAIJA MÄKILÄ (2017)** Effect of processing technologies on phenolic compounds in berry products.
72. **JUHA-MATTI PIHLAVA (2017)** Selected bioactive compounds in cereals and cereal products – their role and analysis by chromatographic methods.
73. **TOMMI KUMPULAINEN (2018)** The complexity of freshness and locality in a food consumption context
74. **XUEYING MA (2018)** Non-volatile bioactive and sensory compounds in berries and leaves of sea buckthorn (*Hippophaë rhamnoides*)
75. **ANU NUORA (2018)** Postprandial lipid metabolism resulting from heated beef, homogenized milk and interesterified palm oil.
76. **HEIKKI AISALA (2019)** Sensory properties and underlying chemistry of Finnish edible wild mushrooms.
77. **YE TIAN (2019)** Phenolic compounds from Finnish berry species to enhance food safety.
78. **MAIJA PAAKKI (2020)** The importance of natural colors in food for the visual attractiveness of everyday lunch.
79. **SHUXUN LIU (2020**) Fermentation with non-*Saccharomyces* yeasts as a novel biotechnology for berry wine production.
80. **MARIKA KALPIO (2020)** Strategies for analyzing the regio- and stereospecific structures of individual triacylglycerols in natural fats and oils.
81. **JOHANNA JOKIOJA (2020)** Postprandial effects and metabolism of acylated anthocyanins originating from purple potatoes.
82. **NIINA KELANNE (2021)** Novel bioprocessing for increasing consumption of Nordic berries.
83. **NIKO MARKKINEN (2021)** Bioprocessing of berry materials with malolactic fermentation.
84. **GABRIELE BELTRAME (2021)** Polysaccharides from Finnish fungal resources.
85. **SALLA LAITO (2022)** Bioactive compounds in oats and gut health.
86. **KANG CHEN (2022)** Multi-omics study on the effects of anthocyanin extracts from bilberries and purple potatoes on type 2 diabetes in Zucker diabetic fatty rats.
87. **WENJIA HE (2022)** Bioprocessing of alcoholic beverages from apples and pears: Effects of raw materials and processes on quality.
88. **TANJA KAKKO (2023)** Alternative approaches to improve the processing and quality of under-utilized fish.
89. **MIKAEL FABRITIUS (2023)** Mass spectrometric methodologies for analysis of triacylglycerol and phospholipid regioisomers in natural fats and oils.
90. **ELLA AITTA (2023)** Green technologies for the extraction of oil and protein from Baltic herring (*Clupea harengus membras*).
91. **AMRUTA KULKARNI (2023)** Effect of omega-3 deficiency and positional distribution of docosahexaenoic acid in triacylglycerols on tissue lipids in rats.
92. **LIZ A. GUTIÉRREZ QUEQUEZANA (2023)** Effect of cultivar, growth environment and developmental stage on phenolic compounds and ascorbic acid in potato tubers grown in Finland.
93. **MINNA ROTOLA-PUKKILA (2024)** The umami compounds in Nordic food raw materials and the effect of cooking.
94. **EIJA AHONEN (2024)** Impact of lipid structure and selected antioxidants on the oxidation of docosahexaenoic acid.
95. **MARINA FIDELIS (2024)** Valorization of underutilized biomass for biorefinery and food applications: Exploring the processing, plant material composition, bioactivity and fortified bread models.
96. **YUQING ZHANG (2025)** Structural analysis of triacylglycerols and bioavailability of docosahexaenoic acid from regio- and enantiopure triacylglycerols.
97. **HANY AHMED (2025)** Molecular insights to gut–brain communication: Metabolomics approach on lifestyle influences.

TURUN
YLIOPISTO
UNIVERSITY
OF TURKU